ENCLOSURE

ATTACHMENT 13.6

SIA Report No. 0800528.402

Nine Mile Point Unit 2 Steam Dryer ASME Stress Analysis

Nine Mile Point Nuclear Station, LLC
May 27, 2009

Report No. 0800528.402.R0
Project No. 0800528
March 2009
☒ Q ☐ Non-Q

Nine Mile Point Unit 2 Steam Dryer
ASME Stress Analysis

Prepared for:

Constellation Energy Group
Oswego, NY
7710698, Rev. 0

Prepared by:

Structural Integrity Associates, Inc.
San Jose, California

Prepared by: _____ Date: 3/27/09
S. S. Tang, P. E.

Reviewed by: _____ Date: 3/27/09
Marcos L. Herrera, P.E.

Approved by: _____ Date: 3/27/09
Karen K. Fujikawa, P.E.

Structural Integrity Associates, Inc.

REVISION CONTROL SHEET

Document Number: 0800528.402

Title: Nine Mile Point Unit 2 Steam Dryer ASME Stress Analysis

Client: Constellation Energy Group

SI Project Number: 0800528 ☒ Q ☐ Non-Q

Section	Pages	Revision	Date	Comments
1.0	1-1	0	3/27/09	Initial Issue
2.0	2-1			
3.0	3-1			
4.0	4-1 – 4-4			
5.0	5-1 – 5-5			
6.0	6-1 – 6-76			
7.0	7-1 – 7-21			
8.0	8-1 – 8-7			
9.0	9-1 – 9-2			
10.0	10-1 – 10-2			

Table of Contents

Section Page

1.0 INTRODUCTION 1-1

2.0 DESIGN CRITERIA 2-1

3.0 LOADS 3-1

3.1 Unit Load Cases 3-1

3.2 Flow Induced Vibration Load 3-1

4.0 LOAD COMBINATIONS 4-1

5.0 ASSUMPTIONS 5-1

6.0 ASME CODE STRESS LIMITS EVALUATION 6-1

6.1 Individual Load Case Results 6-2

6.1.1 Unit Pressure 6-3

6.1.2 Unit Acceleration in Global X-Direction 6-3

6.1.3 Unit Acceleration in Global Y-Direction 6-3

6.1.4 Unit Acceleration in Global Z-Direction 6-3

6.1.5 FIV Loads 6-3

6.1.6 OBE, SSE, SRV and AP Load Cases 6-4

6.2 ASME Code Stress Evaluation, Load Combination Case B-3 6-4

6.3 ASME Code Stress Evaluation, Load Combination Case D-1 6-5

6.4 Reconciliation of Finite Element Model and Assessment of Code Evaluation 6-6

6.5 Assessment of Indications in Upper Support Ring and Drain Channel 6-7

7.0 FATIGUE EVALUATION 7-1

7.1 Stress Range and Mean Stress 7-3

7.2 Fatigue Evaluation 7-3

7.3 Reconciliation of Finite Element Model on Fatigue Evaluation 7-4

8.0 BUCKLING EVALUATION OF LIFTING RODS 8-1

8.1 Technical Approach 8-1

8.2 Design Inputs 8-1

8.3 Assumptions 8-2

8.4 Buckling Calculation 8-2

8.5 Results of Analysis 8-3

8.6 Discussions 8-5

9.0 DISCUSSION AND CONCLUSIONS 9-1

10.0 REFERENCES 10-1

List of Tables

Table | Page

Table 4-1: NMP2 Steam Dryer Load Combinations 4-2
Table 4-2: Delta Pressure Forces 4-3
Table 4-3: Dynamic Loads 4-3
Table 4-4. NMP2 Steam Dryer Limiting Load Combinations 4-4
Table 5-1: Design Stress Intensities and Young's Modulus (ksi) for Typical Stainless Steel 5-2
Table 5-2: Summary of Stress Intensity Limits 5-2
Table 5-3: Allowable Stress Intensities (ksi) 5-2
Table 5-4: Tabulated Values of Fatigue Curves 5-3
Table 6-1: Classification of Stress Intensities 6-9
Table 6-2: Code Evaluation for Load Combination B-3 6-10
Table 6-3: Linearized Stresses at Gusset Section across the Maximum Stress Location for Load Combination Case B-3 6-11
Table 6-4: Code Evaluation for Load Combination D-1 6-12
Table 6-5: Code Interpreted Stresses at the Maximum Stress Location for Level D 6-13
Table 6-6: Comparison of Maximum Stress (ksi) Results due to Model Modification 6-14
Table 6-7: Modified Code Stress Evaluation for Load Combination B-3 6-15
Table 6-8: Modified Linearized Stresses at Gusset Section across the Maximum Stress Location for Load Combination Case B-3 6-16
Table 6-9: Modified Code Stress Evaluation for Load Combination D-1 6-17
Table 6-10: Modified Code Interpreted Stresses at the Maximum Stress Location for Load Combination D-1 6-18
Table 7-1: Fatigue Evaluation for Load Combination B-3 7-5
Table 8-1: Total Lifting Force, Faulted Condition 8-6
Table 8-2: Compressive Load on each Lifting Rod, Faulted Condition 8-6
Table 8-3: Allowable Load due to Axial Compression 8-6

List of Figures

Figure | Page

Figure 5-1: Design Fatigue Curves 5-4
Figure 5-2: Flow Chart for Use of Fatigue Curves 5-5
Figure 6-1: NMP2 Steam Dryer Model 6-19
Figure 6-2: Steam Dryer Boundary Condition 6-20
Figure 6-3: Constraint Equations 6-20
Figure 6-4: Solid Elements, Solid186 and Solid187 6-21
Figure 6-5: Shell Elements, Shell63 6-21
Figure 6-6: Surface Elements, Surf154 6-22
Figure 6-7: Mass Elements, Mass21 6-22
Figure 6-8: Outer Hood 6-23
Figure 6-9: Middle Hood 6-23
Figure 6-10: Inside Hood 6-24
Figure 6-11: Gussets in Hoods 6-24
Figure 6-12: Side Plates 6-25
Figure 6-13: Vane Bank Base Plates 6-25
Figure 6-14: Vertical Plates Inside Vane Banks 6-26
Figure 6-15: Vane Banks 6-27
Figure 6-16: Vane Banks 6-28
Figure 6-17: Drain Pipes 6-28
Figure 6-18: Skirt 6-29
Figure 6-19: Drain Channels 6-29
Figure 6-20: Upper Support Ring 6-30
Figure 6-21: Lower Support Ring 6-30
Figure 6-22: Tie Bars 6-31
Figure 6-23: Lifting Rods 6-31
Figure 6-24: Gussets Between Upper Support Ring and Vane Bank Base Plates 6-32
Figure 6-25: Vessel Brackets and Support Plates 6-32

Figure 6-26: Pressure Loadings 6-33
Figure 6-27: Stress Intensity, Top Surface, due to Unit Pressure 6-34
Figure 6-28: Stress Intensity Distribution, Top Surface, 1 g Acceleration in X-direction 6-35
Figure 6-29: Stress Intensity Distribution, Top Surface, 1 g Static Acceleration in Y-direction 6-36
Figure 6-30: Stress Intensity Distribution, Top Surface, 1 g Static Acceleration in Z-direction 6-37
Figure 6-31: Stress Intensity Distribution, Top Surface, FIV Load - TimeStress_49666_1075 6-38
Figure 6-32: Stress Intensity Distribution, Top Surface, FIV Load - TimeStress_49670_1075 6-39
Figure 6-33: Stress Intensity Distribution, Top Surface, ΔP_u, EPU 6-40
Figure 6-34: Stress Intensity Distribution, Top Surface, ΔP_a, EPU 6-41
Figure 6-35: Stress Intensity Distribution, Top Surface, OBE 6-42
Figure 6-36: Stress Intensity Distribution, Top Surface, SSE 6-42
Figure 6-37: Stress Intensity Distribution, Top Surface, SRV 6-43
Figure 6-38: Stress Intensity Distribution, Top Surface, AP 6-43
Figure 6-39: Outer Hood, Stress Intensity, Case B-3(a) 6-44
Figure 6-40: Middle Hood, Stress Intensity, Case B-3(a) 6-44
Figure 6-41: Inside Hood, Stress Intensity, Case B-3(a) 6-45
Figure 6-42: Gussets in Hoods, Stress Intensity, Case B-3 (a) 6-45
Figure 6-43: Sides Plates, Stress Intensity, Case B-3(a) 6-46
Figure 6-45: Vane Bank Vertical Plates, Stress Intensity, Case B-3(a) 6-47
Figure 6-46: Vane Banks, Stress Intensity, Case B-3(a) 6-47
Figure 6-47: Drain Pipes, Stress Intensity, Case B-3(a) 6-48
Figure 6-48: Skirt, Stress Intensity, Case B-3 (a) 6-48
Figure 6-49: Drain Channels, Stress Intensity, Case B-3(a) 6-49
Figure 6-50: Upper Support Ring, Stress Intensity, Case B-3(a) 6-49
Figure 6-51: Lower Support Ring, Stress Intensity, Case B-3 (a) 6-50
Figure 6-52: Tie Bars, Stress Intensity, Case B-3(a) 6-50
Figure 6-53: Lifting Rods, Stress Intensity, Case B-3(a) 6-51
Figure 6-54: Gussets in Upper Support Ring, Stress Intensity, Case B-3(a) 6-51
Figure 6-55: Outer Hoods Stress Intensity Case B-3 (b) 6-52
Figure 6-56: Middle Hoods, Stress Intensity Case B-3 (b) 6-52

Figure 6-57: Inside Hoods, Stress Intensity, Case B-3 (b) 6-53
Figure 6-58: Gussets in Hoods, Stress Intensity, Case B-3 (b) 6-53
Figure 6-59: Side Plates, Stress Intensity, Case B-3(b) 6-54
Figure 6-60: Vane Bank Base Plates, Stress Intensity, Case B-3(b) 6-54
Figure 6-61: Vane Bank Vertical Plates, Stress Intensity, Case B-3(b) 6-55
Figure 6-62: Vane Bank, Stress Intensity, Case B-3(b) 6-55
Figure 6-63: Drain Pipes, Stress Intensity, Case B-3(b) 6-56
Figure 6-64: Skirt, Stress Intensity, Case B-3(b) 6-56
Figure 6-65: Drain Channels, Stress Intensity, Case B-3(b) 6-57
Figure 6-66: Upper Support Ring, Stress Intensity, Case B-3(b) 6-57
Figure 6-67: Lower Support Ring, Stress Intensity, Case B-3(b) 6-58
Figure 6-68: Tie Bars, Stress Intensity, Case B-3 (b) 6-58
Figure 6-69: Lifting Rods, Stress Intensity, Case B-3(b) 6-59
Figure 6-70: Gussets in Upper Support Ring, Stress Intensity, Case B-3(b) 6-59
Figure 6-71: Gussets in Hoods with the Maximum Stress Intensity, Case B-3(a) 6-60
Figure 6-72: Outer Hoods, Stress Intensity, Case D-1 (a) 6-61
Figure 6-73: Middle Hoods, Stress Intensity, Case D-1 (a) 6-61
Figure 6-74: Inside Hoods, Stress Intensity, Case D-1(a) 6-62
Figure 6-75: Gussets in Hoods, Stress Intensity, Case D-1(a) 6-62
Figure 6-76: Side Plates, Stress Intensity, Case D-1(a) 6-63
Figure 6-77: Vane Bank Base Plates, Stress Intensity, Case D-1 (a) 6-63
Figure 6-78: Vane Bank Vertical Plates, Stress Intensity, Case D-1(a) 6-64
Figure 6-79: Vane Banks, Stress Intensity, Case D-1(a) 6-64
Figure 6-80: Drain Pipes, Stress Intensity, Case D-1(a) 6-65
Figure 6-81: Skirt, Stress Intensity, Case D-1(a) 6-65
Figure 6-82: Drain Channels, Stress Intensity, Case D-1 (a) 6-66
Figure 6-83: Upper Support Ring, Stress Intensity, Case D-1(a) 6-66
Figure 6-84: Lower Support Ring, Stress Intensity, Case D-1(a) 6-67
Figure 6-85: Tie Bars, Stress Intensity, Case D-1(a) 6-67
Figure 6-86: Lifting Rods, Stress Intensity, Case D-1 (a) 6-68

Figure 6-87: Gussets in Upper Support Ring, Stress Intensity, Case D-1 (a) 6-68
Figure 6-88: Outer Hoods, Stress Intensity, Case D-1(b) 6-69
Figure 6-89: Middle, Hoods, Stress Intensity, Case D-1(b) 6-69
Figure 6-90: Inside Hoods, Stress Intensity, Case D-1(b) 6-70
Figure 6-91: Gussets Inside Hoods, Stress Intensity, Case D-1(b) 6-70
Figure 6-92: Side Plates, Stress Intensity, Case D-1(b) 6-71
Figure 6-93: Vane Bank Base Plates, Stress Intensity, Case D-1(b) 6-71
Figure 6-94: Vane Bank Vertical Plates, Stress Intensity, Case D-1(b) 6-72
Figure 6-95: Vane Bank, Stress Intensity, Case D-1(b) 6-72
Figure 6-96: Drain Pipes, Stress Intensity, Case D-1(b) 6-73
Figure 6-97: Skirt, Stress Intensity, Case D-1(b) 6-73
Figure 6-98: Drain Channels, Stress Intensity, Case D-1(b) 6-74
Figure 6-99: Upper Support Ring, Stress Intensity, Case D-1(b) 6-74
Figure 6-100: Lower Support Ring, Stress Intensity, Case D-1(b) 6-75
Figure 6-101: Tie Bars, Stress Intensity, ... 6-75
Figure 6-102: Lifting Rods, Stress Intensity, Case D-1(b) 6-76
Figure 6-103: Gussets in Upper Support Ring, Stress Intensity, Case D-1(b) 6-76
Figure 7-1: Outer Hoods, Alternating Stress Intensity Range, Case B-3 7-6
Figure 7-2: Middle Hoods, Alternating Stress Intensity Range, Load Combination, Case B-3 7-6
Figure 7-3: Inside Hoods, Alternating Stress Intensity Range, Case B-3 7-7
Figure 7-4: Gussets in Hoods, Alternating Stress Intensity Range, Case B-3 7-7
Figure 7-5: Side Plates, Alternating Stress Intensity Range, Case B-3 7-8
Figure 7-6: Vane Bank Base Plates, Alternating Stress Intensity Range, Case B-3 7-8
Figure 7-7: Vane Bank Vertical Plates, Alternating Stress Intensity Range, Case B-3 7-9
Figure 7-8: Vane Banks, Alternating Stress Intensity Range, Case B-3 7-9
Figure 7-9: Drain Pipes, Alternating Stress Intensity Range, Case B-3 7-10
Figure 7-10: Skirt, Alternating Stress Intensity Range, Case B-3 7-10
Figure 7-11: Drain Channels, Alternating Stress Intensity Range, Case B-3 7-11
Figure 7-12: Upper Support Ring, Alternating Stress Intensity Range, Case B-3 7-11
Figure 7-13: Lower Support Ring, Alternating Stress Intensity Range, Case B-3 7-12

Figure 7-14: Tie Bars, Alternating Stress Intensity Range, Case B-3 7-12
Figure 7-15: Lifting Rods, Alternating Stress Intensity Range, Case B-3 7-13
Figure 7-16: Gussets in Upper Support Ring, Alternating Stress Intensity Range, Case B-3 7-13
Figure 7-17: Outer Hoods, Mean Stress Intensity, Case B-3 7-14
Figure 7-18: Middle Hoods, Mean Stress Intensity, Case B-3 7-14
Figure 7-19: Inside Hoods, Mean Stress Intensity, Case B-3 7-15
Figure 7-20: Gussets in Hoods, Mean Stress Intensity, Case B-3 7-15
Figure 7-21: Side Plates, Mean Stress Intensity, Case B-3 7-16
Figure 7-22: Vane Bank Base Plates, Mean Stress Intensity, Case B-3 7-16
Figure 7-23: Vane Bank, Vertical Plates, Mean Stress Intensity, Case B-3 7-17
Figure 7-24: Vane Banks, Mean Stress Intensity, Case B-3 7-17
Figure 7-25: Drain Pipes, Mean Stress Intensity, Case B-3 7-18
Figure 7-26: Skirt, Mean Stress Intensity Range, Case B-3 7-18
Figure 7-27: Drain Channels, Mean Stress Intensity, Case B-3 7-19
Figure 7-28: Upper Support Ring, Mean Stress Intensity, Case B-3 7-19
Figure 7-29: Lower Support Ring, Mean Stress Intensity, Case B-3 7-20
Figure 7-30: Tie Bars, Mean Stress Intensity, Case B-3 7-20
Figure 7-31: Lifting Rods, Mean Stress Intensity, Case B-3 7-21
Figure 7-32: Gussets in Upper Support Ring, Mean Stress Intensity, Case B-3 7-21
Figure 8-1: Loads as Function of Effective Length Factor K 8-7

1.0 INTRODUCTION

As part of implementation of Extended Power Uprate (EPU) at Nine Mile Point Unit 2 (NMP2), the effects of flow induced vibration (FIV) loads need to be considered in the structural analysis of the steam dryer. Thus, an ASME Code [1] Section III analysis has been performed to assess the structural adequacy of the steam dryer. The analysis documented in this report has been performed using the guidance of BWRVIP-182 [2], "Guidance for Demonstration of Steam Dryer Integrity for Power Uprate." The load and load combinations evaluated for the NMP2 steam dryer are considered using the NMP2 plant specific load combinations as well as those provided in BWRVIP-181 [3], "Steam Dryer Repair Design Criteria."

2.0 DESIGN CRITERIA

This evaluation is performed using the guidance of ASME Code, Section III Core Support Structures. As such, the rules of Subarticle NG-3200 of Section III of the ASME Code, 2001 Edition (with 2003 addenda) [1], are used.

3.0 LOADS

3.1 Unit Load Cases

Four static unit load cases were provided by Continuum Dynamics, Inc. (CDI) [4]. They are:

(1) Unit pressure
(2) Static acceleration in global x-direction
(3) Static acceleration in global y-direction
(4) Static acceleration in global z-direction.

3.2 Flow Induced Vibration Load

In addition, a dynamic load case due to the flow induced vibration (FIV) was provided by CDI [4]. This load case is the acoustic loading from the steam line though the steam nozzles to the outer hood of the steam dryer. This load case was performed as a harmonic analysis. The results are only provided for the points of time corresponding to the maximum stress intensity and the maximum alternating stress intensity range in the steam dryer.

4.0 LOAD COMBINATIONS

Per Reference [3], the load combinations are divided into two basic categories, Mark I plants and Mark II/III plants. NMP2 is a BWR-5 Mark II plant, thus, the load combinations contained in Table 7-2 of Reference [3] are used as a guide since NMP2 has plant specific documentation for the steam dryer load combination. The detailed description of individual load cases and how the load cases combined is documented in Reference [5]. The load combinations are summarized in Table 4-1, along with the ΔP in Table 4-2, and scale factors for static acceleration loads in Table 4-3. Based on the review of different load cases and load combinations in References [5] and [6], Table 4-4 lists the load combinations that will be used in the ASME Code stress evaluation.

Table 4-1: NMP2 Steam Dryer Load Combinations

No.	Load Combination	Design Basis	Evaluation Basis
B-1	$NL + \Delta P_N + [OBE^2 + FIV^2]^{1/2}$	Upset	Upset
B-2	$NL + \Delta P_U + [SRV^2 + FIV^2]^{1/2}$	Upset	Upset
B-3	$NL + \Delta P_U + [OBE^2 + SRV^2 + FIV^2]^{1/2}$	Emergency	Upset
C-1	$NL + \Delta P_U + [OBE^2 + SRV^2 + FIV^2]^{1/2}$	Emergency	Emergency
C-2	$NL + \Delta P_U + [CHUG^2 + SRV_{ADS}^2 + FIV^2]^{1/2}$	Emergency	Emergency
D-1	$NL + \Delta P_A + [SSE^2 + AP^2 + FIV^2]^{1/2}$	Faulted	Faulted
D-2	$NL + \Delta P_A + [CHUG^2 + SRV_{ADS}^2 + SSE^2 + FIV^2]^{1/2}$	Faulted	Faulted
D-3	$NL + \Delta P_U + [SSE^2 + SRV^2 + FIV^2]^{1/2}$	Faulted	Faulted
D-4	$NL + \Delta P_I + FIV$	Faulted	Faulted

Notes:

NL	= Normal loads (metal + water weight)
ΔP_N	= Normal delta pressure force
ΔP_U	= Upset delta pressure force
ΔP_A	= Accident LOCA delta pressure force
ΔP_I	= Interlock delta pressure force
FIV	= Flow induced vibration
OBE	= Operating basis earthquake loads
SSE	= Safe shutdown earthquake loads
SRV	= Safety-relief valve discharge loads
SRV_{ADS}	= Loads induced by actuation of safety-relief valves associated with the Automatic Depressurization System
AP	= Annulus pressurization loads
CHUG	= Chugging loads

Dynamic loads are combined by square-root-sum-of the squares (SRSS)

Table 4-2: Delta Pressure Forces

Condition	ΔP (psi) [1]
Normal Condition (ΔP_N)	CLTP: 0.36 EPU: 0.48
Upset Condition (ΔP_U)	CLTP: 0.47 EPU: 0.71
Faulted Condition (ΔP_A, ΔP_I)[2]	CLTP: 6.3 EPU: 4.8

Notes:

1. CLTP = Current Licensed Thermal Power; EPU = Extended Power Uprate
2. Maximum of (ΔP_A, ΔP_I)

Table 4-3: Dynamic Loads

Description	Direction	Load (g)
OBE	Horizontal (X)	0.501
OBE	Horizontal (Y)	0.535
OBE	Vertical	0.186
SSE	Horizontal (X)	0.767
SSE	Horizontal (Y)	0.777
SSE	Vertical	0.327
SRV	Horizontal	0.071
SRV	Vertical	0.132
SRV_{ADS}	Horizontal	0.004
SRV_{ADS}	Vertical	0.128
CHUG	Horizontal (X)	0.078
CHUG	Horizontal (Y)	0.045
CHUG	Vertical (Z)	0.182
AP	Horizontal	0.580*1.6

Table 4-4. NMP2 Steam Dryer Limiting Load Combinations

Case	Load Combination	Evaluation Basis
B-3	$NL + \Delta P_U \pm [OBE^2 + SRV^2 + FIV^2]^{1/2}$	Level B (Upset) [1]
D-1	$NL + \Delta P_A \pm [SSE^2 + AP^2 + FIV^2]^{1/2}$	Level D (Faulted)

Note: 1. The fatigue evaluation does not include the FIV stresses. This load combination is used to evaluate the primary and primary + secondary stresses.

5.0 ASSUMPTIONS

The assumptions are:

(a) All materials in the steam dryer are assumed to be Type 304 stainless steel (A240, Type 304).

(b) The operating temperature is assumed to be 550°F.

(c) The design temperature is assumed to be 600°F.

(d) The vessel brackets are not included in the current ASME Code evaluation.

(e) The weld factor for fatigue evaluation is 1.8 for fillet welds and 1.0 for full penetration welds.

(f) All welds are assumed to be fillet welds.

(g) The quality factor for the weld used in the Code stress evaluation is assumed to be 1.0.

(h) No expansion stress, P_e, is considered in the Code stress evaluation, assuming the thermal stress is insignificant.

(i) The weight of steam is assumed to be negligible.

(j) The water inside the skirt has no effect on the deadweight stress in the steam dryer.

(k) The scale factors for OBE include the effect of the added water mass inside the skirt.

The design stress intensity (S_m), yield strength, ultimate strength and Young's Modulus for Type 304 stainless steel (A-240 Type 304) were obtained from Reference [7] and summarized in Table 5-1 for different temperatures. The summary of stress intensity limits for different service levels and stress categories are obtained from Reference [1] and presented in Table 5-2. The allowable stress intensity for each stress categories are presented in Table 5-3, where P_m: primary membrane, P_b: primary bending, Q: secondary and F: peak.

The material fatigue curves at high cycles are presented in Figure 5-1 [1]. The digitized curves are presented in Table 5-4 [1]. In addition, the guidelines to determine which fatigue curve to be used in the Code evaluation are presented in Figure 5-2 [1].

Table 5-1: Design Stress Intensities and Young's Modulus (ksi) for Stainless Steel (A240 Type 304)

	-20°F to 100°F	500°F	600°F	550°F (1)
S_m	20.0(2)	17.5	16.6	17.05
Yield Strength	30.0(2)	19.4	18.4	18.9
Tensile Strength	75.0(2)	63.4	63.4	63.4
Young's Modulus	28.3×10^3(2)	25.8×10^3	25.3×10^3	25.55×10^3

Notes:

1. Interpolated between 500°F and 600°F
2. At 70°F

Table 5-2: Summary of Stress Intensity Limits

Categories	Levels A and B (Design, Normal & Upset)	Level C (Emergency)	Level D (Faulted)
P_m	S_m	$1.5S_m$	min of $2.4\ S_m$ and $0.7S_u$
$P_m + P_b$	$1.5S_m$	$2.25S_m$	$1.5P_m$
$P_m + P_b + Q$	$3S_m$	n/a	n/a
$P_m + P_b + Q + F$	S_a	n/a	n/a

Notes:

1. Level D uses Section III Appendix F criteria.
2. n/a: not applicable

Table 5-3: Allowable Stress Intensities (ksi)

Categories	Levels A and B (Design, Normal & Upset)	Level C (Emergency)	Level D (Faulted)
P_m	16.6(1)	24.97(1)	min(39.84, 44.38) = 39.84
$P_m + P_b$	24.9(1)	37.35(1)	59.07
$P_m + P_b + Q$(2)	51.15(2)	n/a	n/a
$P_m + P_b + Q + F$	S_a(3)	n/a	n/a

Notes:

1. Used S_m at 600°F for conservatism.
2. Used S_m at 550°F, for bounding average temperature per Figure NG-3221-1, Note (6).
3. See Figure 5-1 and Figure 5-2 and Table 5-4.
4. n/a: not applicable

Table 5-4: Tabulated Values of Fatigue Curves

TABLE I-9.2.2
TABULATED VALUES OF S_a, ksi (MPa), FROM FIG. I-9.2.2[1,2]

Number of Cycles [Note (3)]	Curve A	Curve B	Curve C
1E6	28.2 (194)	28.2 (194)	28.2 (194)
2E6	26.9 (185)	22.8 (157)	22.8 (157)
5E6	25.7 (177)	19.8 (137)	18.4 (127)
1E7	25.1 (173)	18.5 (128)	16.4 (113)
2E7	24.7 (170)	17.7 (122)	15.2 (105)
5E7	24.3 (168)	17.2 (119)	14.3 (99)
1E8	24.1 (166)	17.0 (117)	14.1 (97)
1E9	23.9 (165)	16.8 (116)	13.9 (96)
1E10	23.8 (164)	16.6 (114)	13.7 (94)
1E11	23.7 (163)	16.5 (114)	13.6 (94)

NOTES:
(1) All notes on Fig. I-9.2.2 apply to these data.
(2) Interpolation between tabular values is permissible based upon data representation by straight lines on log-log plot. See Table I-9.1, Note (2).
(3) The number of cycles indicated shall be read as follows:
[E] = I × 10^J, e.g., 5E6 = 5 × 10^6 or 5,000,000

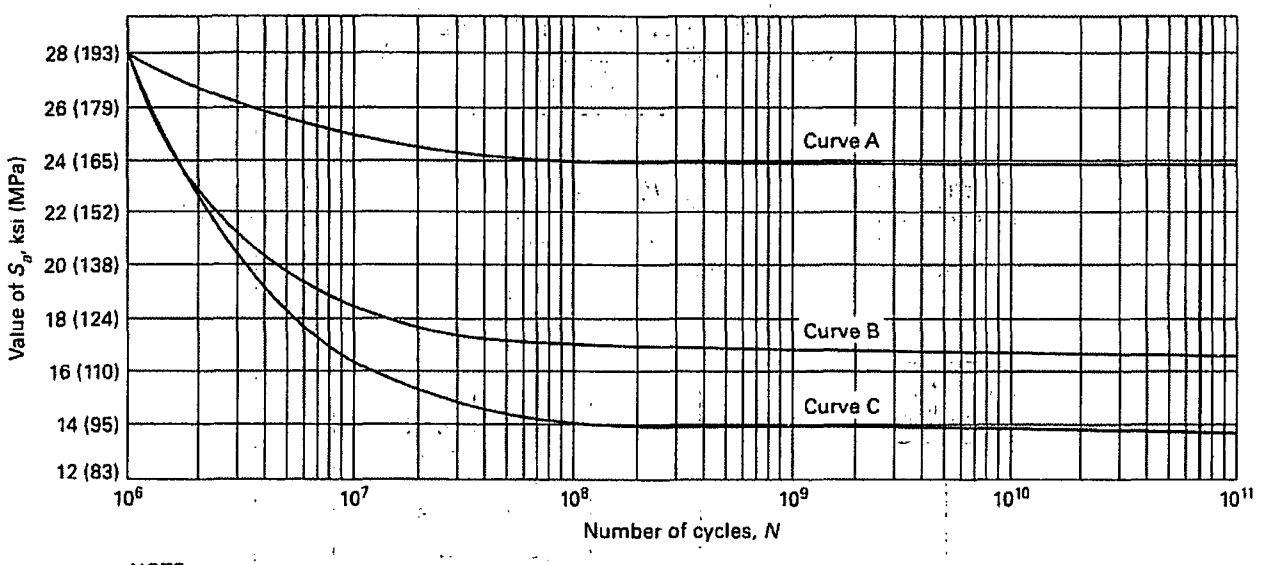

NOTE:
E = 28 3 × 10^6 psi (195 000 MPa)

FIG. I-9.2.2 DESIGN FATIGUE CURVES FOR AUSTENITIC STEELS, NICKEL-CHROMIUM-IRON ALLOY, NICKEL-IRON-CHROMIUM ALLOY, AND NICKEL-COPPER ALLOY FOR $S_a \leq 28.2$ ksi (194 × 10^3 MPa), FOR TEMPERATURES NOT EXCEEDING 800°F (427°C)
(For S_a >28.2 ksi (194 × 10^3 MPa), use Fig. I-9.2.1.)
Table I-9.2.2 Contains Tabulated Values for Accurate Interpolation of This Curve

Figure 5-1: Design Fatigue Curves

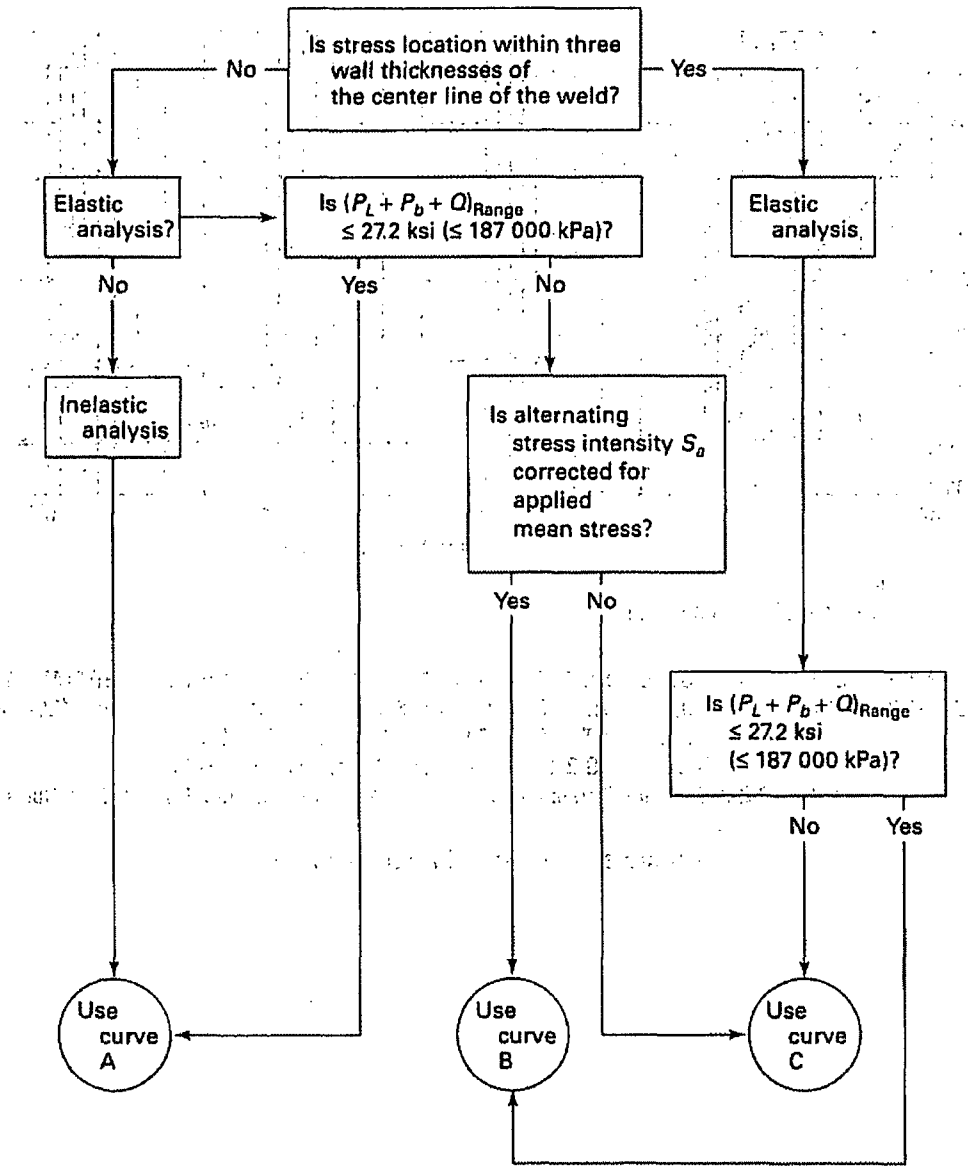

FIG. I-9.2.3 FLOW CHART FOR USE OF CURVES IN FIG. I-9.2.2

Figure 5-2: Flow Chart for Use of Fatigue Curves

6.0 ASME CODE STRESS LIMITS EVALUATION

The individual load cases were combined with the appropriate scale factors for the two load combination cases as shown in Table 4-4. The individual dynamic load cases of OBE, SSE, and SRV are first obtained from the square root of the sum of square (SRSS) from the three static accelerations in the three global directions.

$$OBE = \sqrt{OBE_x^2 + OBE_y^2 + OBE_z^2} \quad (6\text{-}1)$$

$$SSE = \sqrt{SSE_x^2 + SSE_y^2 + SSE_z^2} \quad (6\text{-}2)$$

$$SRV = \sqrt{SRV_x^2 + SRV_y^2 + SRV_z^2} \quad (6\text{-}3)$$

where OBE_i , SSE_i, and SRV_i = load case due to static acceleration excitation in i direction,

i = x, y or z.

After each load case is calculated, then the load case results combined by SRSS depending on the load combinations to obtain the resultant stress components for combinations with the normal load and the delta pressure force load cases.

The resultant load cases of OBE, SSE, and SRV are used in the final load combinations as shown in Table 4-4 for the ASME Code evaluation. The individual load cases are algebraically summed as shown in Table 4-4 for the ASME Code evaluation. The algebraic sum of the SRSS of OBE, SSE, and SRV is both positive and negative to account for the fully reversible nature of these loadings.

The Code stress compliance evaluation was performed on a node by node basis for a simple and direct evaluation. The intent of the Code is to evaluate the stress across a full section per Subarticle NG-3217 and Table NG-3217-1, duplicated in Table 6-1. Therefore, if the stress in a component evaluated on a node by node basis is higher than the required stress allowables, a section per ASME Code guideline is selected through the highest stress location in the component for further evaluation.

The model is shown in Figure 6-1 [4]. The model consists of Shell63, Solid186, Solid187 and Mass21 element types (Figures 6-4 to 6-7) [4]. The model for the unit pressure load case contains element types Surf154 for the pressure inputs (Figure 6-6). It has 157,578 nodes and 122,269 elements (167,122 elements if the Surf154 element type is included). The boundary conditions for the unit pressure load case are shown in Figure 6-2. The steam dryer is constrained at the vessel bracket in all three translational directions. In addition, there are 18,453 constraint equations used in the model, Figure 6-3. These constraint equations are used to couple different components of the steam dryer. The mass elements in Figure 6-7 are inside the Vane Bank to account for the assembly inside the Vane Banks.

For the Code stress evaluation, the steam dryer is separated into different components. The definitions of these components are based on the functionality or proximity in the steam dryer. They are:

1. Outer Hood, Figure 6-8
2. Middle Hood, Figure 6-9
3. Inside Hood, Figure 6-10
4. Gussets in Hoods, Figure 6-11
5. Side Plates, Figure 6-12
6. Vane Bank Base Plates, Figure 6-13
7. Vertical Plates Inside Vane Banks, Figure 6-14
8. Vane Banks, Figure 6-15 and Figure 6-16
9. Drain Pipes, Figure 6-17
10. Skirt, Figure 6-18
11. Drain Channels, Figure 6-19
12. Upper Support Ring, Figure 6-20
13. Lower Support Ring, Figure 6-21
14. Tie Bars, Figure 6-22
15. Lifting Rods, Figure 6-23
16. Gussets Between Upper Support Ring and Vane Bank Base Plates, Figure 6-24

The vessel brackets, Figure 6-25, are not included in the component list for the Code or fatigue evaluation because they are not considered as components in the steam dryer, but instead components in the reactor pressure vessel.

6.1 Individual Load Case Results

The results from the individual load cases are obtained from Reference [4]. Only the EPU condition was considered in this evaluation.

6.1.1 Unit Pressure

The unit pressure loadings on the steam dryer are presented in Figure 6-26. A 1 psi was applied inside the steam dryer, except only at the bottom portion of the skirt. Inside the vane bank, a 0.5 psi was applied to the top plates, side plates and the base plates. The overall stress intensity factor distribution is presented in Figure 6-27. The maximum stress intensity is about 16 ksi, Figure 6-27 (a). The maximum stress location is at the end of the tie bar over the inner hoods, Figure 6-27 (b). The high stress components are the middle and inside hoods.

6.1.2 Unit Acceleration in Global X-Direction

A 1 g acceleration (386.09 in/sec^2 [4]) was applied in the global +x-direction. The global x-direction is shown in Figure 6-4. The overall stress intensity distribution is shown in Figure 6-28 (a). The maximum stress intensity is about 40 ksi. Its location is in one of the vessel bracket, Figure 6-28 (b). This maximum stress is highly localized in the vessel bracket. The stresses in the rest of the steam dryer are much lower.

6.1.3 Unit Acceleration in Global Y-Direction

A 1 g acceleration was applied in the global +y-direction. The overall stress intensity distribution is shown in Figure 6-29 (a). The maximum stress intensity is about 50 ksi. Its location is also at one of the vessel bracket, Figure 6-29 (b). Similar to the previous acceleration case, the stresses in the rest of the steam dryer are lower.

6.1.4 Unit Acceleration in Global Z-Direction

A 1g acceleration was applied in the global +z direction. The overall stress intensity distribution is shown in Figure 6-30 (a). The maximum stress intensity is about 13 ksi. Its location is also at one of the vessel bracket, Figure 6-30 (b). This maximum stress is much lower compared to the other two horizontal acceleration cases.

6.1.5 FIV Loads

Two sets of results were provided from FIV loads [4]. They are identified as:

(1) TimeStress_49666_1075

(2) TimeStress_49670_1075.

These results correspond to the time of maximum stress intensity and the maximum stress intensity range. The overall stress distributions are presented in Figure 6-31 and Figure 6-32. It is shown that case TimeStress_49666_1075 has a higher overall stress intensity. This case is used in the load combinations for the Code stress evaluation.

6.1.6 OBE, SSE, SRV and AP Load Cases

The overall stress distributions for the load cases of ΔP_u, ΔP_a, OBE, SSE, SRV, and AP are presented in Figure 6-33 through Figure 6-38, respectively. These load cases are combined or scaled according to Equations (6-1) to (6-3) or Table 4-3. Only the stresses at the top surface of the shell element types are shown. These load cases are used to perform the load combination, as identified in Table 3-4 for the Code stress and fatigue evaluations.

The load combinations were performed in ANSYS Revision 11.0 [8].

6.2 ASME Code Stress Evaluation, Load Combination Case B-3

To determine whether the steam dryer stresses meet the ASME Code allowable requirements, the steam dryer is divided into major components as identified in Section 6.0. For each component, the stress intensity plots are obtained for the mid, top and bottom surface of the shell elements to determine the primary membrane stress intensity, P_m and the primary membrane and bending stress intensity, P_m+P_b. The results are interpreted from the stress plots based on the nodal basis. These nodal results are readily interpreted and conservative for the ASME Code stress evaluation.

The ASME Code stress evaluation for the load combination Case B-3, a Level B (or upset) service condition, is summarized in Table 6-2. Two conditions for this load case are considered: with (a) positive and (b) negative of the dynamic loads: $[OBE^2 + SRV^2 + FIV^2]^{1/2}$ in the load combinations. The stress intensity distributions for all components are presented from Figure 6-39 thru Figure 6-54 using the positive dynamic loads and from Figure 6-55 to Figure 6-70 using the negative dynamic loads and summarized in Table 6-2. It is shown that all components are below the P_m and P_m+P_b allowables for

the Level B (upset) service condition except the P_m in the component Gussets in Hood from Table 6-2 (a), with stress distribution shown in Figure 6-71 (a).

Since it is assumed that the thermal expansion stress is insignificant, the stress category P_m+P_b+Q is thus the same as P_m+P_b in Table 6-2 (a) and (b)

For the component Gussets in Hood in Load Case B-1(a), the gusset with the maximum stress intensity location is shown in Figure 6-71 (b). The location of the maximum stress is at the bottom corner of the gusset. This maximum stress is very localized and concentrated at a single node. As described in Table NG-3217-1, Table 6-1, for any shell in the core support structure, the location for consideration can be any section across the entire shell, (i.e., component 'Any Shell or Head' under column heading 'Core Support Structure'). Therefore, a section across the gusset at the maximum stress location is selected as shown in Figure 6-71 (b). A linearized stress is obtained for membrane and bending stresses for this section. It is shown that the linearized P_m is 6.53 ksi and the linearized P_m+P_b is 10.17 ksi, Table 6-3. They are below the P_m and P_m+P_b stress allowables of 16.6 ksi and 24.9 ksi, respectively for Load Case B-1.

It should be noted that in Table 6-2, the P_m, P_m+P_b Top and P_m+P_b Bottom are the same for the Upper Support Ring, Lower Support Ring and Tie Bars. It is due that solid elements were used in these components. The nodal stress is taken as both P_m and P_m+P_b.

6.3 ASME Code Stress Evaluation, Load Combination Case D-1

The ASME Code stress evaluation for load combination Case D-1, a Level D (or faulted) service condition, is summarized in Table 6-4 for both positive and negative dynamic load: $[SSE^2 + AP^2 + FIV^2]^{1/2}$ in the load combination. The stress intensity distributions for all components are presented from Figure 6-72 to Figure 6-87 using the positive dynamic loads and Figure 6-88 to Figure 6-103 using the negative dynamic loads and summarized in Table 6-4.

In Table 6-4, it is shown that the components of middle hoods, insides hoods, gussets in hoods, vane bank base plates, vane banks and tie bars are above the allowables either in P_m or P_m+P_b based on the results from nodal stresses. When the stress results are interpreted by linearization of stress in a section

through the maximum stress location and bending stress classified as secondary stress per NG-3213.0 and Table NG-3217-1, most of the components have stresses within the Code stress allowable, Table 6-5, except gussets in hoods and tie bars. Further assessment of this high stress condition is presented in the next section.

6.4 Reconciliation of Finite Element Model and Assessment of Code Evaluation

The ASME Code evaluation was performed based on finite element models and results in Reference [4]. Since then, a modification to the finite element model was incorporated [13]. The unit load cases for the unit pressure and the three unit acceleration were re-analyzed. Since the Code evaluation in Sections 6.2 and 6.3 was performed using the results from the model before the modification, this section provides a reconciliation of the difference in the stress results from these two models to assess the applicability of the current Code evaluation is applicable.

The modifications to the finite element model are described in Reference [13] and summarized below:

1. Reinforcement strips were removed from the innermost hoods (the ones furthest from the MSLs).
2. Dryer support between MSL C and MSL D was shortened to account for the difference in seismic block position.
3. The geometry of the supporting plates was changed in accordance with drawing number 158B8793.

Table 6-6 summarizes the maximum stress intensities in the portion of the steam dryer above the upper support ring for the four unit load cases for the model before the modification and after the modification. The differences in maximum stress intensities are from -14.30% to 41.86%.

In order to evaluate the effect of the model modification on the Code evaluation, the stress intensities results in Tables 6-2 through 6-5 are adjusted by the average of the percentage difference in the last column of Table 6-6. The use of average difference is justified since the load combinations include these four unit load cases as they can cancel each other in the load combination due to acting in the opposite direction. And these unit load cases were scaled by the load factors shown in Table 4-2 to

obtain the resultant stress intensity. The average difference was calculated to be 5.62 %. A scaled factor of 1.06 was used. The modified Code stress evaluation is presented in Table 6-7 to Table 6-10.

For load combination Case B-3, service level conditions A/B, all components remain below the Code stress allowables.

For the Service Level D Code evaluation, the stresses in the same two components, gussets in hoods and tie bars, are higher than the allowable by a maximum of about 30% on the P_m+P_b and 23% on the P_m. Depending on the location, the P_b can be classified as secondary stress per NG-3213.9 such that the P_m+P_b could be within the allowable. In addition, an acceptance criteria using elastic-plastic stress analysis per Appendix F, Rule for Evaluation of Service Loadings with Level D Service Limits, of Reference [1] can be performed to show the Code acceptance of the steam dryer. Since the applied stresses do not significantly exceed the stress allowables, the use of elastic-plastic stress analysis should be able to show that the stresses in these two components could easily satisfy the ASME Code requirement.

6.5 Assessment of Indications in Upper Support Ring and Drain Channel

The baseline inspections [16] of the NMP2 steam dryer identified steam dryer cracking consistent with the BWR fleet operating history as described in Section 2.4 of BWRVIP-139 [18]. The indications that require assessment relative to EPU service conditions are the indications located in the upper support ring, the drain channel to skirt vertical weld, and in the tie bar to hood weld heat affect zone [16]. Indications in the anti-rotation tack welds associated with the tie rod cam nut washers and the lifting lug have been identified as repair locations prior to EPU service.

A fracture mechanics evaluation of the observed indications was performed to determine if a repair is required for these locations for EPU operating conditions [17]. The evaluation in Reference [17] concluded that the reportable indications are expected to experience no significant crack growth during EPU operating conditions. Since the indications are characterized as IGSCC they were evaluated conservatively assuming further IGSCC growth using methods consistent with BWRVIP-14A [19]. The BWRVIP-139 [18] inspection interval is one operating cycle. With this assumption the cracking results in an insignificant change in the section thickness. The remaining ligaments in these components are

sufficient to produce safety factors that are well above the minimum required code safety factors for the all service conditions including the limiting upset and faulted conditions with the EPU FIV load included.

Table 6-1: Classification of Stress Intensities

TABLE NG-3217-1
CLASSIFICATION OF STRESS INTENSITIES FOR SOME TYPICAL CASES

Core Support Structure	Location	Origin of Stress	Type of Stress	Classification	Discontinuity Gross	Discontinuity Local
Cylindrical or spherical shell	Shell plate remote from discontinuities	Pressure difference	General membrane	P_m	No	No
			Gradient through plate thickness	Q	Yes	No
		Axial thermal gradient	Membrane	Q	Yes	No
			Bending	Q	Yes	No
	Junction with head or flange	Pressure difference	Membrane	Q	Yes	No
			Bending	Q	Yes	No
Any shell or head	Any section across entire shell	External load or moment, or pressure difference	General membrane averaged across full section. Stress component perpendicular to cross section	P_m	No	No
		External load or moment	Bending across full section. Stress component perpendicular to cross section	P_m	No	No
	Near nozzle or other opening	External load or moment, or pressure difference	Membrane	Q	Yes	No
			Bending	Q	Yes	No
			Peak (fillet or corner)	F	Yes	Yes
	Any location	Temp. difference between shell and head	Membrane	Q	Yes	No
			Bending	Q	Yes	No
Dished head or conical	Crown	Pressure difference	General membrane	P_m	No	No
			Bending	P_b	No	No
	Knuckle of junction to shell	Pressure difference	Membrane	Q(1)	Yes	No
			Bending	Q	Yes	No
Flat head	Center region	Pressure difference	General membrane	P_m	No	No
			Bending	P_b	No	No
	Junction to shell	Pressure difference	Membrane	Q	Yes	No
			Bending	Q	Yes	No
Perforated head or shell	Typical ligament in a uniform pattern	Pressure difference or external load	General membrane (avg through cross section)	P_m	No	No
			Bending (avg. through width of ligament, but gradient through plate)	P_b	No	No
			Peak	F	No	Yes
	Isolated or atypical ligament	Pressure difference	Membrane	Q	Yes	No
			Bending	F	Yes	Yes
			Peak	F	Yes	Yes

(Table NG-3217-1 continues on next page)

TABLE NG-3217-1 (CONT'D)
CLASSIFICATION OF STRESS INTENSITIES FOR SOME TYPICAL CASES

Core Support Structure	Location	Origin of Stress	Type of Stress	Classification	Discontinuity Gross	Discontinuity Local
Nozzle	Cross section perpendicular to nozzle axis	Pressure difference or external load or moment	General membrane avg across full section. Stress component perpendicular to section.	P_m	No	No
		External load or moment	Bending across nozzle section	P_m	No	No
	Nozzle wall	Pressure difference	General membrane	P_m	No	No
			Membrane	Q	Yes	No
			Bending	Q	Yes	No
			Peak	F	Yes	Yes
		Differential expansion	Membrane	Q	Yes	No
			Bending	Q	Yes	No
			Peak	F	Yes	Yes
Cladding	Any	Differential expansion	Membrane	F	Yes	Yes
			Bending	F	Yes	Yes
Any	Any	Radial thermal gradient through plate thickness(2)	Stress due to equivalent bending portion	Q(3)	Yes	No
			Stress due to nonlinear portion	F	Yes	Yes
Any	Any	Any	Stress concentration (notch effect)	F	Yes	Yes

NOTES:
(1) Consideration must also be given to the possibility of wrinkling and excessive deformation in shells with large diameter-to-thickness ratio
(2) Consider the possibility of thermal stress ratchet
(3) Equivalent linear stress is defined as the linear stress distribution which has the same net bending moment as the actual stress distribution

Table 6-2: Code Evaluation for Load Combination B-3

(a) with positive $[OBE^2 + SRV^2 + FIV^2]^{1/2}$

Component	P_m (ksi)	S_m (ksi)	P_m+P_b (ksi)		$1.5S_m$ (ksi)	P_m+P_b+Q (ksi)		$3S_m$ (ksi)
			Top	Bot		Top	Bot	
Outer Hoods	2.09	16.6	8.69	3.87	24.9	8.69	3.87	51.15
Middle Hoods	4.87	16.6	11.40	10.35	24.9	11.40	10.35	51.15
Inside Hoods	5.34	16.6	12.18	11.18	24.9	12.18	11.18	51.15
Gussets in Hoods	17.15	16.6	17.23	17.24	24.9	17.23	17.24	51.15
Side Plates	4.70	16.6	4.78	4.62	24.9	4.78	4.62	51.15
Vane Bank Base Plates	5.91	16.6	15.35	12.64	24.9	15.35	12.64	51.15
Vertical Plates in Vane Banks	6.34	16.6	8.06	5.82	24.9	8.06	5.82	51.15
Vane Banks	9.10	16.6	10.99	11.32	24.9	10.99	11.32	51.15
Drain Pipes	2.01	16.6	2.69	3.66	24.9	2.69	3.66	51.15
Skirt	2.10	16.6	4.37	6.19	24.9	4.37	6.19	51.15
Drain Channels	2.95	16.6	6.17	6.28	24.9	6.17	6.28	51.15
Upper Support Ring	8.93	16.6	8.93	8.93	24.9	8.93	8.93	51.15
Lower Support Ring	2.68	16.6	2.68	2.68	24.9	2.68	2.68	51.15
Tie Bars	14.05	16.6	14.05	14.05	24.9	14.05	14.05	51.15
Lifting Rods	6.04	16.6	5.66	11.15	24.9	5.66	11.15	51.15
Gussets in Upper Support Ring	2.13	16.6	2.33	1.94	24.9	2.33	1.94	51.15

(b) with negative $[OBE^2 + SRV^2 + FIV^2]^{1/2}$

Component	P_m (ksi)	S_m (ksi)	P_m+P_b (ksi)		$1.5S_m$ (ksi)	P_m+P_b+Q (ksi)		$3S_m$ (ksi)
			Top	Bot		Top	Bot	
Outer Hoods	5.47	16.6	6.24	8.48	24.9	6.24	8.48	51.15
Middle Hoods	4.84	16.6	11.67	10.27	24.9	11.67	10.27	51.15
Inside Hoods	5.29	16.6	12.89	10.96	24.9	12.89	10.96	51.15
Gussets in Hoods	14.03	16.6	14.33	13.74	24.9	14.33	13.74	51.15
Side Plates	10.16	16.6	11.65	9.22	24.9	11.65	9.22	51.15
Vane Bank Base Plates	3.36	16.6	12.16	15.84	24.9	12.16	15.84	51.15
Vertical Plates in Vane Banks	5.36	16.6	6.34	5.09	24.9	6.34	5.09	51.15
Vane Banks	13.14	16.6	13.16	13.13	24.9	13.16	13.13	51.15
Drain Pipes	1.26	16.6	2.82	2.45	24.9	2.82	2.45	51.15
Skirt	2.12	16.6	5.94	3.69	24.9	5.94	3.69	51.15
Drain Channels	2.91	16.6	6.30	6.04	24.9	6.30	6.04	51.15
Upper Support Ring	11.93	16.6	11.93	11.93	24.9	11.93	11.93	51.15
Lower Support Ring	2.13	16.6	2.13	2.13	24.9	2.13	2.13	51.15
Tie Bars	12.52	16.6	12.52	12.52	24.9	12.52	12.52	51.15
Lifting Rods	6.30	16.6	6.24	10.17	24.9	6.24	10.17	51.15
Gussets in Upper Support Ring	2.94	16.6	2.50	3.50	24.9	2.50	3.50	51.15

Table 6-3: Linearized Stresses at Gusset Section across the Maximum Stress Location for Load Combination Case B-3

Surface	P_m (ksi)	P_b (ksi)	P_m+P_b (ksi)
Top	6.53	3.53	10.06
Mid	6.51	3.60	10.12
Bot	6.50	3.67	10.17

Table 6-4: Code Evaluation for Load Combination D-1

(a) with positive $[SSE^2 + AP^2 + FIV^2]^{1/2}$

Component	P_m (ksi)	Min($2.4S_m$,$0.7S_u$) (ksi)	P_m+P_b (ksi)		1.5 P_m Limit (ksi)
			Top	Bottom	
Outer Hoods	9.41	39.84	15.60	12.68	59.07
Middle Hoods	34.91	39.84	78.26	69.22	59.07
Inside Hoods	37.95	39.84	85.47	75.14	59.07
Gussets in Hoods	118.11	39.84	119.12	119.30	59.07
Side Plates	28.34	39.84	32.66	25.34	59.07
Vane Bank Base Plates	38.69	39.84	72.09	66.74	59.07
Vertical Plates in Vane Bank	37.28	39.84	47.58	37.24	59.07
Vane Banks	32.22	39.84	62.44	63.34	59.07
Drain Pipes	9.31	39.84	17.30	15.95	59.07
Skirt	9.91	39.84	25.62	31.86	59.07
Drain Channels	17.48	39.84	7.49	16.62	59.07
Upper Support Ring	34.16	39.84	34.16	34.16	59.07
Lower Support Ring	6.46	39.84	6.46	6.46	59.07
Tie Bars	77.73	39.84	77.73	77.73	59.07
Lifting Rods	13.48	39.84	17.03	31.90	59.07
Gussets in Upper Support Ring	12.90	39.84	14.20	11.66	59.07

(b) with negative $[SSE^2 + AP^2 + FIV^2]^{1/2}$

Component	P_m (ksi)	Min($2.4S_m$,$0.7S_u$) (ksi)	P_m+P_b (ksi)		1.5 P_m Limit (ksi)
			Top	Bottom	
Outer Hoods	9.38	39.84	19.62	13.94	59.07
Middle Hoods	34.36	39.84	78.89	69.06	59.07
Inside Hoods	37.73	39.84	87.15	74.56	59.07
Gussets in Hoods	108.07	39.84	108.39	108.47	59.07
Side Plates	16.19	39.84	21.02	22.40	59.07
Vane Bank Base Plates	32.58	39.84	62.83	62.69	59.07
Vertical Plates in Vane Bank	35.85	39.84	43.35	36.83	59.07
Vane Banks	30.59	39.84	63.12	56.22	59.07
Drain Pipes	8.05	39.84	17.84	12.56	59.07
Skirt	8.55	39.84	29.94	22.12	59.07
Drain Channels	7.38	39.84	20.62	16.24	59.07
Upper Support Ring	22.11	39.84	22.11	22.11	59.07
Lower Support Ring	7.40	39.84	7.40	7.40	59.07
Tie Bars	77.11	39.84	77.11	77.11	59.07
Lifting Rods	14.50	39.84	23.56	17.88	59.07
Gussets in Upper Support Ring	14.64	39.84	12.76	16.98	59.07

Table 6-5: Code Interpreted Stresses at the Maximum Stress Location for Level D

(a) with positive $[SSE^2 + AP^2 + FIV^2]^{1/2}$

Component	Location	P_m (ksi)	Allowable (ksi)	P_m+P_b (ksi)	Allowable (ksi)
Middle Hood(1)	n/a	34.91	39.84	34.91	59.07
Inside Hood(1)	n/a	37.95	39.84	37.95	59.07
Gusset in Hoods(2)	Top	46.14	39.84	65.86	59.07
	Mid	46.21	39.84	65.96	59.07
	Bot	46.28	39.84	66.08	59.07
Vane Banks Base Plate(1)	n/a	38.69	39.84	38.69	59.07
Vane Banks(1)	n/a	32.22	39.84	32.22	59.07
Tie Bars(2)	Vertical	32.18	39.84	62.58	59.07
	Horizontal	27.98	39.84	63.07	59.07
	Diagonal	15.13	39.84	46.79	59.07

(b) with negative $[SSE^2 + AP^2 + FIV^2]^{1/2}$

Component	Location	P_m (ksi)	Allowable (ksi)	P_m+P_b (ksi)	Allowable (ksi)
Middle Hood(1)	n/a	34.36	39.84	34.36	59.07
Inside Hood(1)	n/a	37.73	39.84	37.73	59.07
Gusset in Hoods(2)	Top	40.80	39.84	55.97	59.07
	Mid	40.81	39.84	56.24	59.07
	Bot	40.81	39.84	56.49	59.07
Vane Banks Base Plate(1)	n/a	32.58	39.84	32.58	59.07
Vane Banks(1)	n/a	30.59	39.84	29.09	59.07
Tie Bars(2)	Vertical	8.81	39.84	41.80	59.07
	Horizontal	31.67	39.84	72.23	59.07
	Diagonal	12.78	39.84	38.29	59.07

Note:
(1) Bending stress is classified as Secondary Stress per NG-3213.9 and Table NG-3217-1.
(2) Linearized stress through maximum stress location is used.

Table 6-6: Comparison of Maximum Stress (ksi) Results due to Model Modification

Load Case	Shell Surface	Before Model Modification	After Model Modification	% Difference
Unit Pressure	Top	16.28	16.36	0.49
	Mid	16.28	15.53	-4.61
	Bottom	16.28	15.51	-4.73
X-direction Unit Acceleration	Top	10.36	11.77	13.61
	Mid	8.29	11.76	41.86
	Bottom	9.93	11.75	18.33
Y-direction Unit Acceleration	Top	25.99	22.25	-14.36
	Mid	16.73	15.58	-6.87
	Bottom	26.85	23.01	-14.30
Z-direction Unit Acceleration	Top	6.81	8.36	22.76
	Mid	6.09	7.20	18.23
	Bottom	6.23	6.03	-3.21

Table 6-7: Modified Code Stress Evaluation for Load Combination B-3
(a) with positive $[OBE^2 + SRV^2 + FIV^2]^{1/2}$

Component	P_m (ksi)	S_m (ksi)	P_m+P_b (ksi)		$1.5S_m$ (ksi)	P_m+P_b+Q (ksi)		$3S_m$ (ksi)
			Top	Bot		Top	Bot	
Outer Hoods	2.22	16.6	9.21	4.10	24.9	9.21	4.10	51.15
Middle Hoods	5.16	16.6	12.08	10.97	24.9	12.08	10.97	51.15
Inside Hoods	5.66	16.6	12.91	11.85	24.9	12.91	11.85	51.15
Gussets in Hoods	18.18	16.6	18.26	18.27	24.9	18.26	18.27	51.15
Side Plates	4.98	16.6	5.07	4.90	24.9	5.07	4.90	51.15
Vane Bank Base Plates	6.26	16.6	16.27	13.40	24.9	16.27	13.40	51.15
Vertical Plates in Vane Banks	6.72	16.6	8.54	6.17	24.9	8.54	6.17	51.15
Vane Banks	9.65	16.6	11.65	12.00	24.9	11.65	12.00	51.15
Drain Pipes	2.13	16.6	2.85	3.88	24.9	2.85	3.88	51.15
Skirt	2.23	16.6	4.63	6.56	24.9	4.63	6.56	51.15
Drain Channels	3.13	16.6	6.54	6.66	24.9	6.54	6.66	51.15
Upper Support Ring	9.47	16.6	9.47	9.47	24.9	9.47	9.47	51.15
Lower Support Ring	2.84	16.6	2.84	2.84	24.9	2.84	2.84	51.15
Tie Bars	14.89	16.6	14.89	14.89	24.9	14.89	14.89	51.15
Lifting Rods	6.40	16.6	6.00	11.82	24.9	6.00	11.82	51.15
Gussets in Upper Support Ring	2.26	16.6	2.47	2.06	24.9	2.47	2.06	51.15

(b) with negative $[OBE^2 + SRV^2 + FIV^2]^{1/2}$

Component	P_m (ksi)	S_m (ksi)	P_m+P_b (ksi)		$1.5S_m$ (ksi)	P_m+P_b+Q (ksi)		$3S_m$ (ksi)
			Top	Bot		Top	Bot	
Outer Hoods	5.80	16.6	6.61	8.98	24.9	6.61	8.98	51.15
Middle Hoods	5.13	16.6	12.37	10.89	24.9	12.37	10.89	51.15
Inside Hoods	5.61	16.6	13.66	11.62	24.9	13.66	11.62	51.15
Gussets in Hoods	14.87	16.6	15.19	14.56	24.9	15.19	14.56	51.15
Side Plates	10.77	16.6	12.35	9.77	24.9	12.35	9.77	51.15
Vane Bank Base Plates	3.56	16.6	12.89	16.79	24.9	12.89	16.79	51.15
Vertical Plates in Vane Banks	5.31	16.6	6.54	5.30	24.9	6.54	5.30	51.15
Vane Banks	13.93	16.6	13.95	13.92	24.9	13.95	13.92	51.15
Drain Pipes	1.34	16.6	2.99	2.60	24.9	2.99	2.60	51.15
Skirt	2.25	16.6	6.30	3.91	24.9	6.30	3.91	51.15
Drain Channels	3.08	16.6	6.68	6.40	24.9	6.68	6.40	51.15
Upper Support Ring	12.65	16.6	12.65	12.65	24.9	12.65	12.65	51.15
Lower Support Ring	2.26	16.6	2.26	2.26	24.9	2.26	2.26	51.15
Tie Bars	13.27	16.6	13.27	13.27	24.9	13.27	13.27	51.15
Lifting Rods	6.68	16.6	6.61	10.78	24.9	6.61	10.78	51.15
Gussets in Upper Support Ring	3.12	16.6	2.65	3.71	24.9	2.65	3.71	51.15

Table 6-8: Modified Linearized Stresses at Gusset Section across the Maximum Stress Location for Load Combination Case B-3

Surface	P_m (ksi)	P_b (ksi)	P_m+P_b (ksi)
Top	6.92	3.74	10.66
Mid	6.90	3.82	10.73
Bot	6.89	3.89	10.78

Table 6-9: Modified Code Stress Evaluation for Load Combination D-1
(a) with positive $[SSE^2 + AP^2 + FIV^2]^{1/2}$

Component	P_m (ksi)	Min($2.4S_m$,$0.7S_u$) (ksi)	P_m+P_b (ksi)		1.5 P_m Limit (ksi)
			Top	Bottom	
Outer Hoods	9.97	39.84	16.54	13.44	59.07
Middle Hoods	37.00	39.84	82.96	73.37	59.07
Inside Hoods	40.23	39.84	90.60	79.65	59.07
Gussets in Hoods	125.20	39.84	126.27	126.46	59.07
Side Plates	30.04	39.84	34.62	26.86	59.07
Vane Bank Base Plates	41.01	39.84	76.42	70.74	59.07
Vertical Plates in Vane Bank	39.52	39.84	50.43	39.47	59.07
Vane Banks	34.15	39.84	66.19	67.14	59.07
Drain Pipes	9.87	39.84	18.34	16.91	59.07
Skirt	10.50	39.84	27.16	33.77	59.07
Drain Channels	7.94	39.84	18.53	17.62	59.07
Upper Support Ring	36.21	39.84	36.21	36.21	59.07
Lower Support Ring	6.85	39.84	6.85	6.85	59.07
Tie Bars	82.39	39.84	82.39	82.39	59.07
Lifting Rods	14.29	39.84	18.05	33.81	59.07
Gussets in Upper Support Ring	13.67	39.84	15.05	12.36	59.07

(b) with negative $[SSE^2 + AP^2 + FIV^2]^{1/2}$

Component	P_m (ksi)	Min($2.4S_m$,$0.7S_u$) (ksi)	P_m+P_b (ksi)		1.5 P_m Limit (ksi)
			Top	Bottom	
Outer Hoods	9.94	39.84	20.80	14.78	59.07
Middle Hoods	36.42	39.84	83.62	73.20	59.07
Inside Hoods	39.99	39.84	92.38	79.03	59.07
Gussets in Hoods	114.55	39.84	114.89	114.98	59.07
Side Plates	17.16	39.84	22.28	23.74	59.07
Vane Bank Base Plates	34.53	39.84	66.60	66.45	59.07
Vertical Plates in Vane Bank	38.00	39.84	45.95	39.04	59.07
Vane Banks	32.43	39.84	66.91	59.59	59.07
Drain Pipes	8.53	39.84	18.91	13.31	59.07
Skirt	9.06	39.84	31.74	23.45	59.07
Drain Channels	7.82	39.84	21.86	17.21	59.07
Upper Support Ring	23.44	39.84	23.44	23.44	59.07
Lower Support Ring	7.84	39.84	7.84	7.84	59.07
Tie Bars	81.74	39.84	81.74	81.74	59.07
Lifting Rods	15.37	39.84	24.97	18.95	59.07
Gussets in Upper Support Ring	15.52	39.84	13.53	18.00	59.07

Table 6-10: Modified Code Interpreted Stresses at the Maximum Stress Location for Load Combination D-1

(a) with positive $[SSE^2 + AP^2 + FIV^2]^{1/2}$

Component	Location	P_m (ksi)	Allowable (ksi)	P_m+P_b (ksi)	Allowable (ksi)
Middle Hood(1)	n/a	37.00	39.84	37.00	59.07
Inside Hood(1)	n/a	40.23	39.84	40.23	59.07
Gusset in Hoods(2)	Top	48.91	39.84	69.81	59.07
	Mid	48.98	39.84	69.92	59.07
	Bot	49.06	39.84	70.04	59.07
Vane Banks Base Plate(1)	n/a	41.01	39.84	41.01	59.07
Vane Banks(1)	n/a	34.15	39.84	34.15	59.07
Tie Bars(2)	Vertical	25.12	39.84	66.25	59.07
	Horizontal	34.11	39.84	66.33	59.07
	Diagonal	16.04	39.84	49.60	59.07

(b) with negative $[SSE^2 + AP^2 + FIV^2]^{1/2}$

Component	Location	P_m (ksi)	Allowable (ksi)	P_m+P_b (ksi)	Allowable (ksi)
Middle Hood(1)	n/a	36.42	39.84	36.42	59.07
Inside Hood(1)	n/a	39.99	39.84	39.99	59.07
Gusset in Hoods(2)	Top	43.25	39.84	59.33	59.07
	Mid	43.27	39.84	59.61	59.07
	Bot	43.28	39.84	59.88	59.07
Vane Banks Base Plate(1)	n/a	34.54	39.84	34.53	59.07
Vane Banks(1)	n/a	30.84	39.84	30.84	59.07
Tie Bars(2)	Vertical	9.34	39.84	44.31	59.07
	Horizontal	33.57	39.84	76.56	59.07
	Diagonal	13.55	39.84	40.59	59.07

Note:
(1) Bending stress is classified as secondary stress per NG-3213.9 and Table NG-3217-1.
(2) Linearized stress through maximum stress location is used.

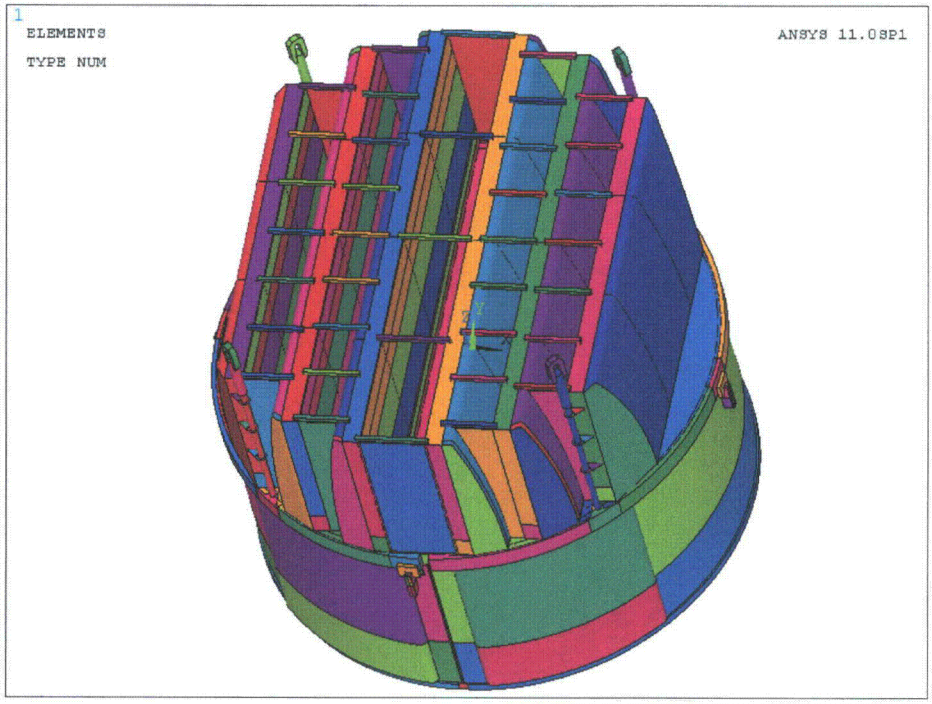

(a) without element edges

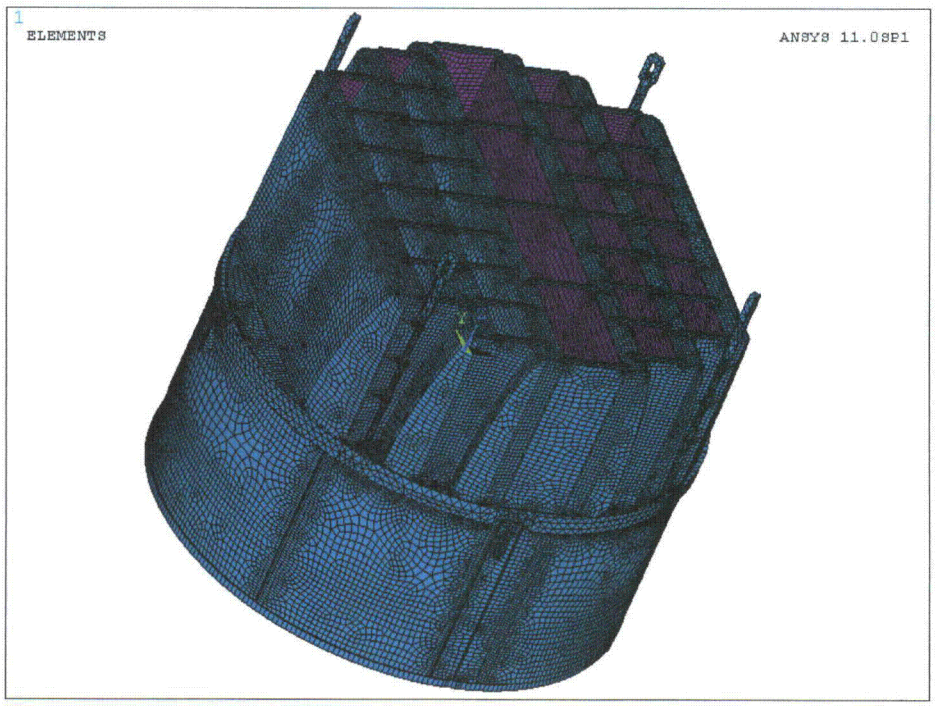

(b) with element edges

Figure 6-1: NMP2 Steam Dryer Model

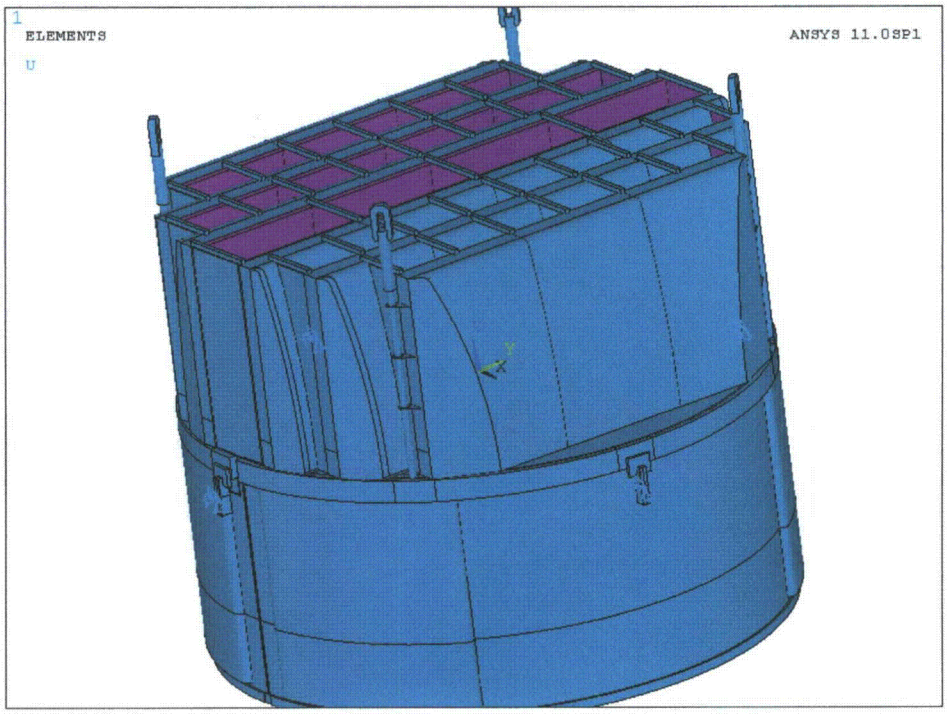

Figure 6-2: Steam Dryer Boundary Condition

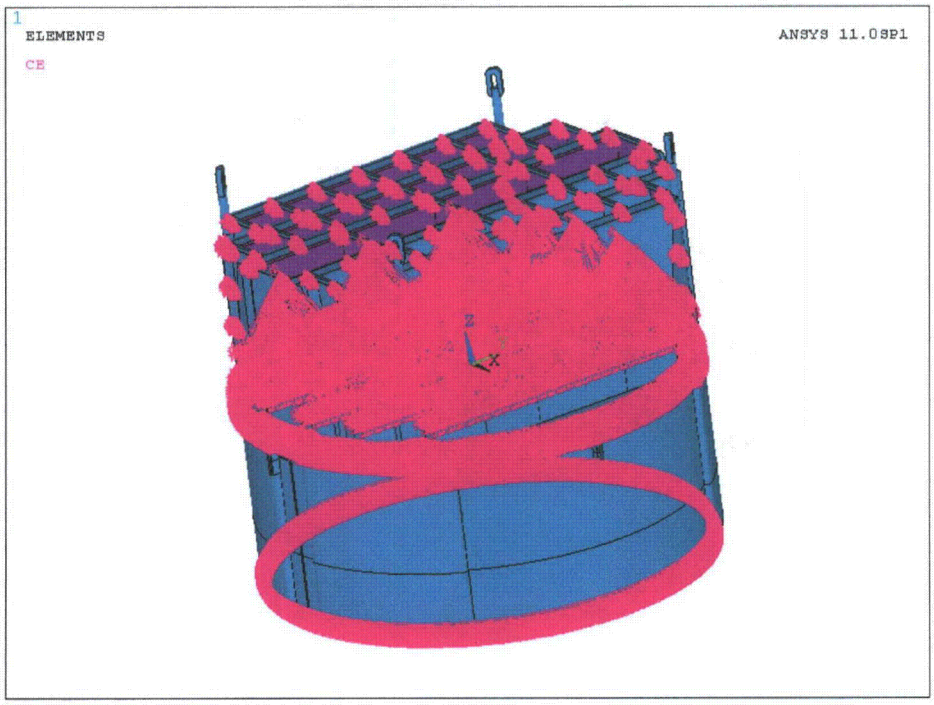

Figure 6-3: Constraint Equations

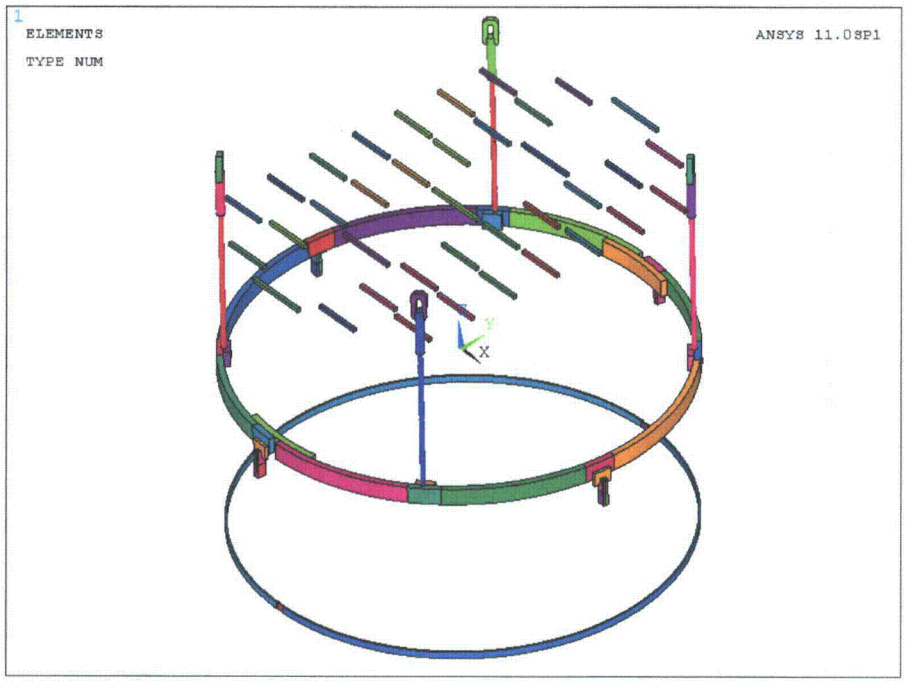

Figure 6-4: Solid Elements, Solid186 and Solid187

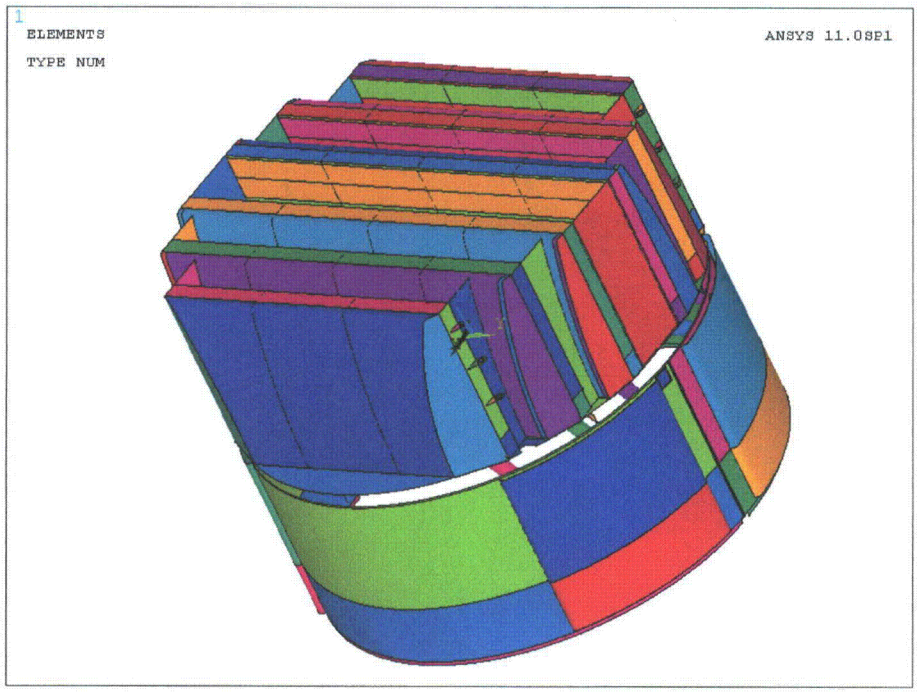

Figure 6-5: Shell Elements, Shell63

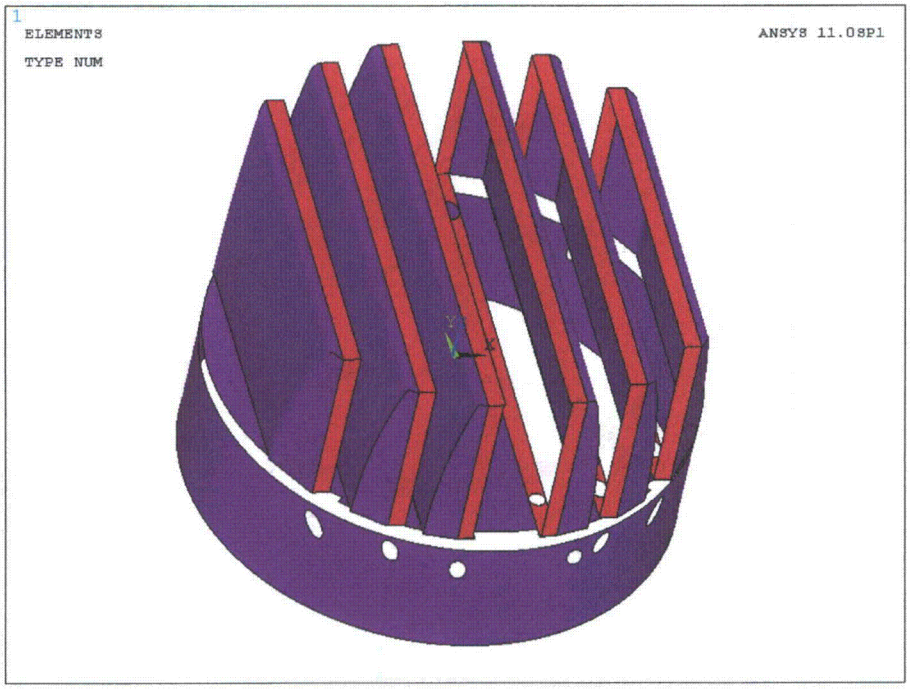

Figure 6-6: Surface Elements, Surf154

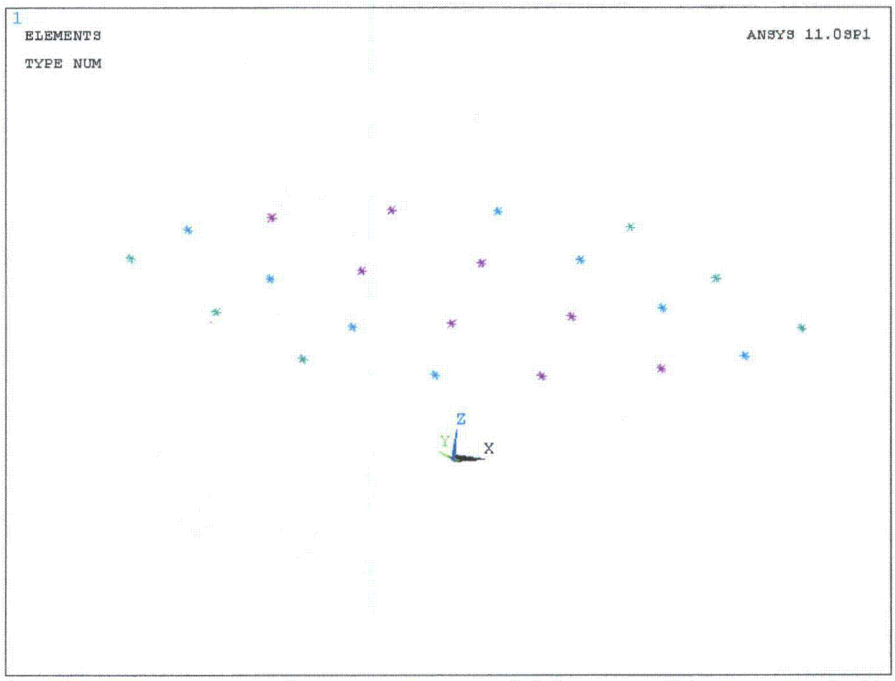

Figure 6-7: Mass Elements, Mass21

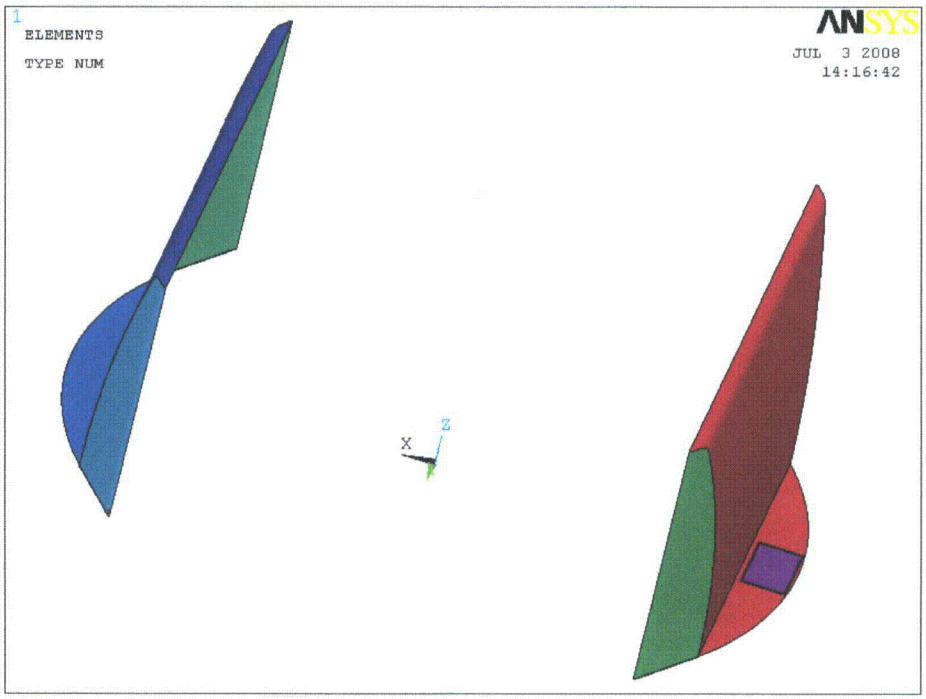

Figure 6-8: Outer Hood

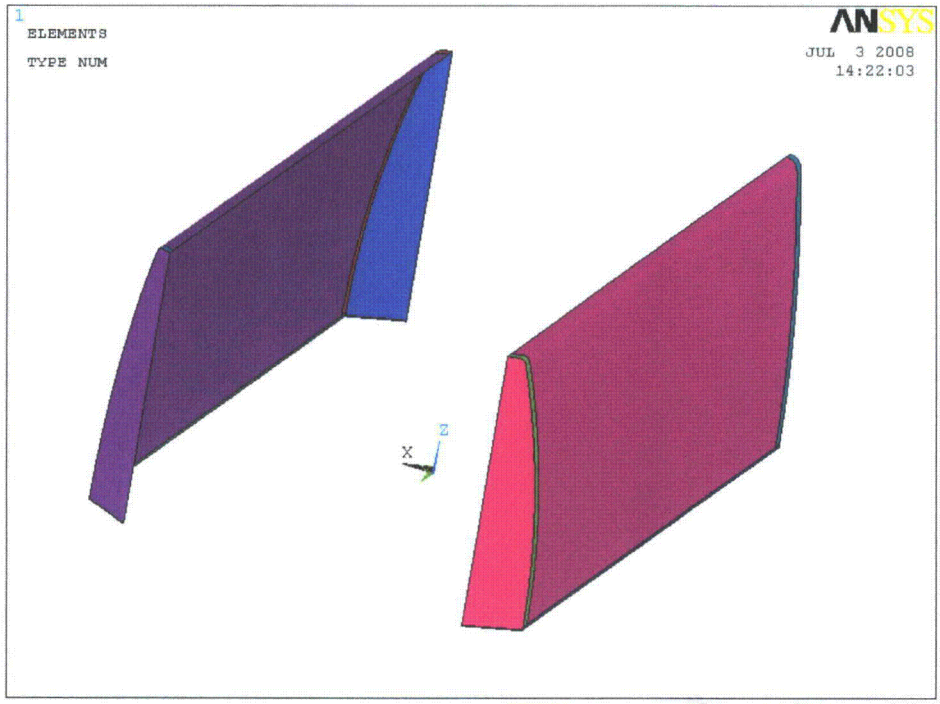

Figure 6-9: Middle Hood

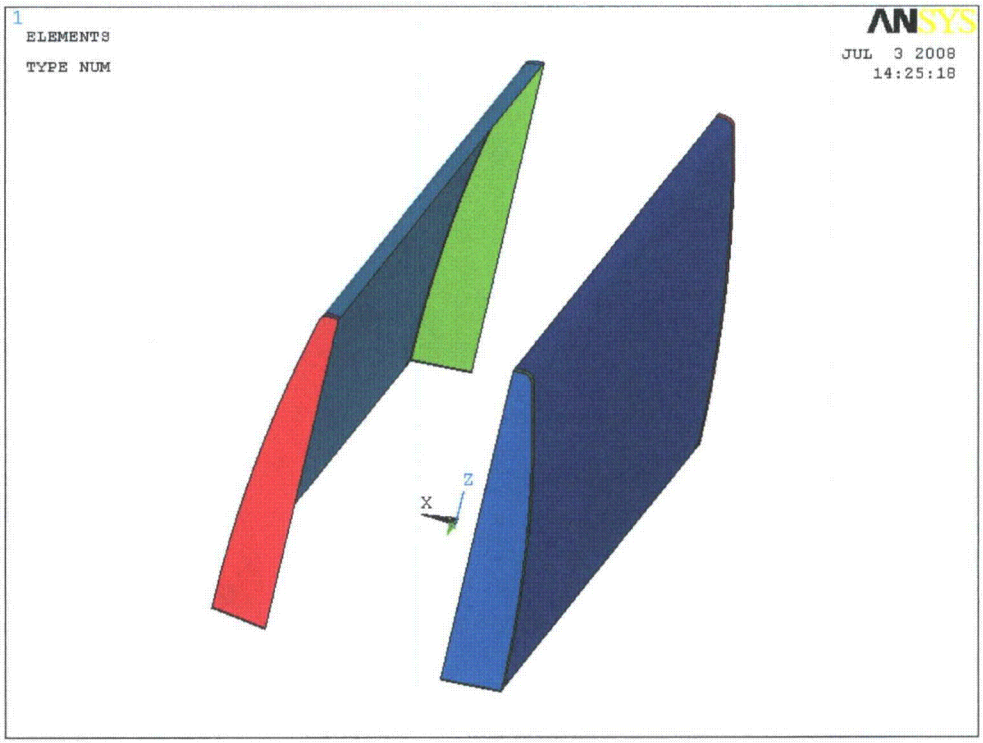

Figure 6-10: Inside Hood

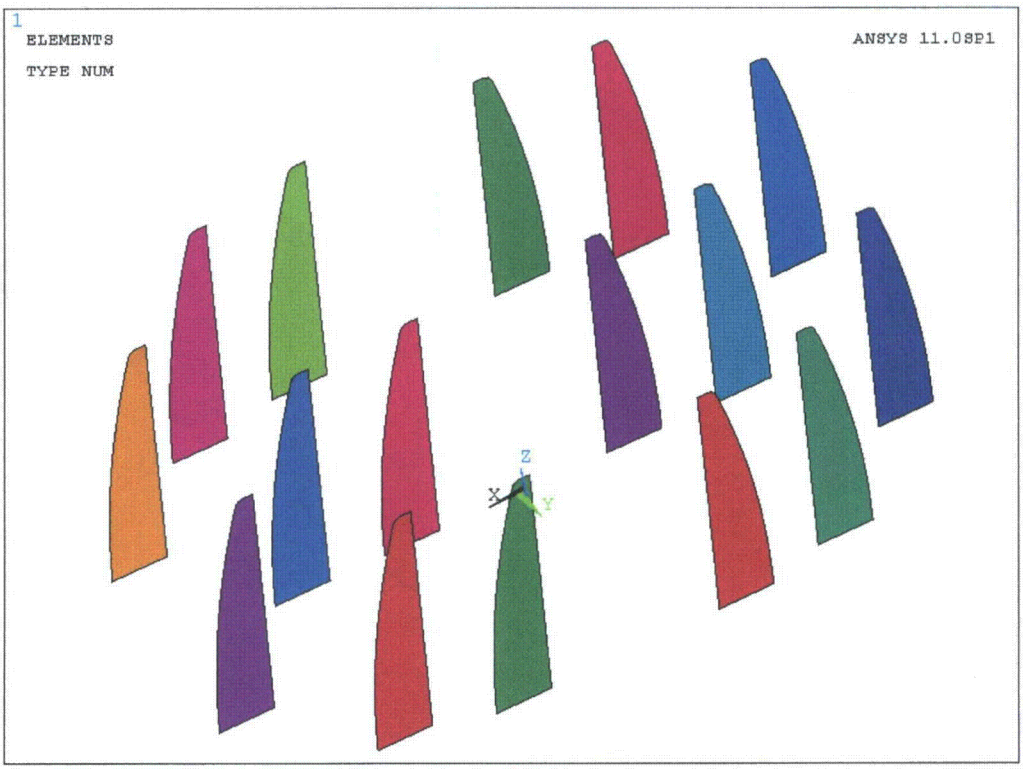

Figure 6-11: Gussets in Hoods

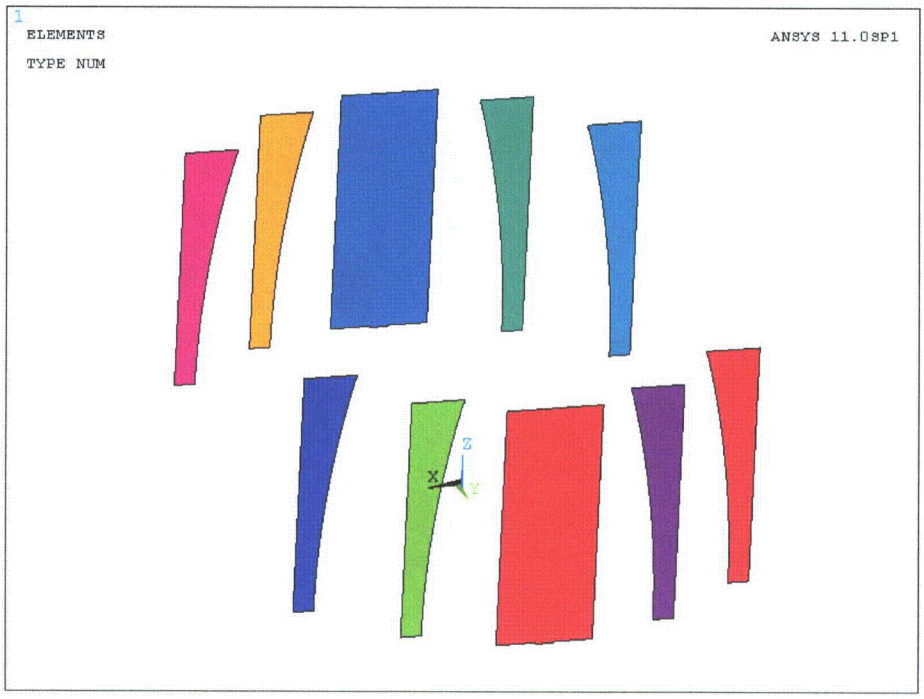

Figure 6-12: Side Plates

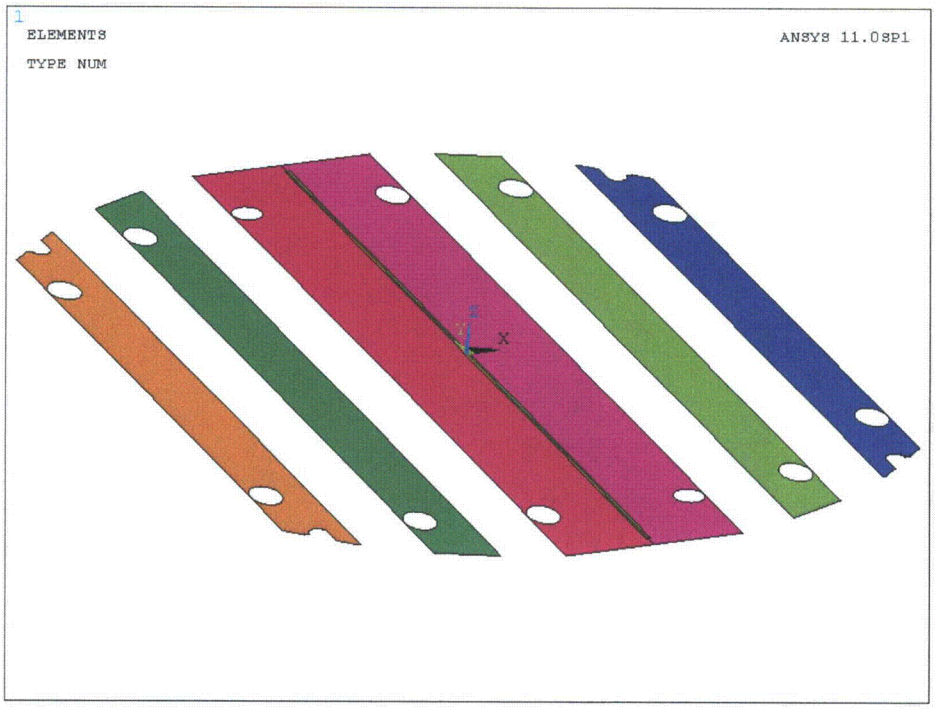

Figure 6-13: Vane Bank Base Plates

Figure 6-14: Vertical Plates Inside Vane Banks

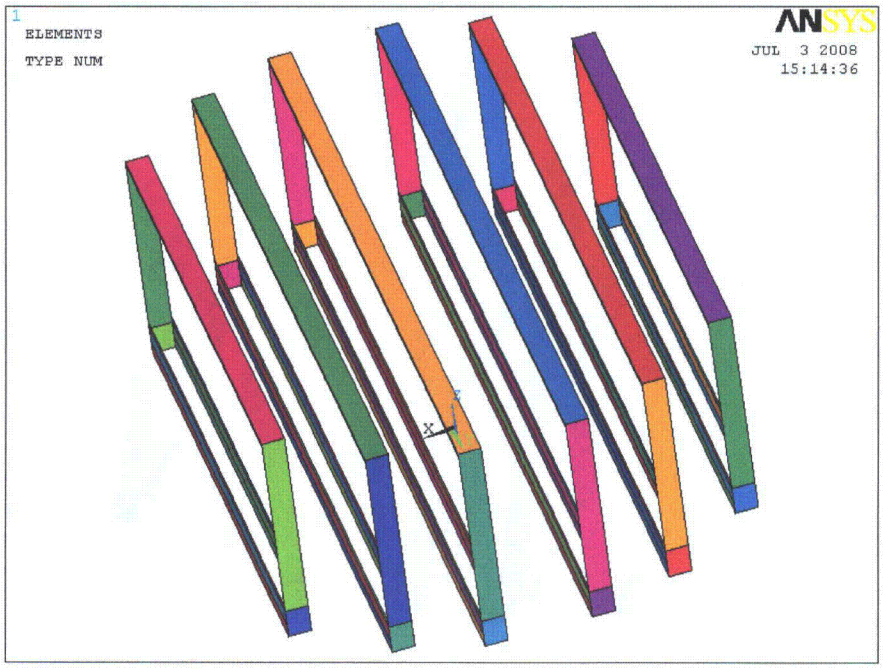

(a) Open View without Perforated Plates

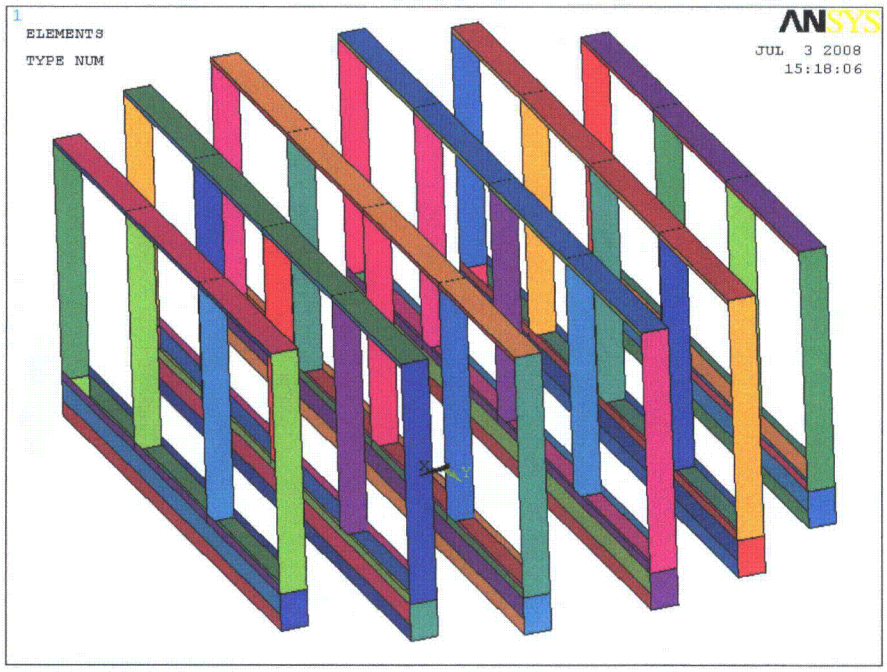

(b) Open View with Vertical Plates

Figure 6-15: Vane Banks

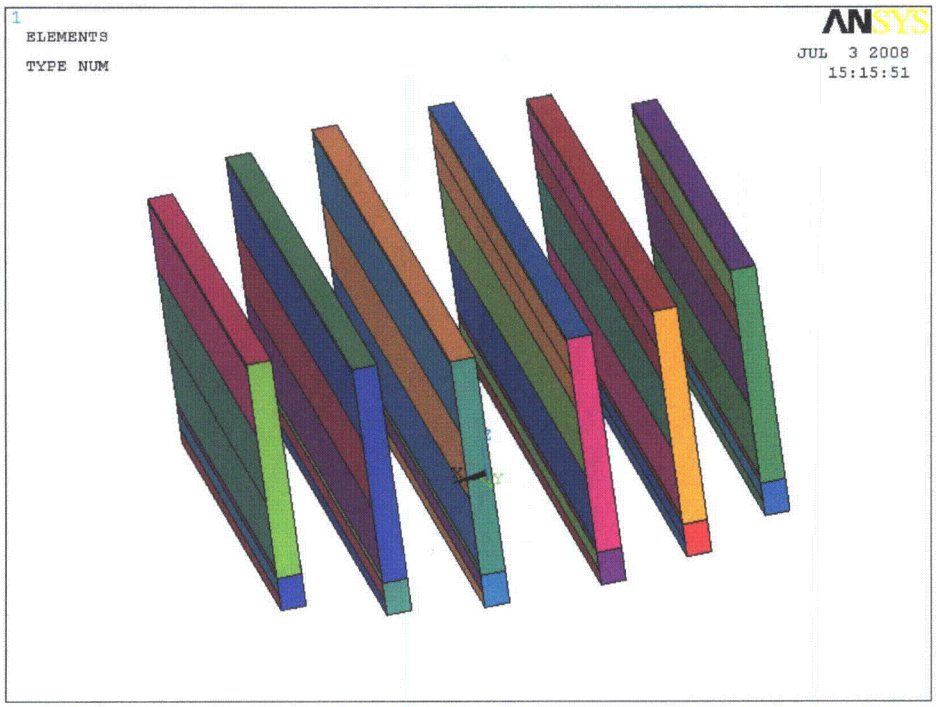

Figure 6-16: Vane Banks

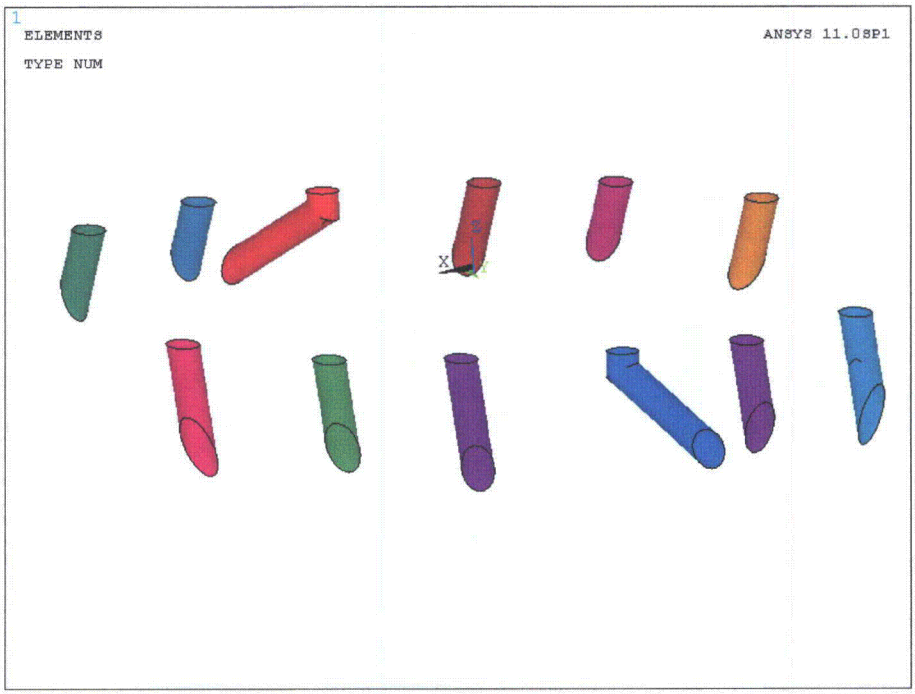

Figure 6-17: Drain Pipes

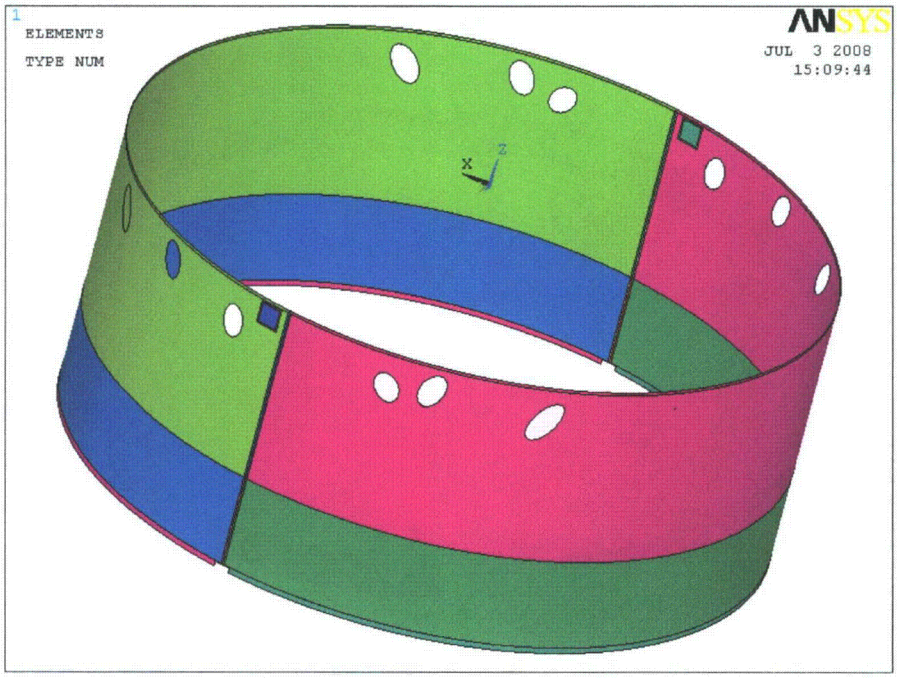

Figure 6-18: Skirt

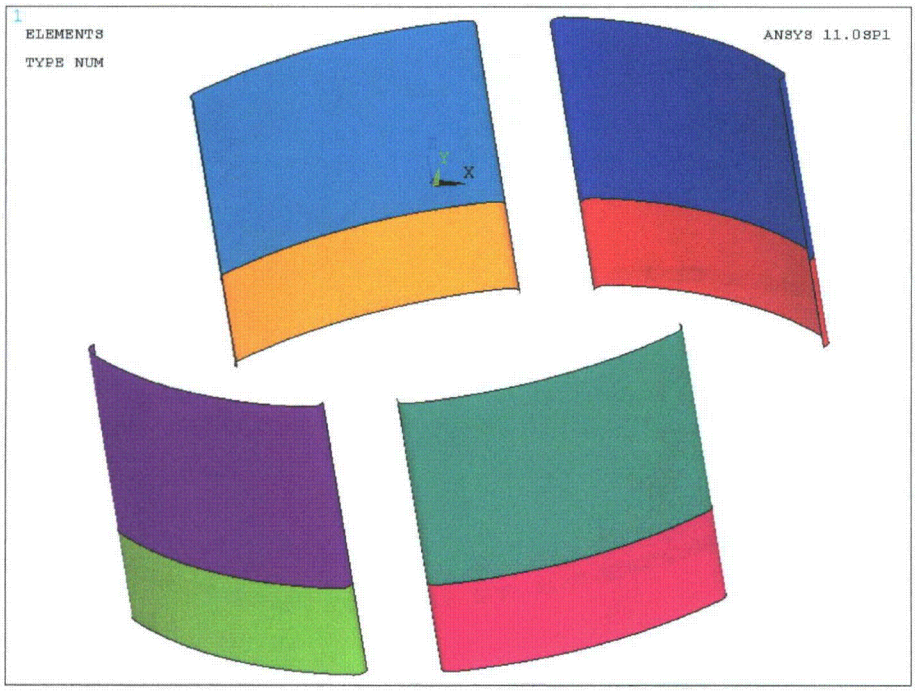

Figure 6-19: Drain Channels

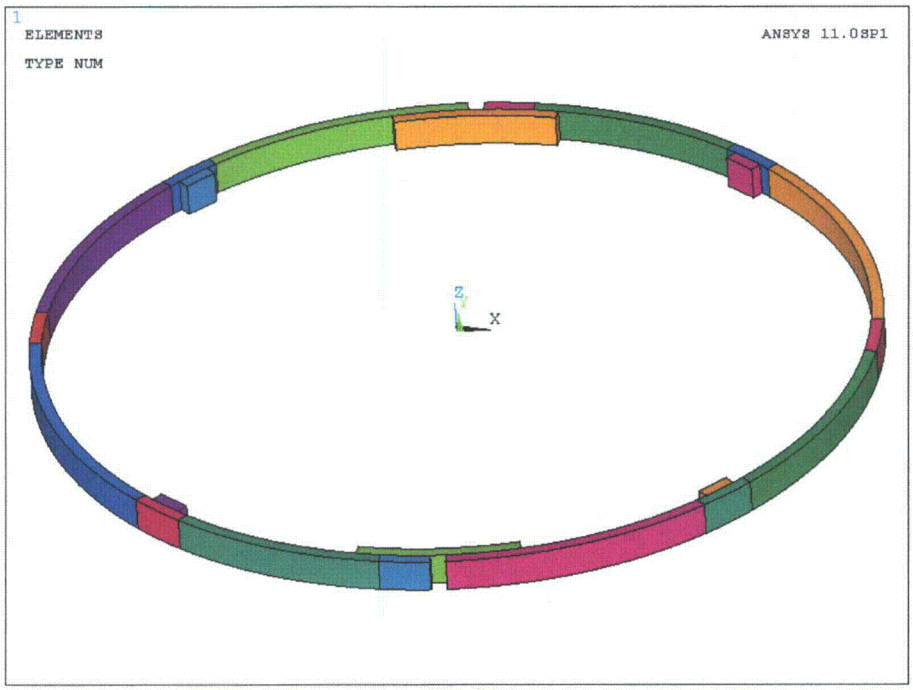

Figure 6-20: Upper Support Ring

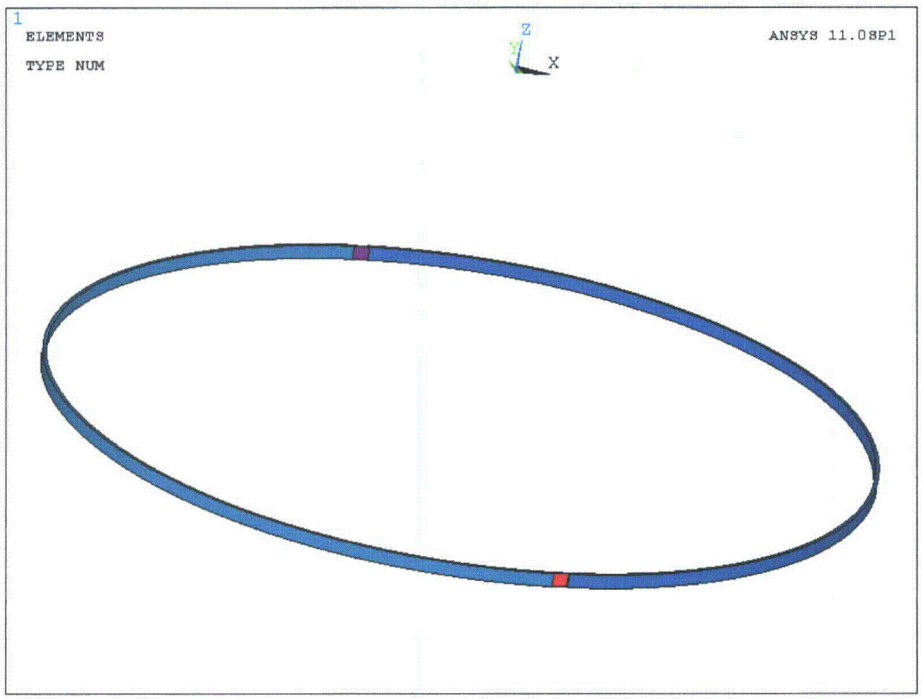

Figure 6-21: Lower Support Ring

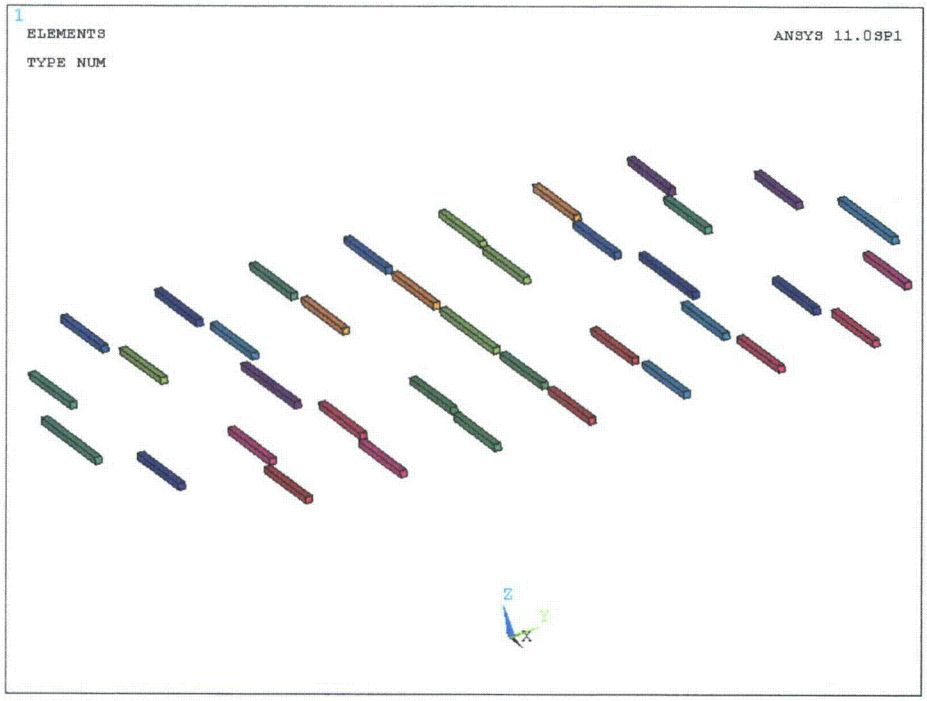

Figure 6-22: Tie Bars

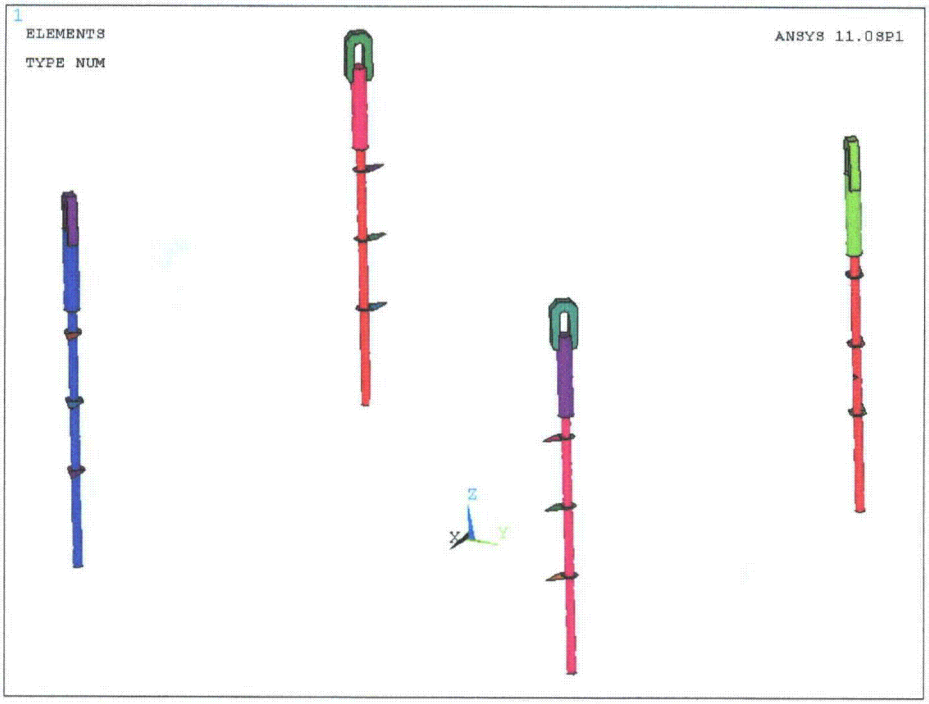

Figure 6-23: Lifting Rods

Figure 6-24: Gussets Between Upper Support Ring and Vane Bank Base Plates

Figure 6-25: Vessel Brackets and Support Plates

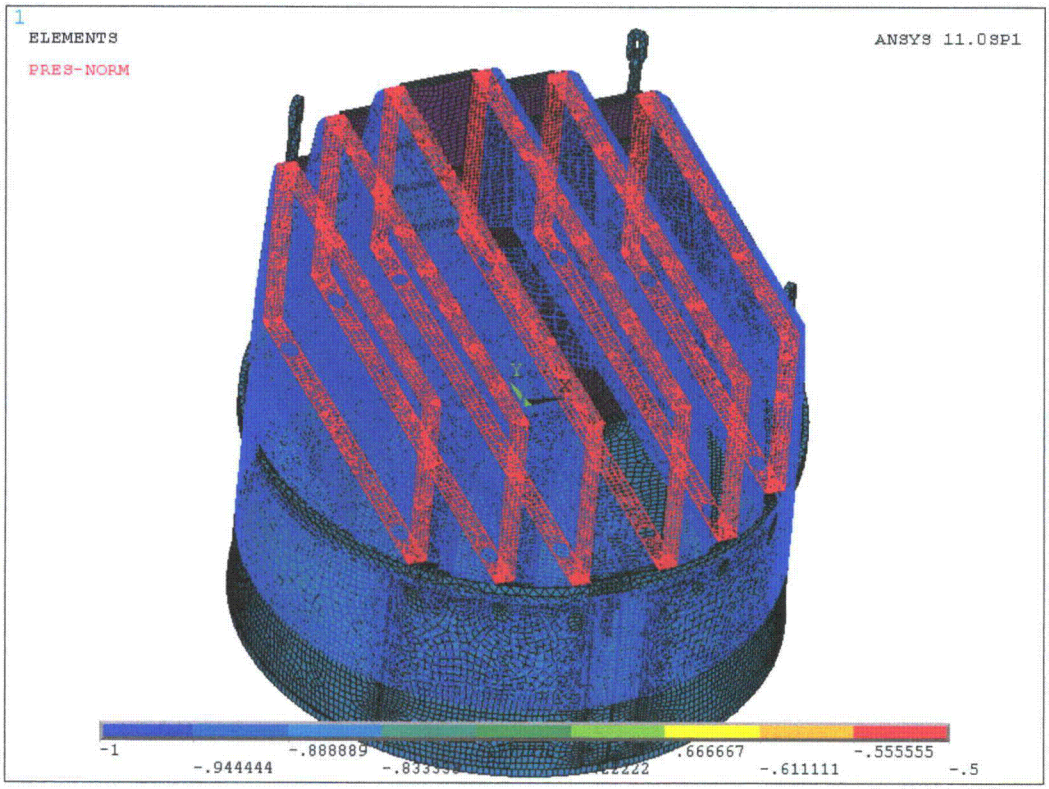

Figure 6-26: Pressure Loadings

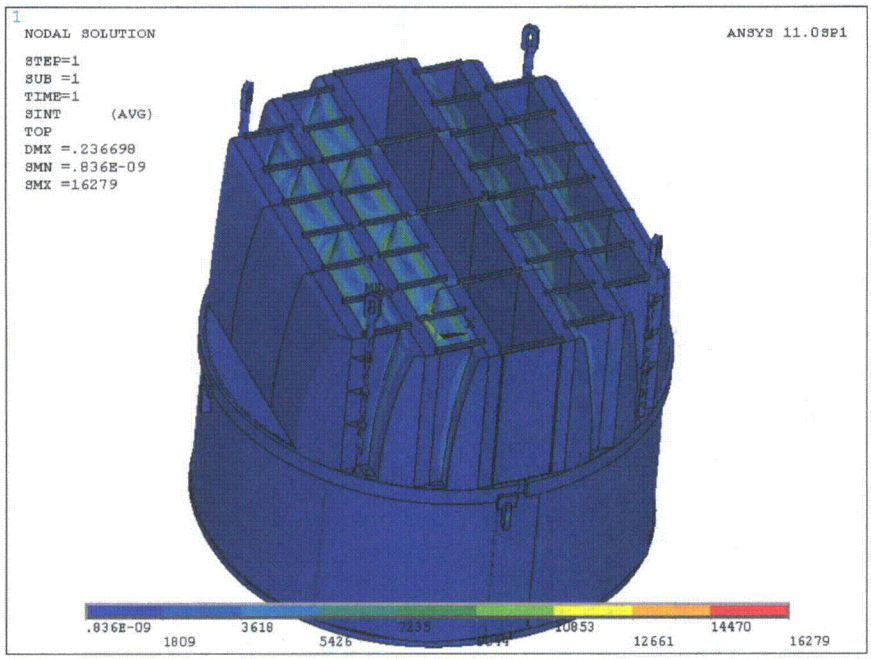

(a) Overall Distribution

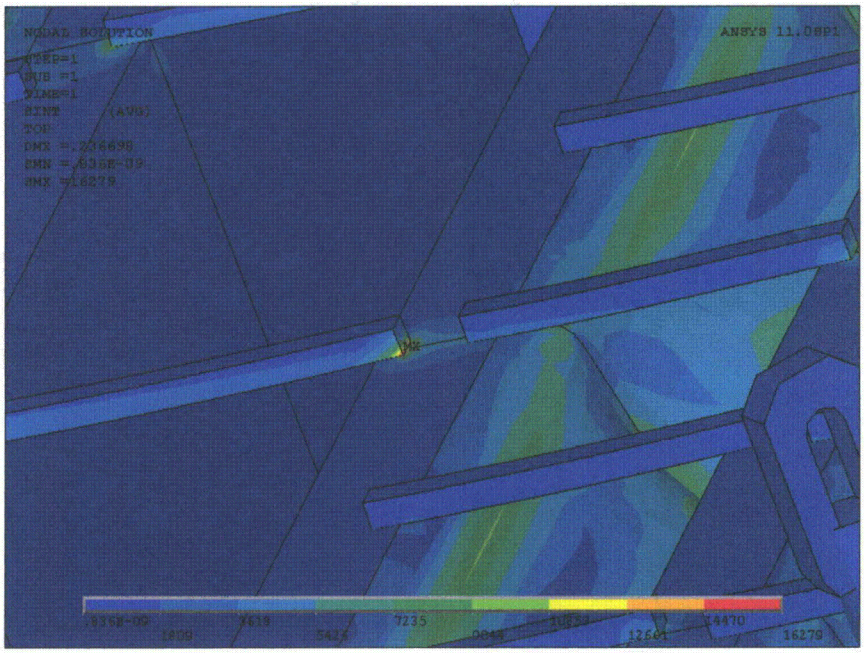

(b) Maximum Stress Location

Figure 6-27: Stress Intensity, Top Surface, due to Unit Pressure

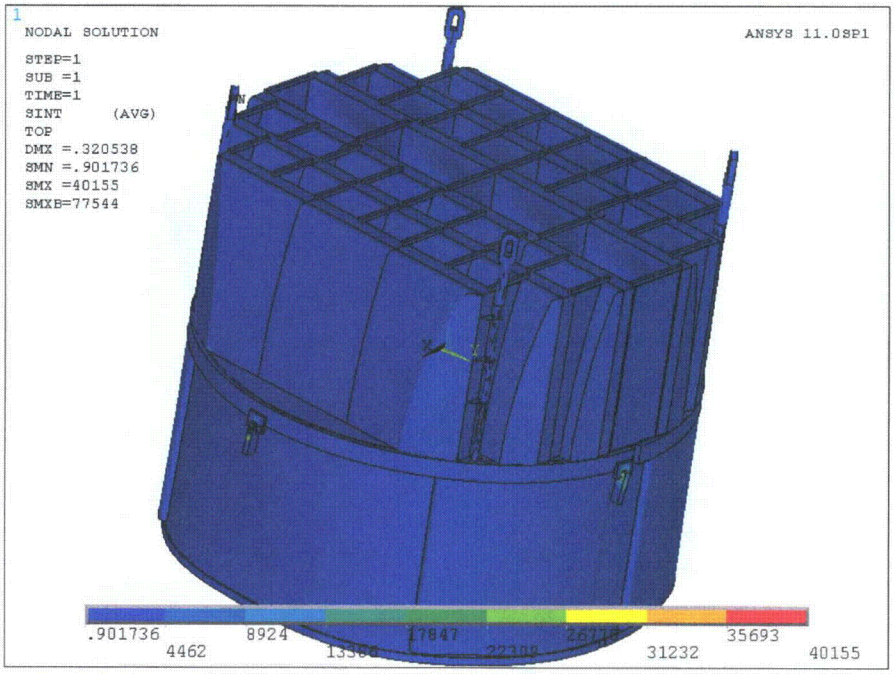

(a) Overall Distribution

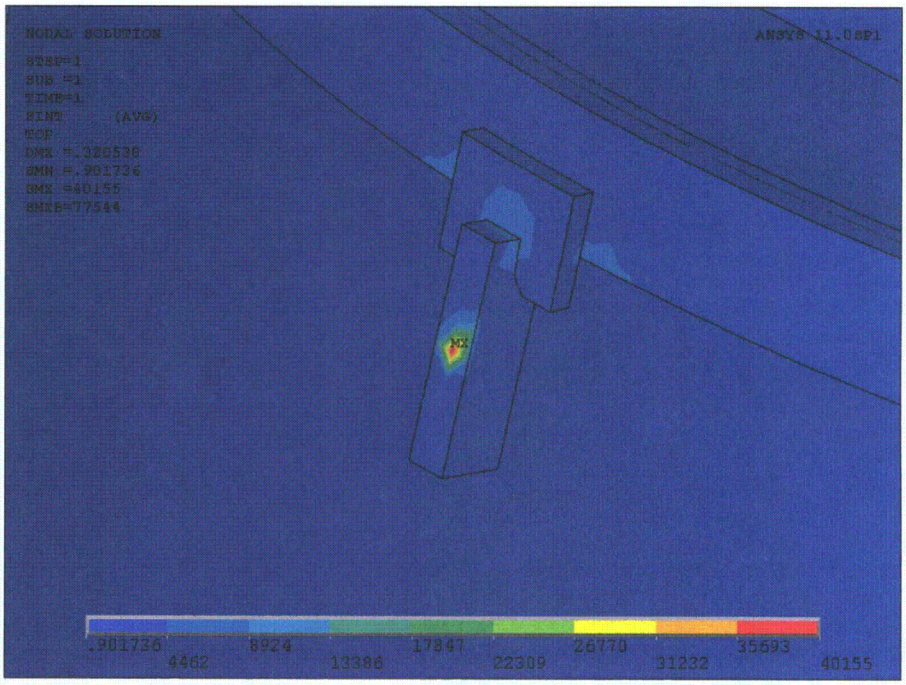

(b) Maximum Stress Location

Figure 6-28: Stress Intensity Distribution, Top Surface, 1 g Acceleration in X-direction

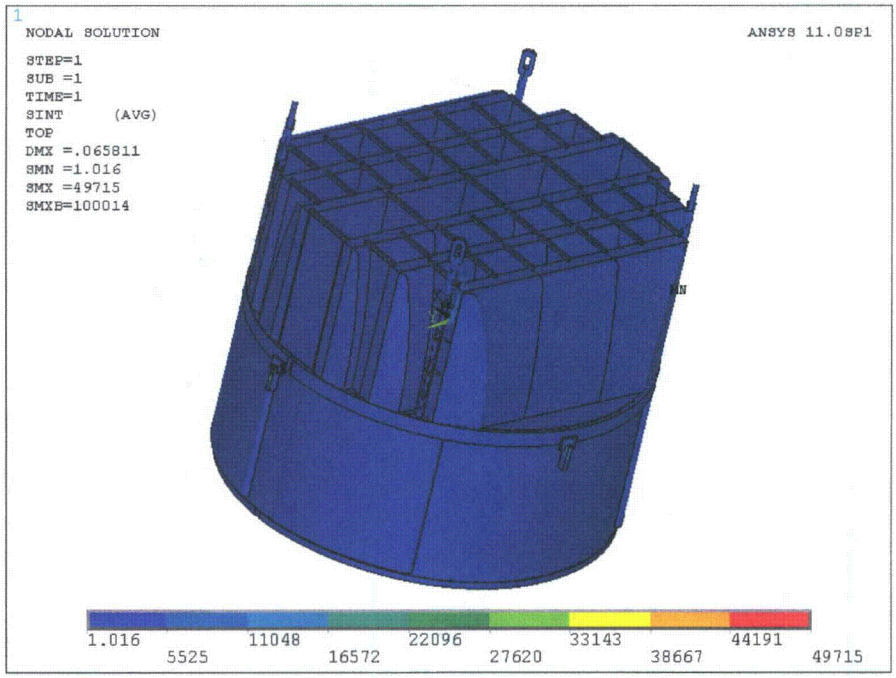

(a) Overall Distribution

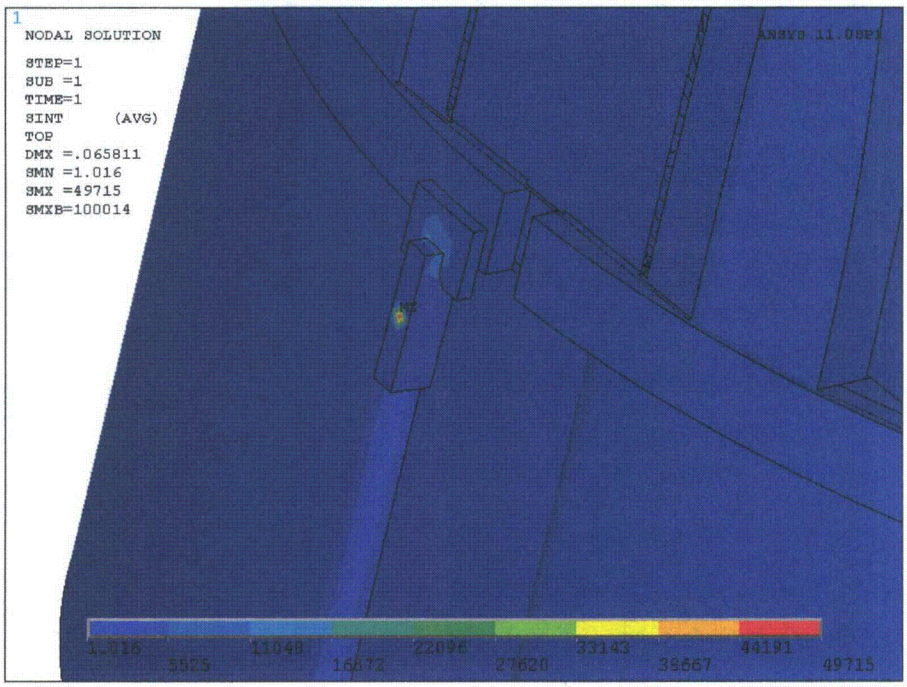

(b) Maximum Stress Location

Figure 6-29: Stress Intensity Distribution, Top Surface, 1 g Static Acceleration in Y-direction

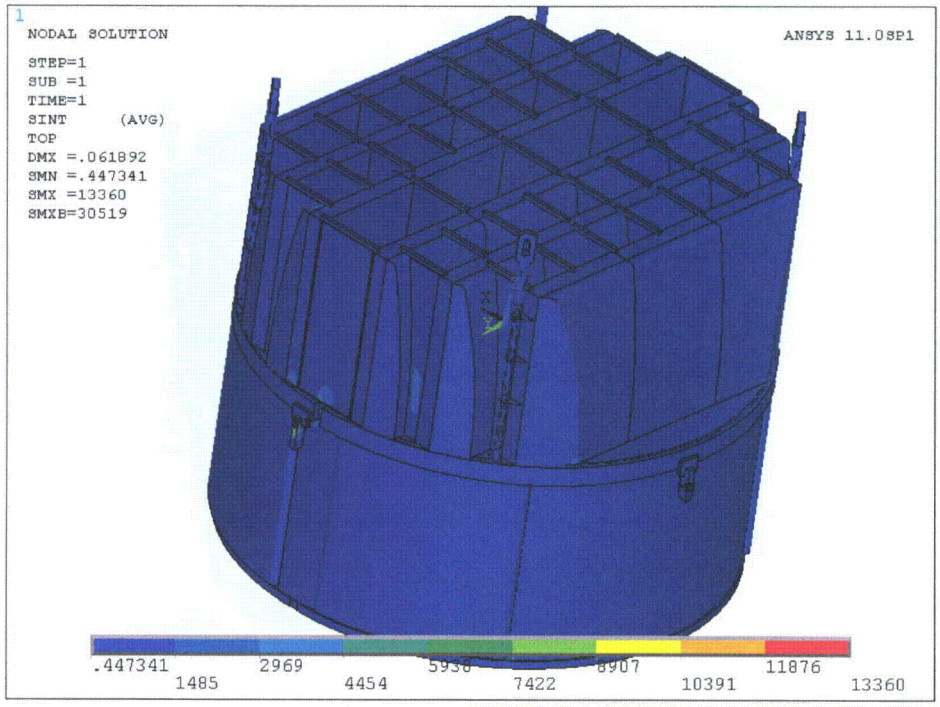

(a) Overall Distribution

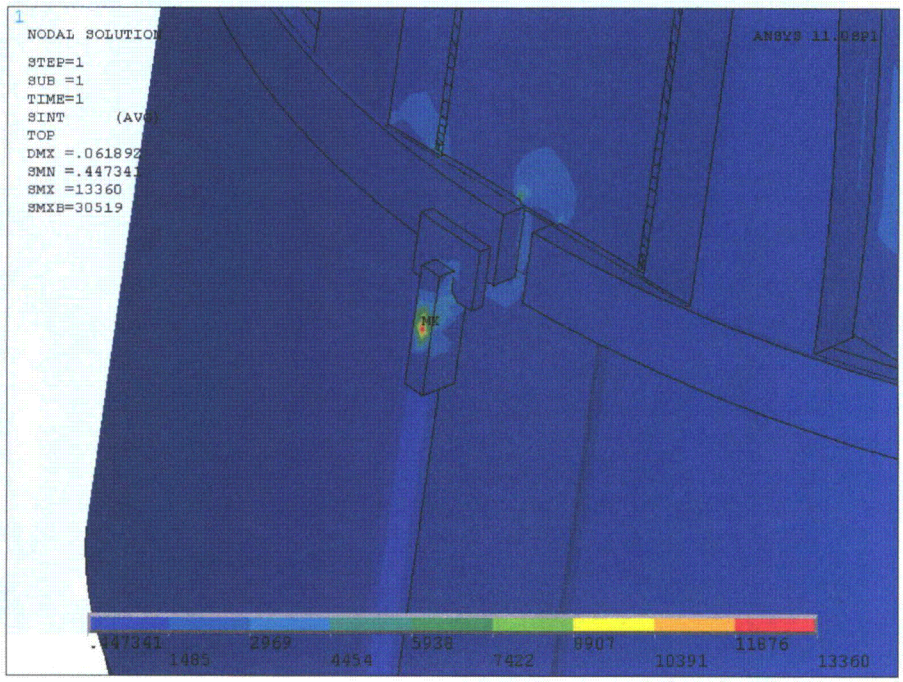

(b) Maximum Stress Location

Figure 6-30: Stress Intensity Distribution, Top Surface, 1 g Static Acceleration in Z-direction

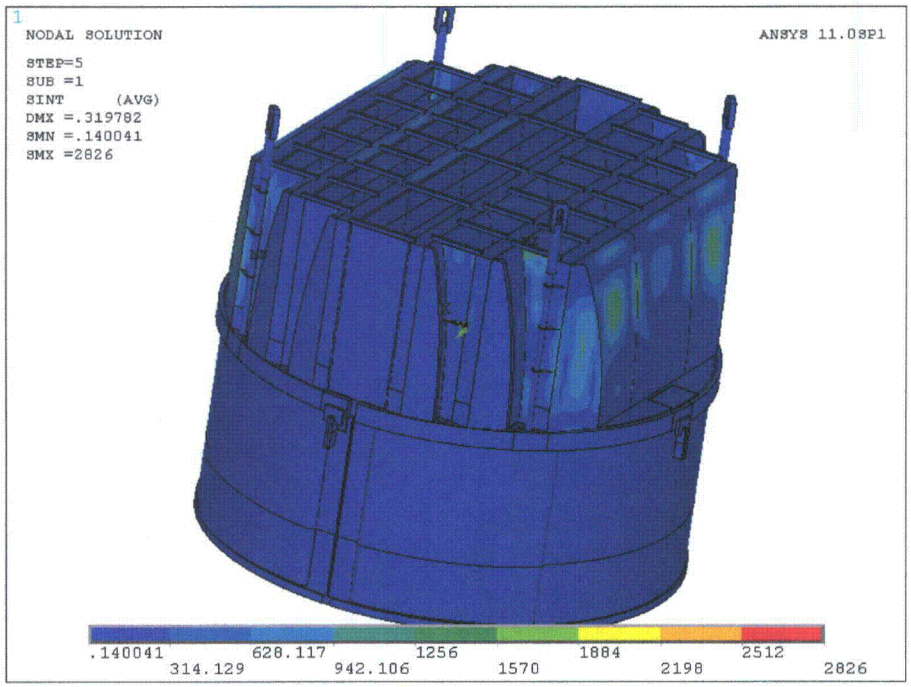

(a) Overall Distribution

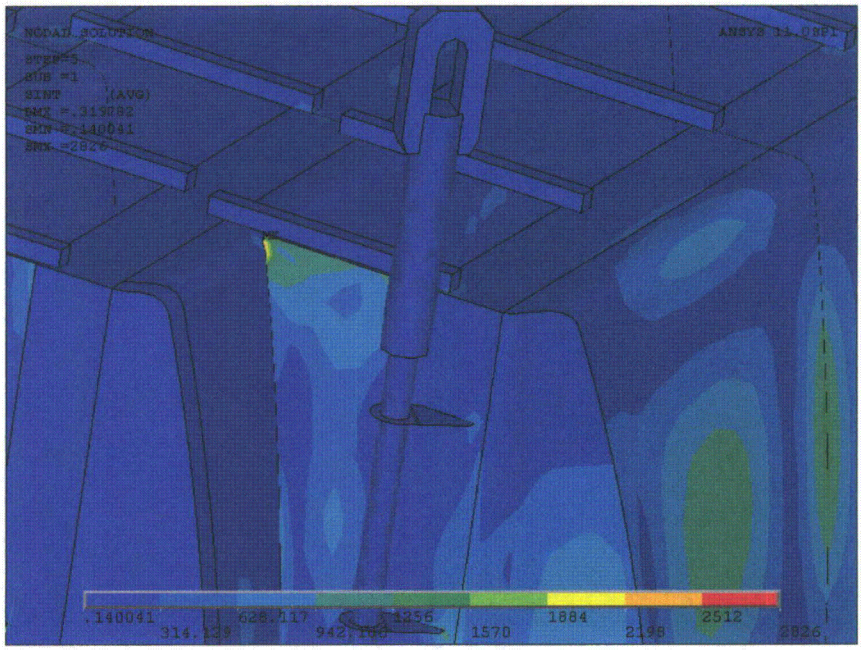

(b) Maximum Stress Location

Figure 6-31: Stress Intensity Distribution, Top Surface, FIV Load - TimeStress_49666_1075

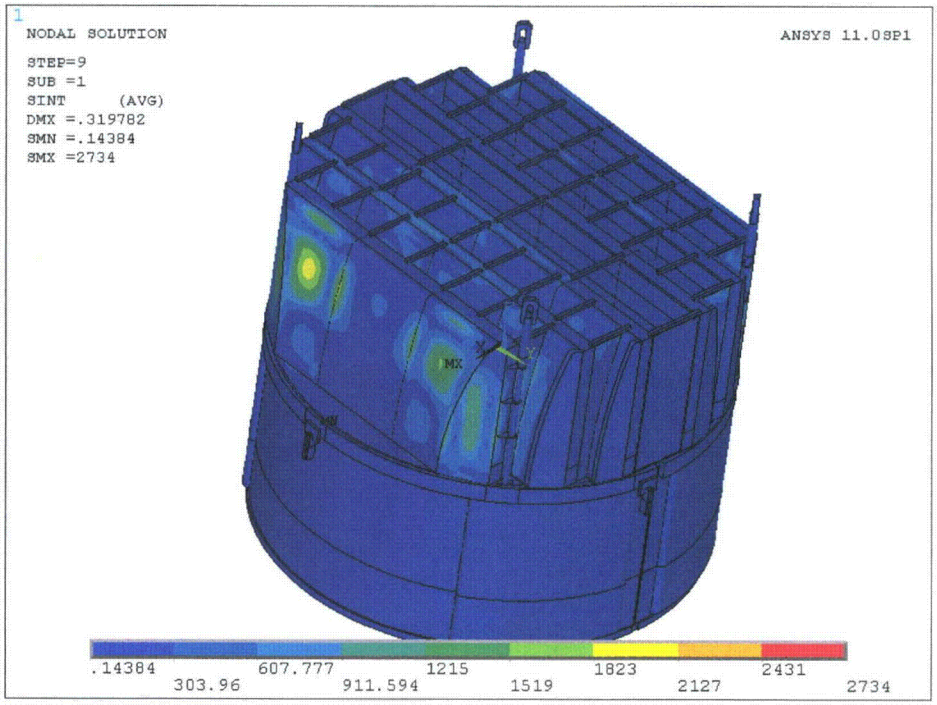

(a) Overall Stress Distribution

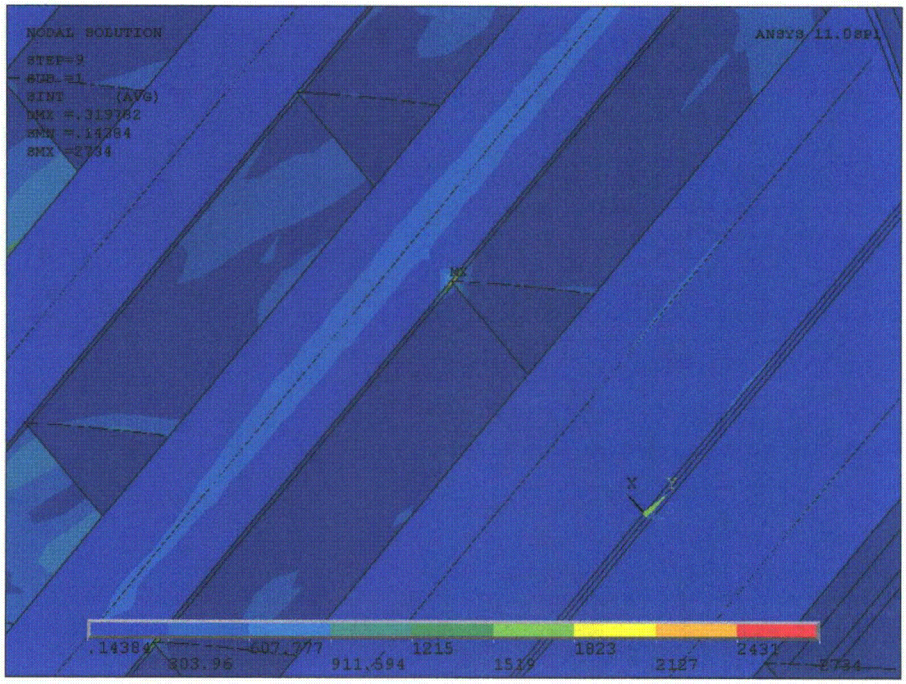

(b) Maximum Stress Location

Figure 6-32: Stress Intensity Distribution, Top Surface, FIV Load - TimeStress_49670_1075

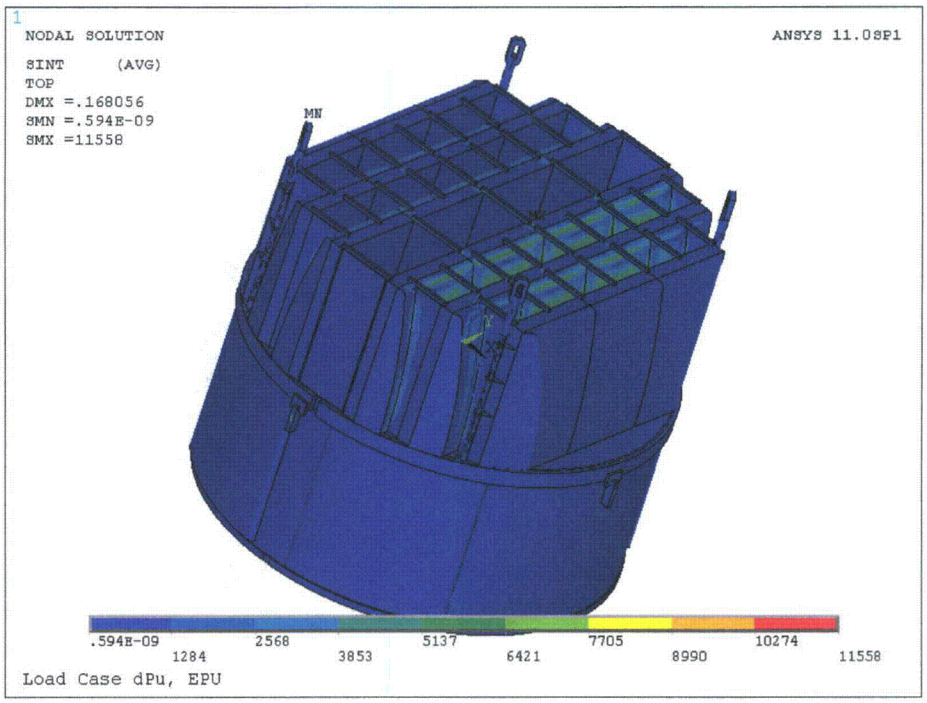

(a) Overall Stress Distribution

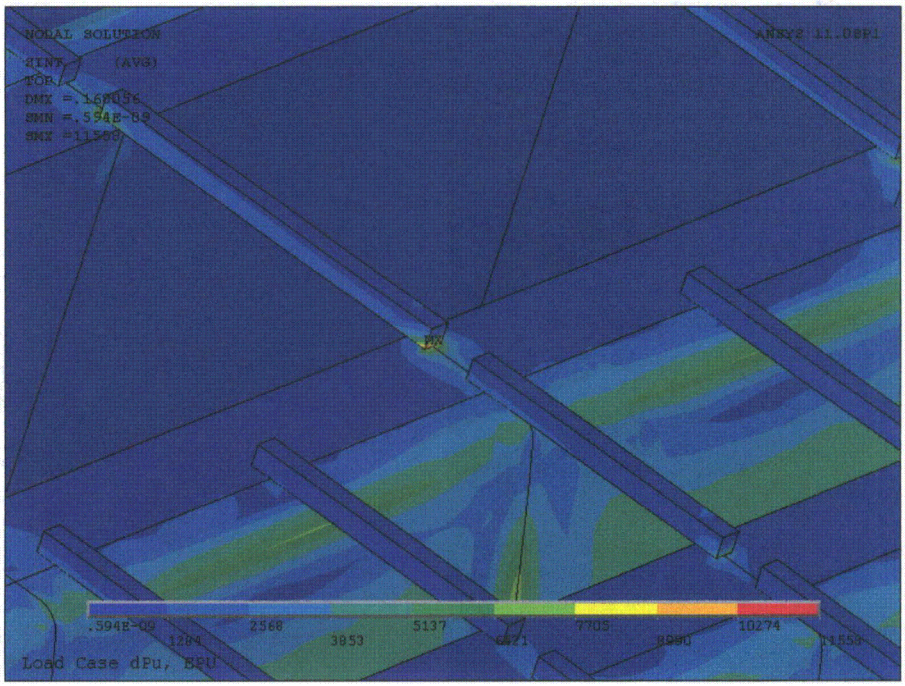

(b) Maximum Stress Location

Figure 6-33: Stress Intensity Distribution, Top Surface, ΔP_u, EPU

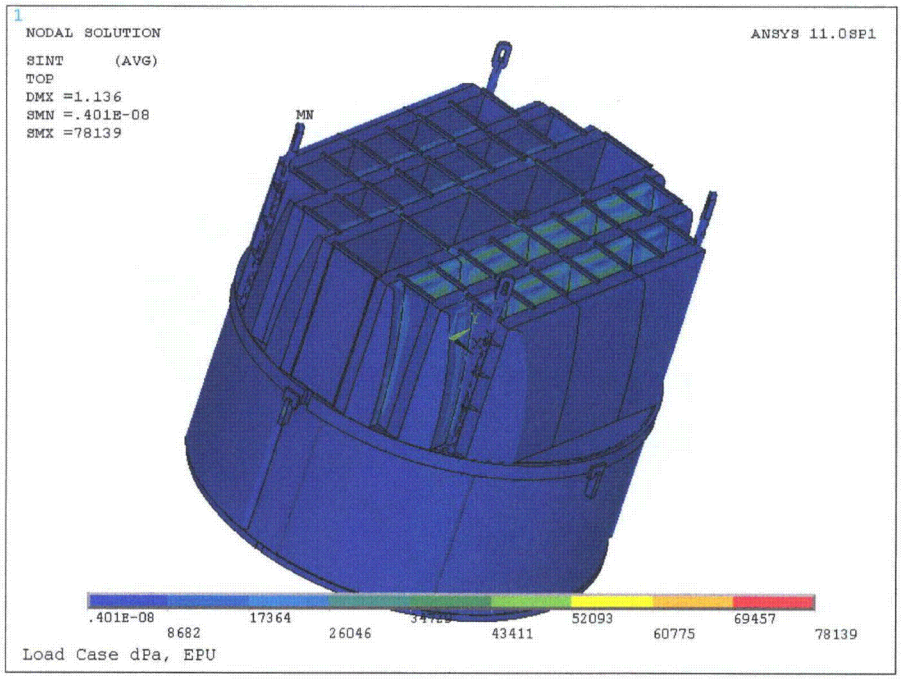

(a) Overall Stress Distribution

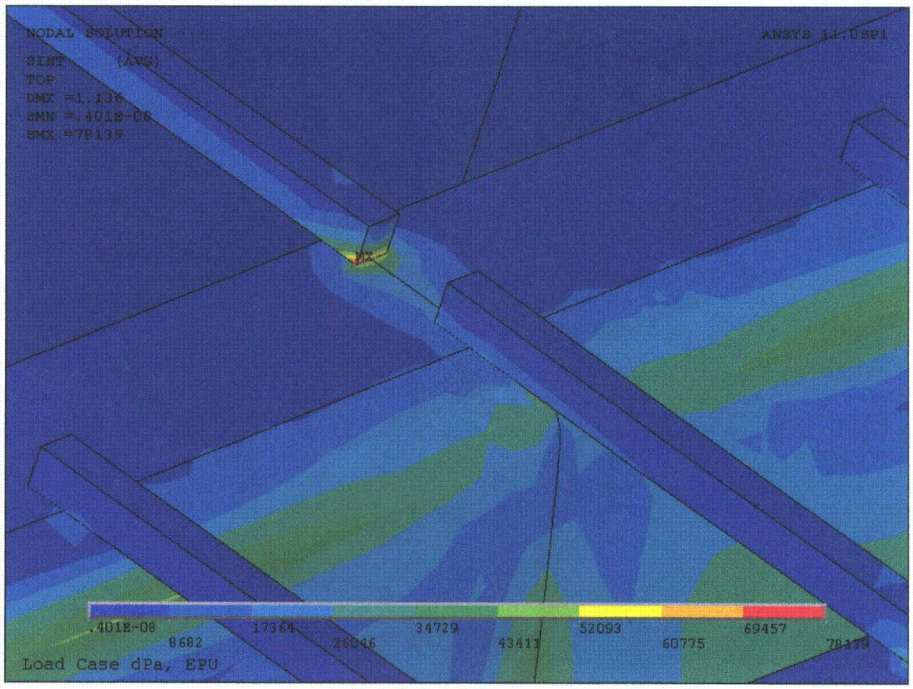

(b) Maximum Stress Location

Figure 6-34: Stress Intensity Distribution, Top Surface, ΔP_a, EPU

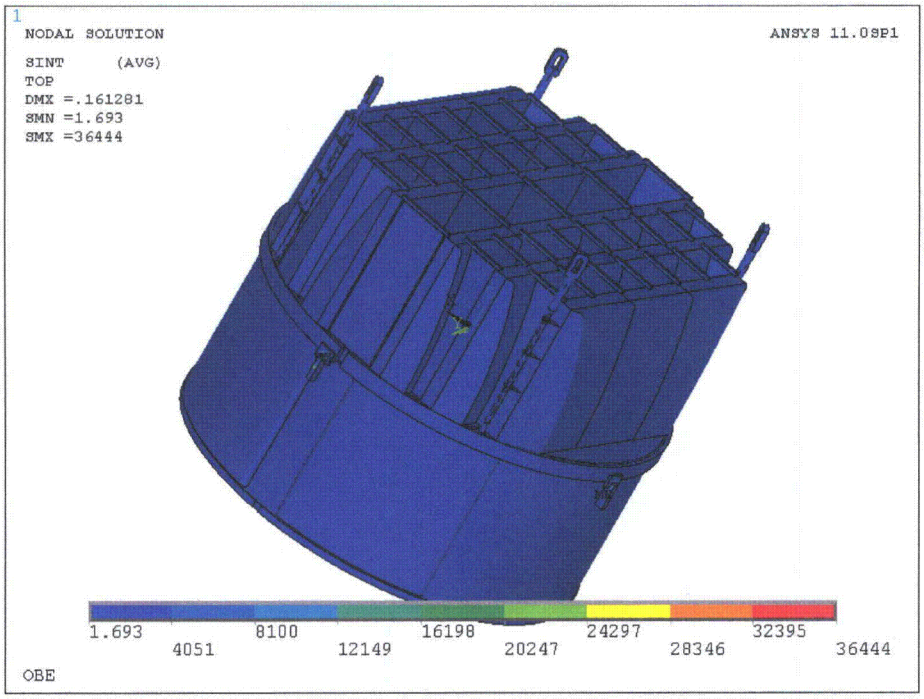

Figure 6-35: Stress Intensity Distribution, Top Surface, OBE

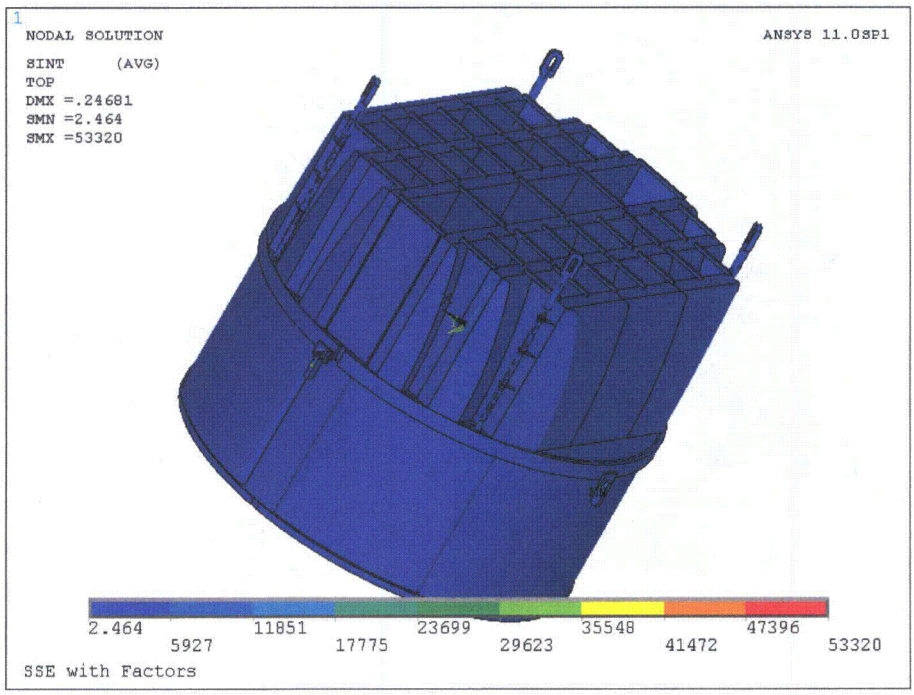

Figure 6-36: Stress Intensity Distribution, Top Surface, SSE

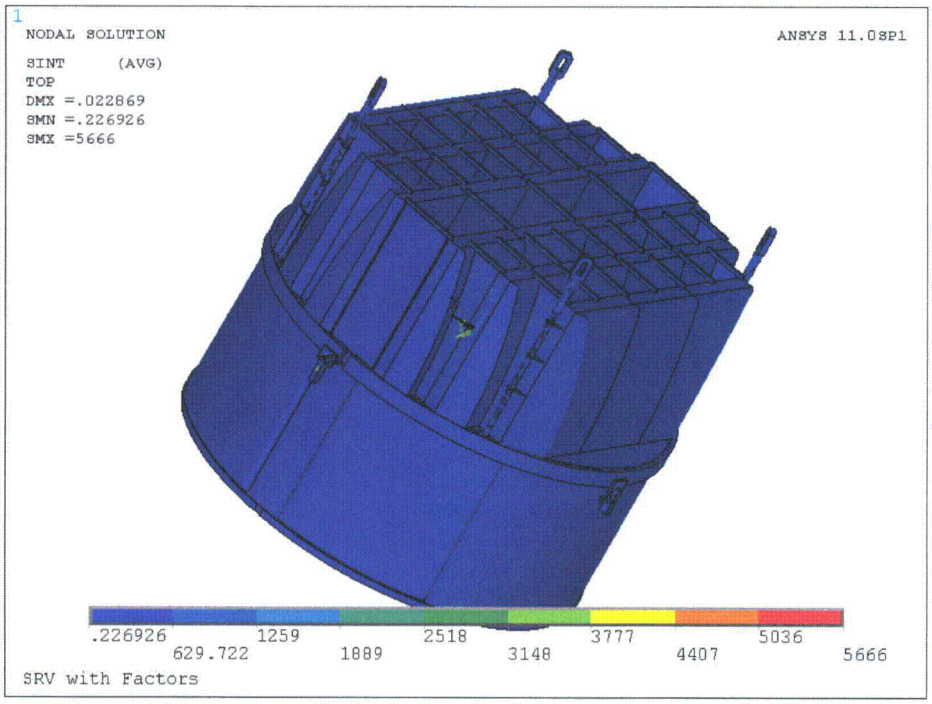

Figure 6-37: Stress Intensity Distribution, Top Surface, SRV

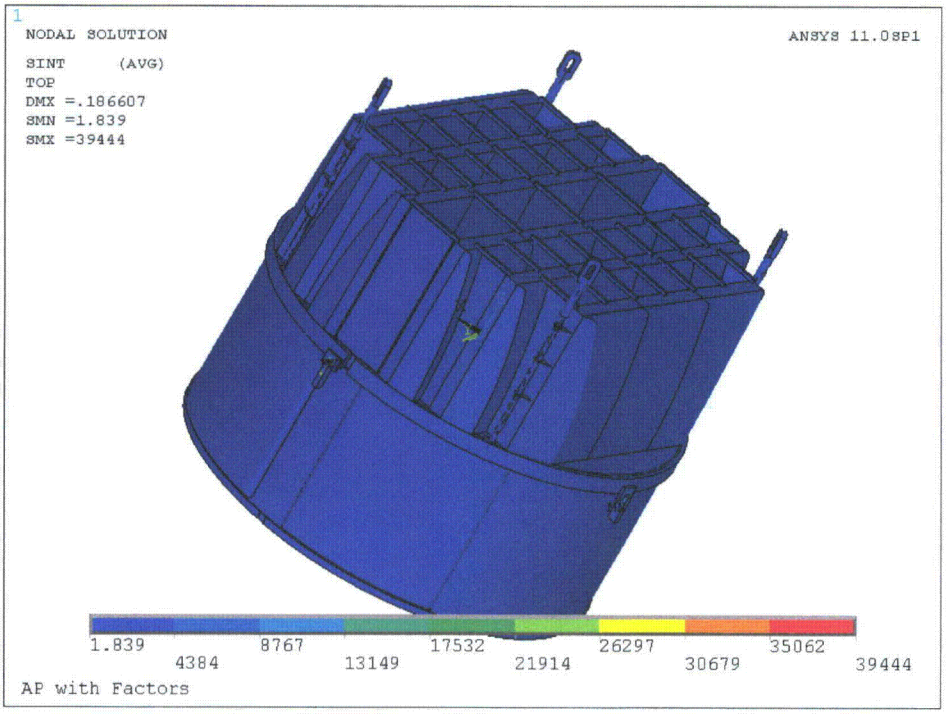

Figure 6-38: Stress Intensity Distribution, Top Surface, AP

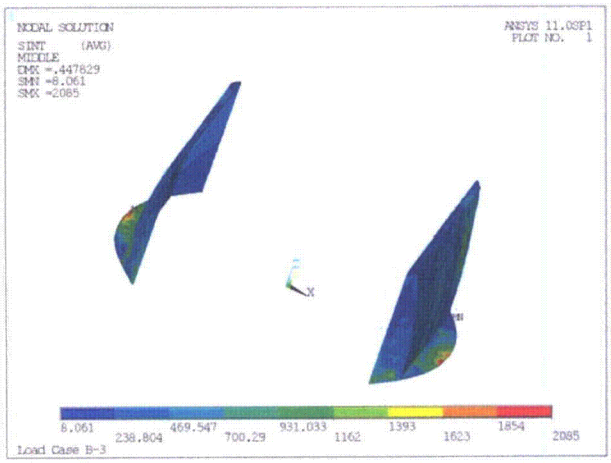

(a) Membrane Stress

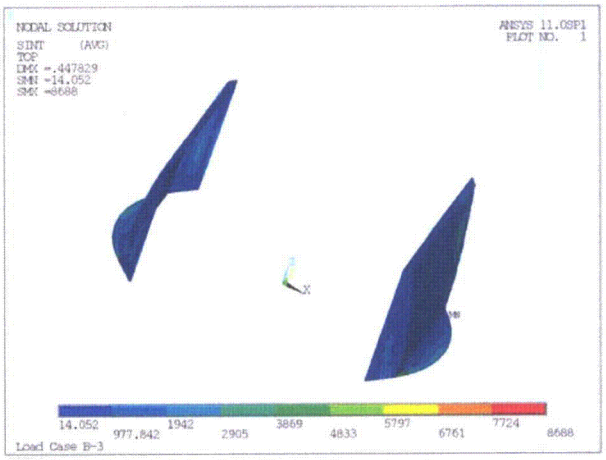

(b) $P_m + P_b$ Stress, Top Surface

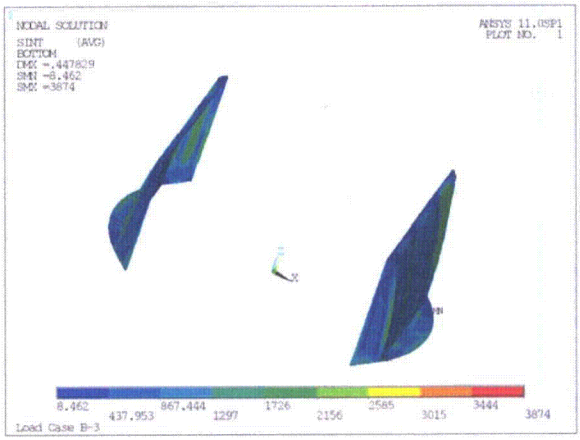

(c), $P_m + P_b$ Stress, Bottom Surface

Figure 6-39: Outer Hood, Stress Intensity, Case B-3(a)

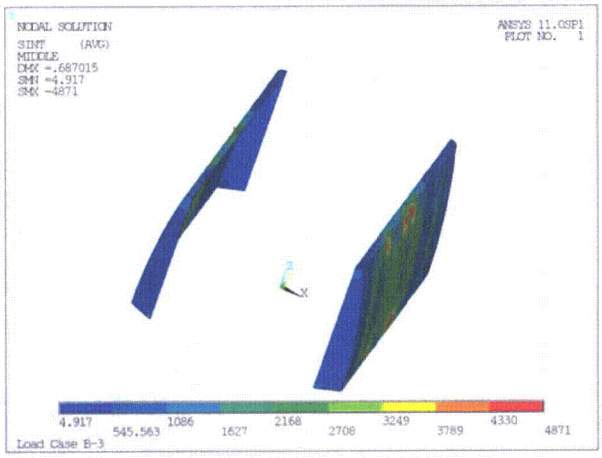

(a) Membrane Stress

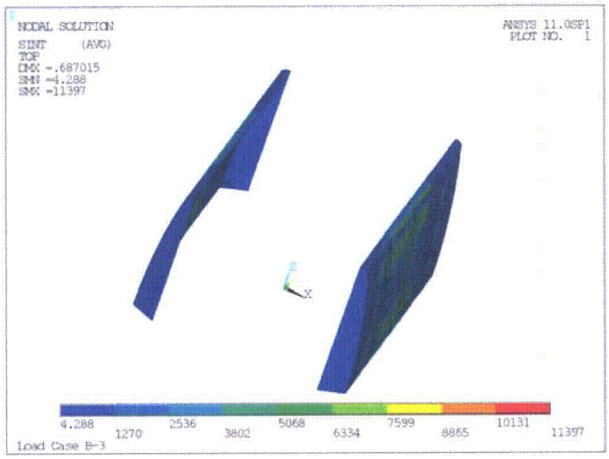

(b) $P_m + P_b$ Stress, Top Surface

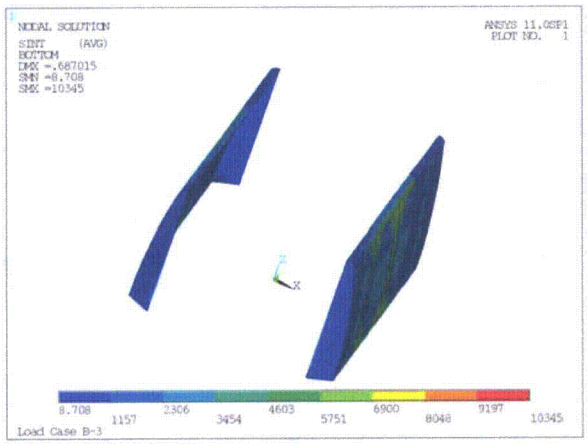

(c) $P_m + P_b$ Stress, Bottom Surface

Figure 6-40: Middle Hood, Stress Intensity, Case B-3(a)

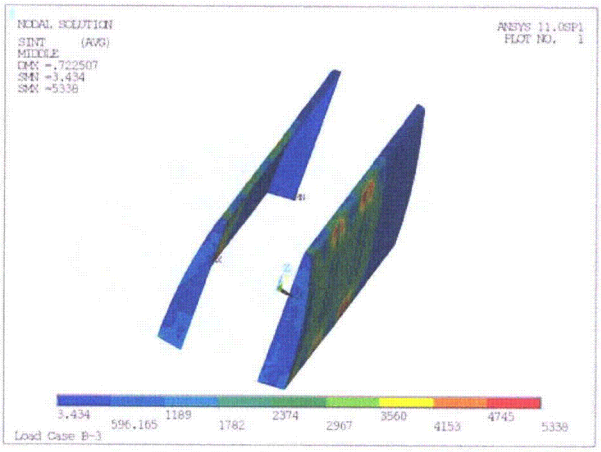

(a) Membrane Stress

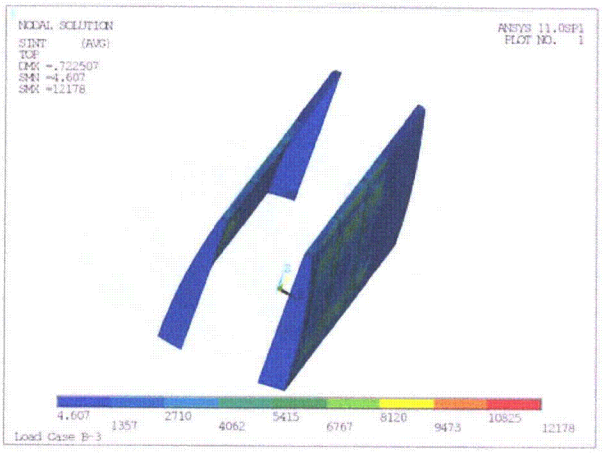

(b) Top Surface, $P_m + P_b$ Stress

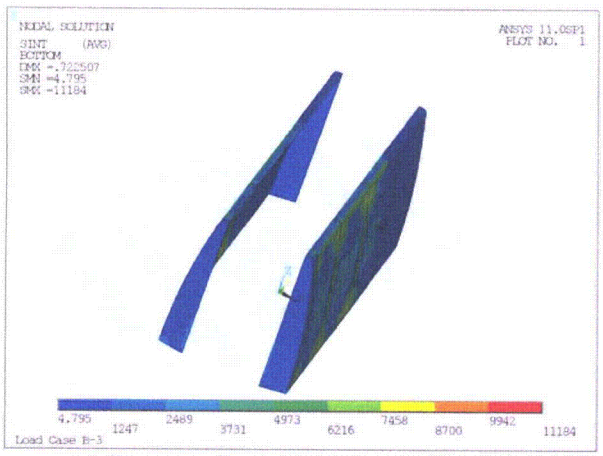

(c) Bottom Surface, $P_m + P_b$ Stress

Figure 6-41: Inside Hood, Stress Intensity, Case B-3(a)

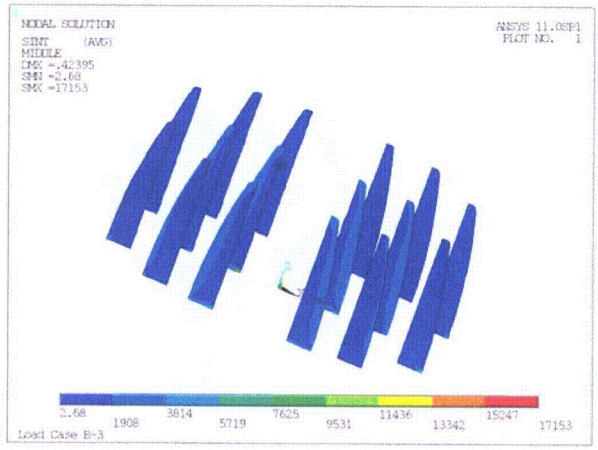

(a) Membrane Stress

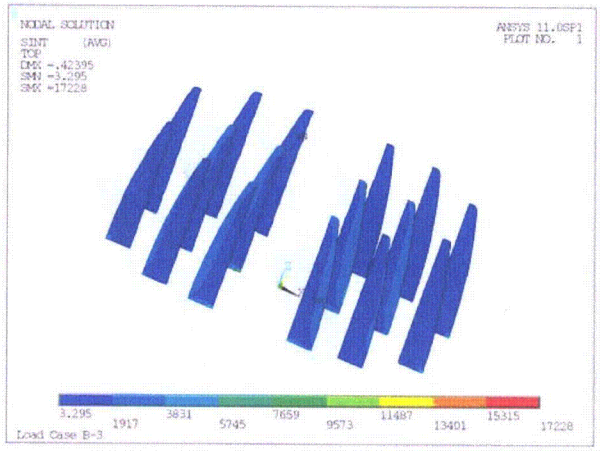

(b) Top Surface, $P_m + P_b$ Stress

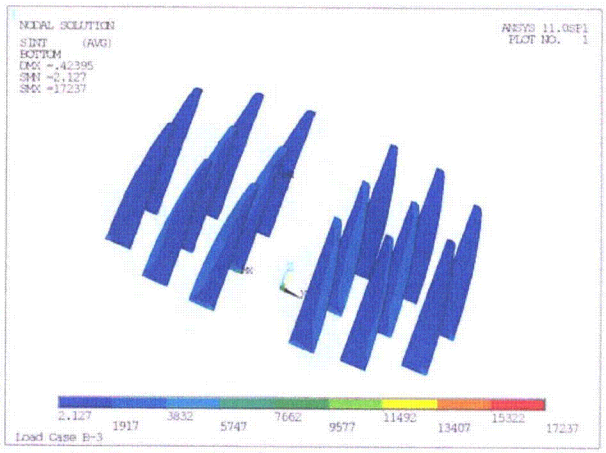

(c) Bottom Surface, $P_m + P_b$ Stress

Figure 6-42: Gussets in Hoods, Stress Intensity, Case B-3 (a)

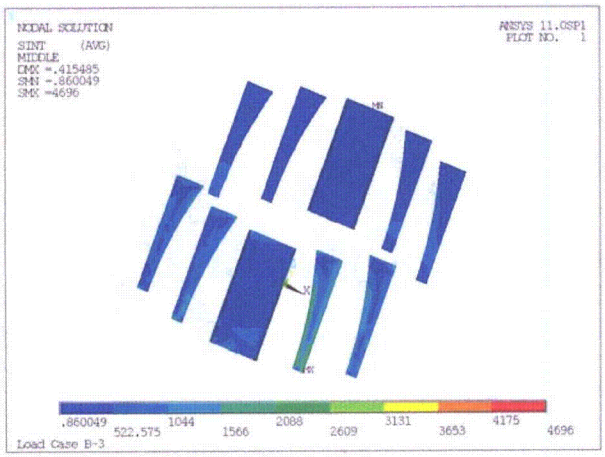

(a) Membrane Stress

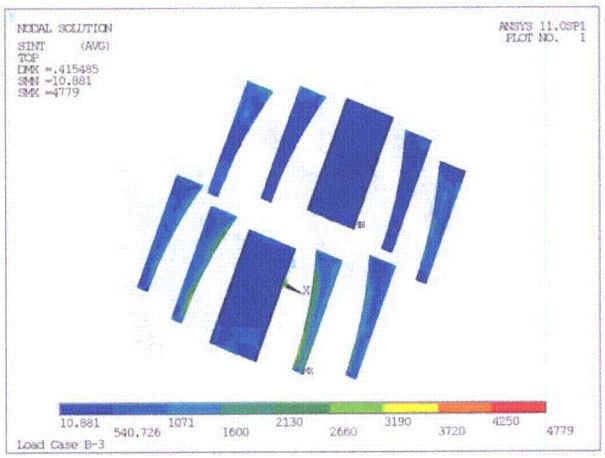

(b) $P_m + P_b$ Stress, Top Surface

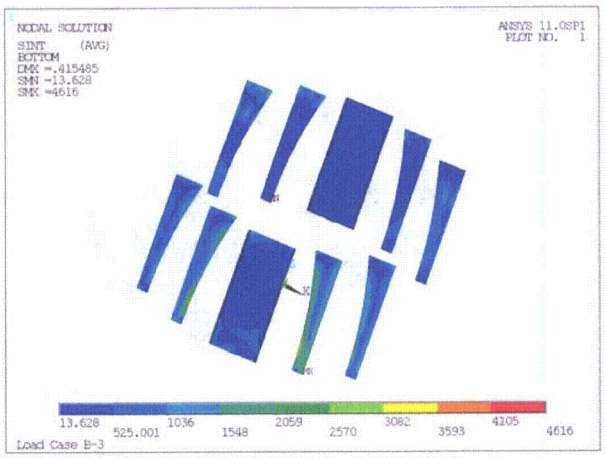

(c) $P_m + P_b$ Stress, Bottom Surface

Figure 6-43: Sides Plates, Stress Intensity, Case B-3(a)

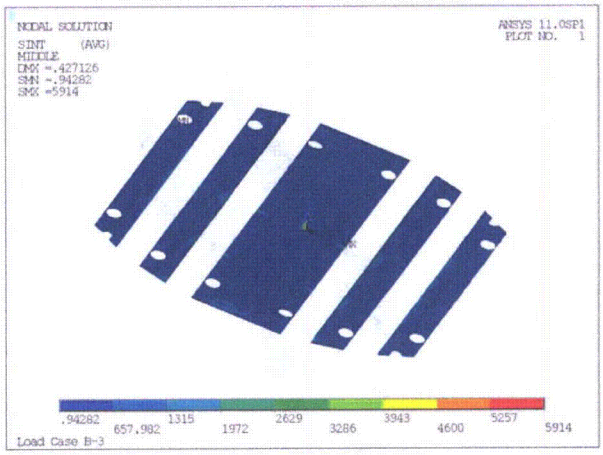

(a) Membrane Stress

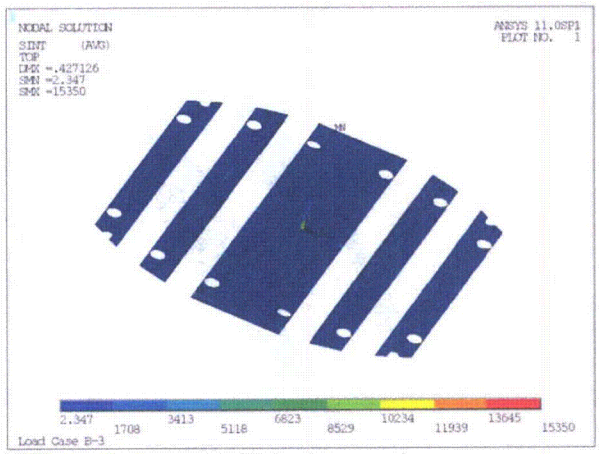

(b) $P_m + P_b$ Stress, Top Surface

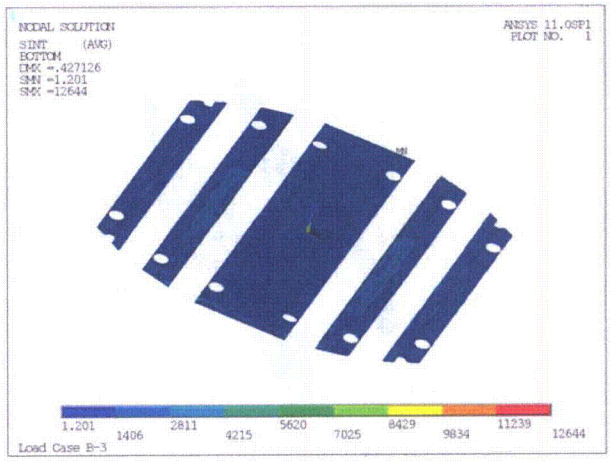

(c) $P_m + P_b$ Stress, Bottom Surface

Figure 6-44: Vane Bank Base Plates, Stress Intensity, Case B-3(a)

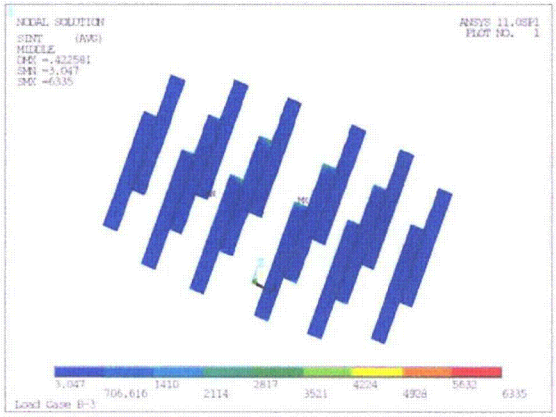

(a) Membrane Stress

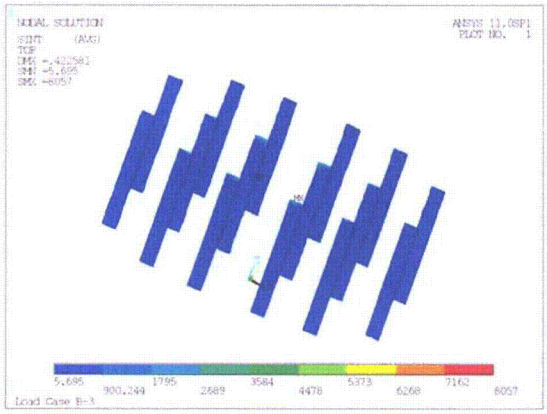

(b) $P_m + P_b$ Stress, Top Surface

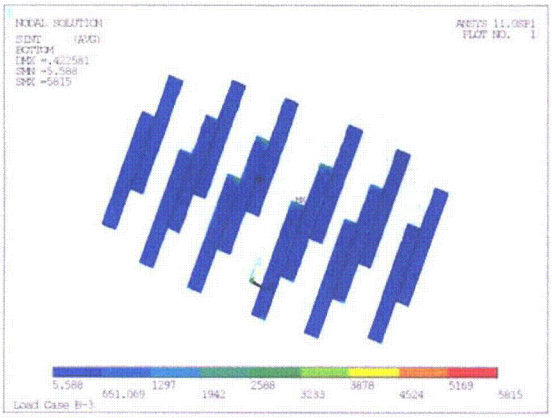

(c) $P_m + P_b$ Stress, Bottom Surface Stress

Figure 6-45: Vane Bank Vertical Plates, Stress Intensity, Case B-3(a)

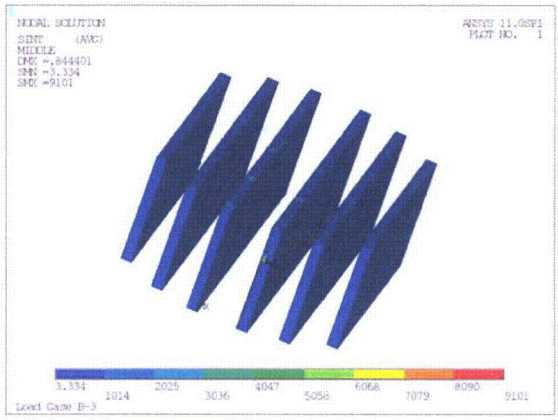

(a) Membrane Stress

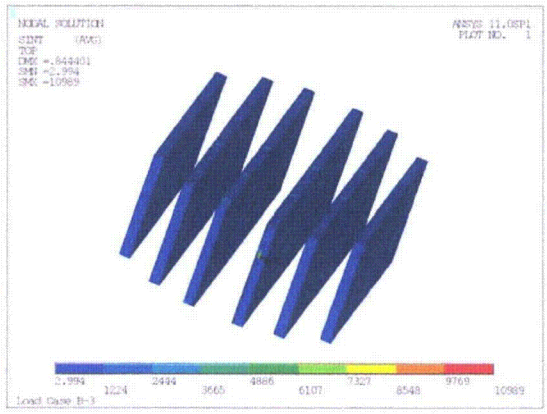

(b) $P_m + P_b$ Stress, Top Surface

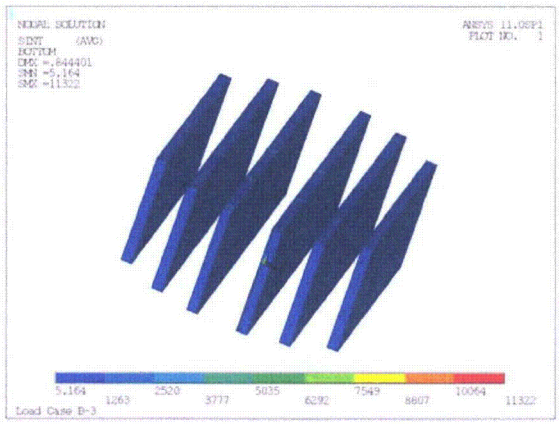

(c) $P_m + P_b$ Stress, Bottom Surface

Figure 6-46: Vane Banks, Stress Intensity, Case B-3(a)

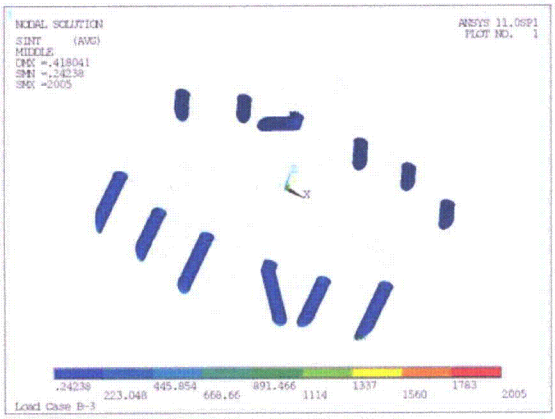

(a) Membrane Stress

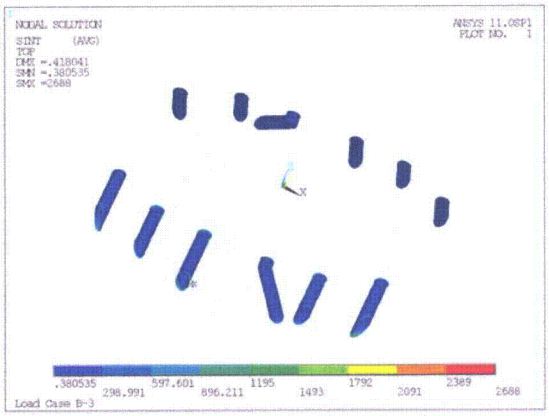

(b) $P_m + P_b$ Stress, Top Surface

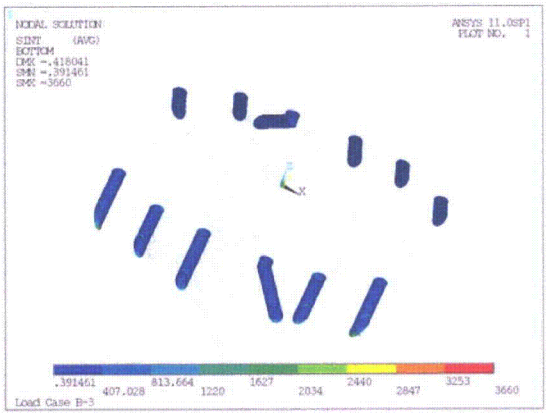

(c) $P_m + P_b$ Stress, Bottom Surface

Figure 6-47: Drain Pipes, Stress Intensity, Case B-3(a)

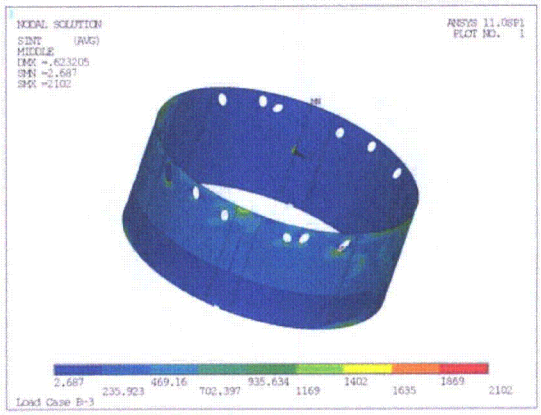

(a) Membrane Stress

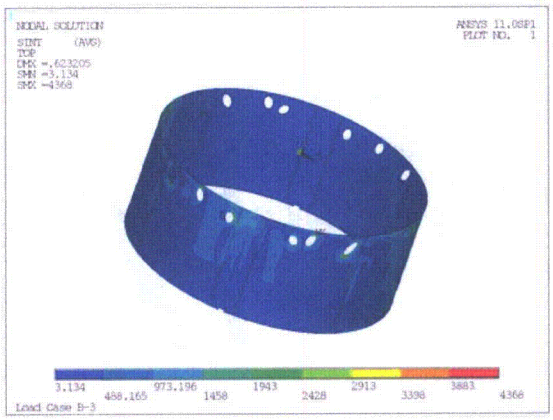

(b) $P_m + P_b$ Stress, Top Surface

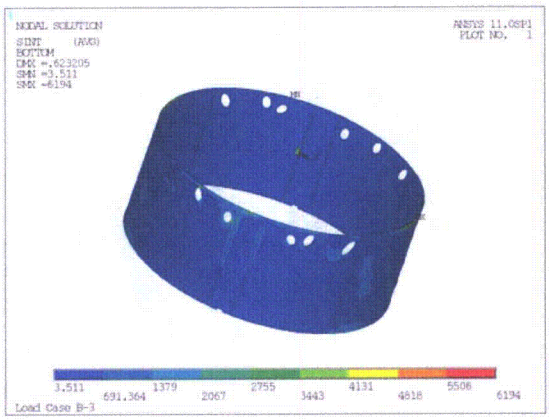

(c) $P_m + P_b$ Stress, Bottom Surface

Figure 6-48: Skirt, Stress Intensity, Case B-3 (a)

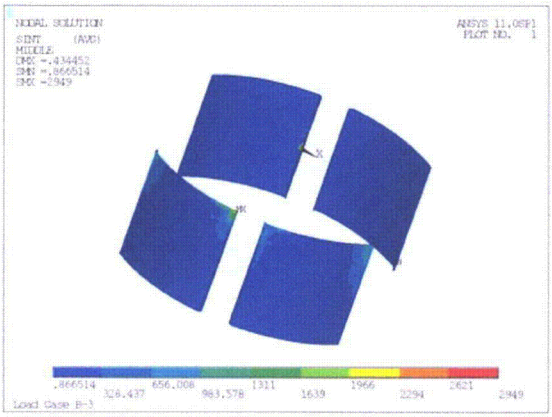

(a) Membrane Stress

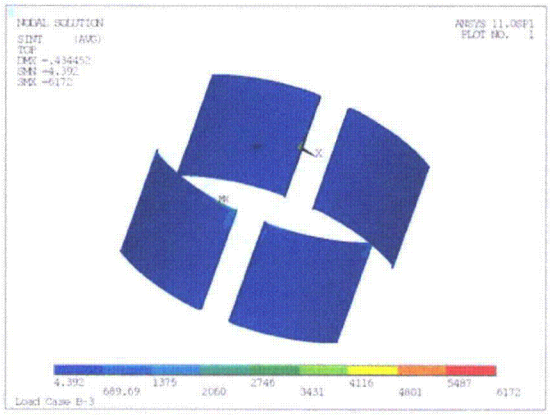

(b) $P_m + P_b$ Stress, Top Surface

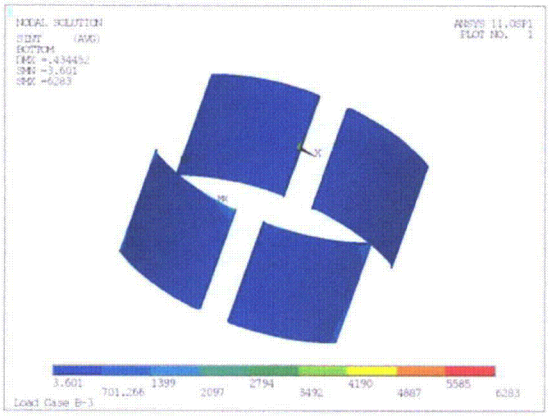

(c) $P_m + P_b$ Stress, Bottom Surface

Figure 6-49: Drain Channels, Stress Intensity, Case B-3(a)

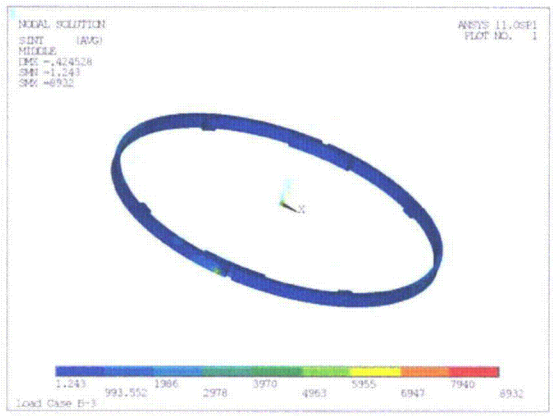

(a) Membrane Stress

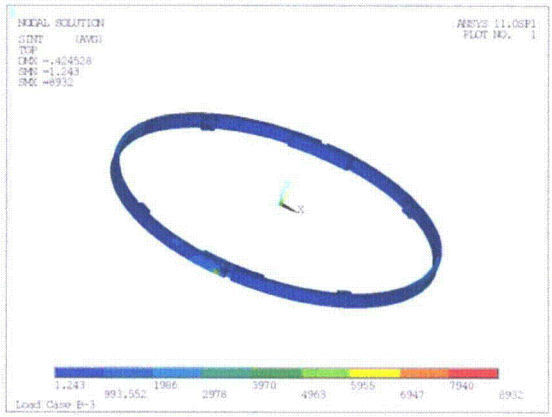

(b) $P_m + P_b$ Stress, Top Surface

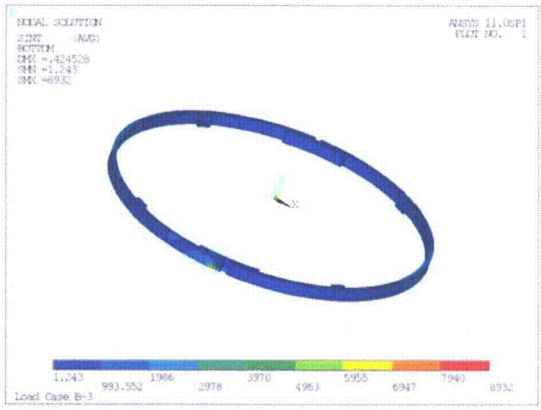

(c) $P_m + P_b$ Stress, Bottom Surface

Figure 6-50: Upper Support Ring, Stress Intensity, Case B-3(a)

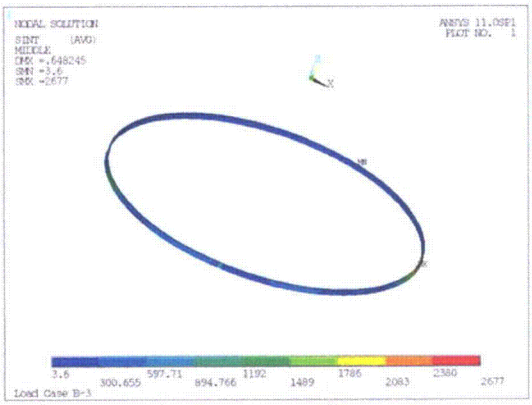

(a) Membrane Stress

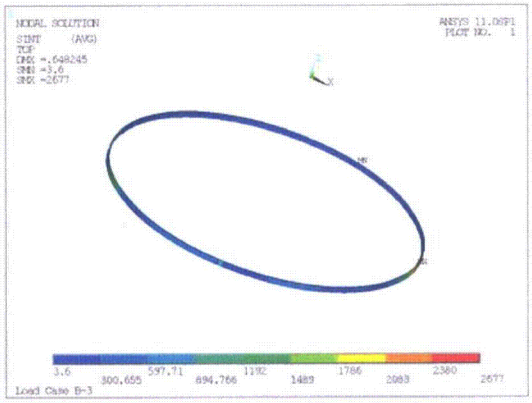

(b) $P_m + P_b$ Stress, Top Surface

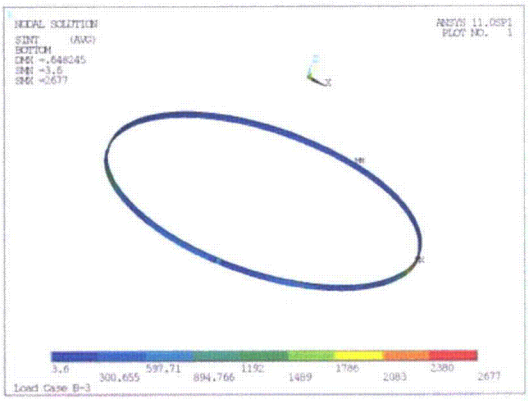

(c) $P_m + P_b$ Stress, Bottom Surface

Figure 6-51: Lower Support Ring, Stress Intensity, Case B-3 (a)

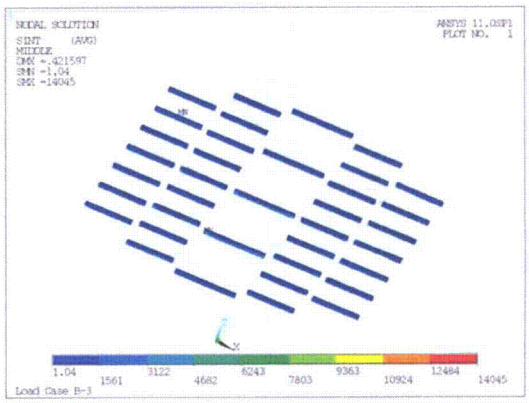

(a) Membrane Stress

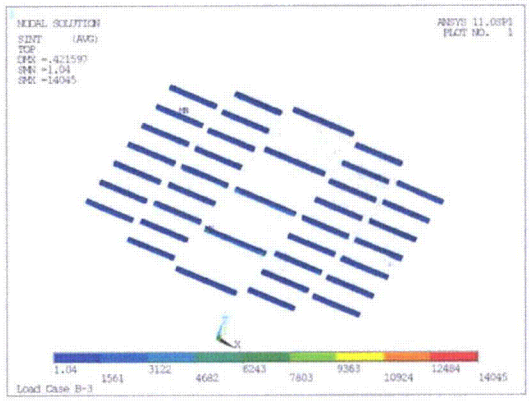

(b) $P_m + P_b$ Stress, Top Surface

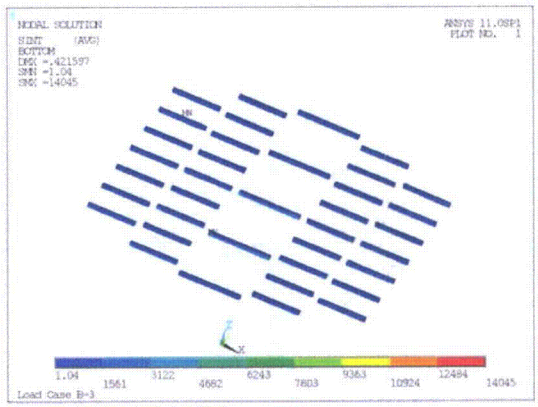

(c) $P_m + P_b$ Stress, Bottom Surface

Figure 6-52: Tie Bars, Stress Intensity, Case B-3(a)

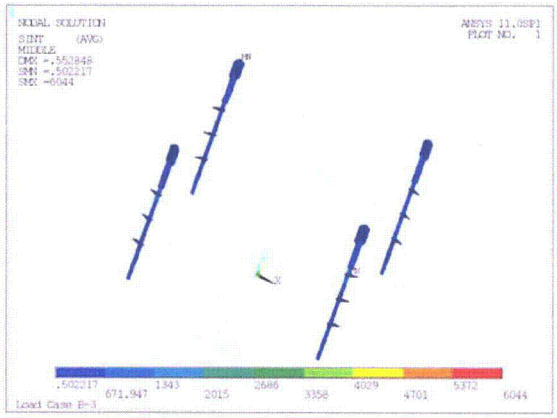

(a) Membrane Stress

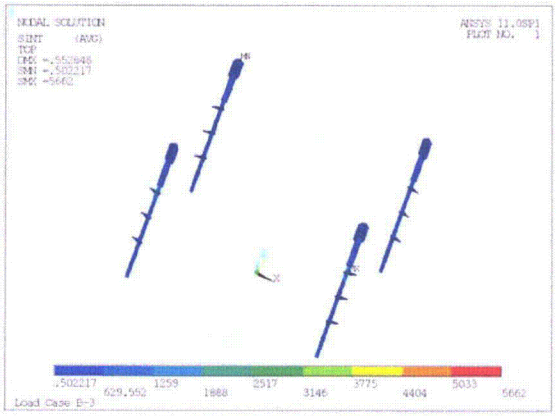

(b) $P_m + P_b$ Stress, Top Surface

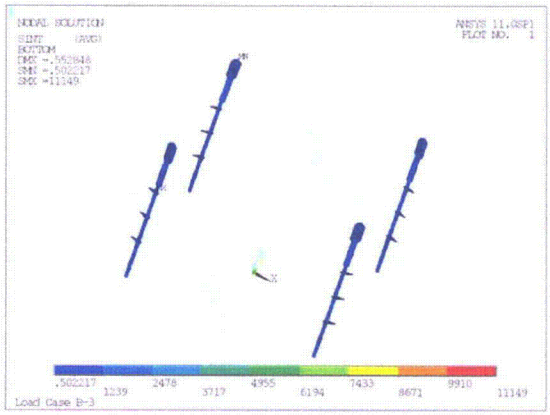

(c) $P_m + P_b$ Stress, Bottom Surface

Figure 6-53: Lifting Rods, Stress Intensity, Case B-3(a)

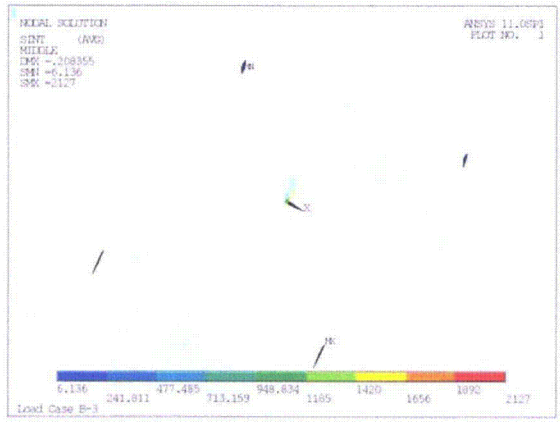

(a) Membrane Stress

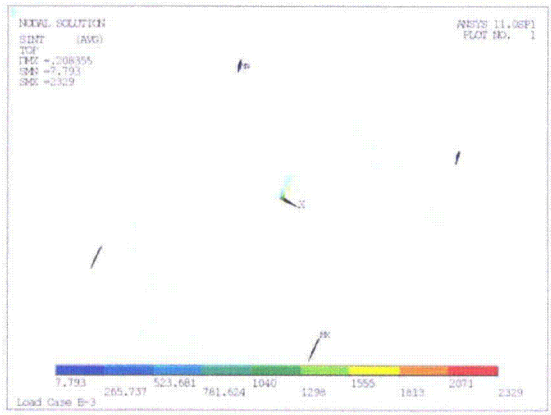

(b) $P_m + P_b$ Stress, Top Surface

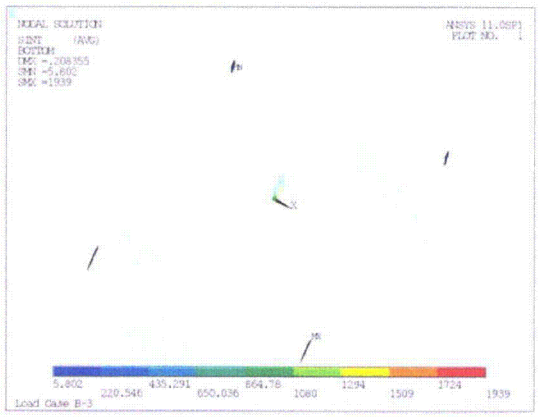

(c) $P_m + P_b$ Stress, Bottom Surface

Figure 6-54: Gussets in Upper Support Ring, Stress Intensity, Case B-3(a)

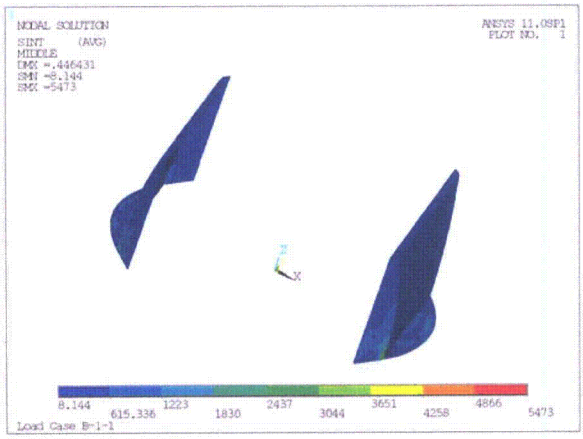

(a) Membrane Stress

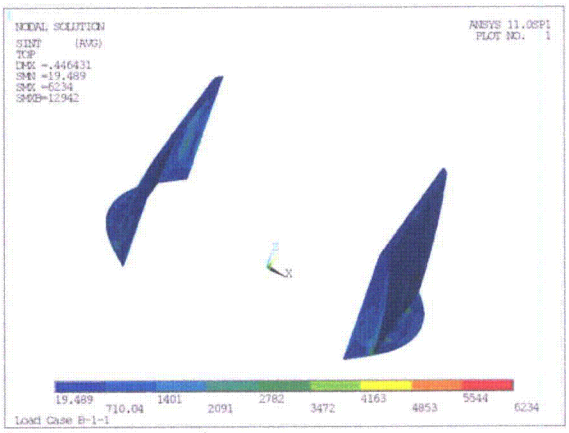

(b) P_m+P_b Stress, Top Surface

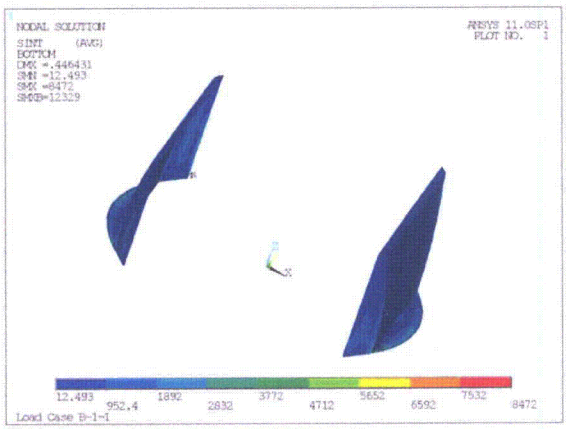

(c) P_m+P_b Stress, Bottom Surface

Figure 6-55: Outer Hoods Stress Intensity Case B-3 (b)

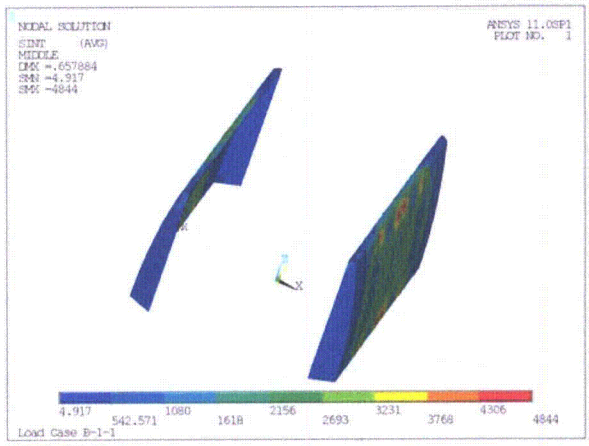

(a) Membrane Stress

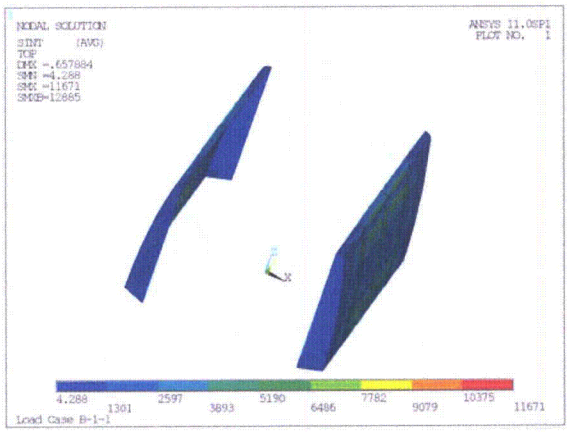

(b) P_m+P_b Stress, Top Surface

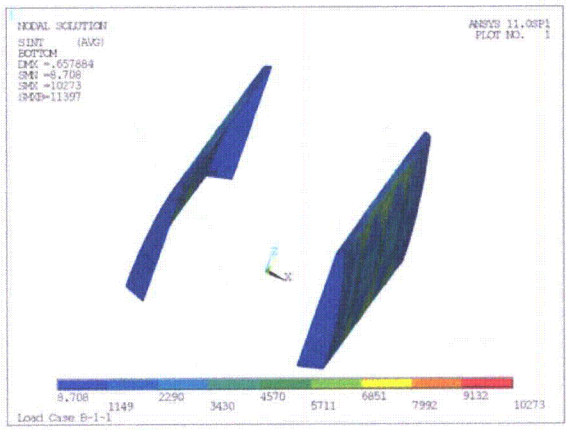

(c) P_m+P_b Stress, Bottom Surface

Figure 6-56: Middle Hoods, Stress Intensity Case B-3 (b)

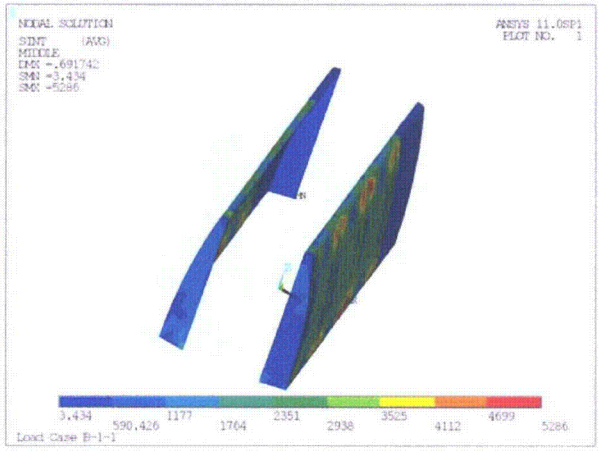

(a) Membrane Stress

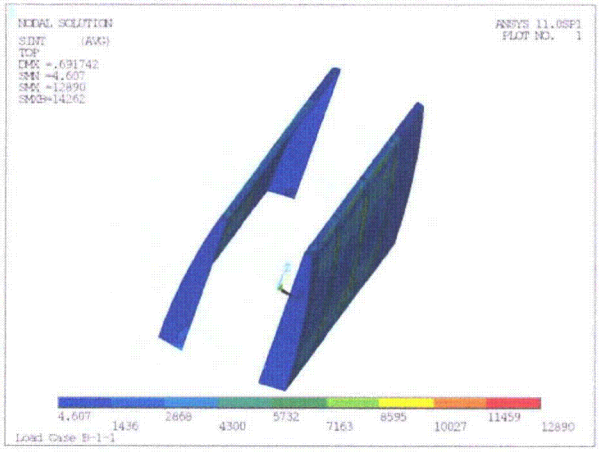

(b) P_m+P_b Stress, Top Surface

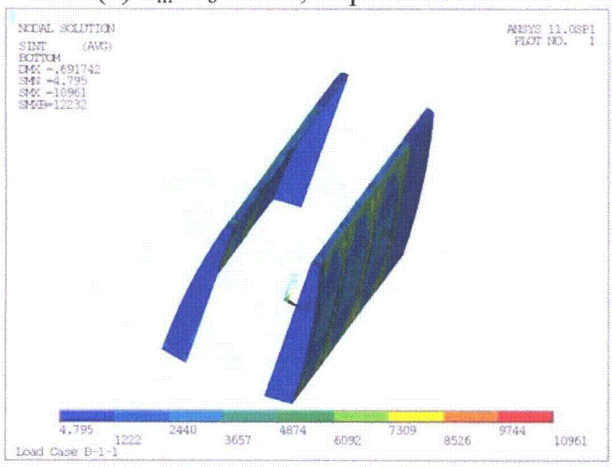

(c) P_m+P_b Stress, Bottom Surface

Figure 6-57: Inside Hoods, Stress Intensity, Case B-3 (b)

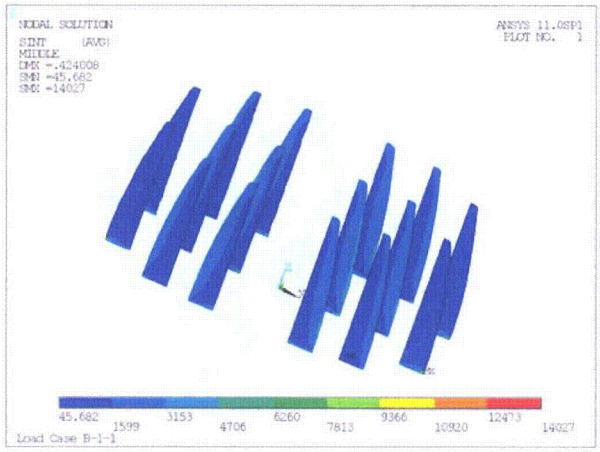

(a) Membrane Stress

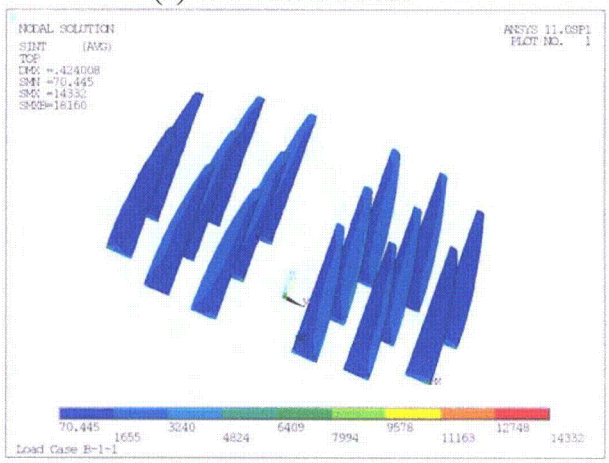

(b) P_m+P_b Stress, Top Surface

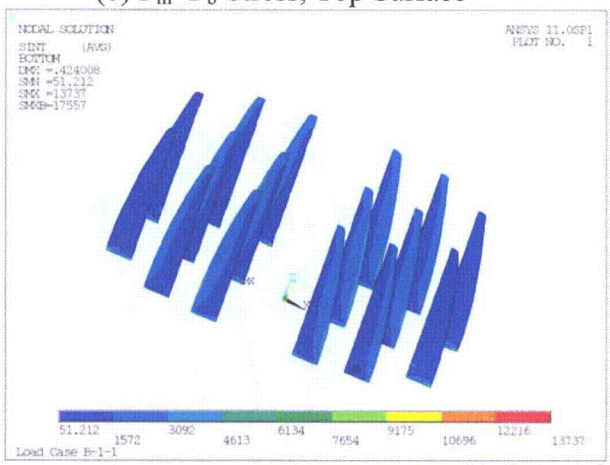

(c) P_m+P_b Stress, Bottom Surface

Figure 6-58: Gussets in Hoods, Stress Intensity, Case B-3 (b)

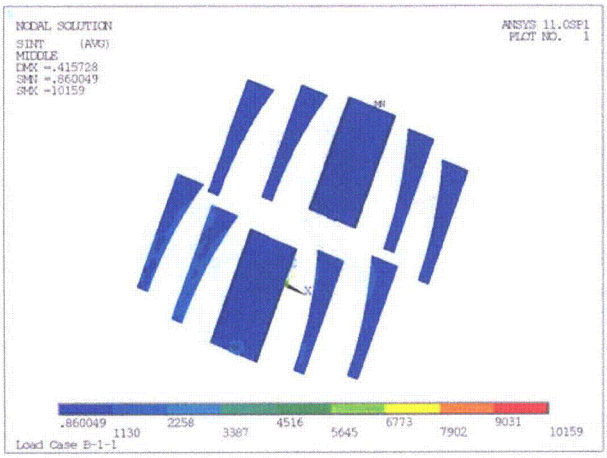

(a) Membrane Stress

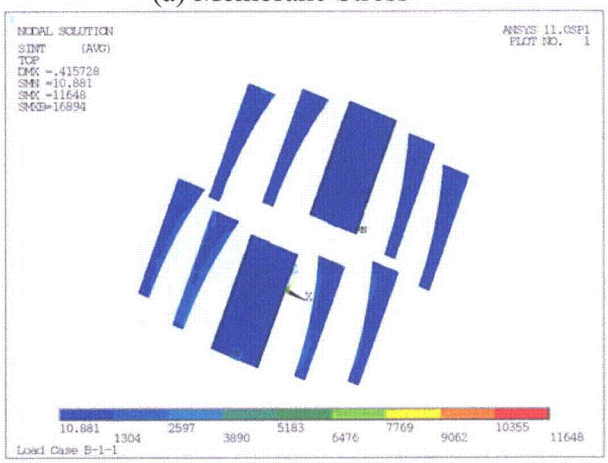

(b) P_m+P_b Stress, Top Surface

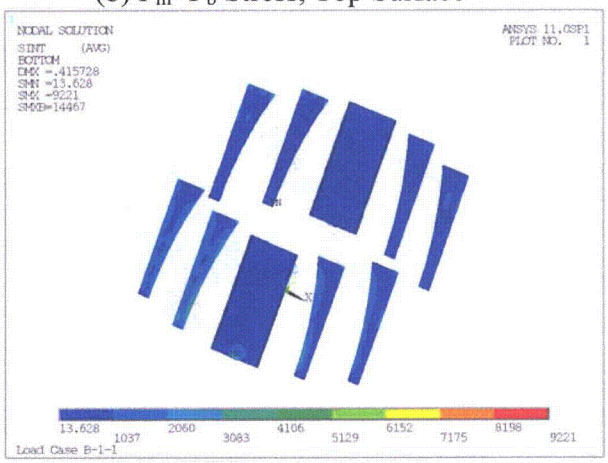

(c) P_m+P_b Stress, Bottom Surface

Figure 6-59: Side Plates, Stress Intensity, Case B-3(b)

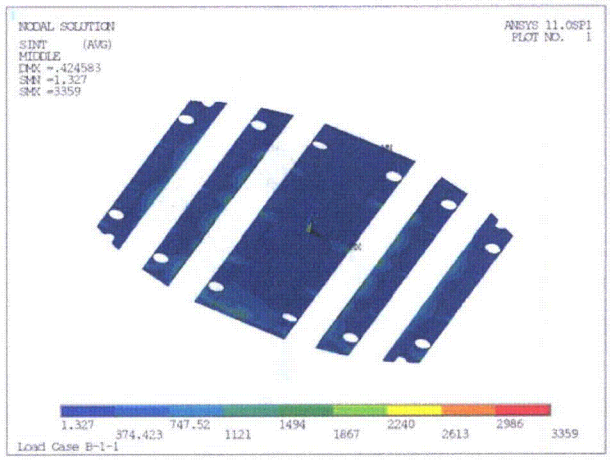

(a) Membrane Stress

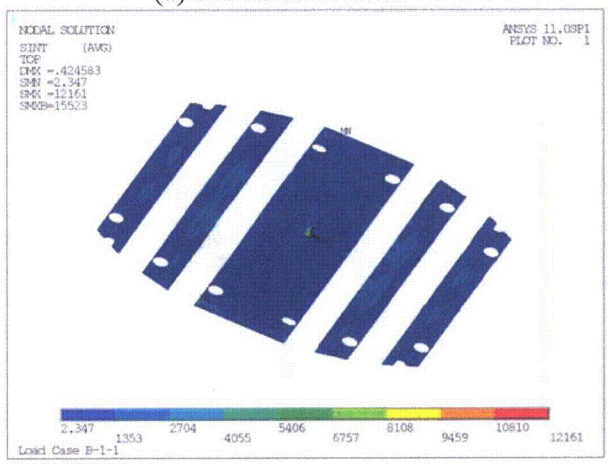

(b) P_m+P_b Stress, Top Surface

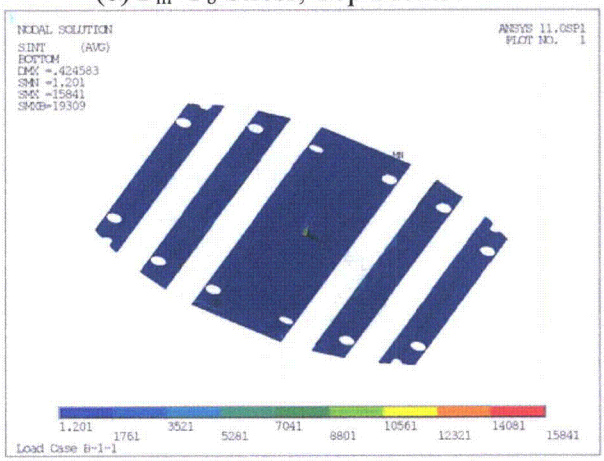

(c) P_m+P_b Stress, Bottom Surface

Figure 6-60: Vane Bank Base Plates, Stress Intensity, Case B-3(b)

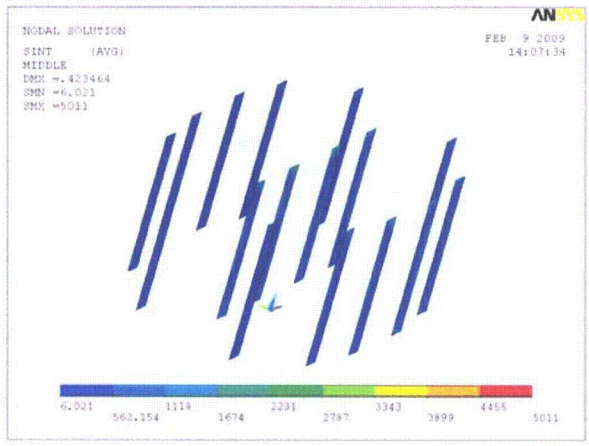

(a) Membrane Stress

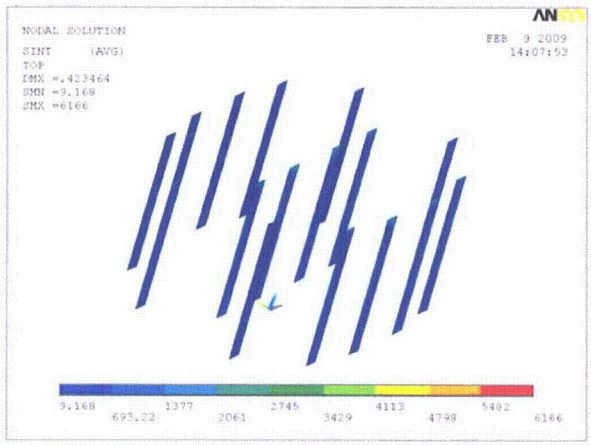

(b) P_m+P_b Stress, Top Surface

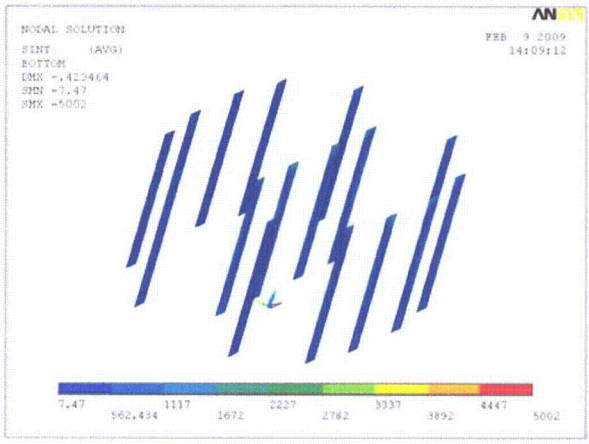

(c) P_m+P_b Stress, Bottom Surface

Figure 6-61: Vane Bank Vertical Plates, Stress Intensity, Case B-3(b)

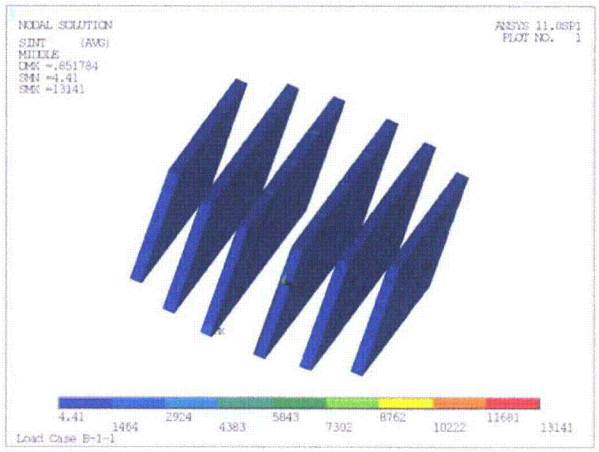

(a) Membrane Stress

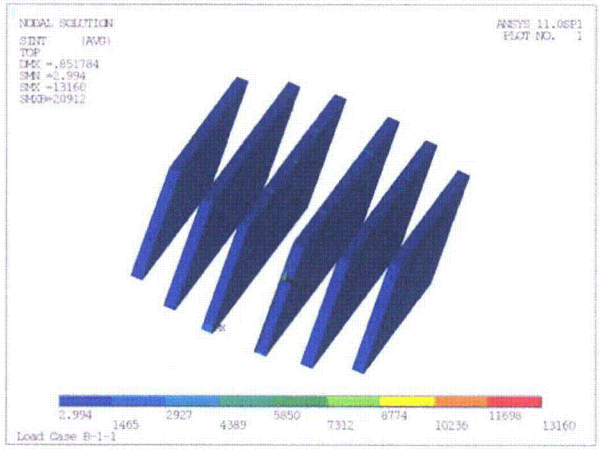

(b) P_m+P_b Stress, Top Surface

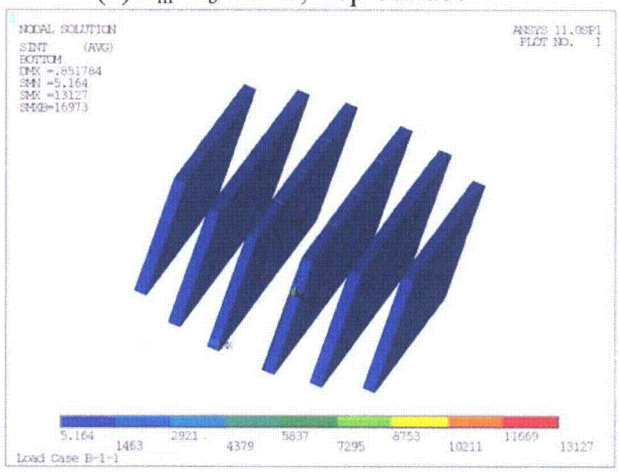

(c) P_m+P_b Stress, Bottom Surface

Figure 6-62: Vane Bank, Stress Intensity, Case B-3(b)

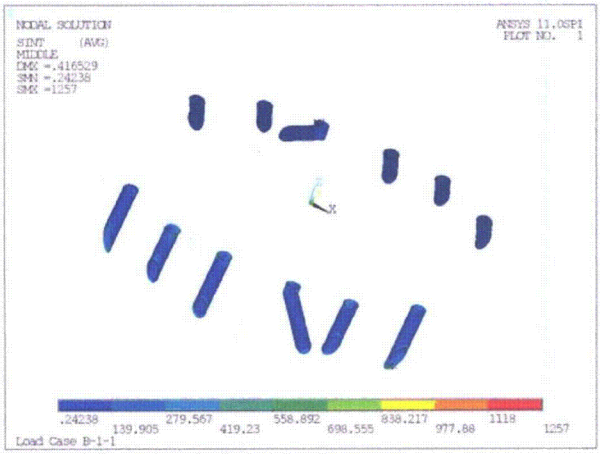

(a) Membrane Stress

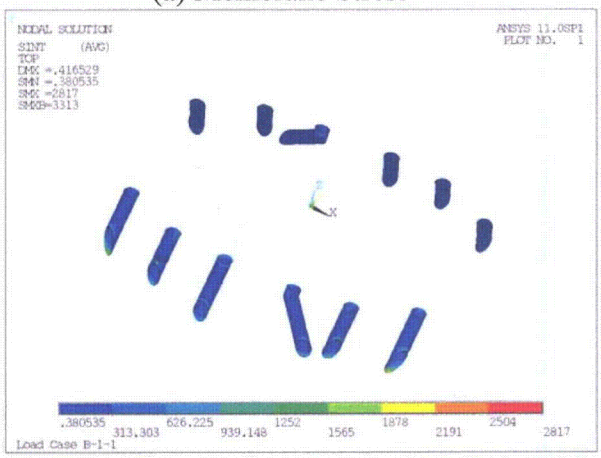

(b) P_m+P_b Stress, Top Surface

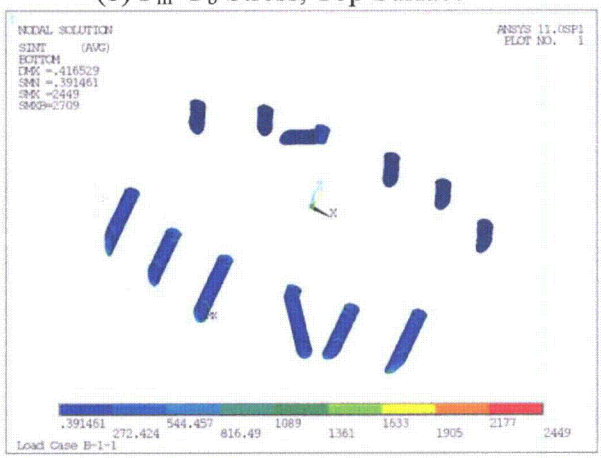

(c) P_m+P_b Stress, Bottom Surface

Figure 6-63: Drain Pipes, Stress Intensity, Case B-3(b)

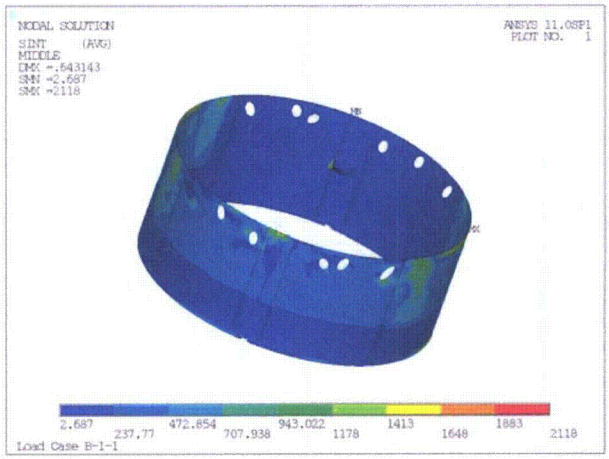

(a) Membrane Stress

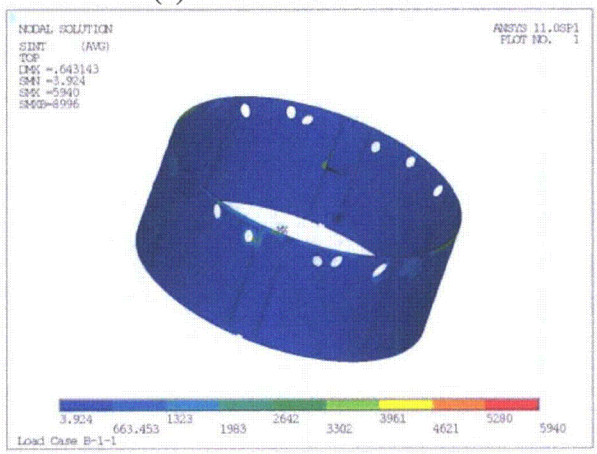

(b) P_m+P_b Stress, Top Surface

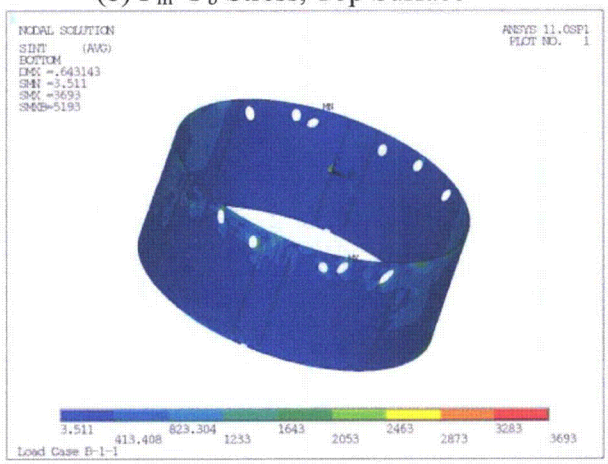

(c) P_m+P_b Stress, Bottom Surface

Figure 6-64: Skirt, Stress Intensity, Case B-3(b)

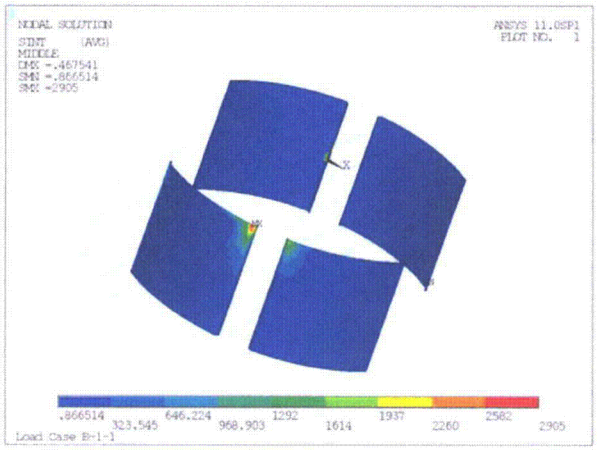

(a) Membrane Stress

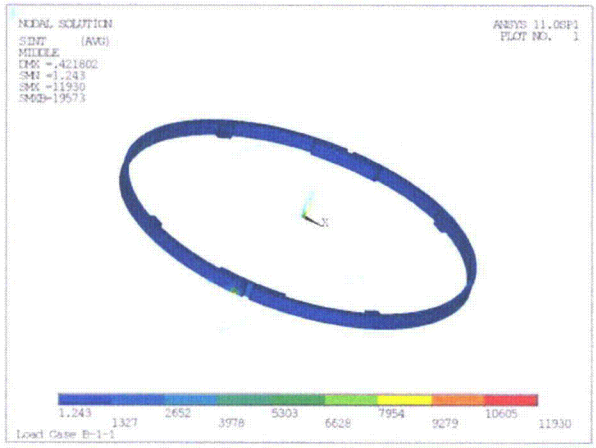

(a) Membrane Stress

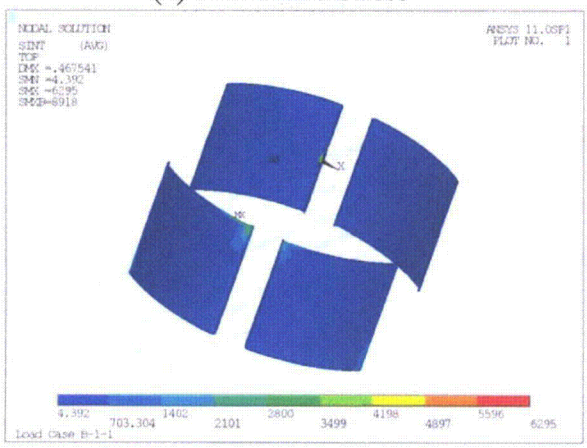

(b) P_m+P_b Stress, Top Surface

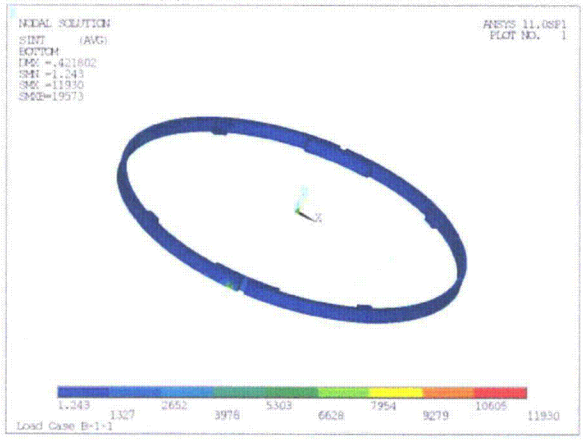

(b) P_m+P_b Stress, Top Surface

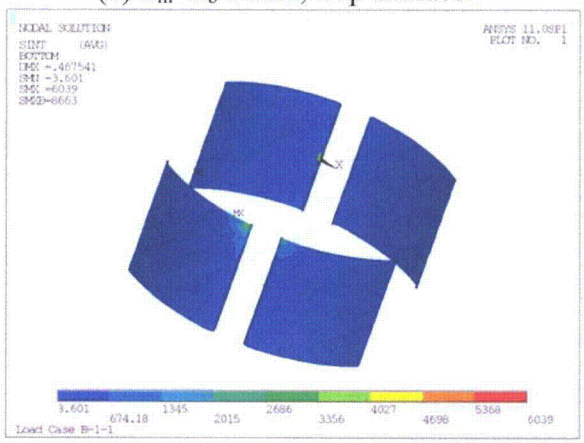

(c) P_m+P_b Stress, Bottom Surface

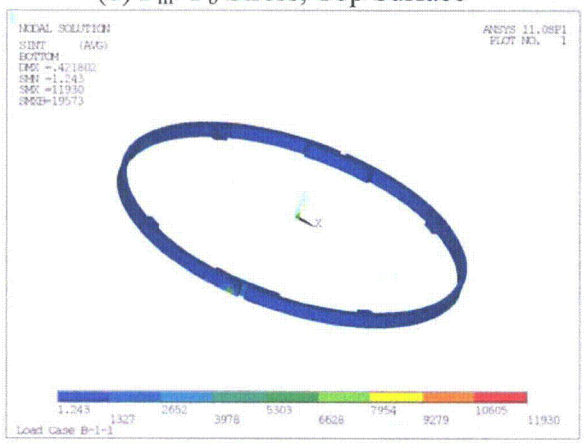

(c) P_m+P_b Stress, Bottom Surface

Figure 6-65: Drain Channels, Stress Intensity, Case B-3(b)

Figure 6-66: Upper Support Ring, Stress Intensity, Case B-3(b)

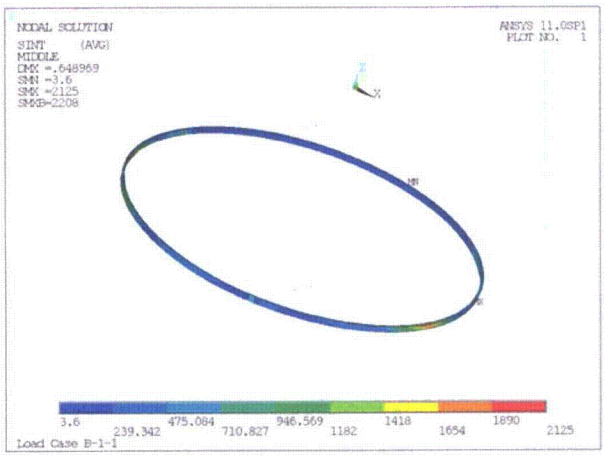

(a) Membrane Stress

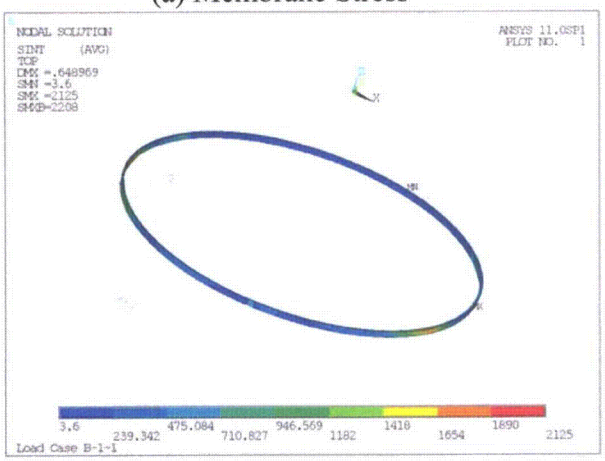

(b) P_m+P_b Stress, Top Surface

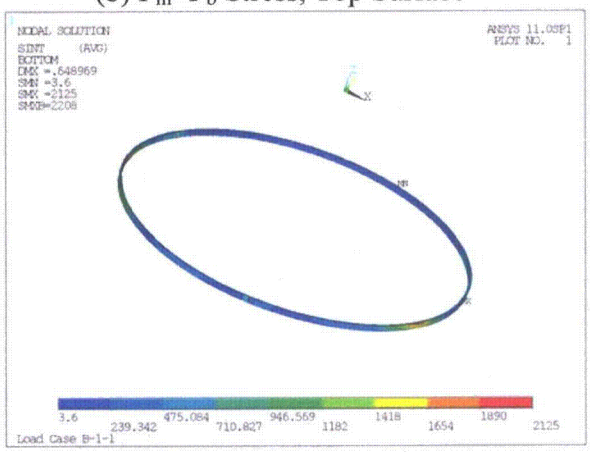

(c) P_m+P_b Stress, Bottom Surface

Figure 6-67: Lower Support Ring, Stress Intensity, Case B-3(b)

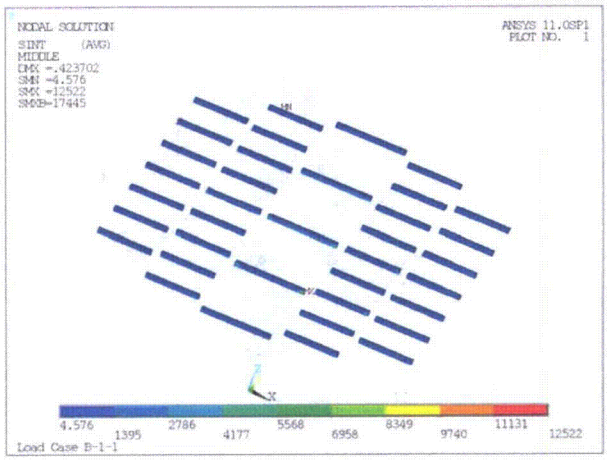

(a) Membrane Stress

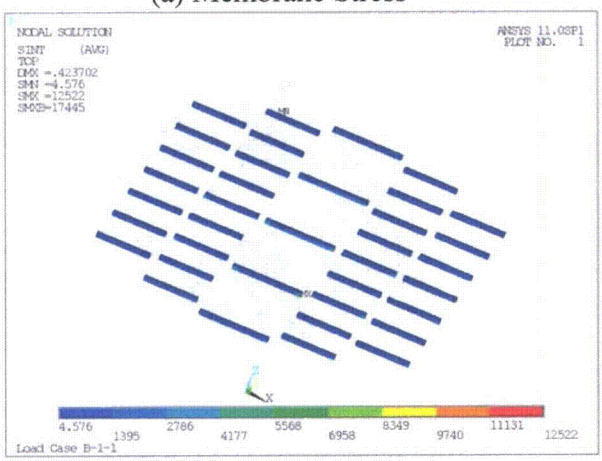

(b) P_m+P_b Stress, Top Surface

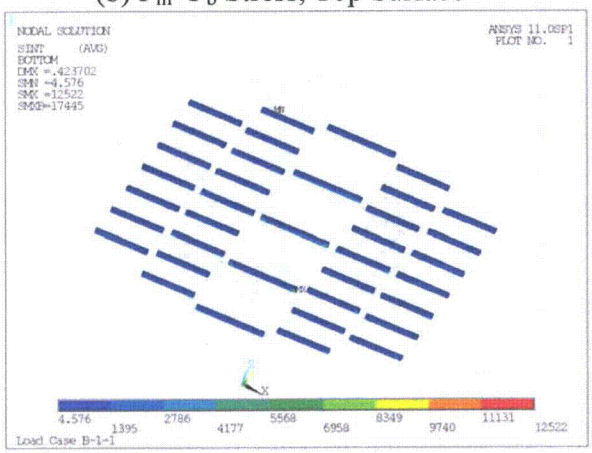

(c) P_m+P_b Stress, Bottom Surface

Figure 6-68: Tie Bars, Stress Intensity, Case B-3 (b)

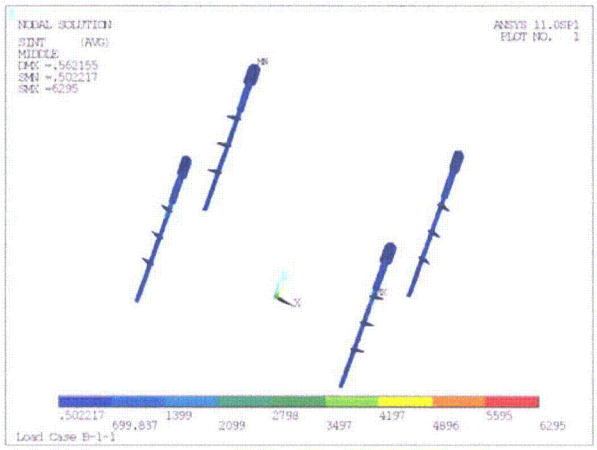

(a) Membrane Stress

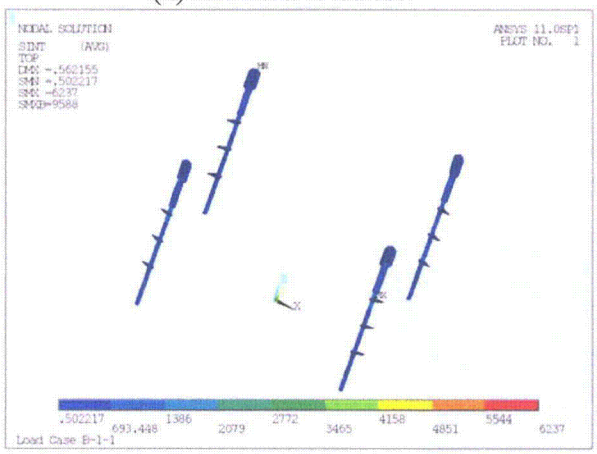

(b) P_m+P_b Stress, Top Surface

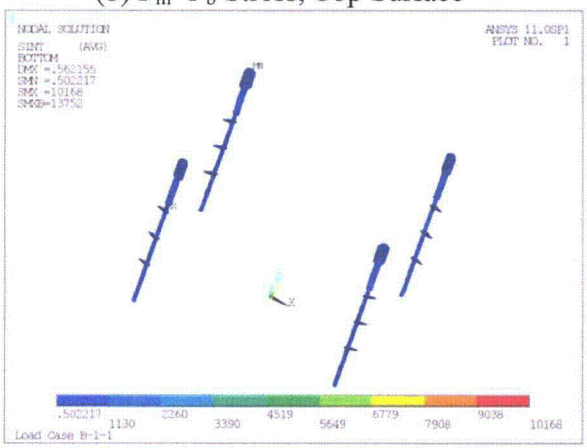

(c) P_m+P_b Stress, Bottom Surface

Figure 6-69: Lifting Rods, Stress Intensity, Case B-3(b)

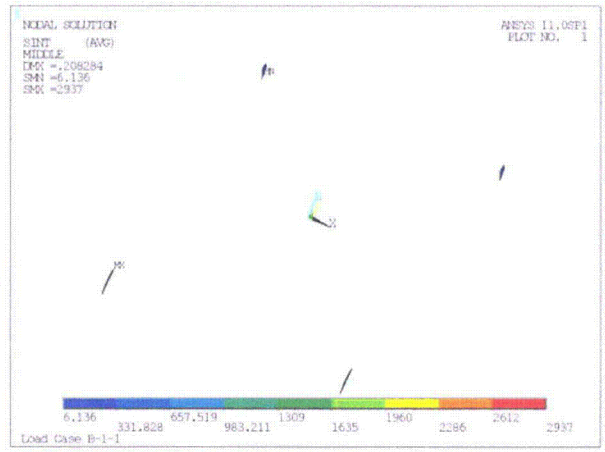

(a) Membrane Stress

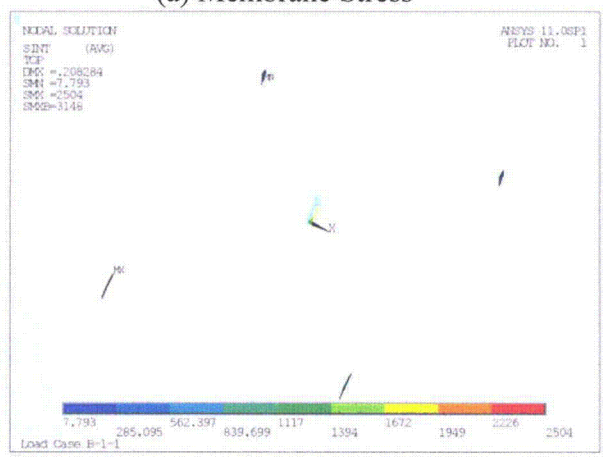

(b) P_m+P_b Stress, Top Surface

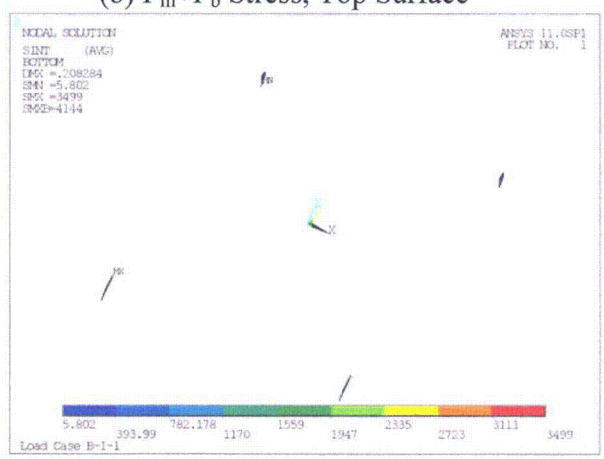

(c) P_m+P_b Stress, Bottom Surface

Figure 6-70: Gussets in Upper Support Ring, Stress Intensity, Case B-3(b)

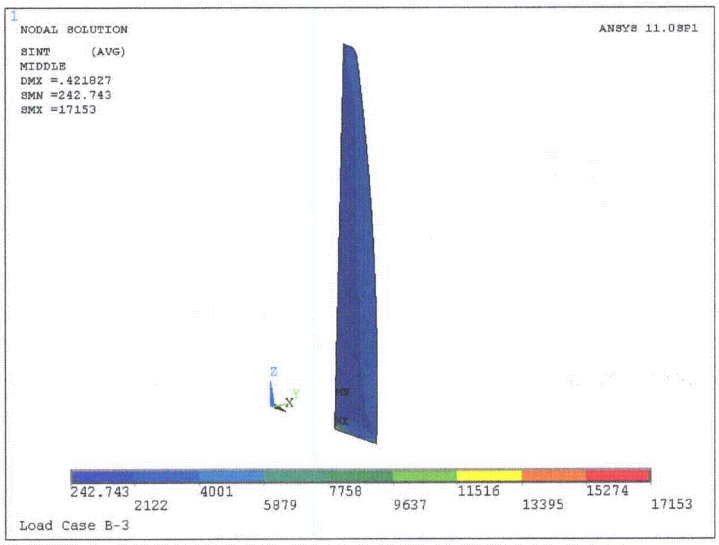

(a) Stress Distribution

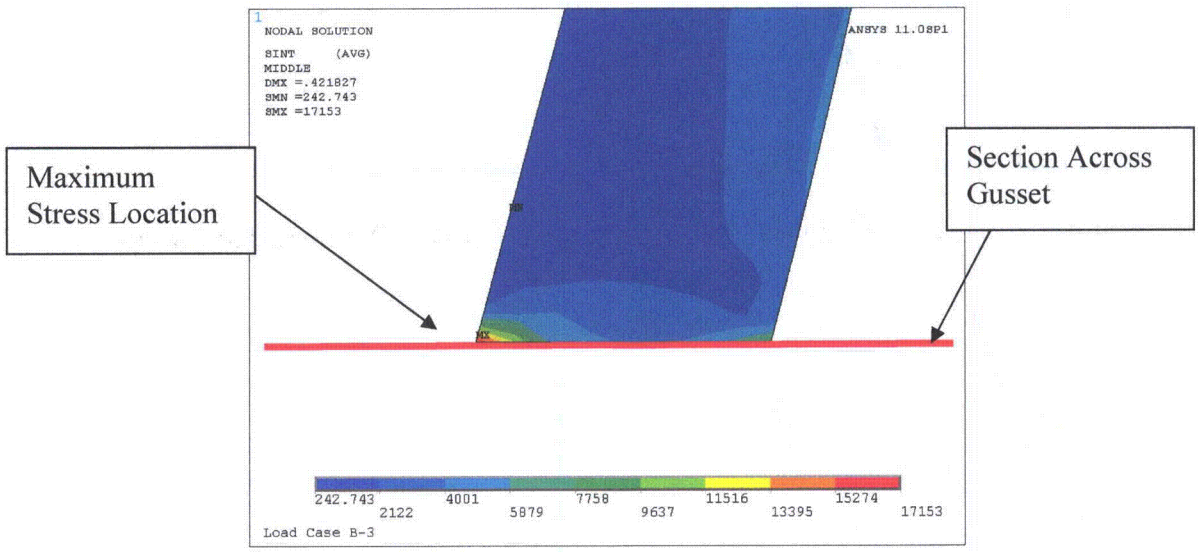

(b) Zoom in View of Localized Maximum Stress

Figure 6-71: Gussets in Hoods with the Maximum Stress Intensity, Case B-3(a)

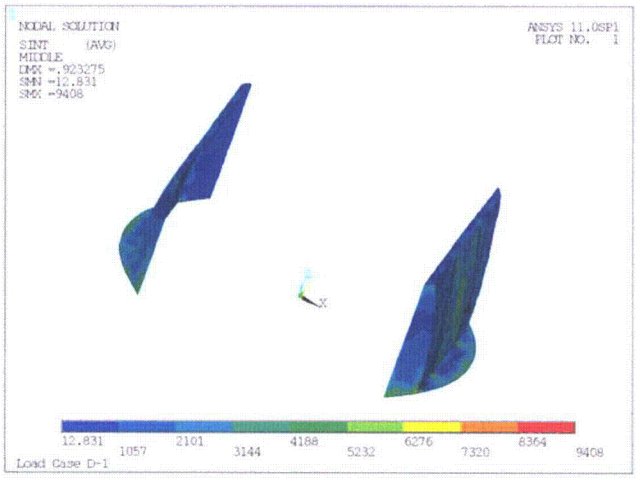

(a) Membrane Stress

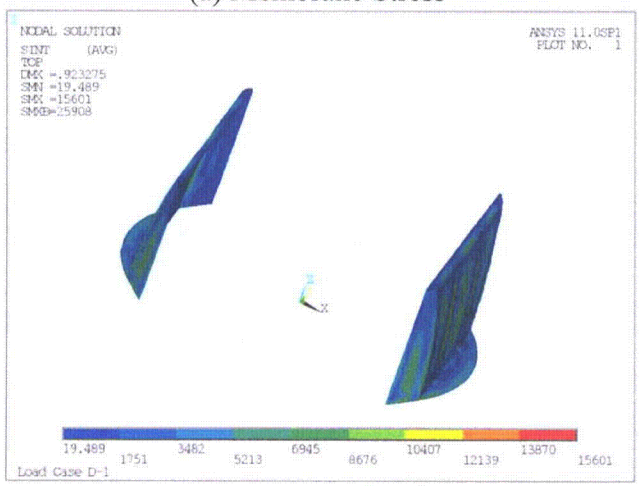

(b) $P_m + P_b$ Stress, Top Surface

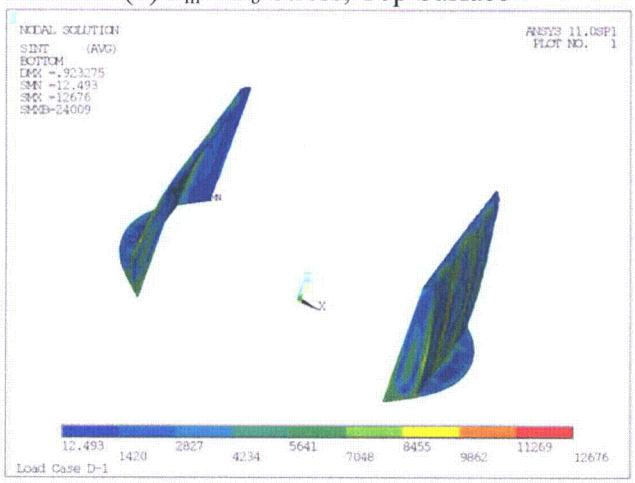

(c) $P_m + P_b$ Stress, Bottom Surface

Figure 6-72: Outer Hoods, Stress Intensity, Case D-1 (a)

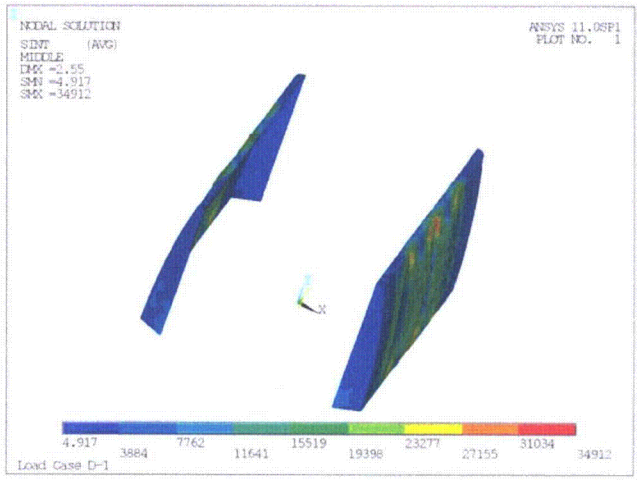

(a) Membrane Stress

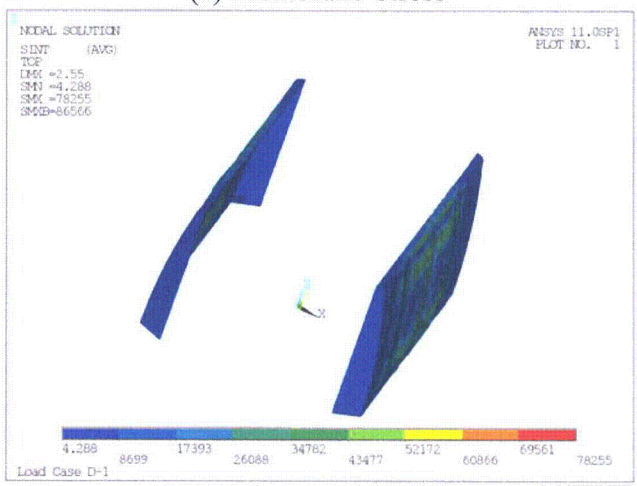

(b) $P_m + P_b$ Stress, Top Surface

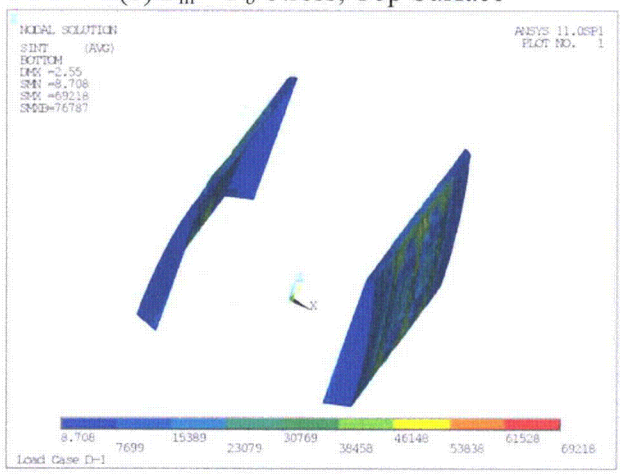

(c) $P_m + P_b$ Stress, Bottom Surface

Figure 6-73: Middle Hoods, Stress Intensity, Case D-1 (a)

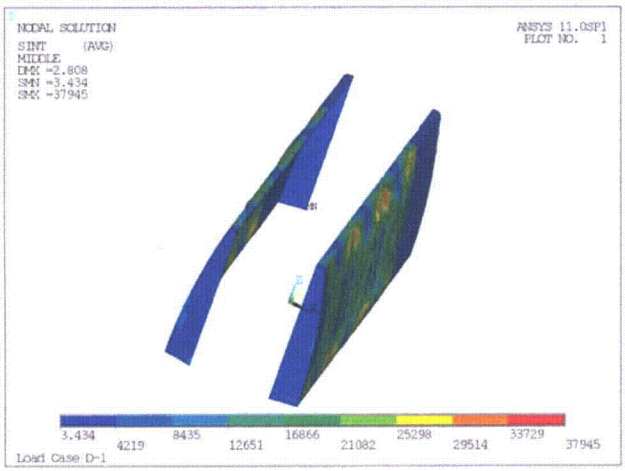

(a) Membrane Stress

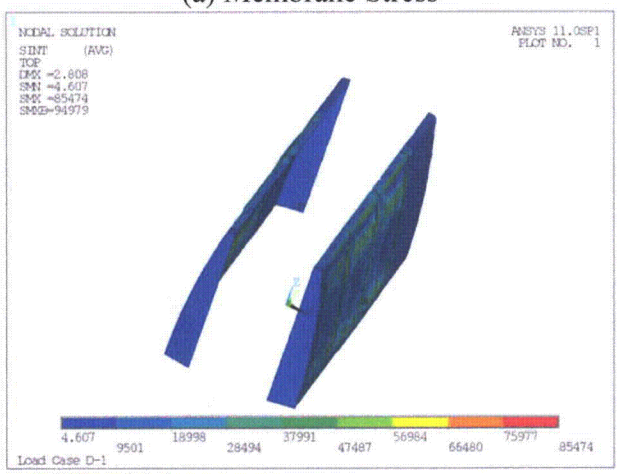

(b) $P_m + P_b$ Stress, Top Surface

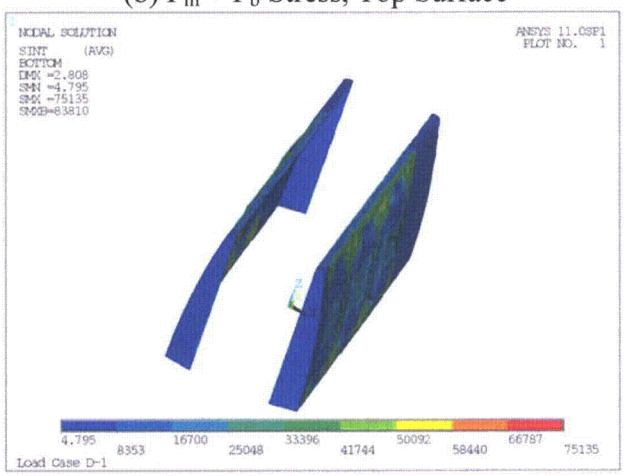

(c) $P_m + P_b$ Stress, Bottom Surface

Figure 6-74: Inside Hoods, Stress Intensity, Case D-1(a)

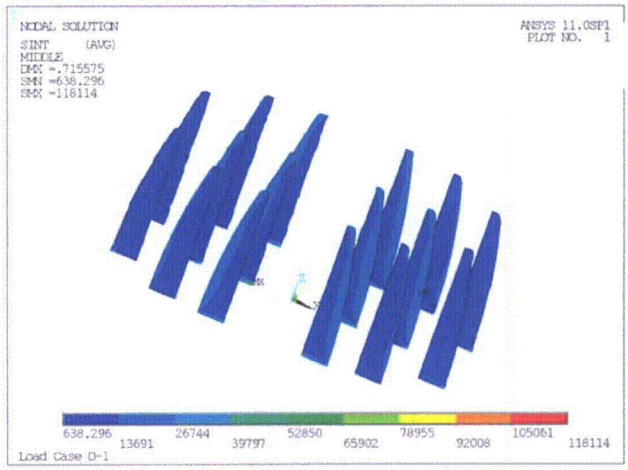

(a) Membrane Stress

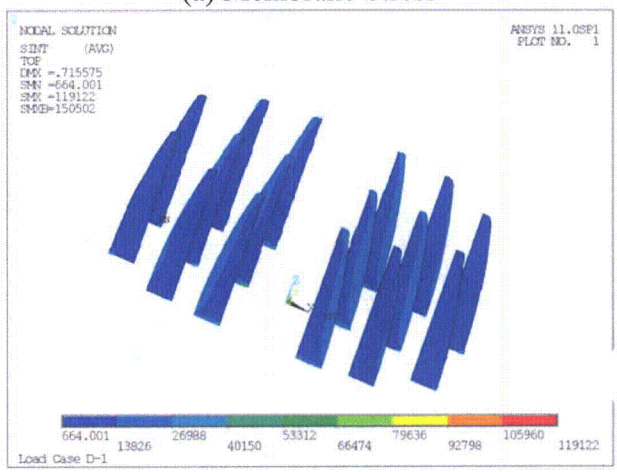

(b) $P_m + P_b$ Stress, Top Surface

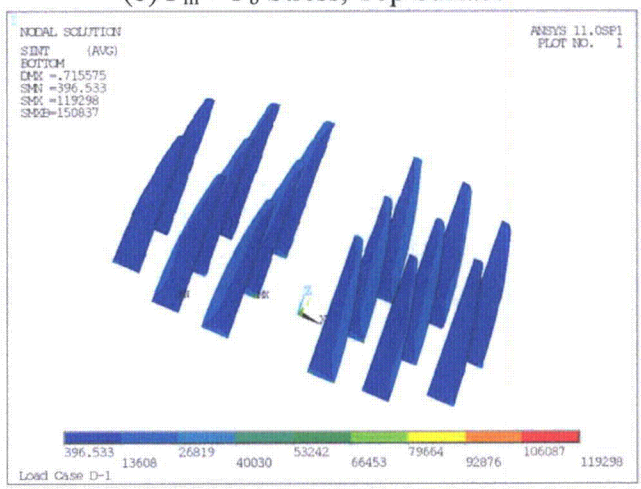

(c) $P_m + P_b$ Stress, Bottom Surface

Figure 6-75: Gussets in Hoods, Stress Intensity, Case D-1(a)

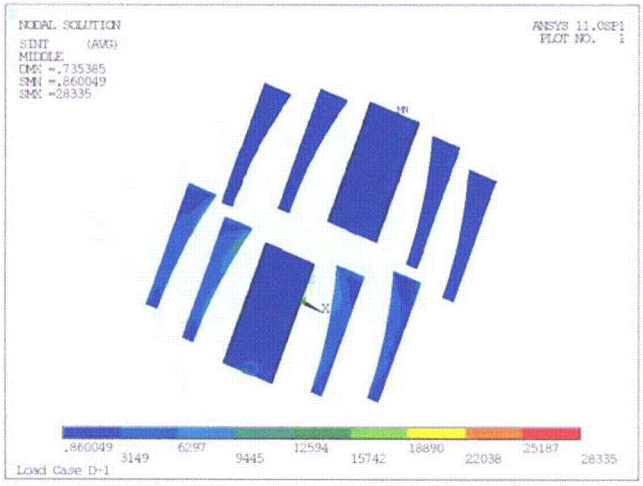

(a) Membrane Stress

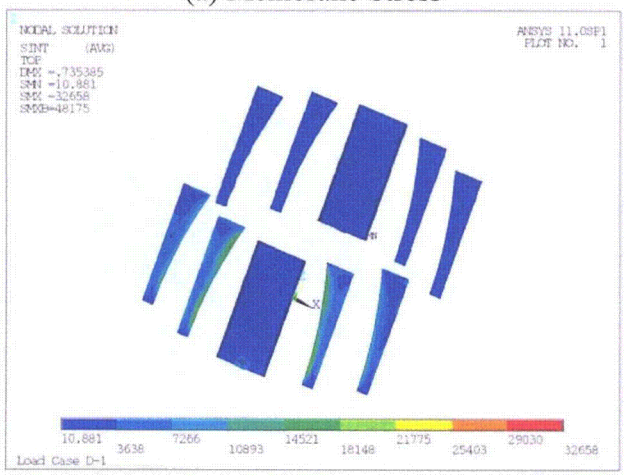

(b) $P_m + P_b$ Stress, Top Surface

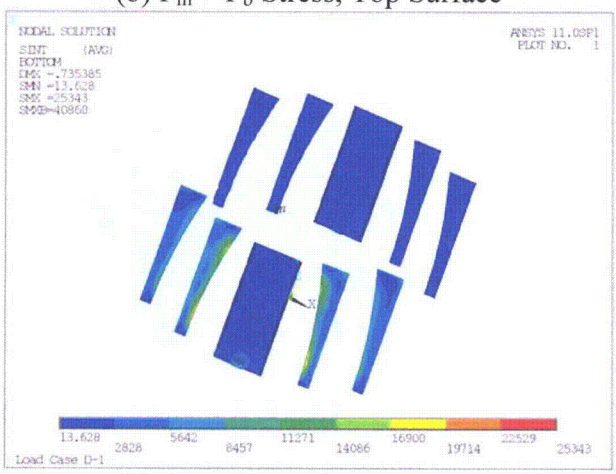

(c) $P_m + P_b$ Stress, Bottom Surface

Figure 6-76: Side Plates, Stress Intensity, Case D-1(a)

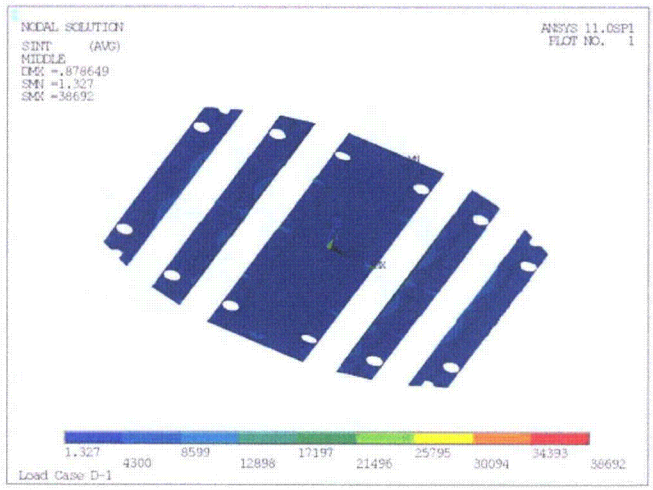

(a) Membrane Stress

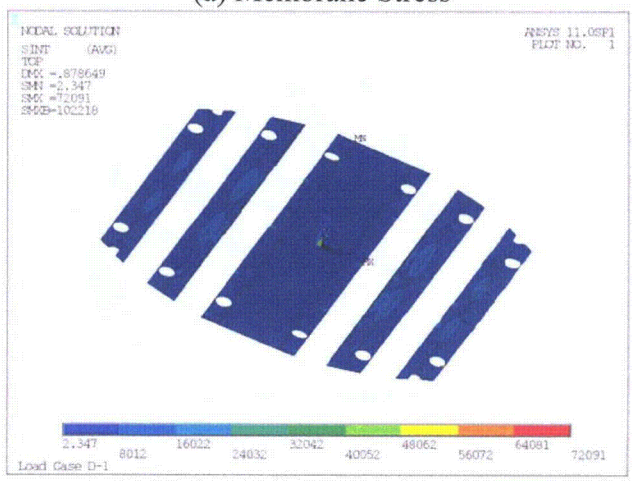

(b) $P_m + P_b$ Stress, Top Surface

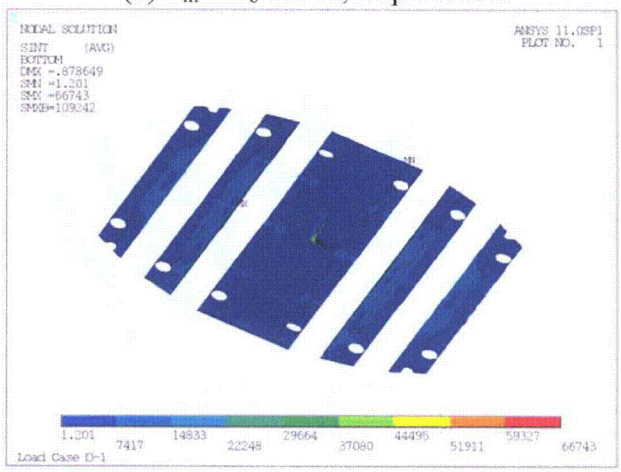

(c) $P_m + P_b$ Stress, Bottom Surface

Figure 6-77: Vane Bank Base Plates, Stress Intensity, Case D-1 (a)

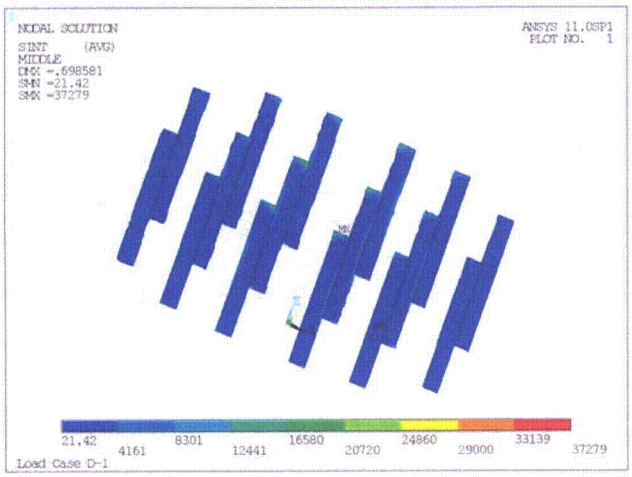

(a) Membrane Stress

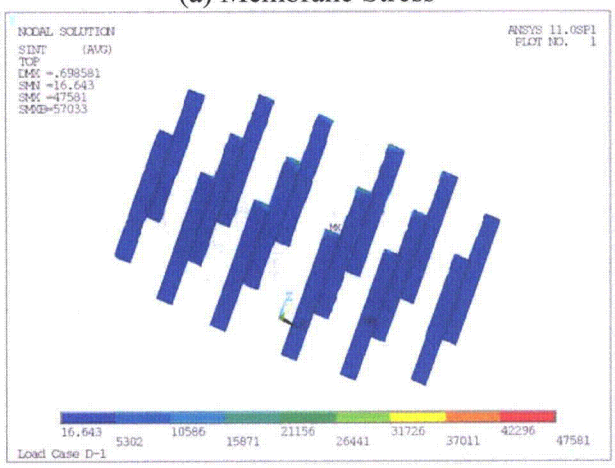

(b) $P_m + P_b$ Stress, Top Surface

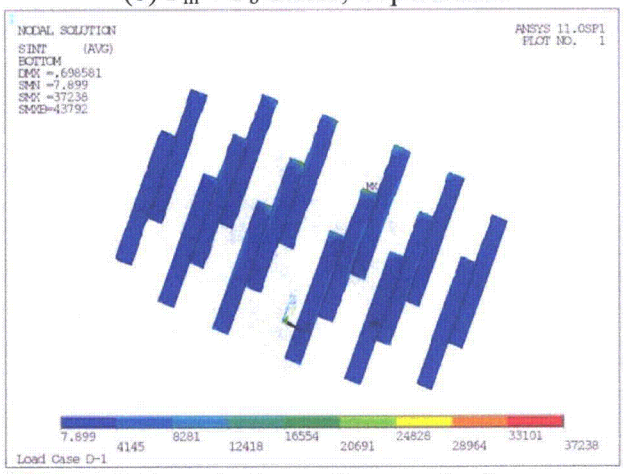

(c) $P_m + P_b$ Stress, Bottom Surface

Figure 6-78: Vane Bank Vertical Plates, Stress Intensity, Case D-1(a)

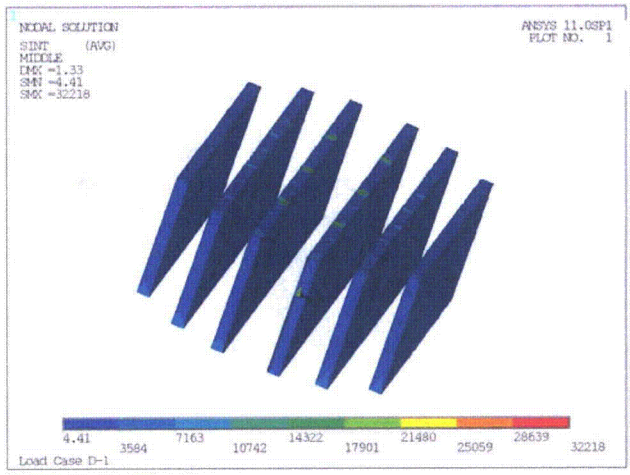

(a) Membrane Stress

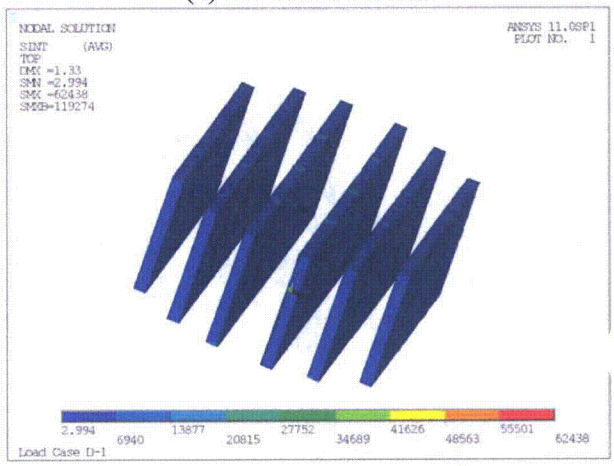

(b) $P_m + P_b$ Stress, Top Surface

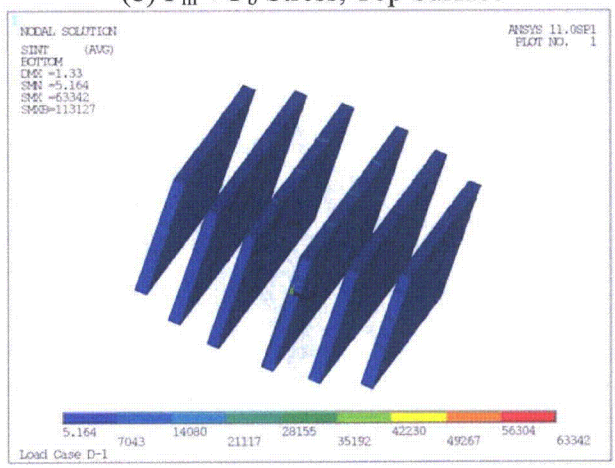

(c) $P_m + P_b$ Stress, Bottom Surface

Figure 6-79: Vane Banks, Stress Intensity, Case D-1(a)

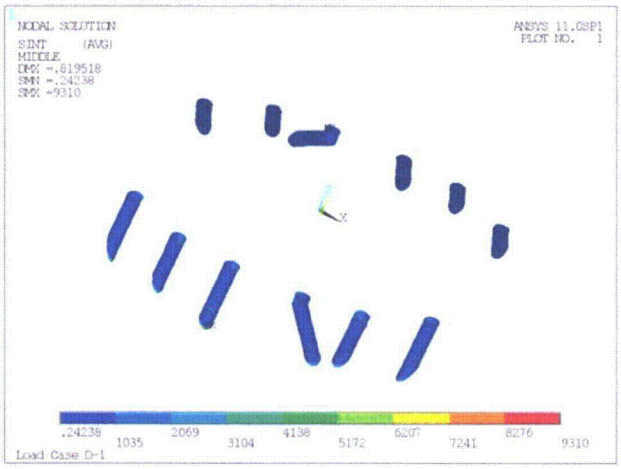

(a) Membrane Stress

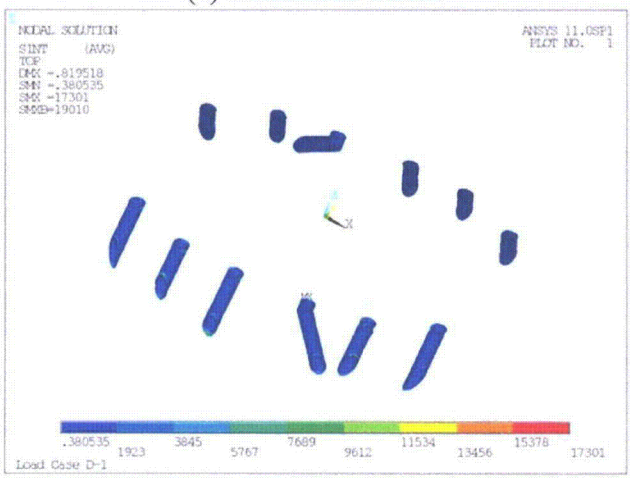

(b) $P_m + P_b$ Stress, Top Surface

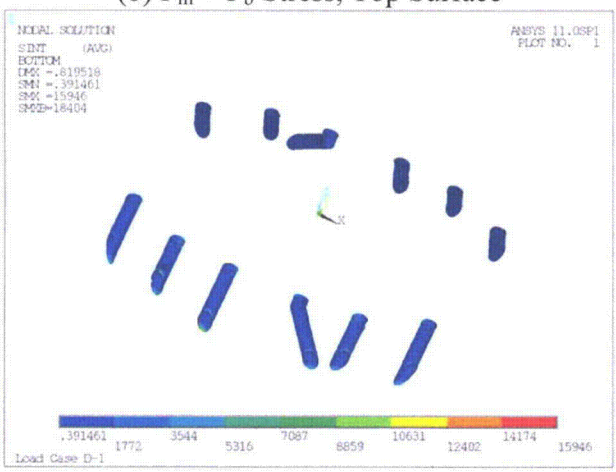

(c) $P_m + P_b$ Stress, Bottom Surface

Figure 6-80: Drain Pipes, Stress Intensity, Case D-1(a)

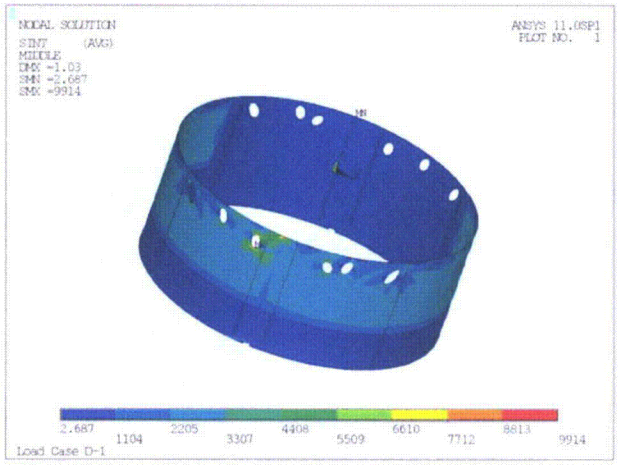

(a) Membrane Stress

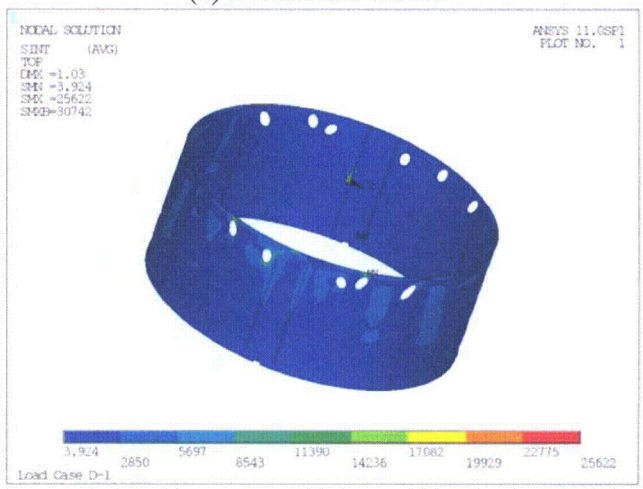

(b) $P_m + P_b$ Stress, Top Surface

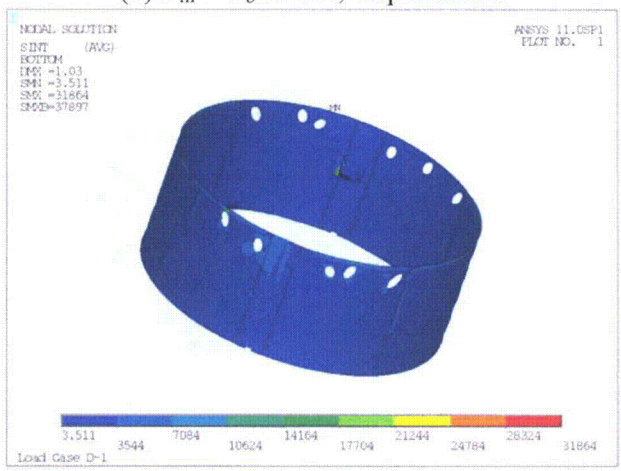

(c) $P_m + P_b$ Stress, Bottom Surface

Figure 6-81: Skirt, Stress Intensity, Case D-1(a)

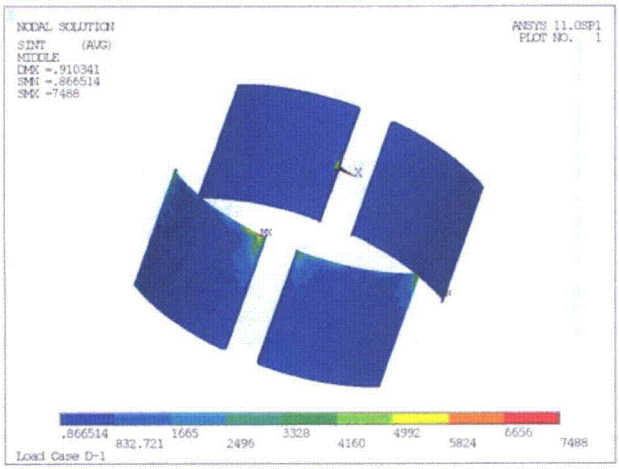

(a) Membrane Stress

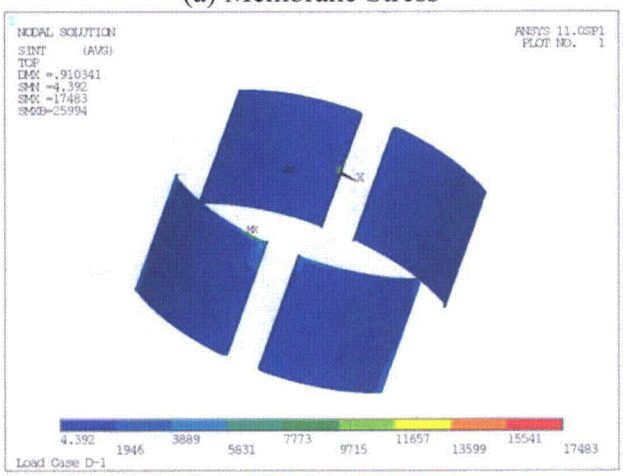

(b) $P_m + P_b$ Stress, Top Surface

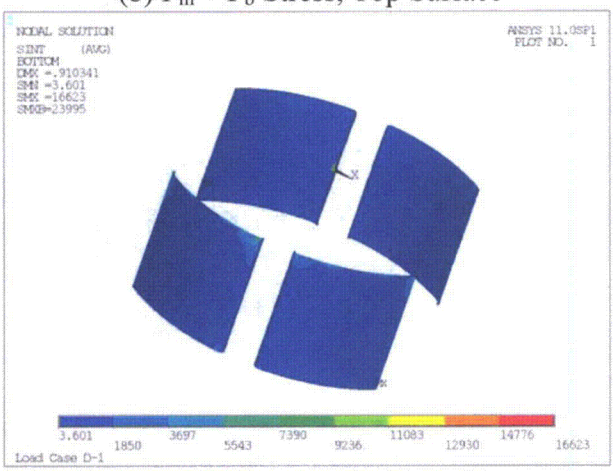

(c) $P_m + P_b$ Stress, Bottom Surface

Figure 6-82: Drain Channels, Stress Intensity, Case D-1 (a)

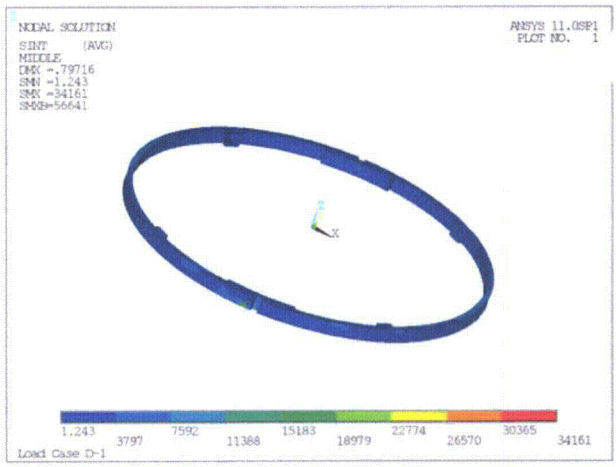

(a) Membrane Stress

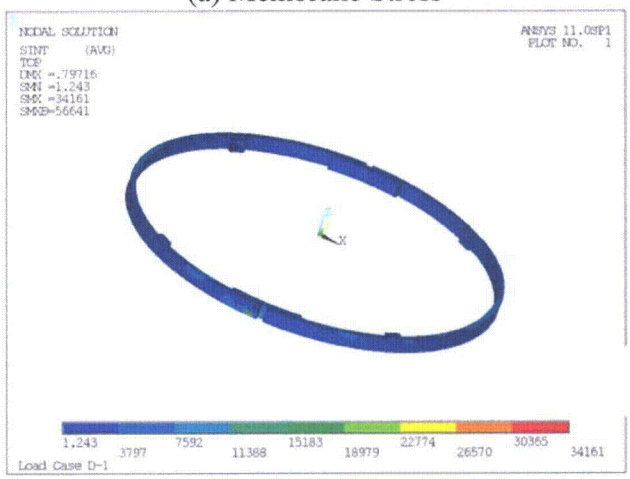

(b) $P_m + P_b$ Stress, Top Surface

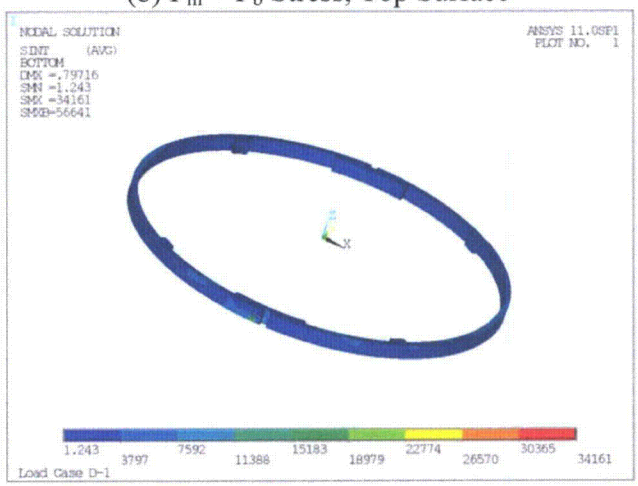

(c) $P_m + P_b$ Stress, Bottom Surface

Figure 6-83: Upper Support Ring, Stress Intensity, Case D-1(a)

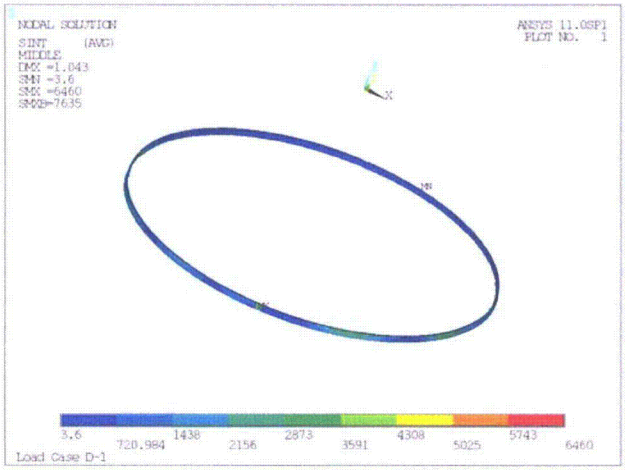

(a) Membrane Stress

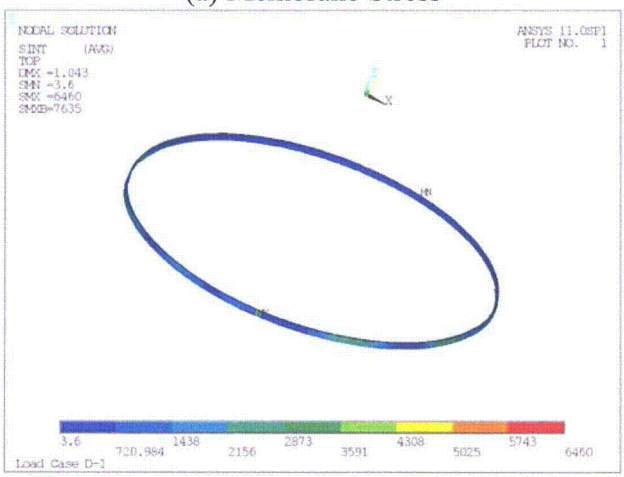

(b) $P_m + P_b$ Stress, Top Surface

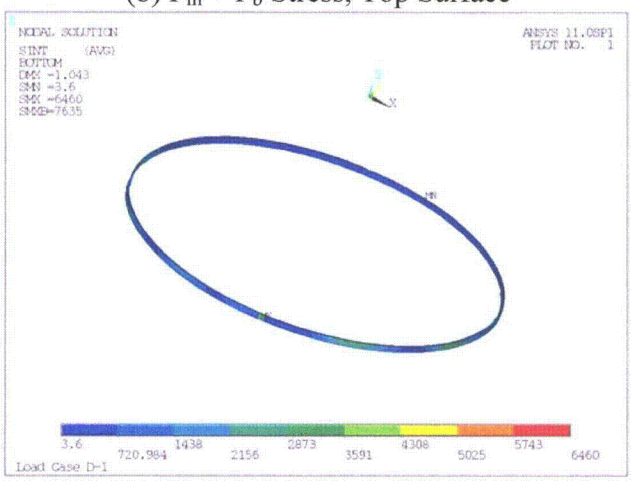

(c) $P_m + P_b$ Stress, Bottom Surface

Figure 6-84: Lower Support Ring, Stress Intensity, Case D-1(a)

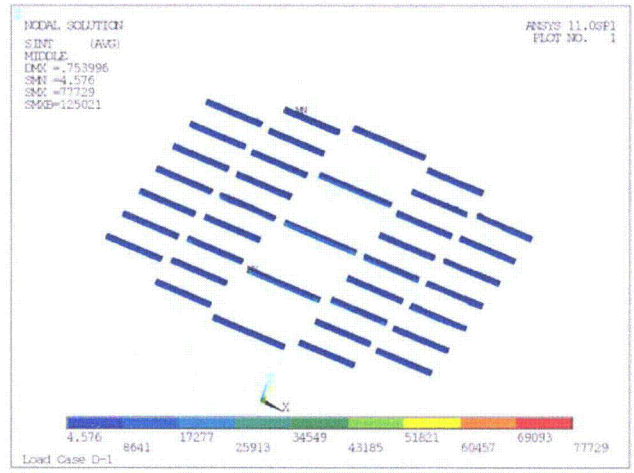

(a) Membrane Stress

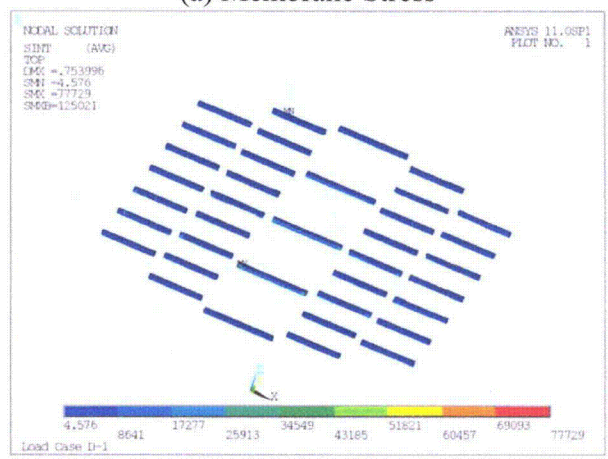

(b) $P_m + P_b$ Stress, Top Surface

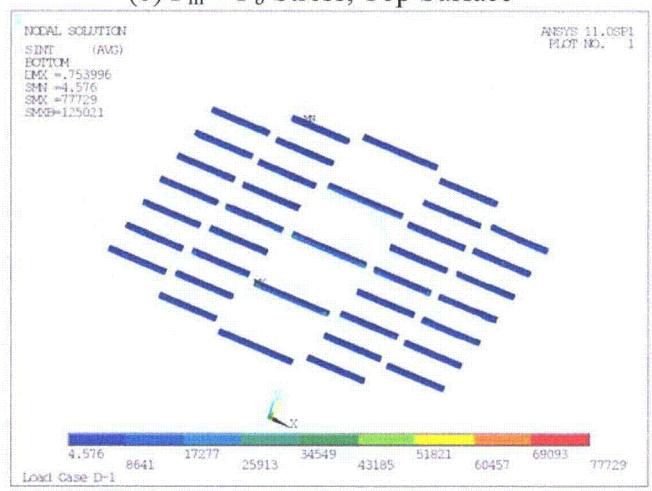

(c) $P_m + P_b$ Stress, Bottom Surface

Figure 6-85: Tie Bars, Stress Intensity, Case D-1(a)

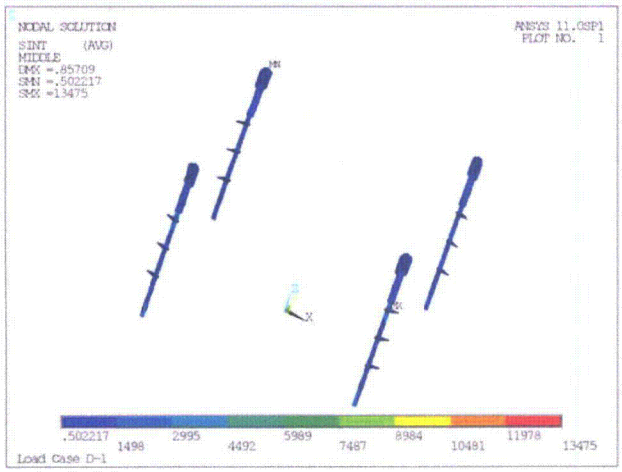

(a) Membrane Stress

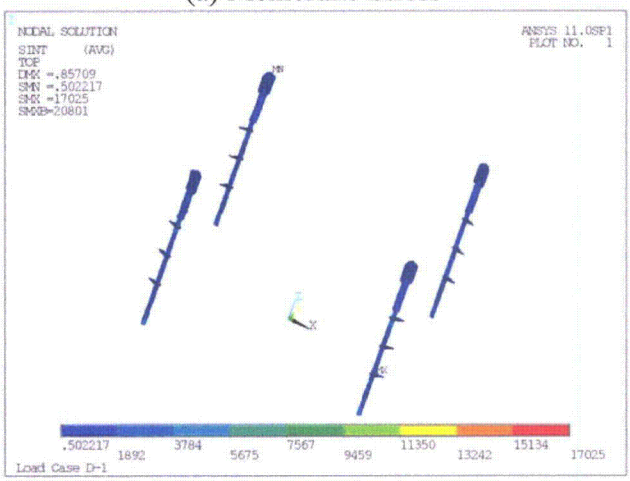

(b) $P_m + P_b$ Stress, Top Surface

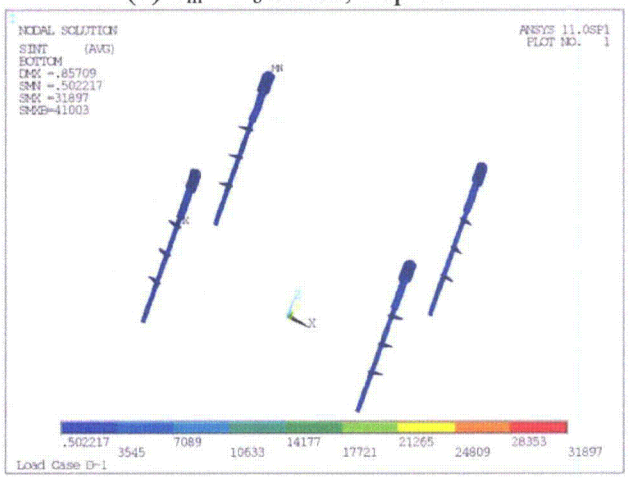

(c) $P_m + P_b$ Stress, Bottom Surface

Figure 6-86: Lifting Rods, Stress Intensity, Case D-1 (a)

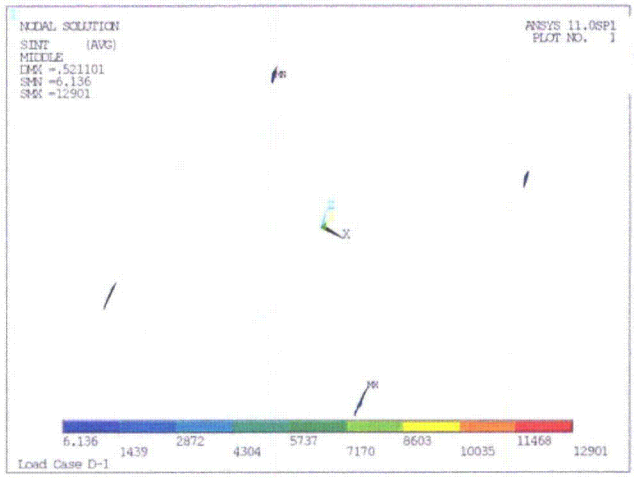

(a) Membrane Stress

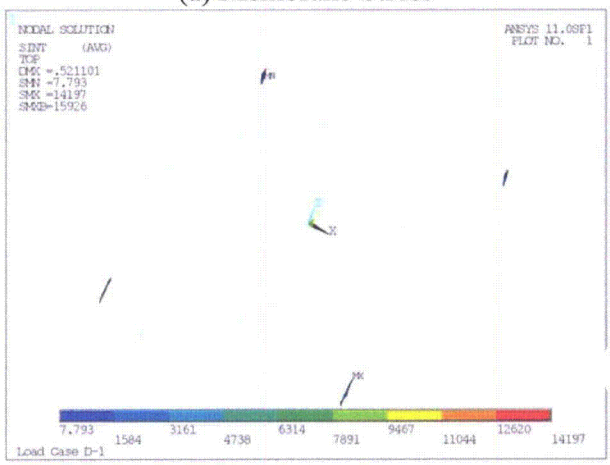

(b) $P_m + P_b$ Stress, Top Surface

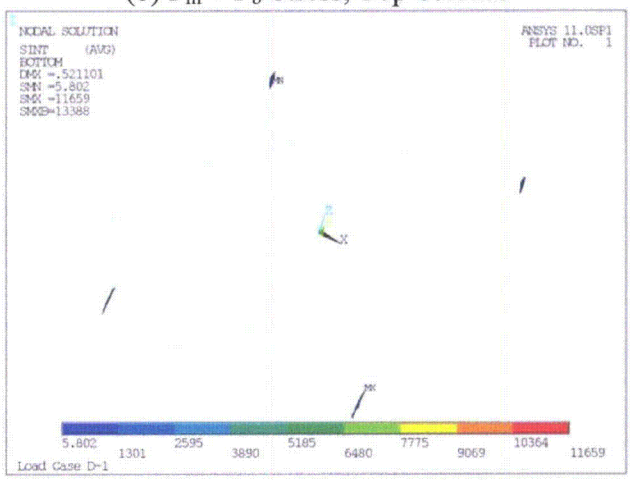

(c) $P_m + P_b$ Stress, Bottom Surface

Figure 6-87: Gussets in Upper Support Ring, Stress Intensity, Case D-1 (a)

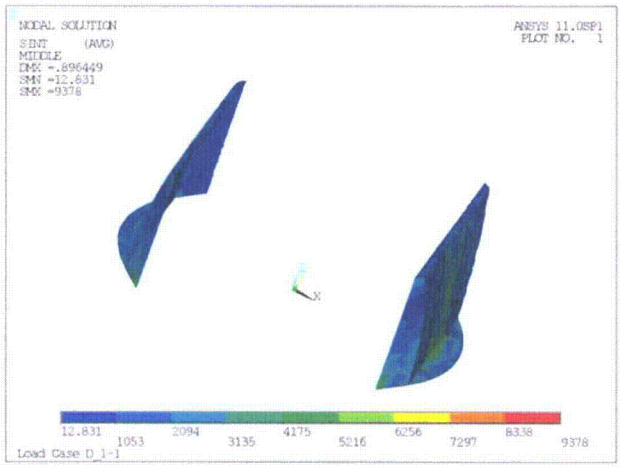

(a) Membrane Stress

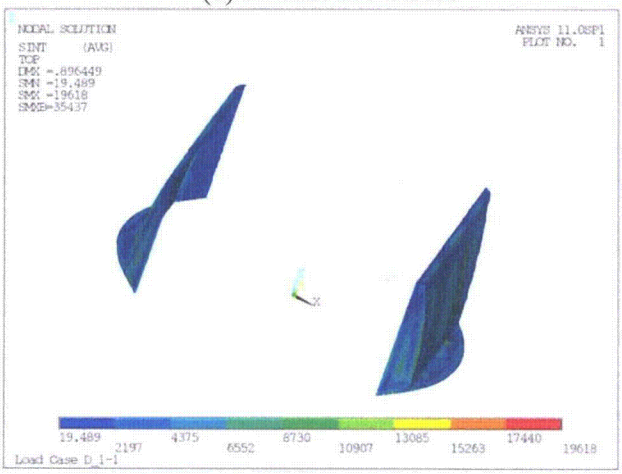

(b) P_m+P_b Stress, Top Surface

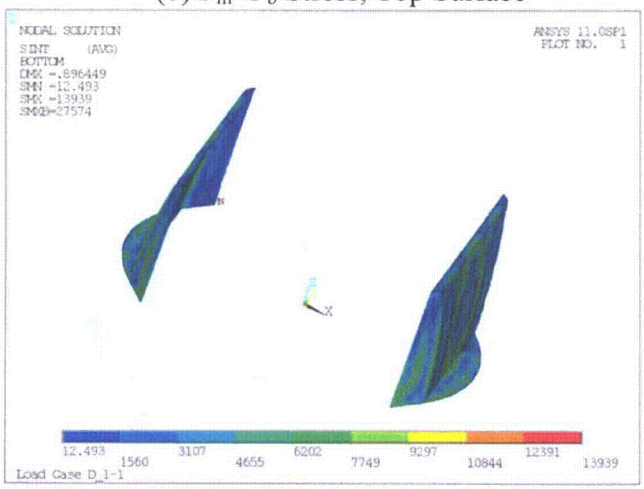

(c) P_m+P_b Stress, Bottom Surface

Figure 6-88: Outer Hoods, Stress Intensity, Case D-1(b)

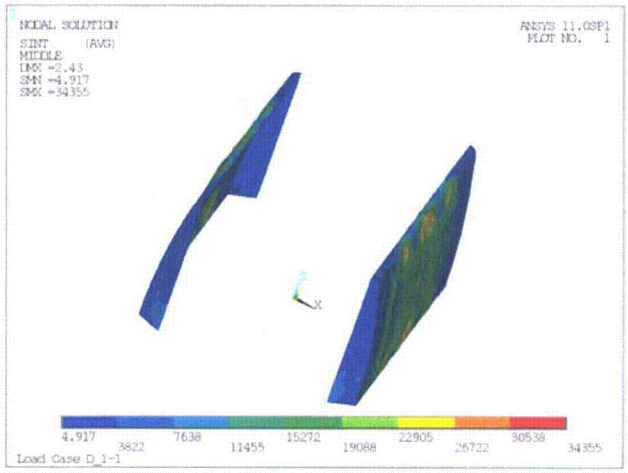

(a) Membrane Stress

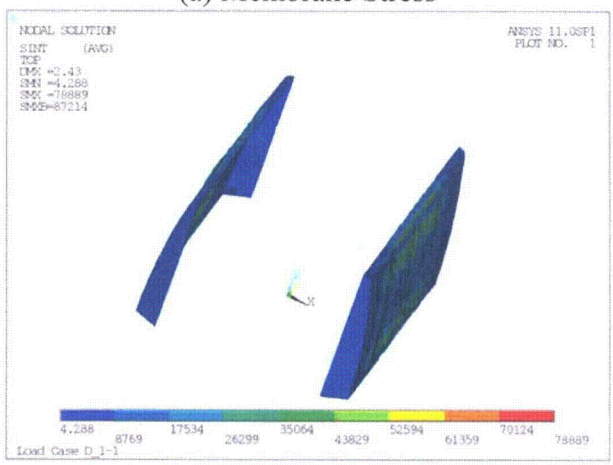

(b) P_m+P_b Stress, Top Surface

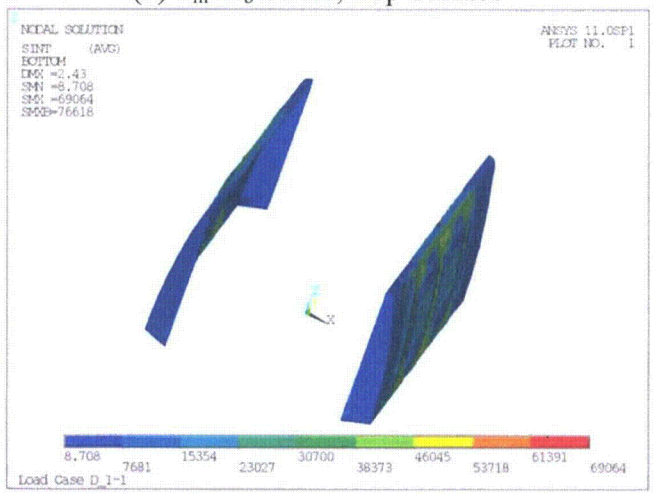

(c) P_m+P_b Stress, Bottom Surface

Figure 6-89: Middle, Hoods, Stress Intensity, Case D-1(b)

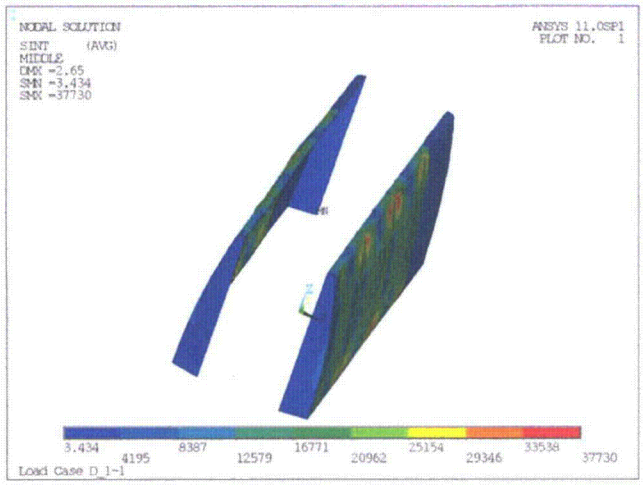

(a) Membrane Stress

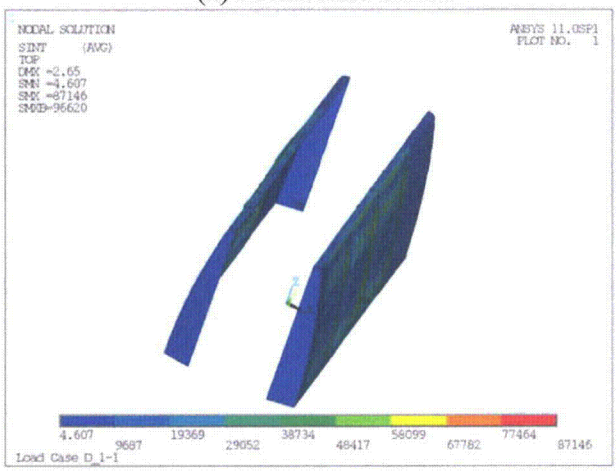

(b) P_m+P_b Stress, Top Surface

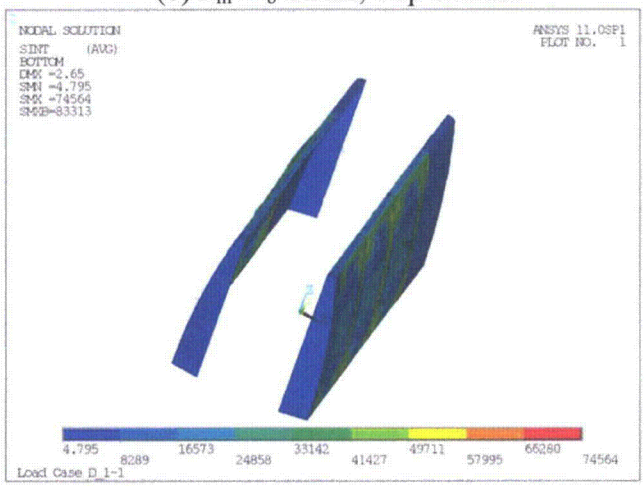

(c) P_m+P_b Stress, Bottom Surface

Figure 6-90: Inside Hoods, Stress Intensity, Case D-1(b)

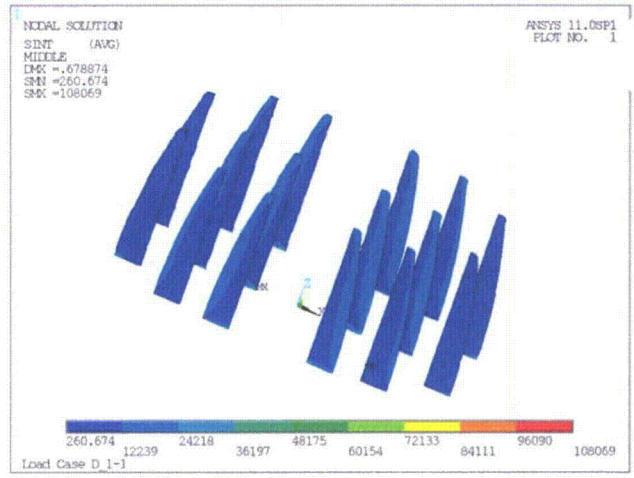

(a) Membrane Stress

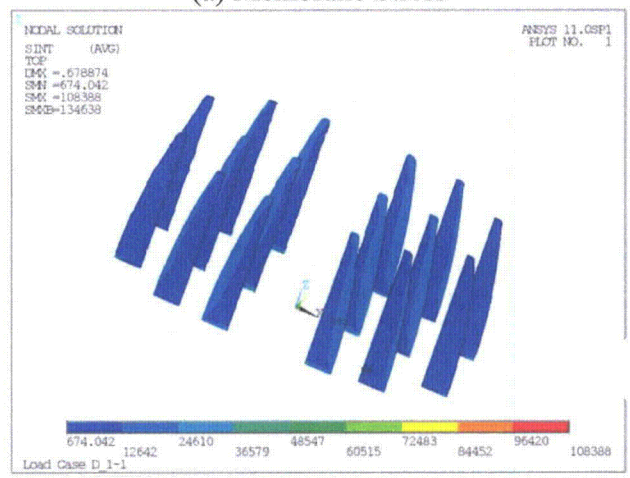

(b) P_m+P_b Stress, Top Surface

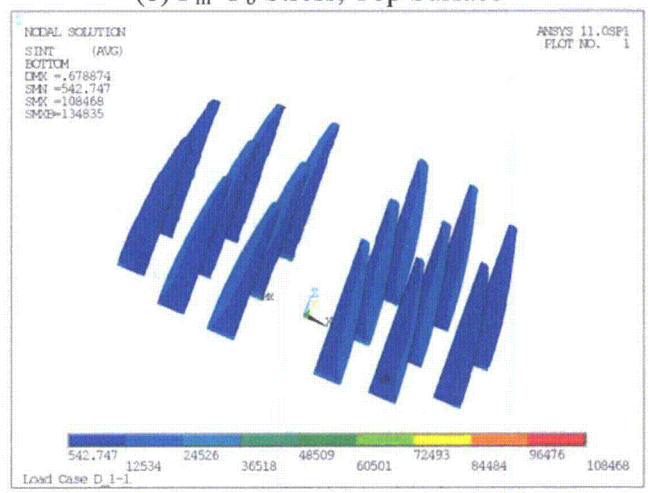

(c) P_m+P_b Stress, Bottom Surface

Figure 6-91: Gussets Inside Hoods, Stress Intensity, Case D-1(b)

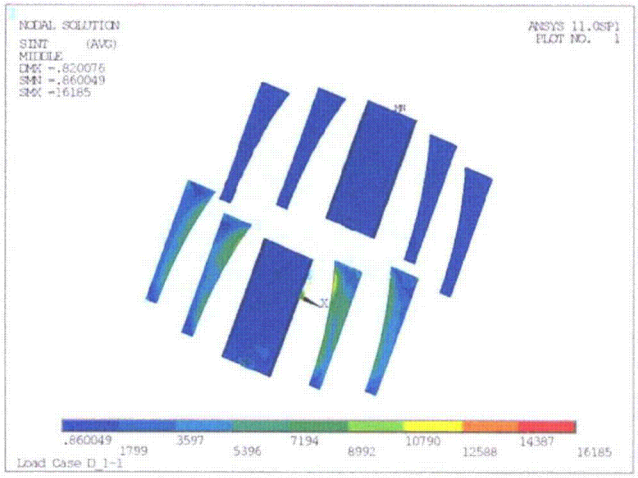

(a) Membrane Stress

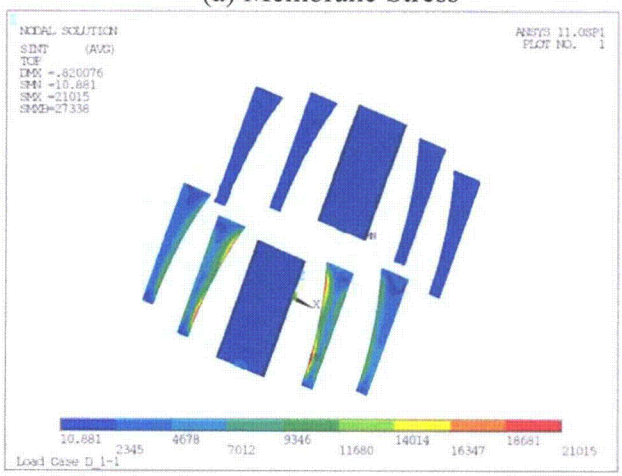

(b) P_m+P_b Stress, Top Surface

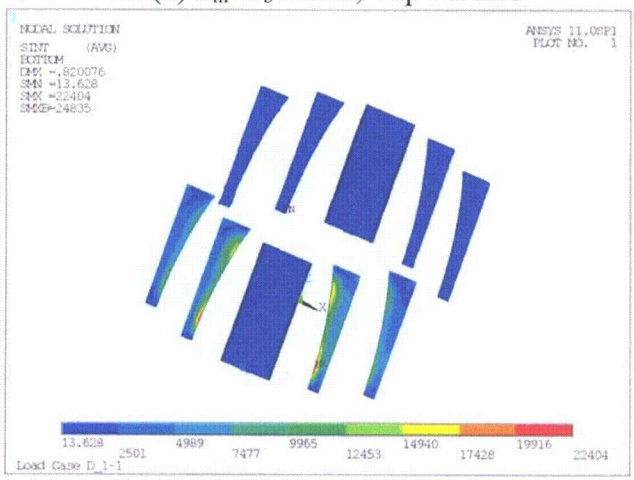

(c) P_m+P_b Stress, Bottom Surface

Figure 6-92: Side Plates, Stress Intensity, Case D-1(b)

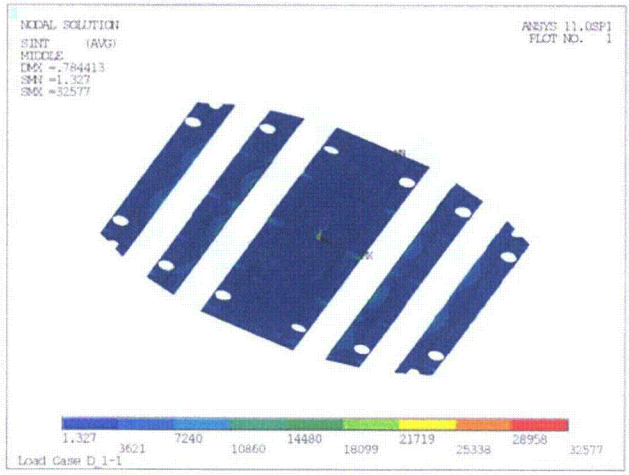

(a) Membrane Stress

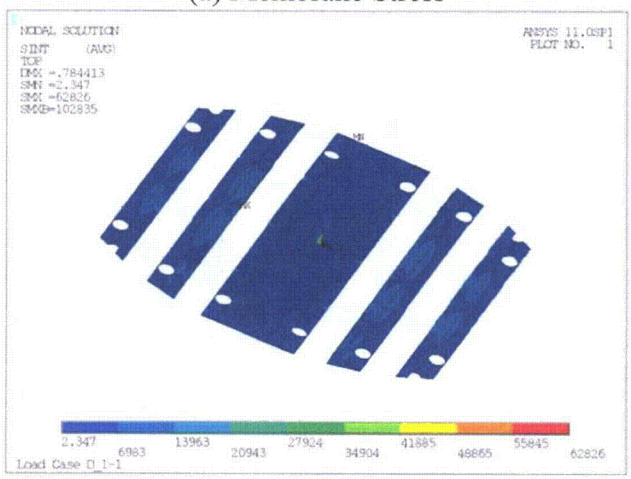

(b) P_m+P_b Stress, Top Surface

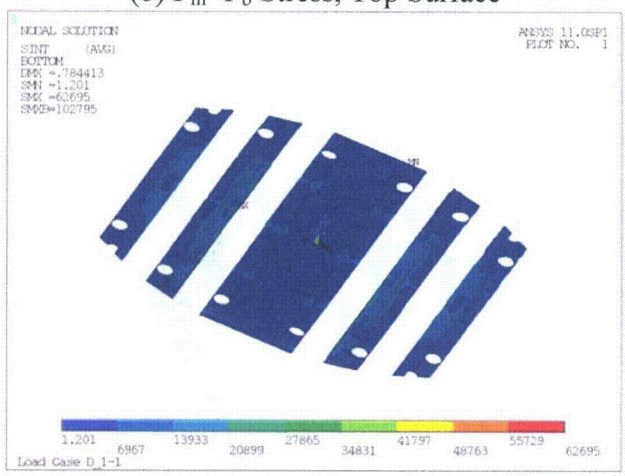

(c) P_m+P_b Stress, Bottom Surface

Figure 6-93: Vane Bank Base Plates, Stress Intensity, Case D-1(b)

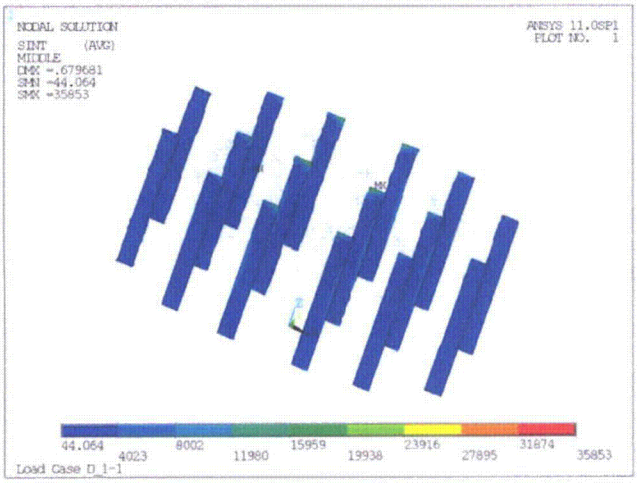

(a) Membrane Stress

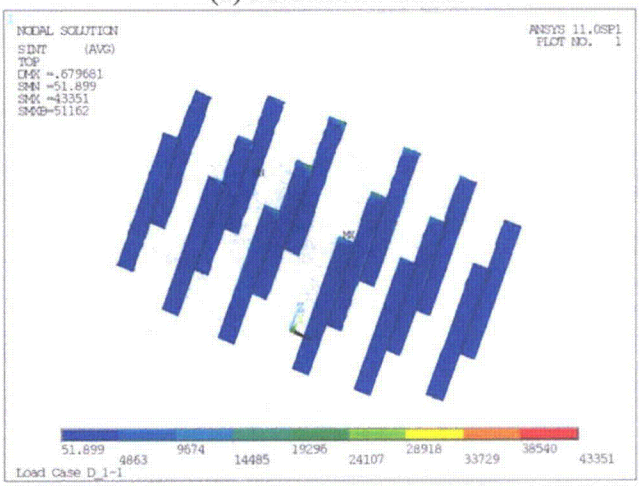

(b) P_m+P_b Stress, Top Surface

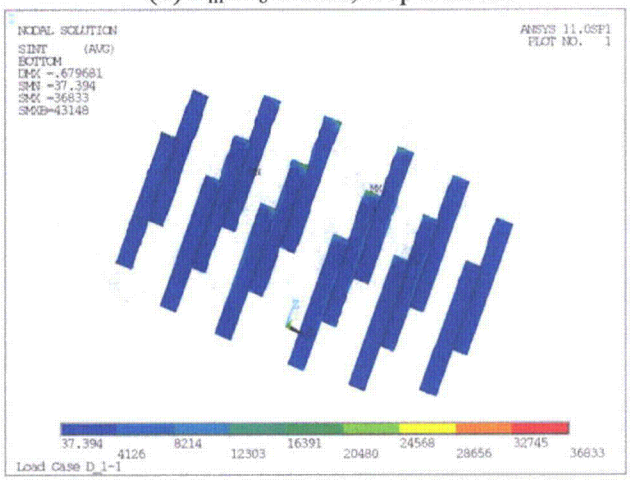

(c) P_m+P_b Stress, Bottom Surface

Figure 6-94: Vane Bank Vertical Plates, Stress Intensity, Case D-1(b)

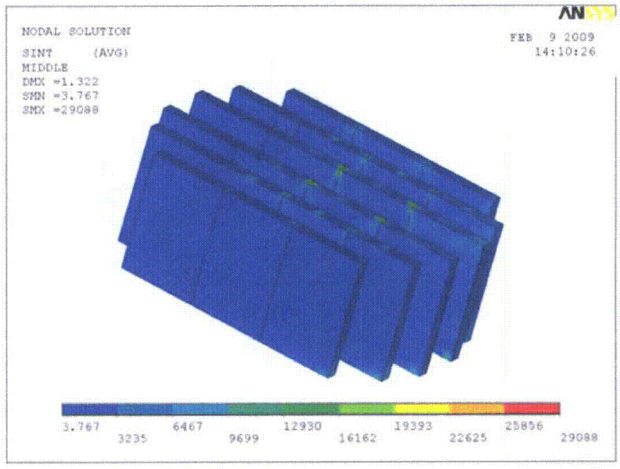

(a) Membrane Stress

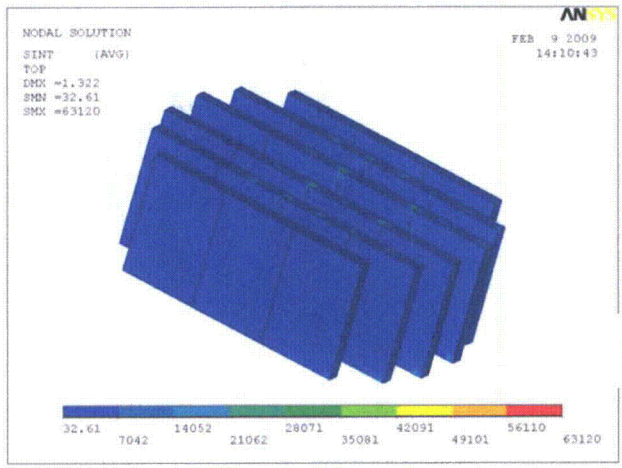

(b) P_m+P_b Stress, Top Surface

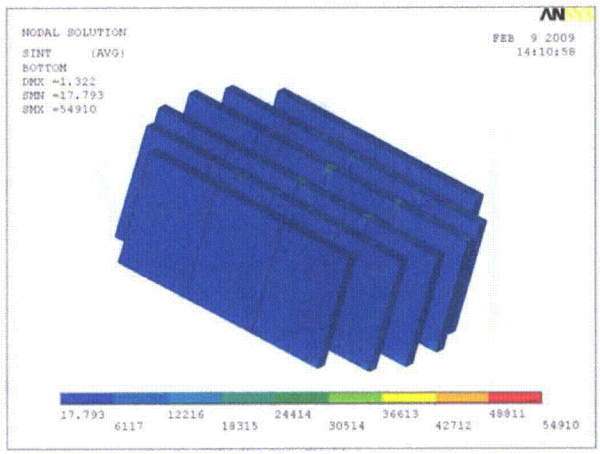

(c) P_m+P_b Stress, Bottom Surface

Figure 6-95: Vane Bank, Stress Intensity, Case D-1(b)

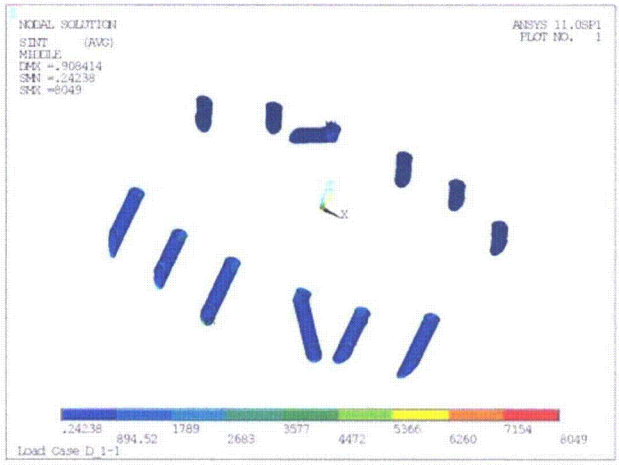

(a) Membrane Stress

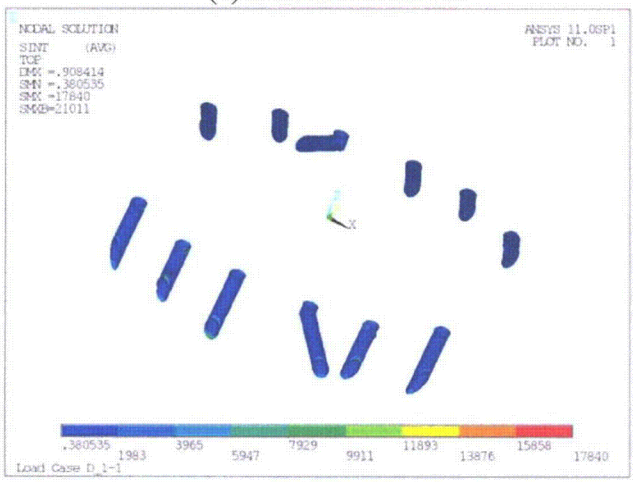

(b) P_m+P_b Stress, Top Surface

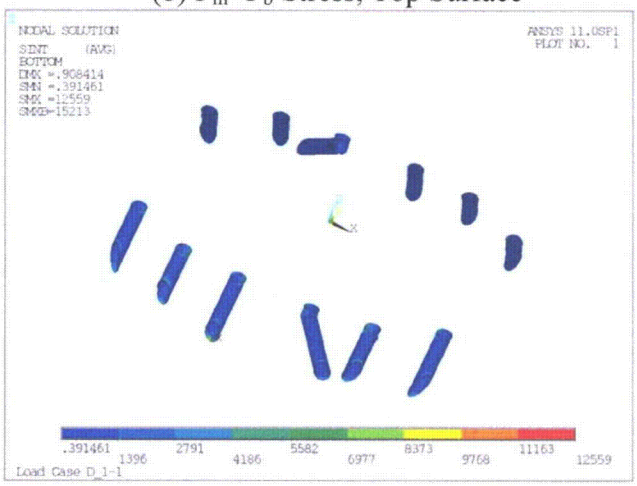

(c) P_m+P_b Stress, Bottom Surface

Figure 6-96: Drain Pipes, Stress Intensity, Case D-1(b)

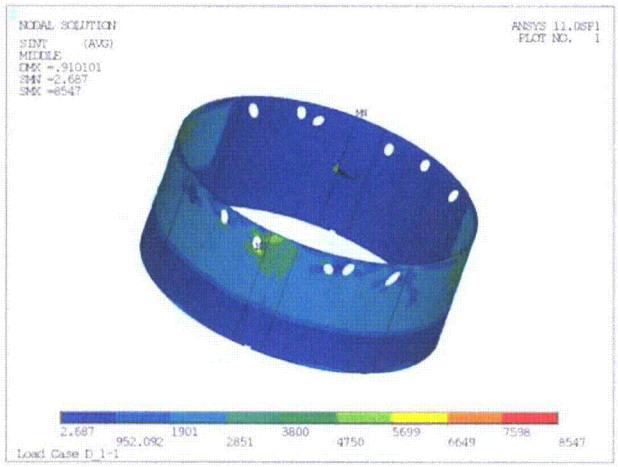

(a) Membrane Stress

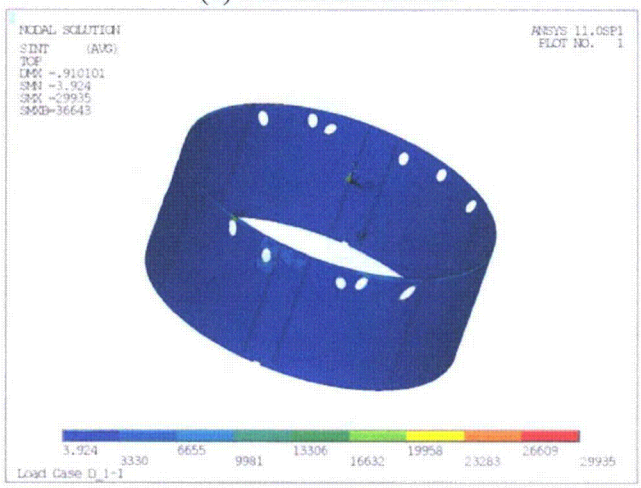

(b) P_m+P_b Stress, Top Surface

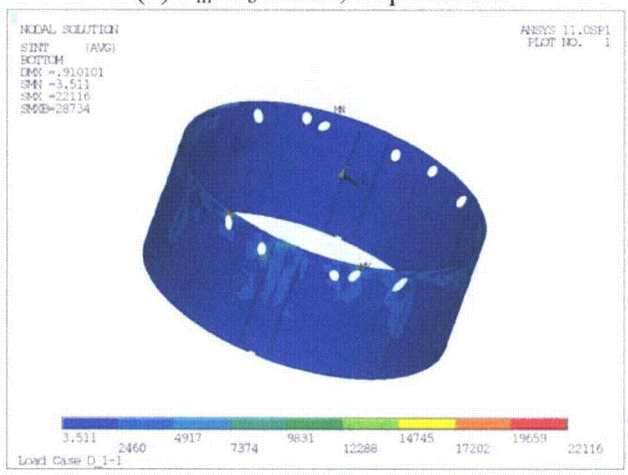

(c) P_m+P_b Stress, Bottom Surface

Figure 6-97: Skirt, Stress Intensity, Case D-1(b)

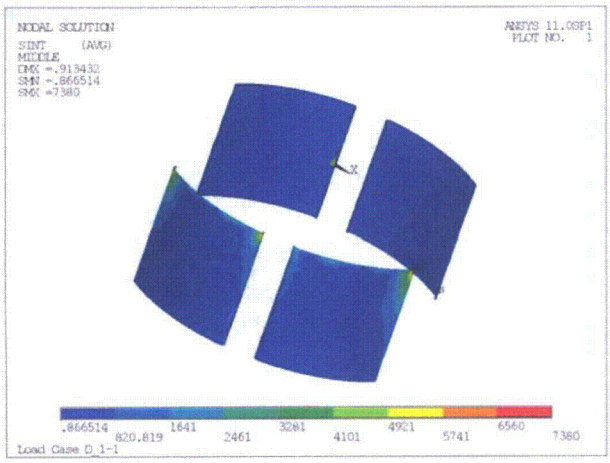

(a) Membrane Stress

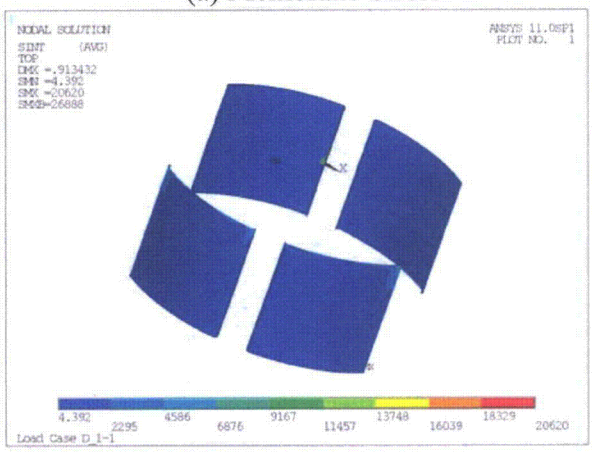

(b) P_m+P_b Stress, Top Surface

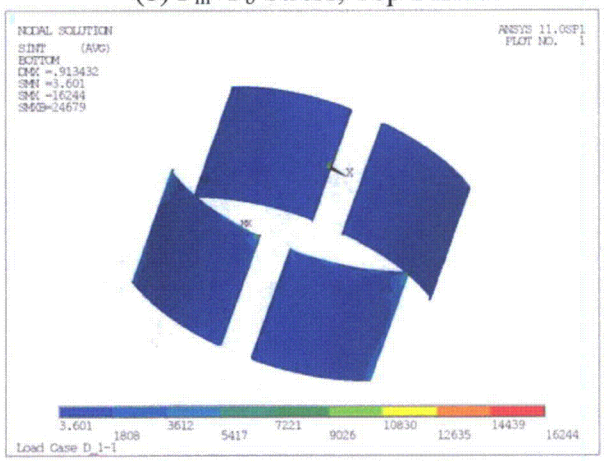

(c) P_m+P_b Stress, Bottom Surface

Figure 6-98: Drain Channels, Stress Intensity, Case D-1(b)

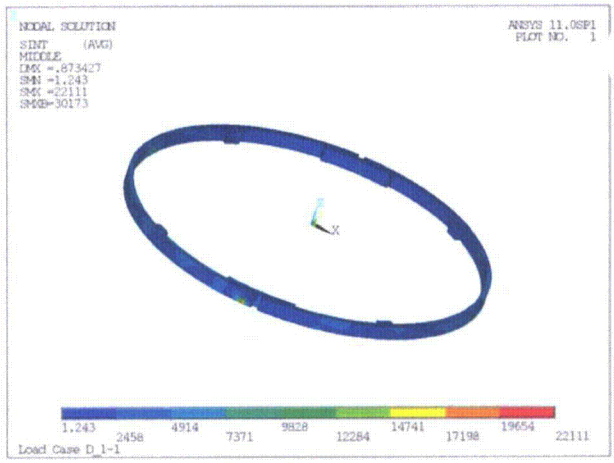

(a) Membrane Stress

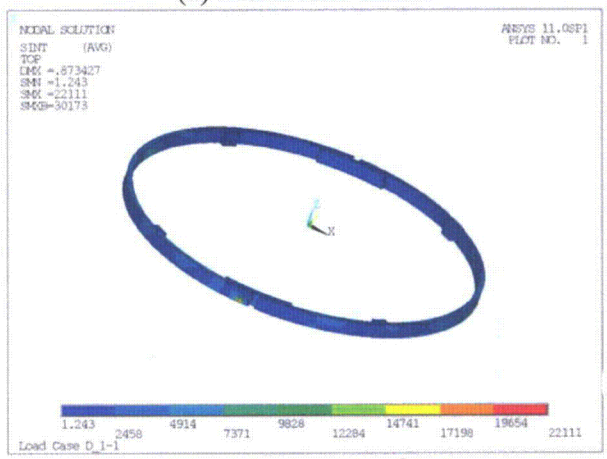

(b) P_m+P_b Stress, Top Surface

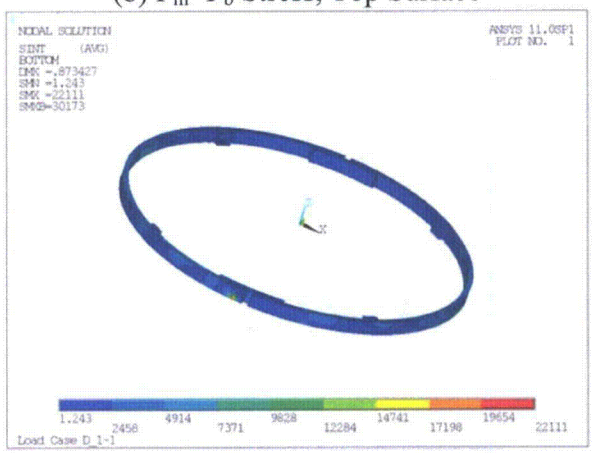

(c) P_m+P_b Stress, Bottom Surface

Figure 6-99: Upper Support Ring, Stress Intensity, Case D-1(b)

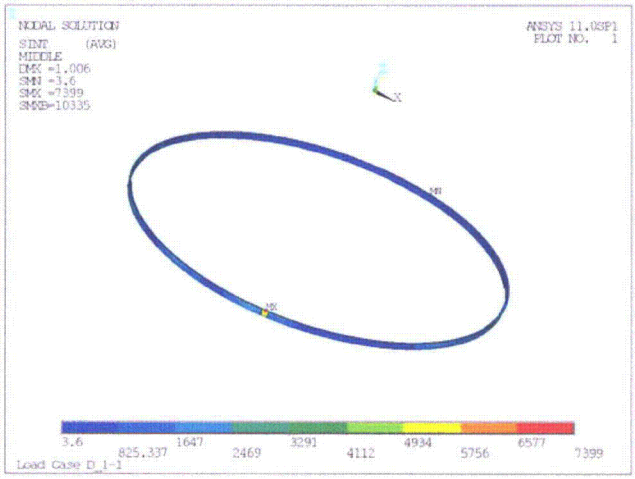

(a) Membrane Stress

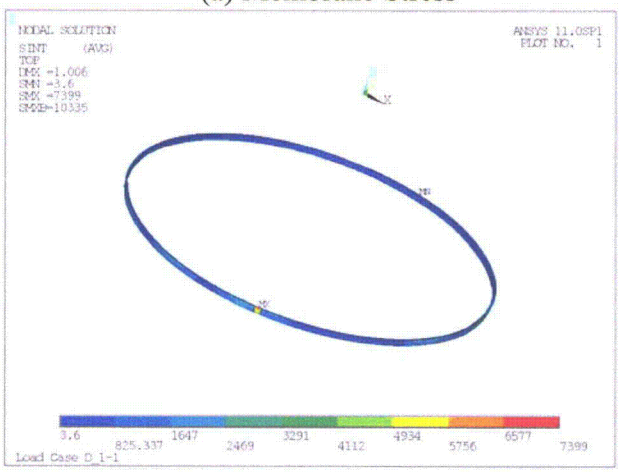

(b) P_m+P_b Stress, Top Surface

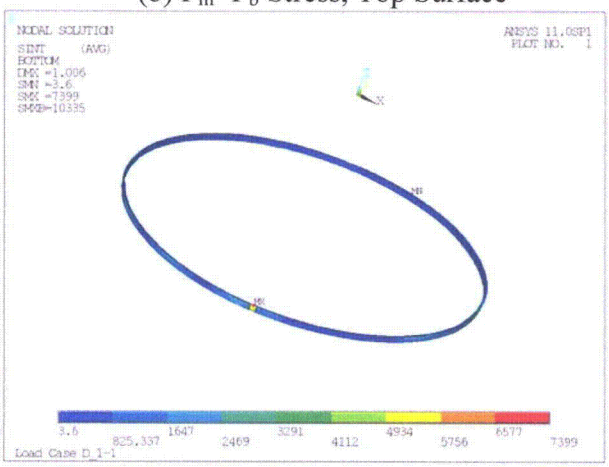

(c) P_m+P_b Stress, Bottom Surface

Figure 6-100: Lower Support Ring, Stress Intensity, Case D-1(b)

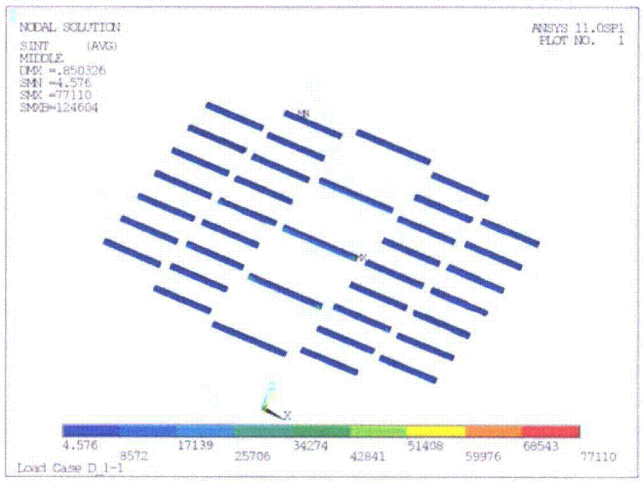

(a) Membrane Stress

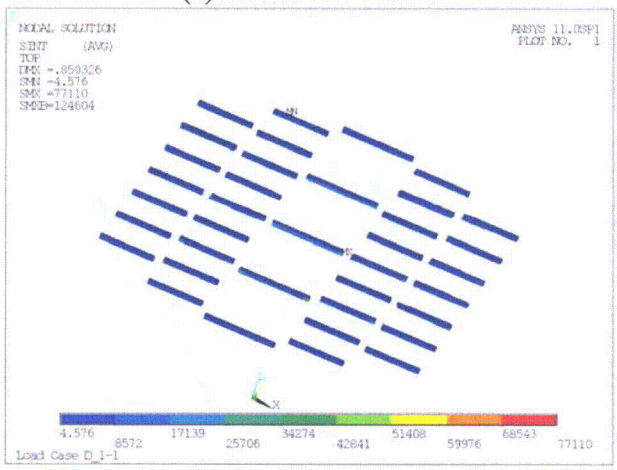

(b) P_m+P_b Stress, Top Surface

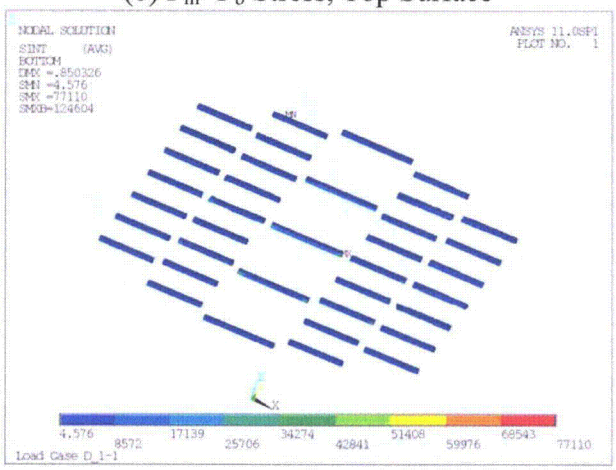

(c) P_m+P_b Stress, Bottom Surface

Figure 6-101: Tie Bars, Stress Intensity, Case D-1(b)

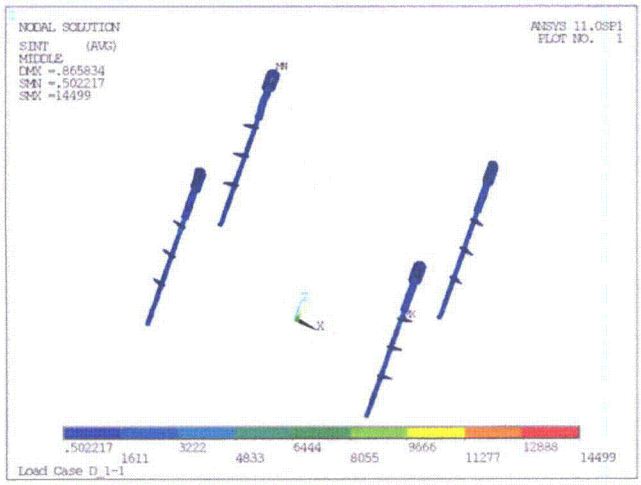

(a) Membrane Stress

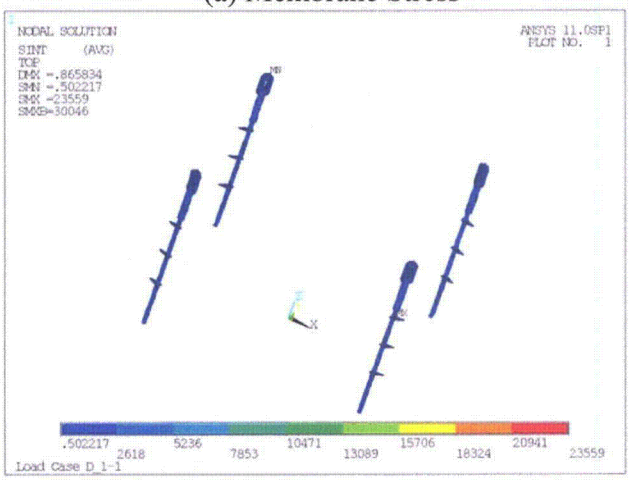

(b) P_m+P_b Stress, Top Surface

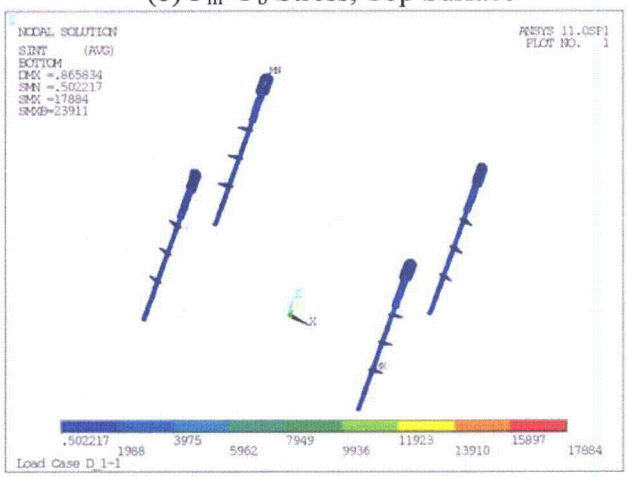

(c) P_m+P_b Stress, Bottom Surface

Figure 6-102: Lifting Rods, Stress Intensity, Case D-1(b)

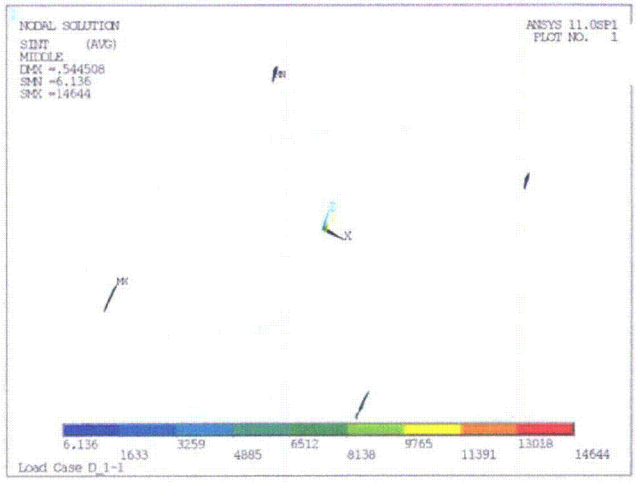

(a) Membrane Stress

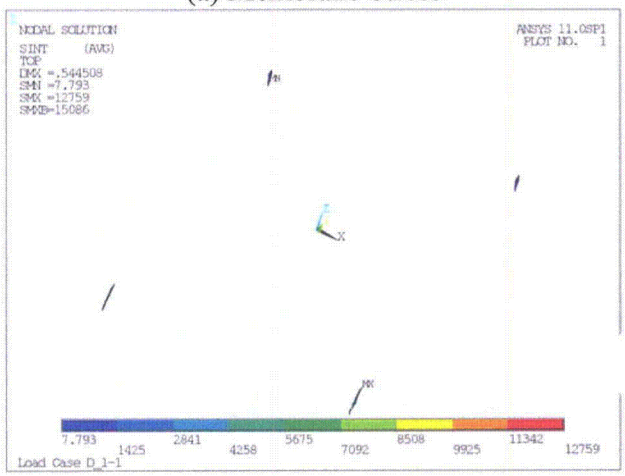

(b) P_m+P_b Stress, Top Surface

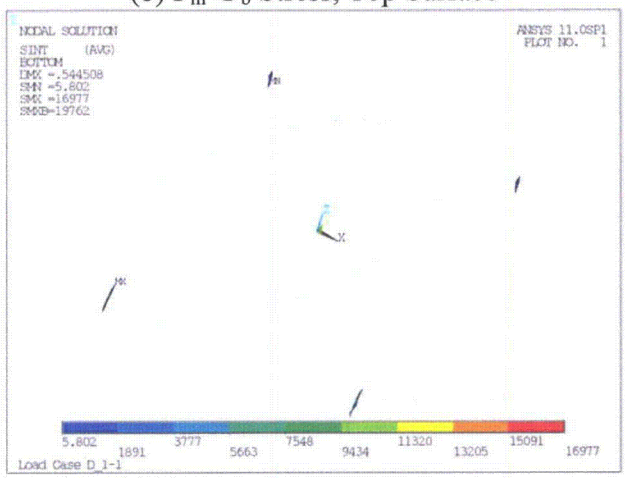

(c) P_m+P_b Stress, Bottom Surface

Figure 6-103: Gussets in Upper Support Ring, Stress Intensity, Case D-1(b)

7.0 FATIGUE EVALUATION

The Code fatigue evaluation is only required for Levels A and B [1]. Calculation of the alternating stress, S_a follows NG-3216.2 [1] which states for varying principal stress direction:

"(b) Choose a point in time when the conditions are one of the extremes for the cycle (either maximum or minimum, algebraically) and identify the stress components at this time by the subscripts i.

(c) Subtract each of the six stress components σ_{ti}, σ_{li}, etc., from the corresponding stress components σ_t, σ_l, etc., at each point in time during the cycle and call the resulting component σ_t', σ_l', etc.

(d) At each point in time during the cycle, calculate the principle stresses σ'_1, σ'_2, $\sigma'3$ derived from the six stress components σ'_t, σ'_l, etc.

(e) Determine the stress differences $S'_{12} = \sigma'_1-\sigma'_2$, $S'_{23} = \sigma'_2-\sigma'_3$, $S'_{31} = \sigma'_3 - \sigma'_1$ versus time for the complete cycle and find the largest absolute magnitude of any stress differences at any time. The alternating stress intensity S_{alt} is one-half of this magnitude."

To determine the maximum stress alternating stress, the loading combination is performed using ANSYS [8] as follows:

for Case B-3:

$\sigma_m = (OBE + SRV)_{max}$ as in item (b) (7-1)

$\sigma_n = (OBE + SRV)_{min}$ as σ_t, σ_l, in item (c) (7-2)

$\sigma'_k = \sigma_m - \sigma_n$ as in item (c) (7-3)

where: k, m, n = the six stress components t, l, etc as identified in item (c)

$(OBE+SRV)_{max}$,

$(OBE+SRV)_{min}$.

The load combinations are subtracted algebraically between the maximum and minimum. Then the principle stresses, σ'_i and the stress intensities, S'_{ij} where i = 1, 2, and 3, are computed in ANSYS [8] and extracted for fatigue evaluation.

In the fatigue evaluation, the alternating stress intensities was calculated using maximum stress intensities S'_{ij} from the top surface or the bottom surface of the shells along with the weld factor. The alternating stress intensity, S_{alt} is calculated as follows:

$$S_{alt} = \frac{\max\left|S'_{ij}\right|}{2}\frac{30x10^6}{E}F \qquad (7\text{-}4)$$

where: E = Young's modulus in psi at temperature

F = weld factor

S'_{ij}= as defined in item (e) above

The fatigue curve to be used, depending on the location and the stress intensity, is depicted in the flow chart in Figure 5-2.

As shown in Figure I-9.2.3 [1], fatigue curve B can be used if the alternating stress intensity S_{alt} is corrected for applied mean stress as follows [9]:

$$S_{eq} = \frac{S_{alt}}{1 - \frac{S_{mean}}{S_u}} \qquad (7\text{-}5)$$

where:

S_{eq} = value of stress to be used in entering the fatigue curve to find the allowable of number of cycles

S_{mean} = adjusted value of mean stress

= S'_{mean} if $S_{alt} + S'_{mean} \leq S_y$

= $S_y - S_{alt}$ if $S_{alt}+S'_{mean} > S_y$ and $S_{alt} < S_y$

= 0 if $S_{alt} \geq S_y$

S'_{mean} = basic value of mean stress (calculated directly from loading cycle)

S_u = ultimate tensile strength

As shown in Table 4-4, Case B-3 is comprised of load cases NL, ΔP_u, OBE, SRV, and FIV. Only OBE, SRV, and FIV are alternating in nature. In the current evaluation, only the OBE and SRV loads are used in the fatigue evaluation and the fatigue usage factor is calculated per NG-3222.4.

The number of events in OBE and SRV are obtained from Reference [12]. There are 10 occurrences for OBE and 8 occurrences for SRV. It is assumed that each of these events has 100 fully reversed cycles in the loadings for a total number of 1800 cycles.

The fatigue evaluation is performed for the load combination Case B-3 (Level B service condition) due to OBE and SRV load per the guidance in Section III, Subsection NG, paragraph NG-3216 and Appendix I [1]. To reduce the conservatism, the criteria for use of difference fatigue curves, Figure 5-2, per Appendix I, Figure I-9.2.3 of Reference [1] is also considered. This would allow the fatigue curves A or B to be used if either the mean stress is considered, the P_l+P_b+Q is less than 27.2 ksi or the location is away from the weld.

7.1 Stress Range and Mean Stress

The alternating stress intensities are obtained from the SRSS of two load cases, OBE and SRV. The maximum alternating stress intensity ranges due to these two load cases for all components are presented from Figure 7-1 through Figure 7-16. The mean stress intensity due to the NL and ΔP_u loads are presented from Figure 7-17 through Figure 7-32. The maximum alternating stress intensity ranges and mean stress intensities in these figures were extracted to perform the fatigue evaluation.

7.2 Fatigue Evaluation

The results of fatigue evaluation, which includes the use of Equations (7-4) and (7-5), are summarized in Table 7-1. The maximum alternating and mean stress intensity for each component is obtained from Figures 7-1 through 7-32. The P_l+P_b+Q for each component is obtained from Table 6-2. It should be noted that these maximum alternating stress intensity amplitude, maximum mean stress intensity and the P_l+P_b+Q can be at different nodal locations. But these were used as if they are at the same nodal location.

From References [10] and [11], it is shown that most of the welds in the steam dryer are fillet welds. Not all the welds are identified in these two references. For conservatism, it is assumed that all welds are fillet welds with a weld factor of 1.8. In addition, it is assumed that all maximum alternating stress intensity ranges are at or close to the weld locations (less than 3 inches from the weld centerline per Appendix I of Reference [1]).

Since the P_l+P_b+Q range for all components are less than the 27.2 ksi requirements per Figure I-9.2.3 of Section III, Appendix I [1], fatigue curve B in Figure 5-1 can be used. Fatigue curve B has an endurance limit of 16.5 ksi. For conservatism, fatigue curve C in Figure 5-1 was used to calculate the fatigue usage. After accounting for the mean stress effect, the alternating stress amplitudes, S_{eq}, in all steam dryer components are less than 16 ksi.

It is assumed that there are a total of 18 events for OBE and SRV. In each event, there are 100 cycles. The allowable cycles for each component were obtained and the fatigue usages were calculated. Although fatigue curve B can be used, for conservatism, the fatigue usage was calculated using fatigue curve C. The largest fatigue usage is 9.84×10^{-5} in the Vane Bank Base Plates. This fatigue usage is less than the Code fatigue usage allowable of 1.

7.3 Reconciliation of Finite Element Model on Fatigue Evaluation

As shown in Table 7-1, the fatigue usage using the results from the original model is very small, 9.84×10^{-5}. Even with the increase of 6% in the alternating stress ranges, the increase in the fatigue usage is not significant and still under the allowable.

Table 7-1: Fatigue Evaluation for Load Combination B-3

Case B-3, OBE and SRV						Max|S'ij| Range (ksi)									Curve C	
Component	At Weld	Fillet Weld	Wld Cl < 3 thk	P_L+P_B+Q (ksi)	S'_{mean} (ksi)	Top	Bottom	Max|S'ij|alt (ksi)	E Ratio	Weld Factor	S_{alt} (ksi) Eq (7)	Fatigue Curve	S_{mean} (ksi)	S_{eq}(ksi) Eq (8)	Allowable Cycle	Fatigue Usage
Outer Hoods	Yes	Yes	Yes	8.69	3.69	5.02	4.85	2.51	1.11	1.8	5.00	B	3.69	5.31	1.00E+11	1.80E-08
Middle Hoods	Yes	Yes	Yes	11.67	11.53	3.69	2.78	1.85	1.11	1.8	3.68	B	11.53	4.50	1.00E+11	1.80E-08
Inside Hoods	Yes	Yes	Yes	12.89	12.53	4.01	3.06	2.01	1.11	1.8	4.00	B	12.53	4.98	1.00E+11	1.80E-08
Gussets in Hoods	Yes	Yes	Yes	17.24	14.44	6.36	6.15	3.18	1.11	1.8	6.34	B	12.56	7.91	1.00E+11	1.80E-08
Side Plates	Yes	Yes	Yes	11.65	7.63	4.17	3.80	2.09	1.11	1.8	4.16	B	7.63	4.73	1.00E+11	1.80E-08
Vane Bank Base Plates	Yes	Yes	Yes	15.84	9.15	13.76	14.26	7.13	1.11	1.8	14.22	B	4.68	15.35	18286322	9.84E-05
Vertical Plates in Vane Banks	Yes	Yes	Yes	8.06	7.10	1.30	0.95	0.65	1.11	1.8	1.30	B	7.10	1.46	1.00E+11	1.80E-08
Vane Banks	Yes	Yes	Yes	13.16	9.44	11.32	11.13	5.66	1.11	1.8	11.28	B	7.62	12.83	1.00E+11	1.80E-08
Drain Pipes	Yes	Yes	Yes	3.66	2.71	2.31	2.11	1.16	1.11	1.8	2.30	B	2.71	2.41	1.00E+11	1.80E-08
Skirt	Yes	Yes	Yes	6.19	3.07	3.43	3.65	1.83	1.11	1.8	3.64	B	3.07	3.82	1.00E+11	1.80E-08
Drain Channels	Yes	Yes	Yes	6.30	1.90	6.23	6.16	3.12	1.11	1.8	6.21	B	1.90	6.40	1.00E+11	1.80E-08
Upper Support Ring	Yes	Yes	Yes	11.93	2.13	12.22	12.22	6.11	1.11	1.8	12.18	B	2.13	12.61	1.00E+11	1.80E-08
Lower Support Ring	Yes	Yes	Yes	2.68	1.33	1.38	1.38	0.69	1.11	1.8	1.38	B	1.33	1.41	1.00E+11	1.80E-08
Tie Bars	Yes	Yes	Yes	14.05	11.78	3.46	3.46	1.73	1.11	1.8	3.45	B	11.78	4.24	1.00E+11	1.80E-08
Lifting Rods	Yes	Yes	Yes	11.15	3.93	5.95	11.04	5.52	1.11	1.8	11.01	B	3.93	11.73	1.00E+11	1.80E-08
Gussets in Upper Support Ring	Yes	Yes	Yes	3.50	1.52	1.48	2.06	1.03	1.11	1.8	2.05	B	1.52	2.10	1.00E+11	1.80E-08

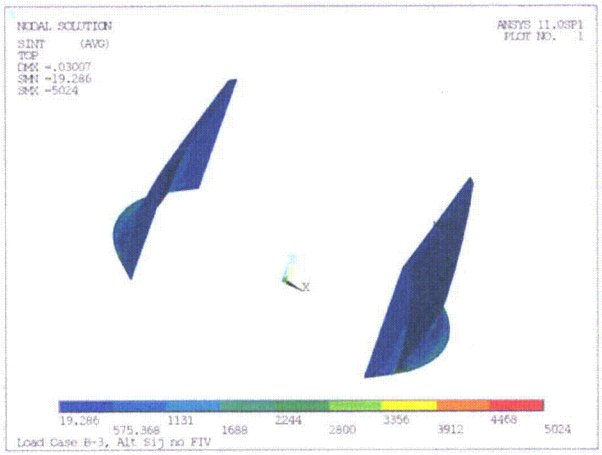

(a) Top Surface

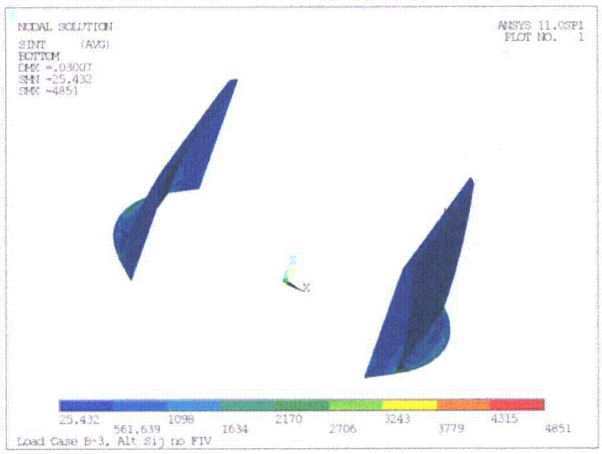

(b) Bottom Surface

Figure 7-1: Outer Hoods, Alternating Stress Intensity Range, Case B-3

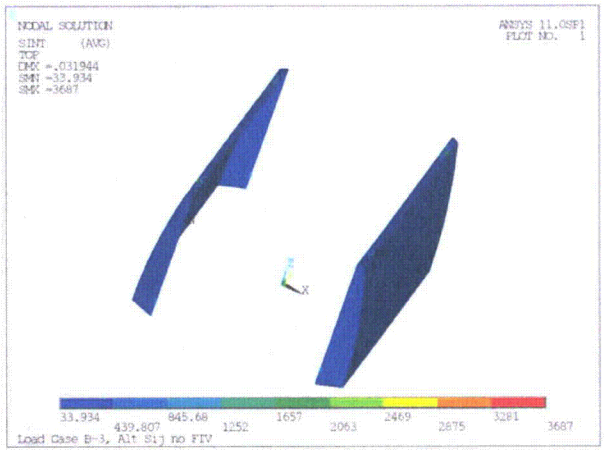

(a) Top Surface

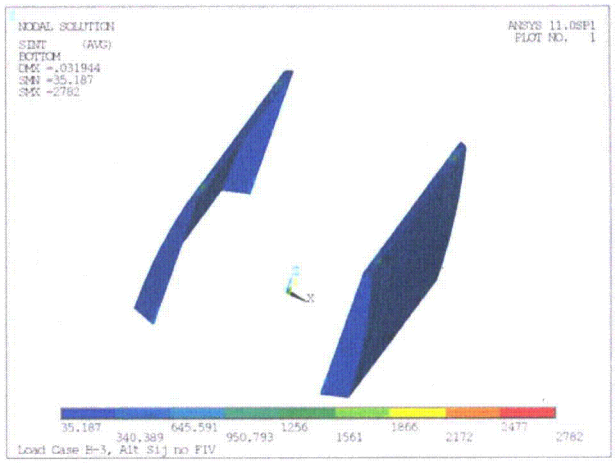

(b) Bottom Surface

Figure 7-2: Middle Hoods, Alternating Stress Intensity Range, Load Combination, Case B-3

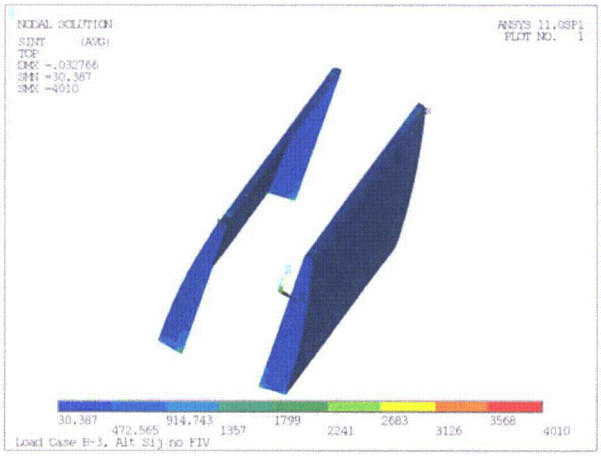

(a) Top Surface

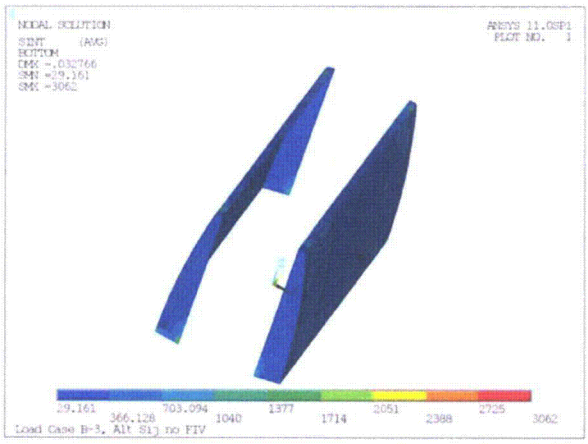

(b) Bottom Surface

Figure 7-3: Inside Hoods, Alternating Stress Intensity Range, Case B-3

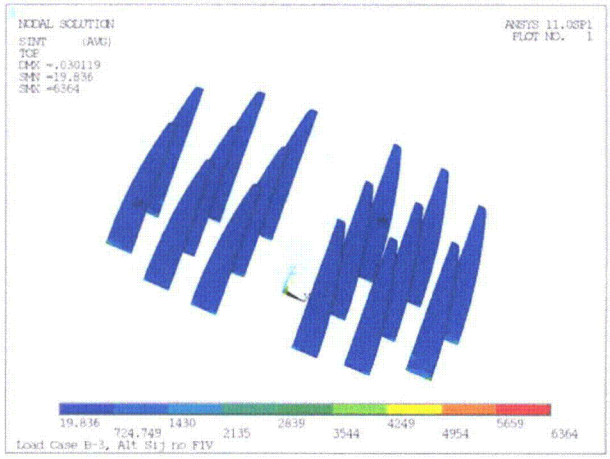

(a) Top Surface

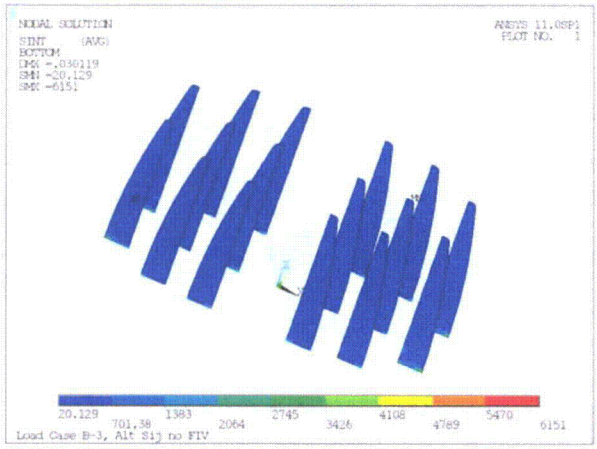

(b) Bottom Surface

Figure 7-4: Gussets in Hoods, Alternating Stress Intensity Range, Case B-3

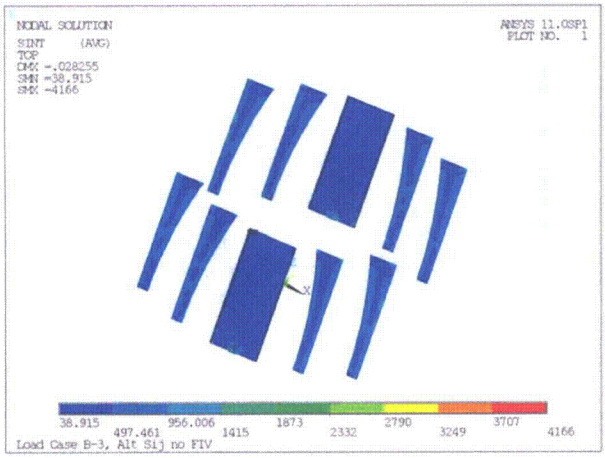

(a) Top Surface

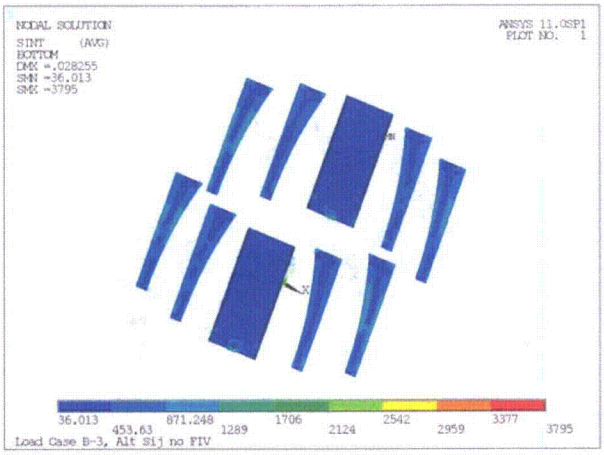

(b) Bottom Surface

Figure 7-5: Side Plates, Alternating Stress Intensity Range, Case B-3

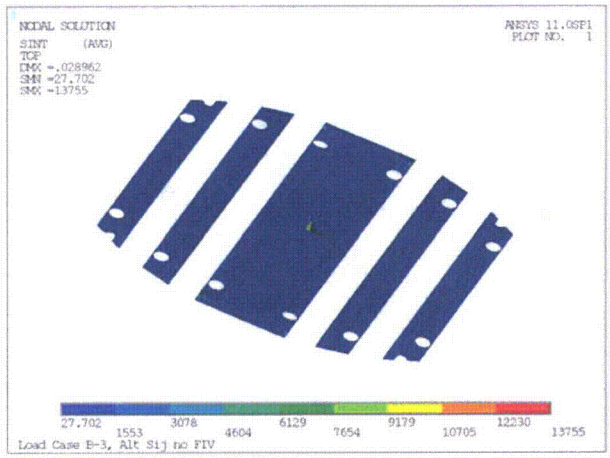

(a) Top Surface

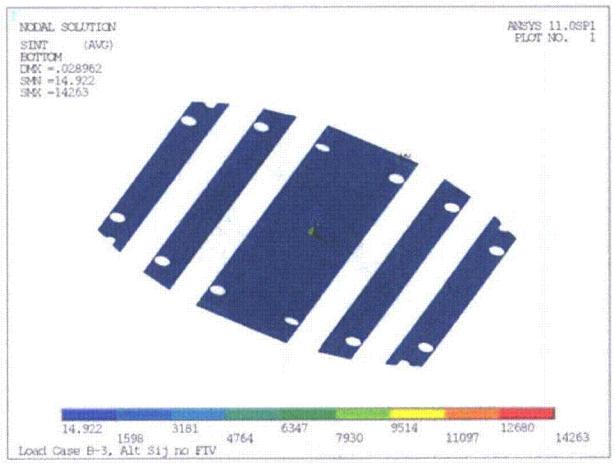

(b) Bottom Surface

Figure 7-6: Vane Bank Base Plates, Alternating Stress Intensity Range, Case B-3

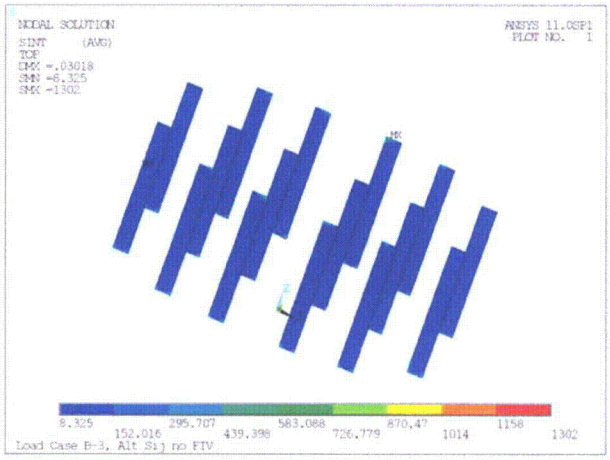

(a) Top Surface

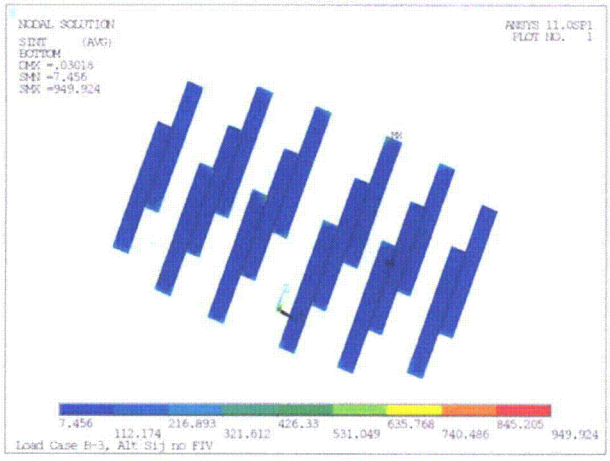

(b) Bottom Surface

Figure 7-7: Vane Bank Vertical Plates, Alternating Stress Intensity Range, Case B-3

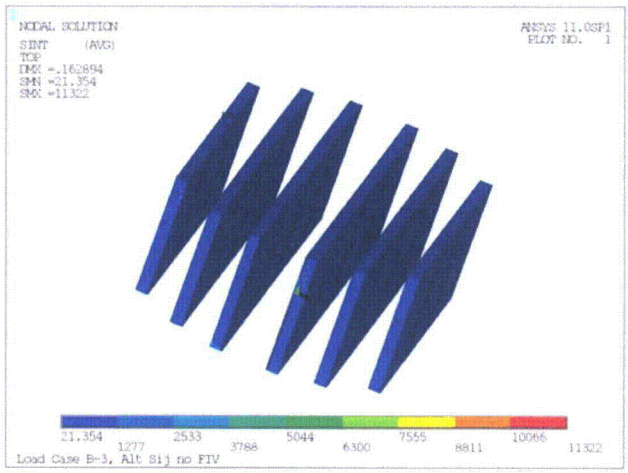

(a) Top Surface

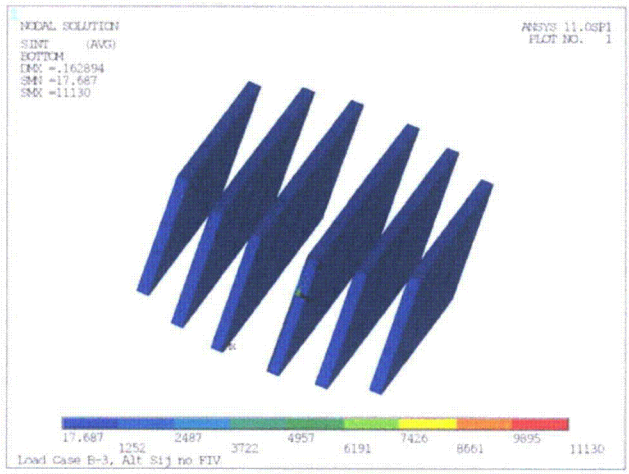

(b) Bottom Surface

Figure 7-8: Vane Banks, Alternating Stress Intensity Range, Case B-3

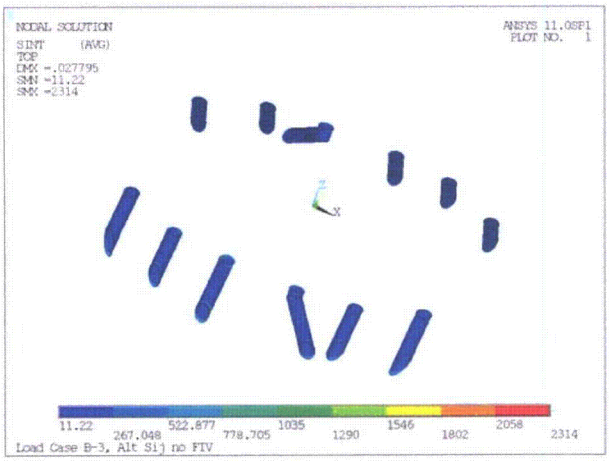

(a) Top Surface

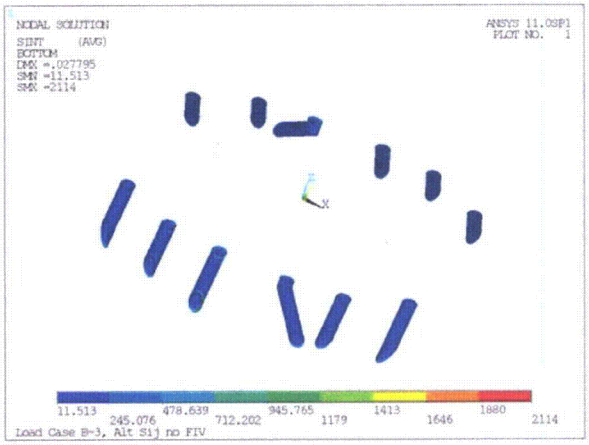

(b) Bottom Surface

Figure 7-9: Drain Pipes, Alternating Stress Intensity Range, Case B-3

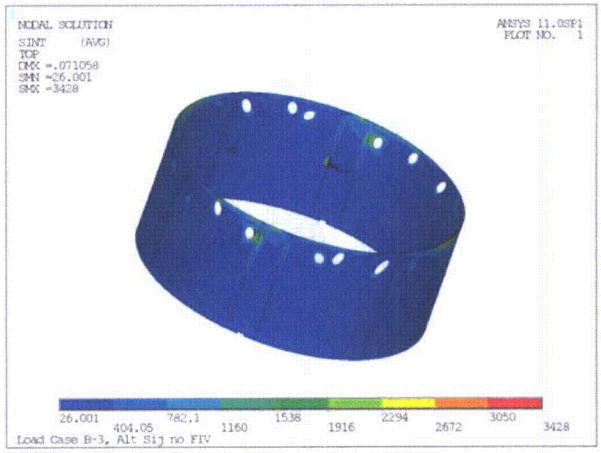

(a) Top Surface

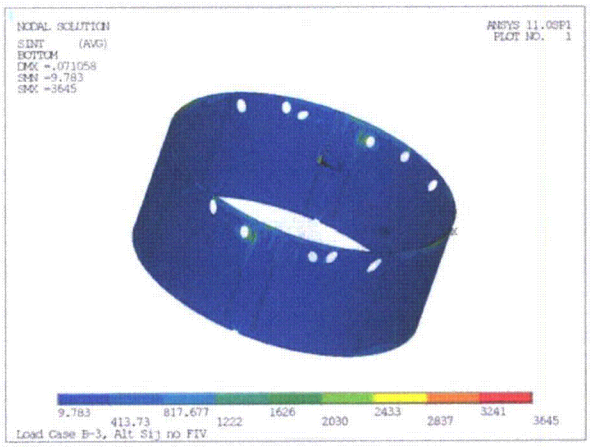

(b) Bottom Surface

Figure 7-10: Skirt, Alternating Stress Intensity Range, Case B-3

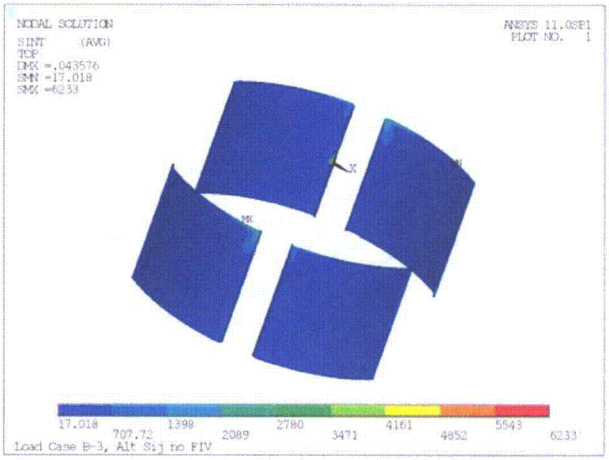

(a) Top Surface

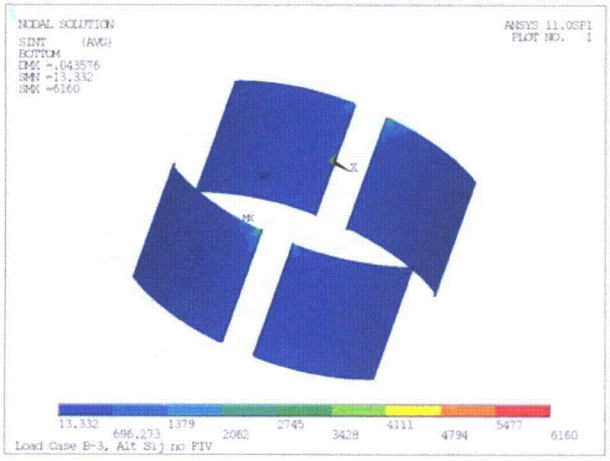

(b) Bottom Surface

Figure 7-11: Drain Channels, Alternating Stress Intensity Range, Case B-3

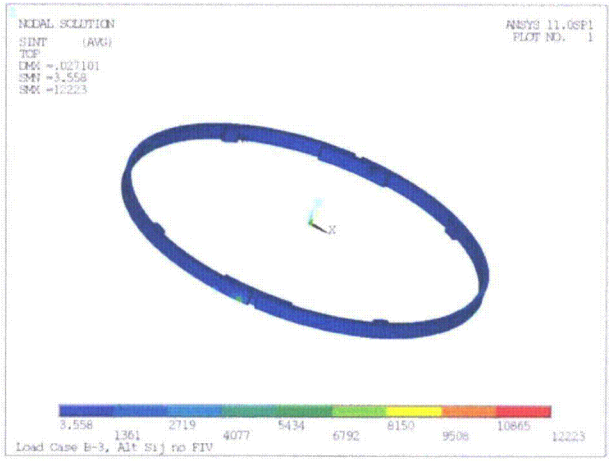

(a) Top Surface

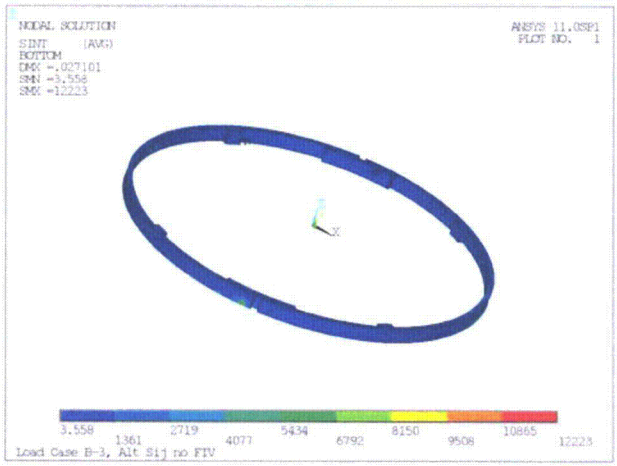

(b) Bottom Surface

Figure 7-12: Upper Support Ring, Alternating Stress Intensity Range, Case B-3

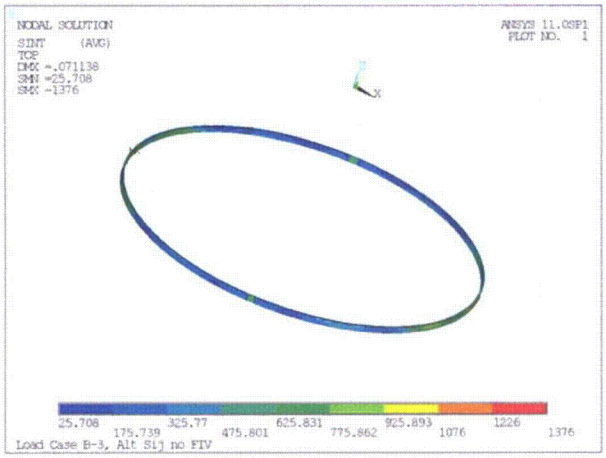

(a) Top Surface

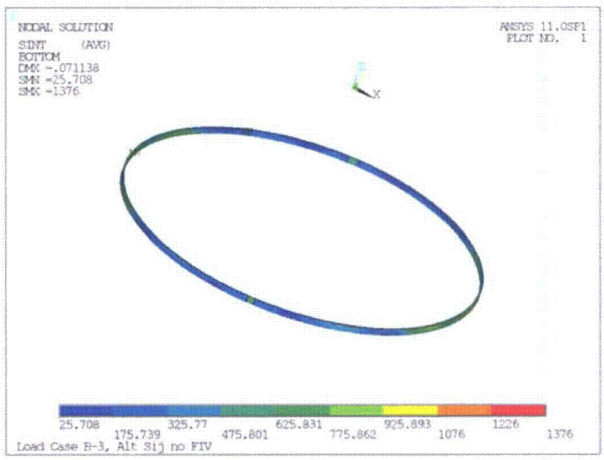

(b) Bottom Surface

Figure 7-13: Lower Support Ring, Alternating Stress Intensity Range, Case B-3

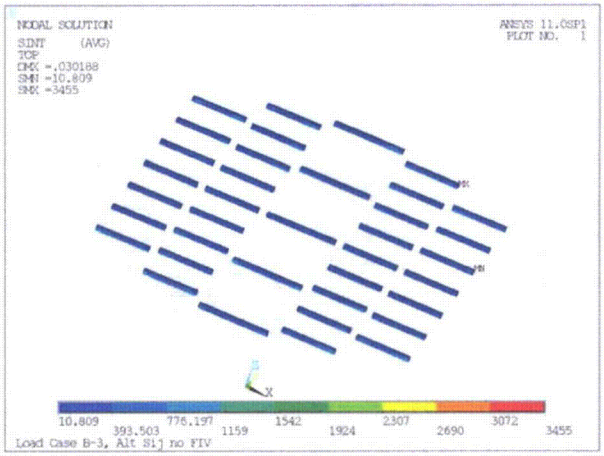

(a) Top Surface

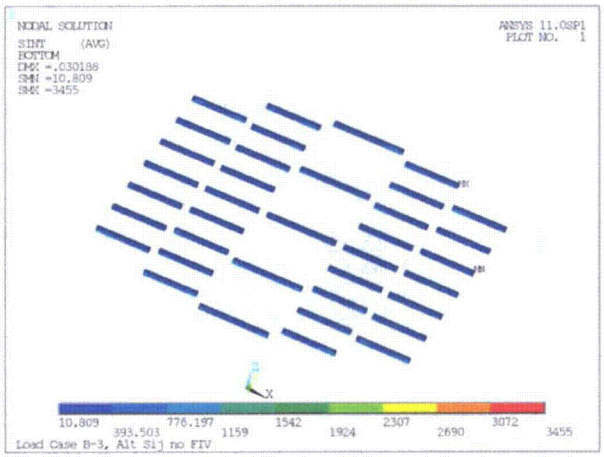

(b) Bottom Surface

Figure 7-14: Tie Bars, Alternating Stress Intensity Range, Case B-3

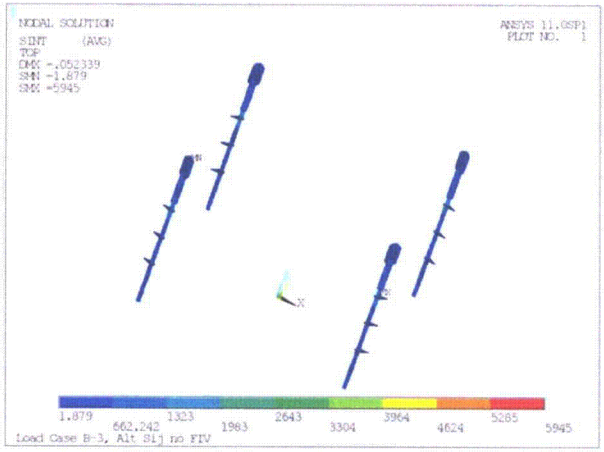

(a) Top Surface

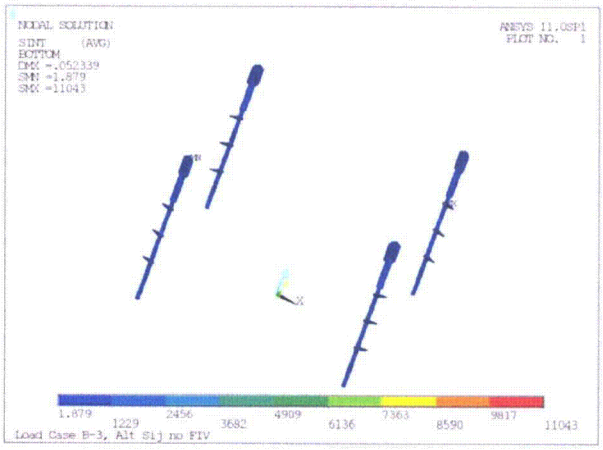

(b) Bottom Surface

Figure 7-15: Lifting Rods, Alternating Stress Intensity Range, Case B-3

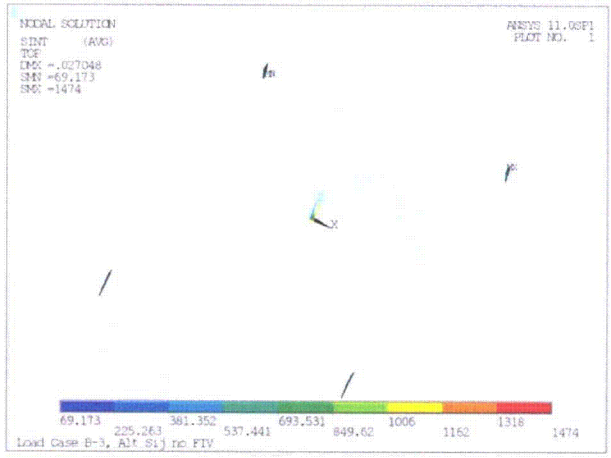

(a) Top Surface

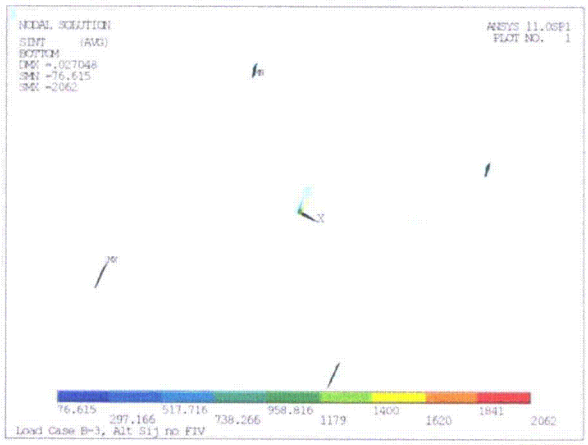

(b) Bottom Surface

Figure 7-16: Gussets in Upper Support Ring, Alternating Stress Intensity Range, Case B-3

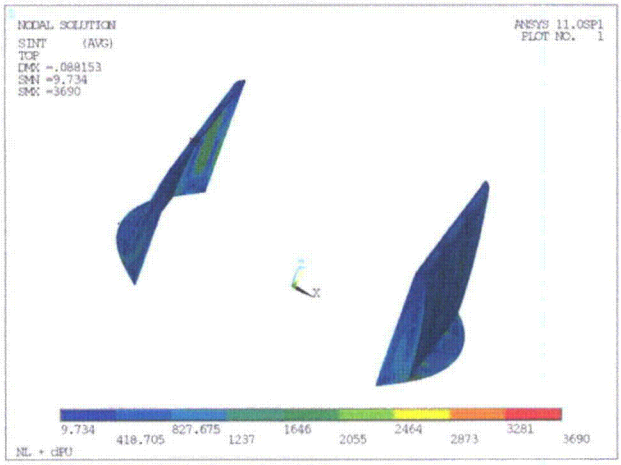

(a) Top Surface

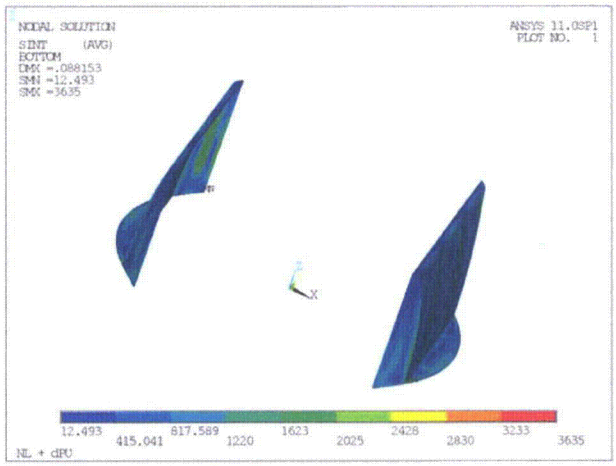

(b) Bottom Surface

Figure 7-17: Outer Hoods, Mean Stress Intensity, Case B-3

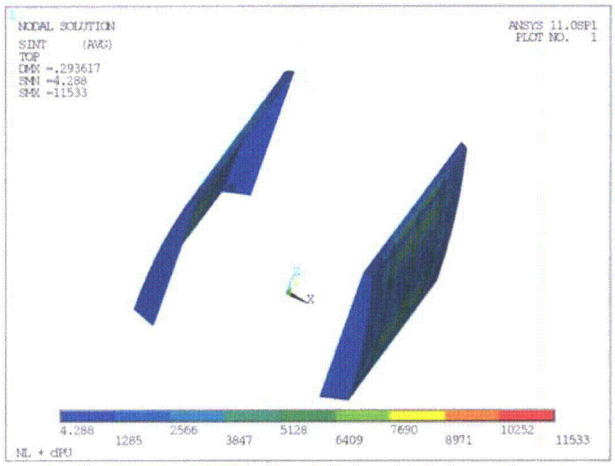

(a) Top Surface

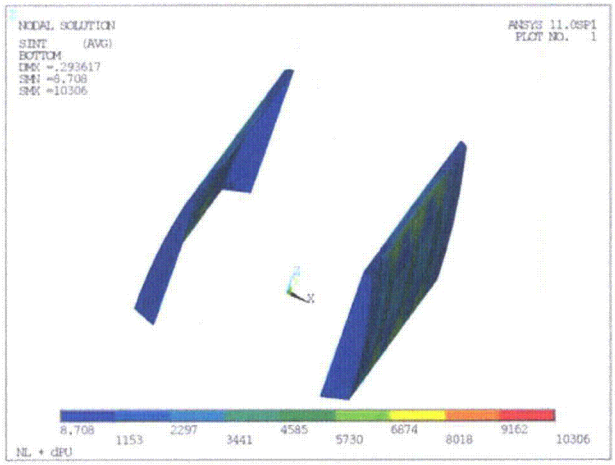

(b) Bottom Surface

Figure 7-18: Middle Hoods, Mean Stress Intensity, Case B-3

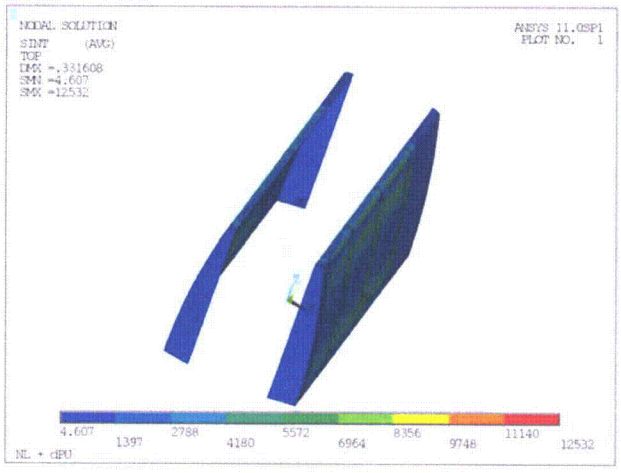

(a) Top Surface

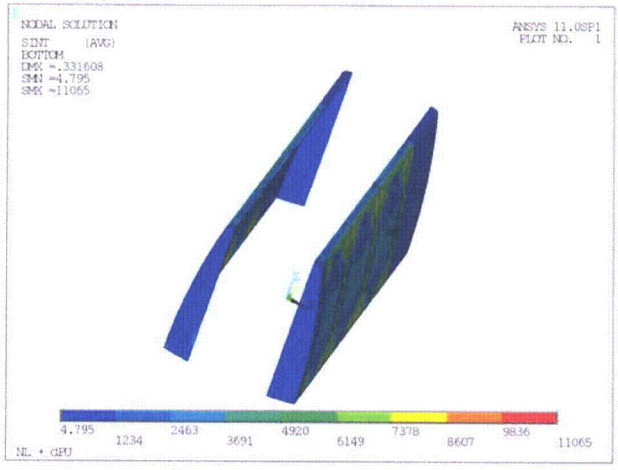

(b) Bottom Surface

Figure 7-19: Inside Hoods, Mean Stress Intensity, Case B-3

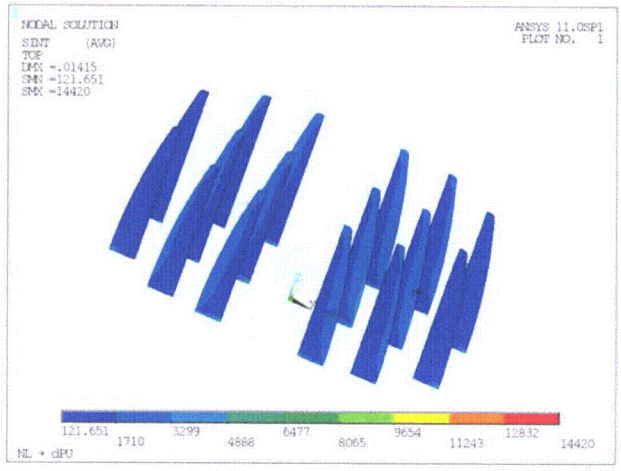

(a) Top Surface

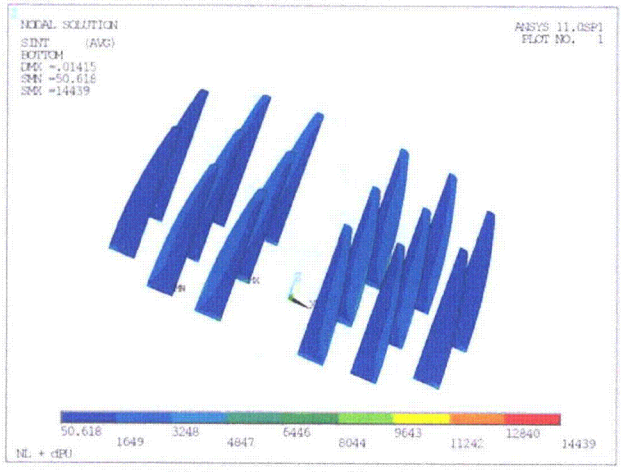

(b) Bottom Surface

Figure 7-20: Gussets in Hoods, Mean Stress Intensity, Case B-3

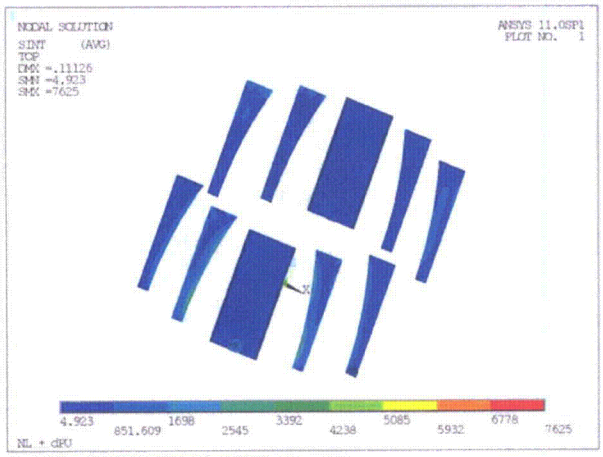

(a) Top Surface

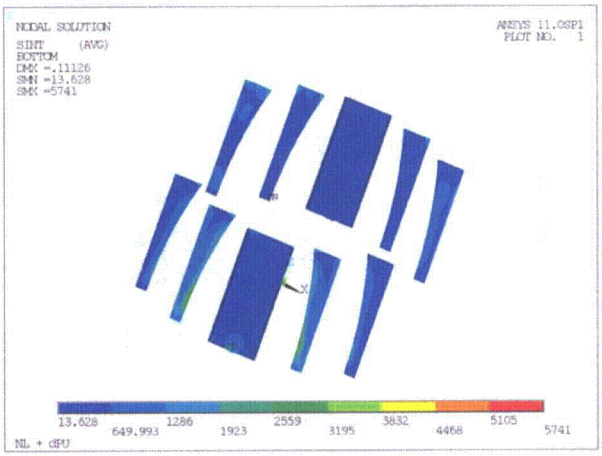

(b) Bottom Surface

Figure 7-21: Side Plates, Mean Stress Intensity, Case B-3

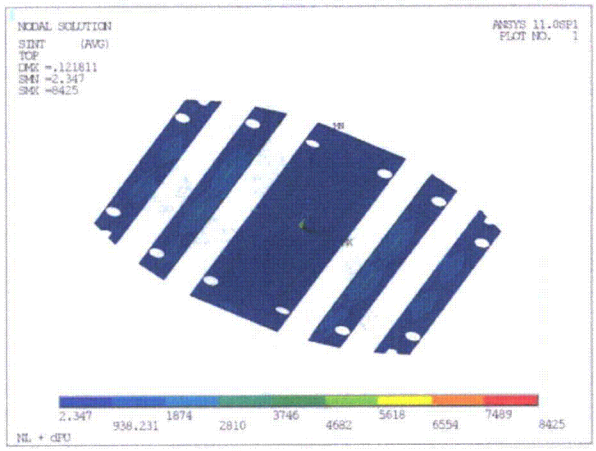

(a) Top Surface

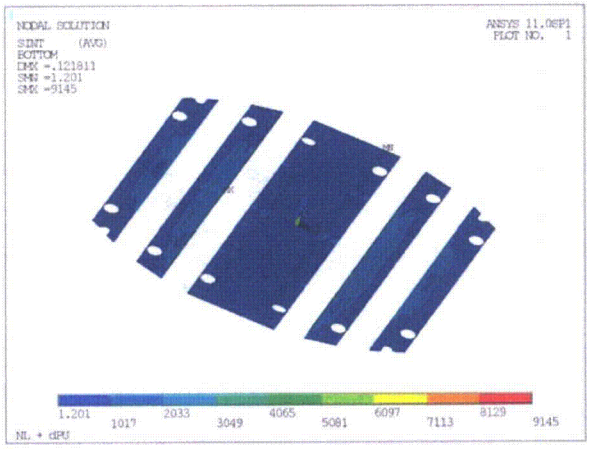

(b) Bottom Surface

Figure 7-22: Vane Bank Base Plates, Mean Stress Intensity, Case B-3

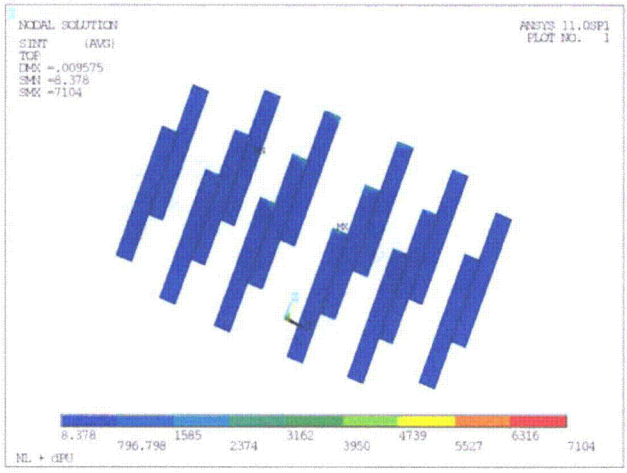

(a) Top Surface

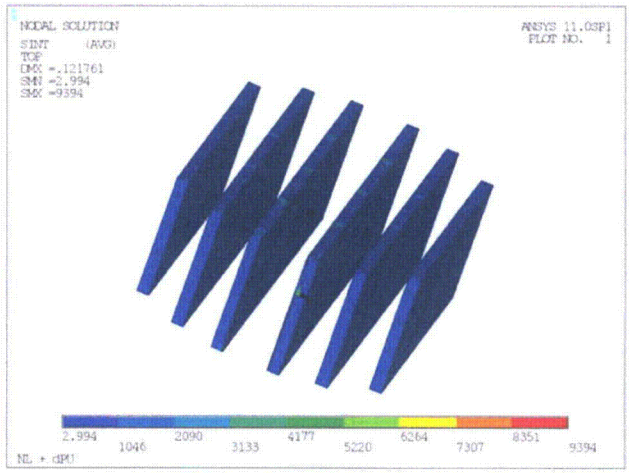

(a) Top Surface

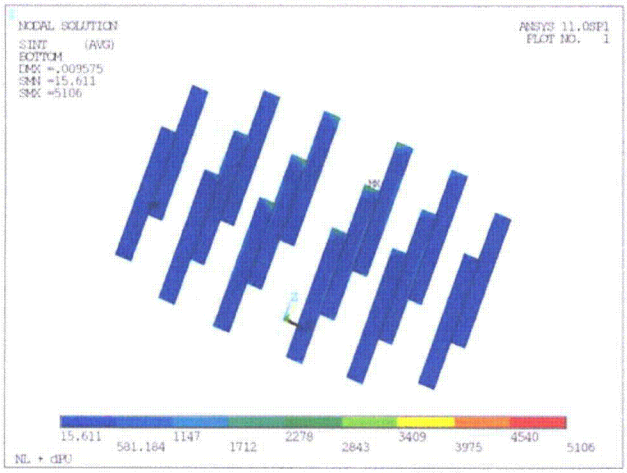

(b) Bottom Surface

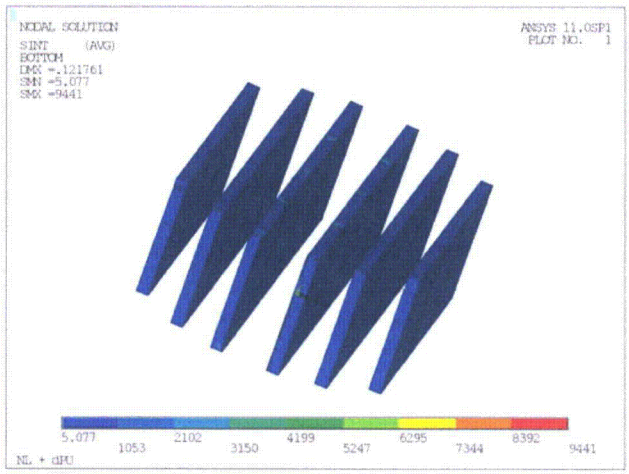

(b) Bottom Surface

Figure 7-23: Vane Bank, Vertical Plates, Mean Stress Intensity, Case B-3

Figure 7-24: Vane Banks, Mean Stress Intensity, Case B-3

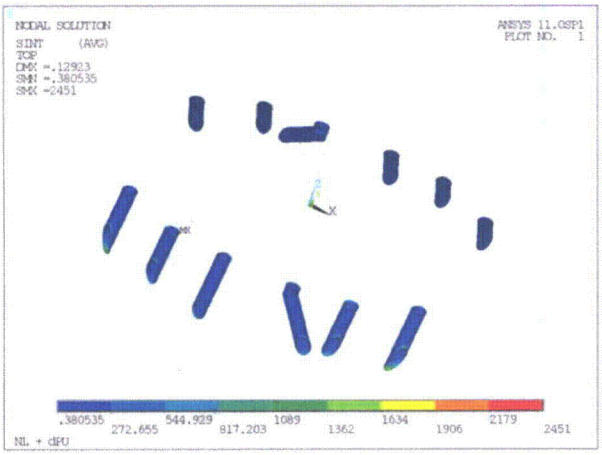

(a) Top Surface

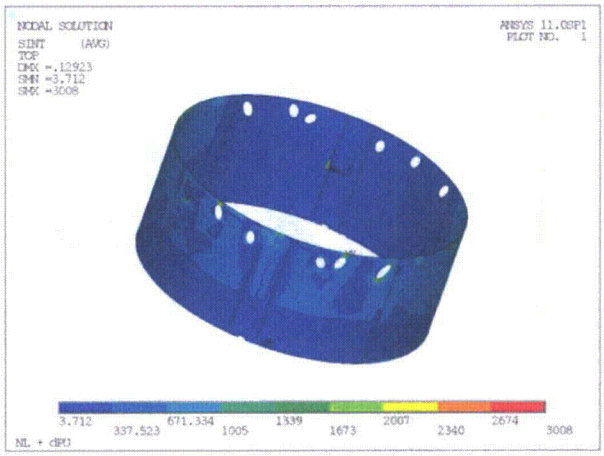

(a) Top Surface

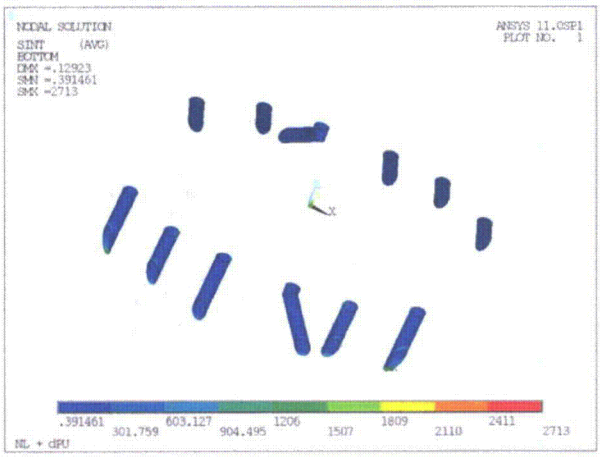

(b) Bottom Surface

Figure 7-25: Drain Pipes, Mean Stress Intensity, Case B-3

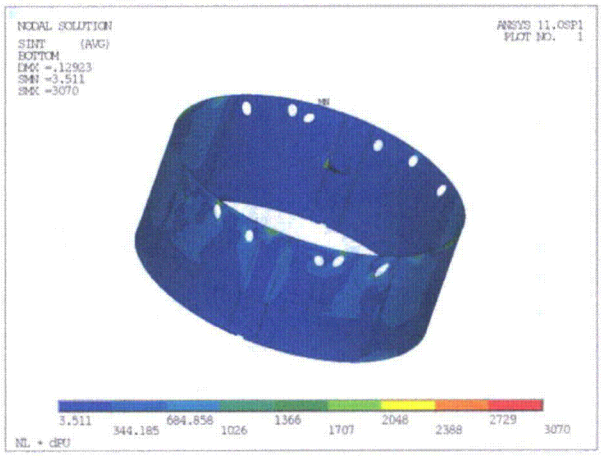

(b) Bottom Surface

Figure 7-26: Skirt, Mean Stress Intensity Range, Case B-3

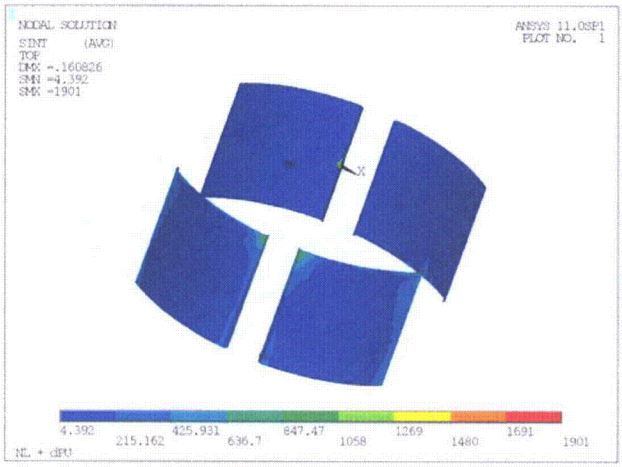

(a) Top Surface

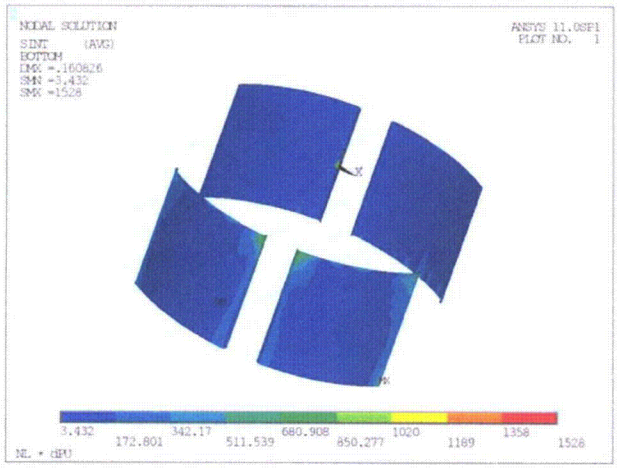

(b) Bottom Surface

Figure 7-27: Drain Channels, Mean Stress Intensity, Case B-3

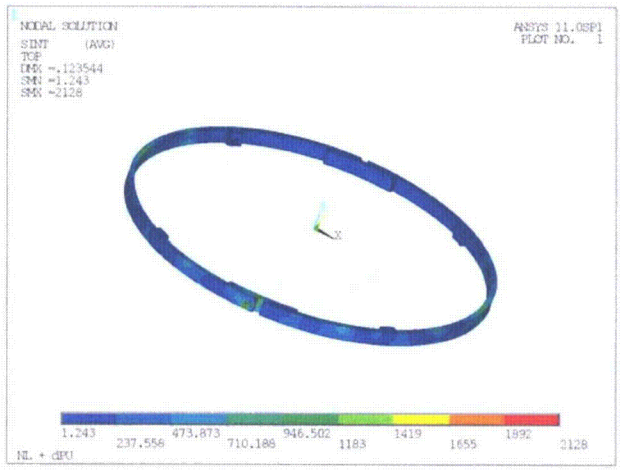

(a) Top Surface

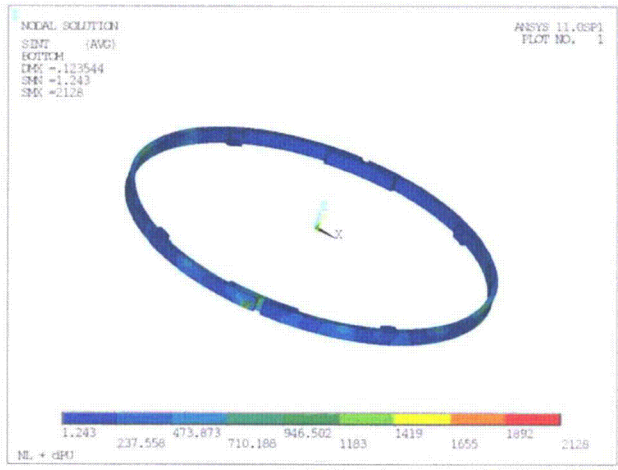

(b) Bottom Surface

Figure 7-28: Upper Support Ring, Mean Stress Intensity, Case B-3

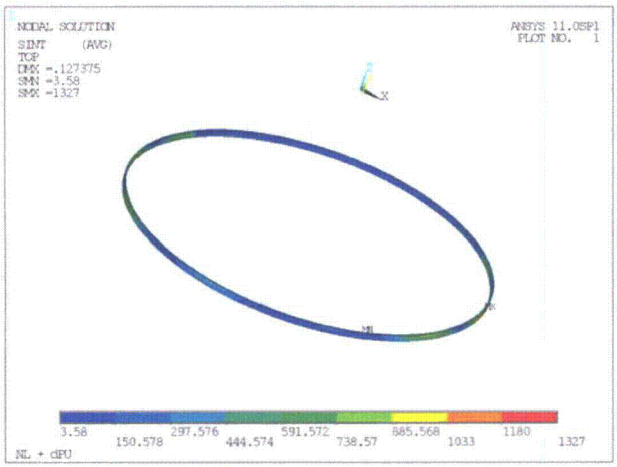

(a) Top Surface

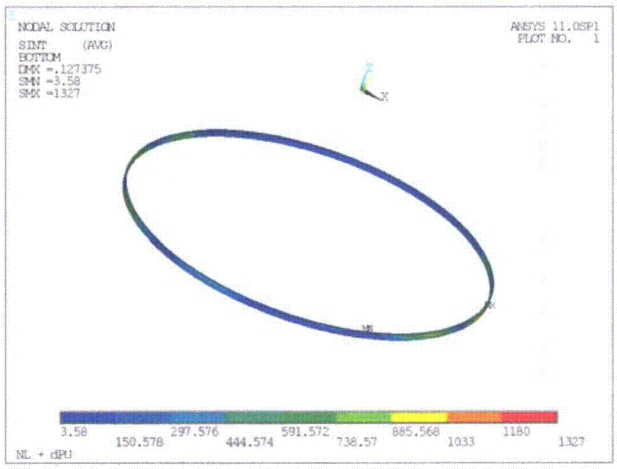

(b) Bottom Surface

Figure 7-29: Lower Support Ring, Mean Stress Intensity, Case B-3

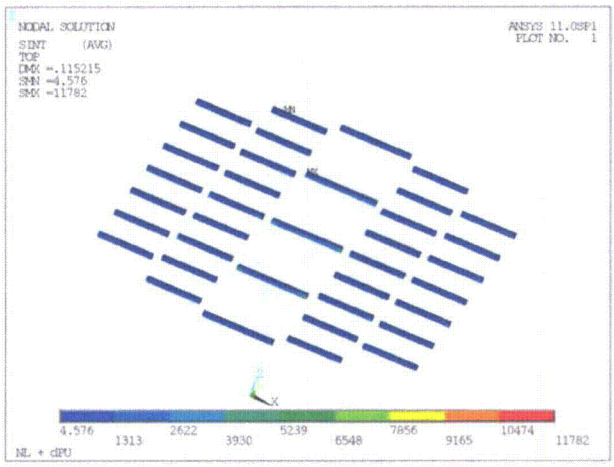

(a) Top Surface

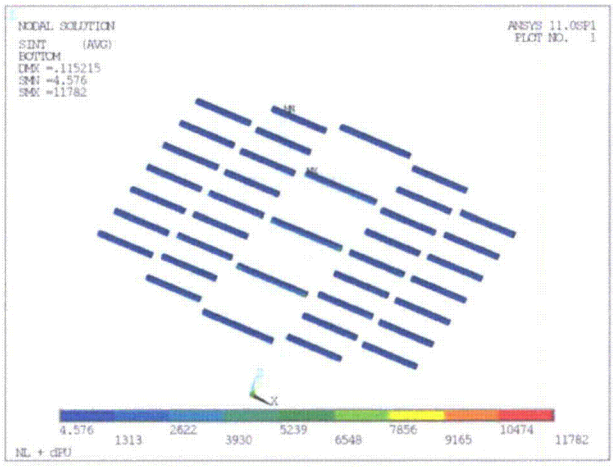

(b) Bottom Surface

Figure 7-30: Tie Bars, Mean Stress Intensity, Case B-3

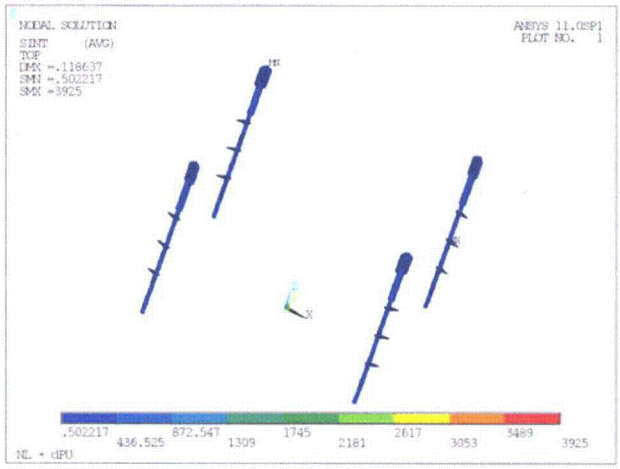

(a) Top Surface

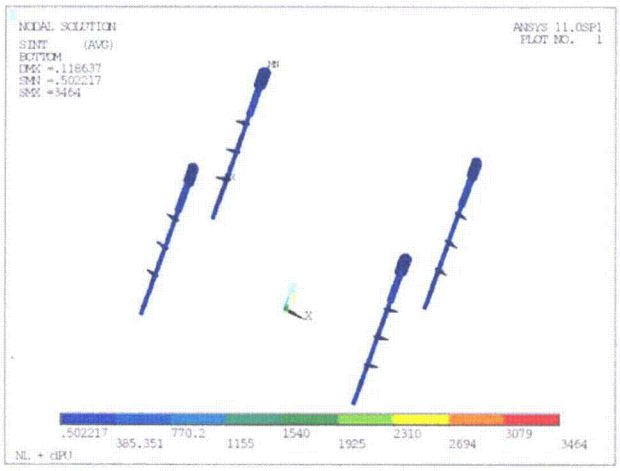

(b) Bottom Surface

Figure 7-31: Lifting Rods, Mean Stress Intensity, Case B-3

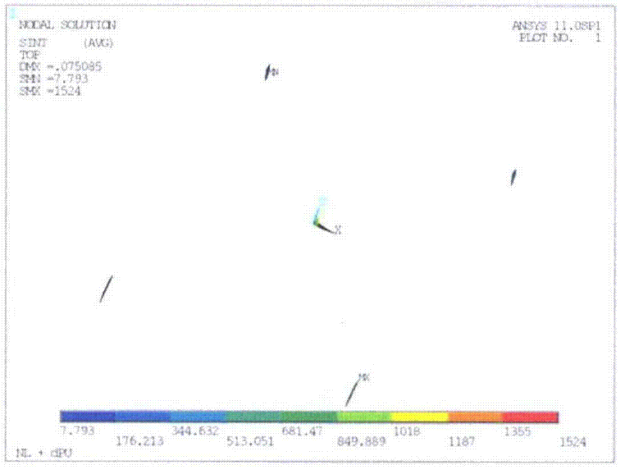

(a) Top Surface

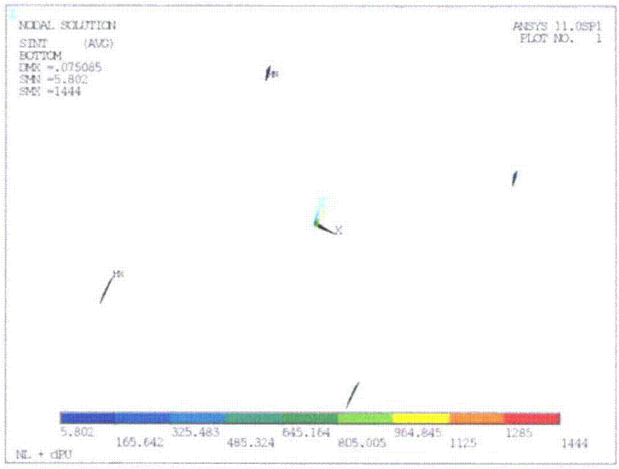

(b) Bottom Surface

Figure 7-32: Gussets in Upper Support Ring, Mean Stress Intensity, Case B-3

8.0 BUCKLING EVALUATION OF LIFTING RODS

In Reference [14], the critical component of the steam dryer is the lifting rods due to buckling when the steam dryer lifts up and the lifting rods hit the stops in the top head. This section describes the evaluation of buckling under the Level D condition for the lifting rods.

8.1 Technical Approach

The Code evaluation of the steam dryer was evaluated according to the rules of ASME Section III, Subsection NG [1]. The only buckling evaluation, as described in Subsection NG, is only for cylindrical shell, spherical shell or tubular product under external pressure. Since the buckling of the steam dryer lifting rods is evaluated for the faulted condition, the rules of Appendix F of Section III are used.

8.2 Design Inputs

Each lifting rod is 3 inches in diameter and 82 inches long [4]. There are three gusset plates providing lateral support along the length of each rod, Figure 6-1. The longest unbraced length for each lifting rod is 32 inches.

The pressure difference for the faulted condition in the steam dryer is 6.3 psi for the CLTP and 4.8 psi for the EPU [4].

The typical material of the lifting rods is Type 304 stainless steel [5]. The operating temperature for the steam dryer is 550°F [5]. The yield strength of the Type 304 stainless steel at operating temperature is 18.9 ksi.

The weight of the steam dryer is 80,000 lbs [15]. The SSE load in the vertical direction is 0.327g [5].

8.3 Assumptions

The following assumptions are used in the evaluation:

1. The lifting rods are assumed to be a linear type support such that the criteria for linear type support in Appendix F, F-1334 could be used.
2. The loads on the lifting rods are assumed to be from the lifting of the steam dryer due to the pressure differential across the steam dryer in the faulted condition.
3. The lifting load is uniformly distributed among the four lifting rods.
4. The buckling occurs assuming the lifting of the steam dryer hitting the dryer stops in the reactor vessel top head.
5. The effect of the gap between the lifting rods and the stops is neglected, (i.e., the gap is assumed to be closed).
6. The buckling load is assumed to be axially load only.
7. Elastic buckling is assumed.
8. Stresses resulting from constraint of free end displacement are considered as primary stress.
9. Only the vertical load from SSE is assumed to cause buckling in the lifting rods.
10. The gravity is assumed to have no effect on the lifting force.

8.4 Buckling Calculation

Per Appendix F, F-1334.3, maximum load in axially load compression members shall be limited to:

For $0 \leq \lambda \leq 1$

$$\frac{P}{P_y} = \frac{1 - \frac{\lambda^2}{4}}{1.11 - 0.5\lambda + 0.17\lambda^2 - 0.28\lambda^3} \tag{8-1}$$

For $1 \leq \lambda \leq \sqrt{2}$

$$\frac{P}{P_y} = \frac{2}{3}\left(1 - \frac{\lambda^2}{4}\right) \tag{8-2}$$

For $\lambda > \sqrt{2}$

$$\frac{P}{P_y} = \frac{2}{3\lambda^2} \tag{8-3}$$

where:

P	= maximum allowable load, lb
P_y	= $S_y A_g$, lb
A_g	= area of gross section, in^2
λ	$= \left(\frac{KL}{r}\right)\frac{1}{\pi}\sqrt{\frac{S_y}{E}}$
E	= modulus of elasticity, psi
S_y	= yield strength, psi
K	= effective length factor
L	= unbraced length, in.
r	= radius of gyration, in.

8.5 Results of Analysis

The total lifting load is calculated using the project horizontal area of the steam dryer and the pressure differential for the CLTP and EPU. The projected horizontal area was calculated conservatively using the outside diameter of the upper support ring, about 245 inches as estimated from Reference [4]. The total lifting forces due to pressure differential are presented in Table 8-1.

Assuming the lifting load is evenly distributed among the four lifting rods, the load in each rod is shown in Table 8-2. The axial load on each lifting rod due to the SSE is 80,000*0.327/4 = 6,540 lbs.

The compressive loads acting on each lifting rod due to different loading conditions are summarized in Table 8-2.

From Reference [4], it is shown that the lifting rods are braced at two different elevations with the longest unbraced length of about 32 inches from the top of the support ring to the lowest bracing gusset.

The effective length factor, K, for a slender column can be ranged from 1 to a large number depending on the end support conditions and material properties. Typically, the value of K is from 1 to 5 for a solid circular column with different support conditions.

A parametric study was performed to obtain the allowable compressive load for a value of K from 1 to 5. The allowable compressive loads were calculated using Equations (8-1) through (8-3) depending on λ. For circular column, the radius of gyration is the same as the column radius.

The calculation results are summarized in Table 8-3 and Figure 8-1. Also, the compressive loads due to the pressure differential from either CLTP or EPU and the SSE vertical acceleration are also plotted in Figure 8-1. It is shown that the applied compressive loads do not exceed the allowable until the K reaches 3.8.

From Reference [14], it is shown that the most critical condition was the buckling of lifting rods. The design basis allowable load for the buckling of the faulted condition is 88.99 kips [14, page 2-19]. This design basis criterion is also plotted in Figure 8-1. It is shown that the compressive loads due to CLTP/EPU are lower than the design criterion. Also, it also gives an indication that an effective length factor of 3 was probably used in Reference [14]. In addition, the applied compressive load calculated in Reference [14] is 75.18 kips using an absolute sum of the load

cases. This compressive load is comparable to the applied compressive loads, 80.79 kips for CLTP and 63.11 kips for EPU, obtained in this calculation.

8.6 Discussions

A buckling evaluation of the lifting rods was performed for the faulted condition. The evaluation was performed for the CLTP and EPU conditions. The loadings are due to the pressure differential in the CLTP and EPU conditions, in addition to the vertical acceleration from the SSE.

The evaluation was performed according to ASME B&PV Code Section III, Appendix F. The allowable compressive load was calculated using equations in F-1334.3. A parametric evaluation was performed on the allowable compressive loads as a function of effective length factor K.

It is shown that the applied compressive loads in the lifting rods are less than the allowable compressive loads per Appendix F, F-1334.3 if the effective length factor is less than 3.8 for the CLTP condition. For EPU condition, the applied compressive load is below the allowable compressive load even beyond an effective length factor of 5. From the results presented in Reference [5], the design basis buckling load corresponds to an effective length factor of 3. Also, the applied compressive loads calculated per the CLTP and EPU pressure differential are less than the design basis criteria for buckling presented in Reference [15].

Table 8-1: Total Lifting Force, Faulted Condition

Conditions	Pressure Differential (psi)	Lifting Force (lbs)
CLTP	6.3	297004
EPU	4.8	226289

Table 8-2: Compressive Load on each Lifting Rod, Faulted Condition

Conditions	Axial Load (kips)
CLTP	74.25
EPU	56.57
SSE, vertical g	6.54

Table 8-3: Allowable Load due to Axial Compression

Effective Length Factor, K	λ	Allowable Load (lbs)
1	0.1860	109722
2	0.3719	98826
3	0.5579	88427
4	0.7439	78805
5	0.9298	69962

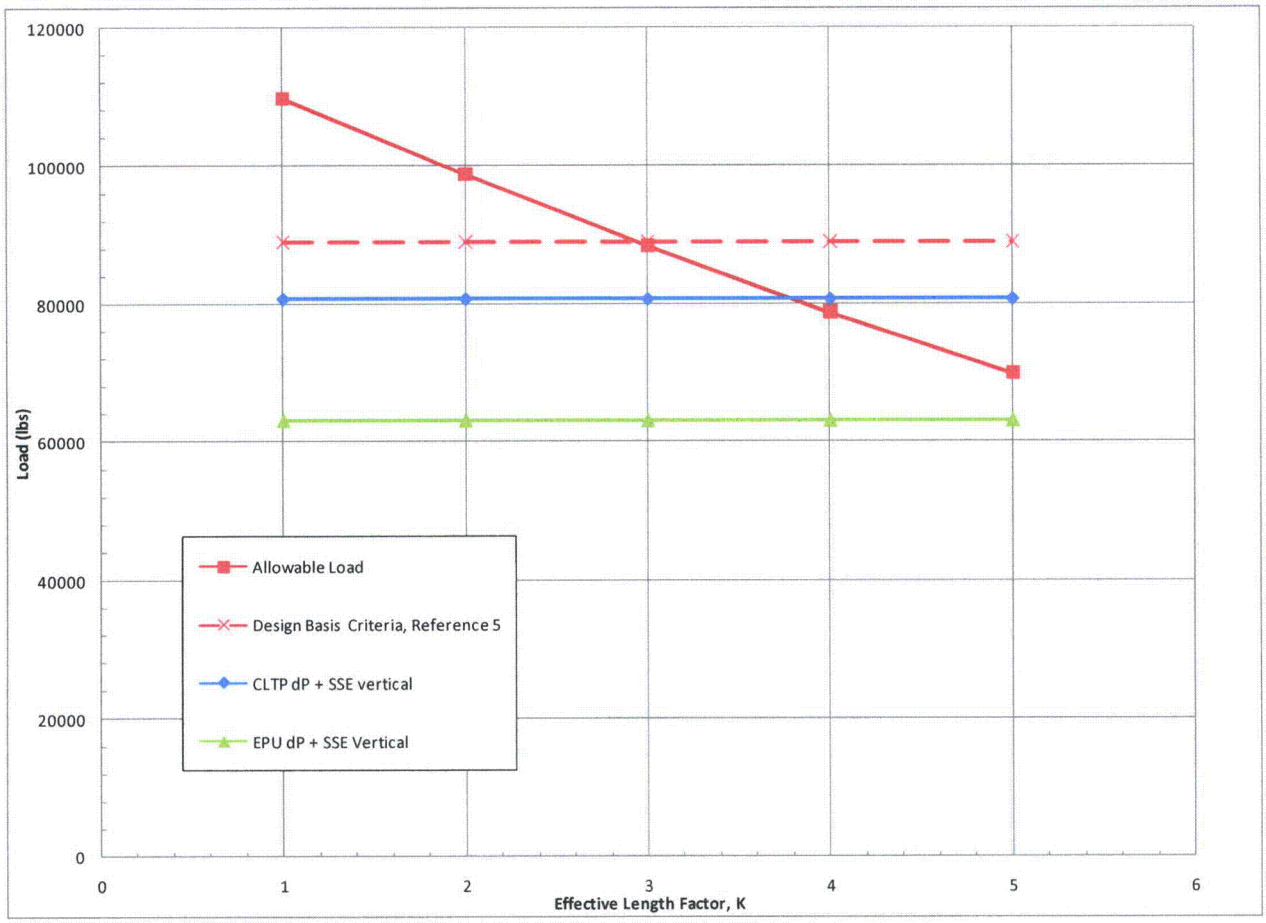

Figure 8-1: Loads as Function of Effective Length Factor K

9.0 DISCUSSION AND CONCLUSIONS

An evaluation was performed for the NMP 2 steam dryer for EPU conditions. It includes an ASME Code evaluation for stress allowables and fatigue.

The evaluation was performed per the guidance on the demonstration of steam dryer integrity for plants implementing power uprate. The basic load combinations were provided in Reference [5]. The stress results for individual load cases used in the load combinations are based on the four unit load cases: one unit pressure and three unit static accelerations in the three global directions. In addition, results from two points of time in the FIV transient were provided in Reference [4] for use in the Code stress allowable and fatigue evaluation.

A review of the load combinations in Reference [5] shows that two load combination cases identified as load Case B-3 for the Service Levels A and B and load Case D-1 for the service Levels C and D are bounding.

The resultant stresses for these two load cases were obtained from the four unit load cases with the appropriate scaling factors with the FIV loads. The alternating stress intensity ranges were obtained from the difference between the two points of time in the FIV load transient.

The Code evaluation was performed per Subsection NG of ASME B&PV Code Section III [1]. The evaluation shows that the allowable requirements for all stress categories are met for all service levels based on the nodal interpretation of the finite element results. The stress in the gussets in the hoods and tie bars for the faulted load combination exceed the stress allowable, Table 6-10. However, these components do not significantly exceed the stress allowable and application of elastic-plastic stress analysis method would likely show that the stresses in these two components satisfy the Appendix F rule for evaluation of service loadings with Level D Service Limits. It is noted that the hood gusset location is dominated by the accident differential pressure (ΔP_A or ΔP_I) loading and the EPU faulted differential pressure load is reduced compared to that for the original licensed thermal power conditions. The overall conclusion is that the hood gusset location remains within the original design basis margin for the faulted load

case for the EPU condition. Using the stress for a section through the component, the stresses are within the ASME Code stress allowables for the Service Level B condition.

The cumulative fatigue was evaluated per the guidance in Section III Appendix I of Reference [1]. With the consideration of mean stress effect, the P_l+P_b+Q stress range limits and the location of the peak stress, it is shown that the maximum alternating stress amplitude, S_{eq}, in all steam dryer components are below the endurance limit of fatigue curve B of 16.5 ksi. Even with the more conservative fatigue Curve C, the fatigue usage is very small.

10.0 REFERENCES

1. ASME Boiler and Pressure Vessel Code, Section III, Subsection NG and Appendices, 2001 Edition with all Addenda.
2. EPRI Report, "BWRVIP-182: BWR Vessel and Internals Project, Guidance for Demonstration of Steam Dryer Integrity for Power Uprate," Report No. 1016166, EPRI, Palo Alto, CA 2008, SI File No. 0800528.210P.
3. EPRI Report, "BWRVIP-181: BWR Vessel and Internals Project, Steam Dryer Repair Design Criteria," Report 1013403, EPRI, Palo Alto, CA 2008, SI File No. 0800528.210P.
4. CDI ANSYS Databases and Results, July 1, 2008, SI File No. 0800528.212.
5. SI Report 0800528.401, Revision 0, "Nine Mile Point 2 Stream Dryer EPU Loads and Load Combination," SI File No. 0800528.401.
6. GE Document No. NEDC-31145, February 1986, "Niagara Mohawk Power Corporation Nine Mile Point Unit 2 NSSS New Loads Design Adequacy Education Final Summary Report," SI File 0800528.201.
7. ASME Boiler and Pressure Vessel Code, Section II, Part D, 2001 Edition with all Addenda.
8. ANSYS Revision 11.0, ANSYS, Inc., August, 2007.
9. ASME, "Criteria of the ASME Boiler and Pressure Vessel Code for Design by Analysis in Sections III and VIII, Division 2," Pressure Vessels and Piping Design and Analysis, A Decade of Progress, Vol. I Analysis, ASME Publication, 1972.
10. Drawing 796E258, "Dryer Half, Steam Dryer," Rev. C, SI File No. 0800528.215.
11. Drawing 0016010001729, "Dryer Section, Steam Dryer," Sheet 1, Rev. 2, SI File No. 0800528.215.
12. Nine Mile Point Unit 2 FSAR, SI File No. 0800528.207.
13. E-mail, A. Boschitsch (CDI)/K. Fujikawa (SI), "Subject: Response to 10-14 phone message," October 16, 2008, SI File No. 0800528.103.
14. Lattin, N. F., "Niagara Mohawk Power Corporation Nine Mile Point Unit 2, NSSS New Loads Design Adequacy Evaluation Final Summary Report," General Electric Report NEDC-31145, ERM BMB-1588, Class II, February 1986.
15. E-mail, Alex Boschitsch (CDI)/Karen Fujikawa (SI), 'Re: NMP2 Steam Dryer Weight,' November 4, 2008, SI File No. 0800528.103.
16. "Invessel Visual Inspection (IVVI) of Reactor Pressure Vessel Components for the Nine Mile Point Unit 2 Nuclear Station During the Spring 2008 Outage," Report No. G9M12-N2R11-309718, April 2008, Westinghouse, SI File No. 0801273.201.
17. SI Report No. 0801273.401, Rev. 1, "Flaw Evaluation and Vibration Assessment of the Nine Mile Point Unit 2 Steam Dryer for Extended Power Uprate Operating Conditions."

18. EPRI Report 1011463, "BWRVIP-139: BWR Vessel and Internals Project Steam Dryer Inspection and Flaw Evaluation Guidelines," EPRI, Palo Alto, CA 2005.

19. EPRI Report TR-105873-A, "BWR Vessel and Internals Project: Evaluation of Crack Growth in BWR Stainless Steel RPV Internals (BWRVIP-14A)," March 2003.